# APPLICATION OF PRECISION ENGINEERING FOR NANOMETRE FOCUSSING OF HARD X-RAYS IN SYNCHROTRON BEAM LINES

A thesis submitted for the degree of Master of Philosophy

by

Stewart Mark Scott

Department of Advanced Manufacturing and Enterprise Engineering
Brunel University

November 2011

## Corrections

| Issue No | Date |
|---|---|
| 1st Draft | 8 September 2011 |
| 2nd Draft | 31 October 2011 |
| Issued for examination | 29 November 2011 |
| Viva comments incorporated | 7 February 2012 |

## Abstract

Many modern synchrotron beamlines are able to focus X-rays to a few microns in size. Although the technology to achieve this is well established, performing routine experiments with such beams is still time consuming and requires careful set up. Furthermore there is a need to be able to carry out experiments using hard X-ray beams with even smaller beams of between 100nm and 10nm. There are focussing optics that are able to do this but integrating these optics into a stable and a usable experimental set up are challenging. Experiments can often take some hours and any change in position of the beam on the sample will adversely affect the quality of the results. Experiments will often require scanning of the beam across the sample and so mechanisms suitable for high resolution but stable scanning are required.

Performing routine experiments with nanometre sized beams requires mechanical systems to be able to position the sample, focussing optics, detectors and diagnostics with significantly higher levels of stability and motion resolution than is required from so called micro focus beam lines.

This dissertation critically reviews precision engineering and associated technologies that are relevant for building nano focus beamlines, and the following key issues are explored:

- Long term position stability due to thermal effects
- Short term position stability due to vibration
- Position motion with nanometre incremental motion
- Results of some tests are presented and recommendations given.

Some test results are presented and guidance on designing nano focus beamlines presented.

## Acknowledgements

The Author would like to thank the support of Prof Kai Cheng of Brunel University and Dr Andy Dent, Mr Jim Kay and Dr Kawal Sawhney of Diamond Light Source Ltd in carrying out this work. I also thank Diamond Light Source for the funding and use of equipment.

All diagrams and images are the authors unless stated.

Table of Contents

Chapter 1. Introduction ..... 1

1.1 Synchrotrons ..... 1

1.1.1 History ..... 1

1.1.2 How synchrotrons work ..... 1

1.2 Diamond Light source ..... 2

1.3 Hard X- ray applications ..... 3

1.4 Requirements for nanometre precision mechanics ..... 4

1.5 Aims and Objectives ..... 4

1.6 Scope of the dissertation ..... 5

1.6.1 Specification ..... 5

1.6.2 To determine what are the technical problems to be addressed ..... 5

1.6.3 To highlight what are the current technologies ..... 5

1.6.4 To review trends in current research ..... 5

1.6.5 To carry out some test and development ..... 6

1.6.6 To make recommendations in any changes of design methodology or technology that Diamond Light Source should adopt in the future ..... 6

Chapter 2. Scientific requirements and challenges ..... 7

2.1 Science at the nanometre scale. ..... 7

2.2 Nano beamlines ..... 7

2.2.1 APS ..... 7

2.2.2 Soleil ..... 7

2.2.3 ESRF ..... 8

2.2.4 NSLSII ..... 9

2.2.5 PETRA III ..... 9

2.2.6 Spring 8 ..... 9

2.2.7 ANKA ..... 10

2.2.8 Diamond ..... 10
2.3 Focussing optics ..... 10
2.3.1 Kirkpatrick-Baez mirrors ..... 10
2.3.2 Refractive lenses ..... 12
2.3.3 Fresnel Zone plates ..... 15
2.3.4 Multi layer laue lenses ..... 16
2.3.5 Capillary tubes ..... 16
2.3.6 Waveguides ..... 17
2.3.7 Diffraction limit ..... 18
2.3.8 Summary of focussing optics ..... 18
2.4 Types of experiments suitable for nano focus ..... 19
2.4.1 Nano diffraction ..... 19
2.4.2 Micro fluorescence ..... 19
2.4.3 Transmisive imaging ..... 21
2.4.4 Phase contrast imaging ..... 22
2.5 Technical challenges for a sub 100nm beam experiment station ..... 22
2.5.1 Focussing distance ..... 22
2.5.2 Positional stability ..... 23
2.5.3 Sample alignment ..... 23
2.5.4 Sample scanning ..... 24
2.5.5 User sample mounting ..... 25
2.5.6 Detector integration ..... 25
2.5.7 Alignment and diagnostics ..... 25
2.5.8 Sample mounting and sample changing ..... 27
2.5.9 Integration into existing beamlines ..... 30
Chapter 3. Thermal stability ..... 32
3.1 Thermal stability issues ..... 32
3.2 Low thermal expansion materials ..... 32
3.2.1 Glass ceramics ..... 32
3.2.2 Sialon ..... 34
3.2.3 36% Nickel iron alloys ..... 35

3.2.4 Metal matrix composites ..... 36
3.2.5 Carbon fibre composites ..... 38
3.2.6 Silicon carbide ..... 40
3.2.7 Nexcera ..... 42
3.2.8 Ceramic composites ..... 43
3.2.9 Granite ..... 43
3.2.10 Titanium ..... 44
3.2.11 Aluminium Alloys ..... 45
3.2.12 Summary of low CTE materials ..... 45
3.3 Phase change materials ..... 46
3.3.1 Salt based PCMs ..... 47
3.3.2 Organic PCMs ..... 48
3.3.3 Embedded PCMs ..... 49
3.3.4 Conclusion ..... 50
3.4 Minimisation of internal air ..... 50
3.5 Minimisation of heat load variation ..... 51
3.5.1 2 phase stepper motors ..... 51
3.5.2 Pneumatic actuators ..... 52
3.5.3 Lighting ..... 53
3.5.4 Conclusions ..... 53
3.6 Thermal expansion compensation ..... 53
3.7 Thermal centre ..... 55
3.8 Minimisation of heat loads ..... 55
3.9 Reduce stabilisation time ..... 56
3.10 Active temperature stabilisation methods ..... 56
3.10.1 Laboratory water circulator ..... 57
3.10.2 Pressure pulse reduction system ..... 57
3.10.3 Peltier to water exchanger ..... 60
3.10.4 Peltier to air exchanger ..... 61
3.10.5 Thermal mass ..... 61

3.10.6 Reduction of heat transfer from ambient air ..... 62
3.11 Thermal insulation ..... 62
3.12 Reduction in surface area ..... 64
3.13 Temperature control through air heat exchange ..... 65
3.13.1 Natural convection ..... 65
3.13.2 Forced Convection ..... 67
3.13.3 Temperature stability using air flow ..... 68
3.14 Separate metrology frame ..... 68
3.15 Improvements in hutch temperature control ..... 69
3.15.1 Improvement of temperature control of hutches at the ESRF ..... 69
3.15.2 Improvements of temperature control at Diamond ..... 69
3.15.3 Figure of merit ..... 79
3.16 Temperature measurement ..... 81
3.16.1 Thermocouples ..... 81
3.16.2 Resistance thermometers ..... 83
3.16.3 Thermisters ..... 84
3.17 Trends in current research and development ..... 85
3.18 Recommendations to improve thermal stability ..... 86
3.18.1 Materials ..... 86
3.18.2 Design ..... 87
Chapter 4. Vibration stability ..... 88
4.1 Sources of vibration at Diamond ..... 88
4.2 Vibration criteria ..... 89
4.3 Transmissibility and resonance ..... 92
4.4 External passive vibration isolation ..... 93
4.4.1 Introduction ..... 93
4.4.2 Minus K negative spring system. ..... 94
4.4.3 Pneumatic isolators ..... 94

4.5 External active vibration isolation ..... 95
4.5.1 Introduction ..... 95
4.5.2 Kolibri system from TNO ..... 95
4.5.3 HWI Scientific Instruments ..... 96
4.5.4 Halcyonics GmbH ..... 96
4.5.5 CERN Magnet isolation system ..... 96
4.5.6 Giant Magnetostrictive Hybrid actuation system ..... 96
4.6 Internal passive damping ..... 97
4.6.1 Damping using shunted piezos ..... 97
4.6.2 Damping using visco elastic materials ..... 98
4.6.3 Constrained layer damping ..... 99
4.6.4 Structural damping ..... 99
4.6.5 Tuned mass dampers ..... 101
4.6.6 Internal viscous damping ..... 101
4.6.7 Damping using granular materials ..... 102
4.7 Vibration reduction at source ..... 102
4.7.1 Summary ..... 103
Chapter 5. Acoustic stability ..... 105
5.1 Human ear response to sound ..... 105
5.2 Sound effect on samples ..... 109
5.3 Sound reflection coefficient ..... 109
5.4 Sound absorption ..... 110
5.4.1 Porous absorbers ..... 110
5.4.2 Panel absorbers ..... 111
5.4.3 Resonators ..... 111
5.4.4 Micro perforated panel absorbers ..... 111
5.5 Noise source frequency ..... 115
5.6 Sound reduction ..... 115
5.7 Reverberation time ..... 115

5.8 Room modes ..... 116
5.9 Acoustic vibration summary ..... 118
Chapter 6. Position control ..... 119
6.1 Actuators ..... 119
6.1.1 Stepper motors ..... 119
6.1.2 DC Motor ..... 121
6.1.3 Piezo actuators ..... 122
6.1.4 Voice coil actuators ..... 123
6.1.5 Piezo slip/stick devices ..... 124
6.1.6 Linear motors ..... 125
6.1.7 Giant Magnetostrictive actuators ..... 126
6.1.8 Pneumatic actuators ..... 126
6.1.9 Hydraulic actuators ..... 127
6.1.10 Magnetic Shape memory alloy actuators ..... 127
6.2 Bearings ..... 128
6.2.1 Aerostatic bearings (air bearings) ..... 128
6.2.2 Hydrostatic bearings ..... 132
6.2.3 Rotary stroke bearings ..... 132
6.2.4 Roller bearings ..... 133
6.2.5 Re-circulating ball bearings ..... 135
6.2.6 Linear crossed Roller bearings ..... 136
6.2.7 Magnetic bearings ..... 137
6.3 Drives ..... 137
6.3.1 Lead screws ..... 137
6.3.2 Ball screws ..... 137
6.3.3 Satellite roller screws ..... 138
6.3.4 Harmonic drive gearboxes ..... 139
6.3.5 Low backlash gears ..... 140
6.3.6 Flexures ..... 141
6.4 Position feedback ..... 142

6.4.1 Introduction ..... 142
6.4.2 Incremental optical scale encoders ..... 142
6.4.3 Absolute optical encoders ..... 146
6.4.4 Laser interferometer encoders ..... 146
6.4.5 Capacitive sensors ..... 148
6.4.6 Inductive (Eddy current) Sensors ..... 148
Chapter 7. Laser interferometer tests ..... 149
7.1 Introduction ..... 149
7.2 Test set up ..... 149
7.2.1 Laser Encoder ..... 150
7.2.2 Encoder and mirror mount ..... 151
7.2.3 Vibration reduction ..... 152
7.2.4 Temperature stability ..... 152
7.2.5 Pressure measurement ..... 153
7.2.6 Humidity measurement ..... 153
7.2.7 Location ..... 153
7.2.8 Air turbulence ..... 153
7.2.9 Test procedure ..... 153
7.2.10 Sources of error ..... 154
7.3 Results ..... 163
7.4 Measurement Stability ..... 164
7.5 Measurement Uncertainty ..... 165
7.6 Discussion ..... 166
7.7 Experience obtained ..... 168
7.7.1 Local thermal stabilisation enclosure ..... 168
7.7.2 Hutch temperature controller settings ..... 170
7.7.3 Rigid coupling of optics to sample stage ..... 170
7.7.4 Voice coil actuators ..... 171
7.7.5 Slip stick piezo actuators ..... 171
7.7.6 Pneumatic actuators ..... 171

7.7.7 Flexures ..... 172
7.7.8 Granite blocks ..... 172
7.7.9 Silicon Carbide ..... 173
7.7.10 Low thermal expansion ceramics ..... 173
7.7.11 Laser encoders ..... 173
7.7.12 Capacitive sensors ..... 174
7.8 Exact constraint design ..... 174
7.9 Introduction ..... 174
7.10 Thermal expansion fixed point. ..... 174
7.11 Fixing weak to strong ..... 175
7.12 Over-constrained motion ..... 175
7.13 Kinematic Mounts ..... 175
7.13.1 Preload ..... 176
7.13.2 Materials ..... 176
7.14 Experimental tests ..... 176
Chapter 8. Conclusions and recommendations for future Work ..... 178
8.1 Summary of work conducted ..... 178
8.2 Main findings ..... 178
8.3 Recommendations ..... 180
8.3.1 Thermal stability ..... 180
8.3.2 Acoustic vibration ..... 181
8.3.3 Floor transmitted vibrations ..... 181
8.3.4 Motion control ..... 182
8.3.5 Keeping up to date with latest developments ..... 183
References ..... 187
Appendix A – Development and testing of a carbon fibre pyramidal end structure ..... 197
Appendix B – Active vibration using positional feedback ..... 206
Appendix C – Adjustable length platform ..... 209

Appendix D - Vibrometer tests.....213

Appendix E – Temperature stabilised enclosure tests.....232

Appendix F – Vibration isolation test.....237

Appendix G – Tests of MinusK table.....243

## List of figures

Figure 1 – KB Mirror system ..... 11
Figure 2- 2D lenses produced at Aachen ..... 13
Figure 3 - lens holder 1D lenses ..... 13
Figure 4 - Silicon cuniform lenses ..... 14
Figure 5 - Fresnel zone plate and Order sorting aperture ..... 15
Figure 6 - Schematic of a Fresnel zone plate ..... 16
Figure 7- Mono capillary tube ..... 17
Figure 8 - Tapered capillary tube ..... 17
Figure 11 - Mulit element germanium detector used at B18 Core spectroscopy beamline at Diamond ..... 20
Figure 14 – Example of fluorescence experiments ..... 21
Figure 16 – Hampton Research mount ..... 28
Figure 18– Water jet cut Corning ULE parts ..... 33
Figure 19–CTE of Invar™ and Super Invar™ ..... 35
Figure 20–Examples of Silicon Carbide section from Newport Spectra Physics ..... 41
Figure 21–Broken slab of Nexcera ..... 43
Figure 22– Summary of CTE of some materials ..... 46
Figure 23– Expansion compensated triangle ..... 54
Figure 24– Plot of vertical height change vs leg angle ..... 54
Figure 25- Pressure pot circuit ..... 58
Figure 26- Pressure pot ..... 59
Figure 27- Sketch of pressure pot ..... 60
Figure 28 – Hutch roof mounted air chiller and fan ..... 70
Figure 29 - B16 Hutch showing air distribution socks ..... 70
Figure 30 – Location of 3 port valve outside the hutch ..... 71
Figure 31 Hutch air temperature control schematic ..... 72
Figure 32 – Air temperature control panel ..... 72
Figure 33 – Temperature profiles for different Xp values ..... 75
Figure 34 – Tuning result with Zeigler-Nichols parameters ..... 76

Figure 35 – Tuning results with Tyreus-Luyben parameters ..... 77
Figure 36 – Linear valve characteristic ..... 78
Figure 37 – Equal percentage valve characteristic ..... 78
Figure 38 –Temperature distribution of block ..... 79
Figure 39 – Location of constraints of block ..... 80
Figure 40 – Deflection of Aluminium as a function of thermal expansion ..... 80
Figure 41 – Deflection of Aluminium a a function of thermal conductivity ..... 81
Figure 42 – Vibration measurements on B16 ..... 89
Figure 43 – Vibration criteria ..... 91
Figure 44 Ground vibrations measured at various sites. ..... 92
Figure 45 – Vibration displacement measurements ..... 93
Figure 46 – Negative stiffness spring ..... 94
Figure 47 – Volture piezo energy harvester ..... 98
Figure 48 – Loss factor of RA218 against temperature and frequency ..... 98
Figure 49 – Shear modulus of RA218 against temperature and frequency ..... 99
Figure 50 – Loss factor of Paragon MPM ..... 100
Figure 51 – CSA Tuned mass damper ..... 101
Figure 52 – Water pump plinth and spring supports ..... 102
Figure 53 - Graph of Sound filter response against frequency ..... 106
Figure 54 - Absorption of Clearsorber™ micro perforated film ..... 112
Figure 55 - British museum Atrium ..... 112
Figure 56 - Absorption of Clearsorber™ honeycomb ..... 113
Figure 57 – Modex panel ..... 114
Figure 58- Diagram of RPG Modex panel ..... 114
Figure 59 - Axial room modes ..... 116
Figure 60 - Tangential Room modes, ½ energy of axial modes ..... 117
Figure 61 - Oblique Room modes, ¼ energy of axial modes ..... 117
Figure 62 – 2 and 5 phase motors ..... 120
Figure 63 – Cedrat amplified piezo actuator ..... 122
Figure 66 – New focus slip stick piezo actuator ..... 125

Figure 68 – Hydraulic actuators ..... 127
Figure 69 - Pressure distribution of different orifice arrangements ..... 129
Figure 70 – Rotary stroke bearing ..... 133
Figure 71 – NSK Liner bearing ..... 135
Figure 72 – Linear crossed roller bearing ..... 136
Figure 73 – Ball screw ..... 138
Figure 74 - Rollvis Swiss satellite roller screw ..... 139
Figure 75 - Harmonic drive ..... 140
Figure 76- OTT anti backlash worm and wheel ..... 141
Figure 77 – Signal collection scheme for the Laser interferometer tests ..... 150
Figure 78 - Renishaw RLU10 laser unit ..... 151
Figure 79– Renishaw detector head ..... 151
Figure 80 - Peltier heat pump ..... 152
Figure 81– National Instruments cRIO, back plane and C series modules ..... 154
Figure 82– Encoder position during door opening test ..... 156
Figure 83– Pressure reading during door opening test ..... 157
Figure 84 - Measured position ..... 158
Figure 85 - Measured pressure ..... 158
Figure 86 - Pressure compensated position ..... 159
Figure 87 - Pressure variation ..... 160
Figure 88 – Temperature of air over a 11.5 hour period ..... 163
Figure 89– Pressure compensated position over a 11.5 hour period ..... 164
Figure 90 – Example of a kinematic mounts ..... 175
Figure 91 – Simple steel fabrication ..... 198
Figure 92 – 3 legged structure ..... 198
Figure 93 – 4 legged, 4 brace structure ..... 199
Figure 94 – 4 legged, 12 brace structure ..... 199
Figure 95 – 3 legged, triple tripod structure ..... 200
Figure 96 – 4 legged, 8 brace structure ..... 201
Figure 97 – Testing of 4 legged structure ..... 202

Figure 98 – measured vertical vibrations of 4 legged structure ..... 203
Figure 99 – Measured horizontal vibrations of 4 legged structure ..... 203
Figure 100 – Design of adjustable length platform ..... 209
Figure 101 – Actuator leg ..... 210
Figure 102 – Schematic of actuator leg ..... 210
Figure 103- Actuator leg under test ..... 211
Figure 104- Feedback results of actuator ..... 212
Figure 105 – Polytec Vibromter ..... 213
Figure 106 – Vibrometer rubber feet test ..... 214
Figure 107 - Vibrometer Test with rubber feet ..... 215
Figure 108 - Stationary attocube ..... 216
Figure 109 - Attocube at 500Hz, 20 Volts ..... 217
Figure 110 - Attocube at 500Hz, 10 volts ..... 217
Figure 111 – Attocube at 500Hz, 2 Volts ..... 218
Figure 112 – Attocube at 250Hz, 2 Volts ..... 218
Figure 113 – Most stable test ..... 219
Figure 114 – Vibrometer mounted on detector stage ..... 221
Figure 115 – Vibration target mounted on diagnostics stage ..... 222
Figure 116 – Vibration results between detector stage and diagnostics stage ..... 223
Figure 117 – Vibration test with piezo stage at 5 volts ..... 223
Figure 118 – Vibration results between detector and optics stage (Test 3) ..... 224
Figure 119 – Vibration results between detector stage and optics stage at different heights (Test 4 & 5) ..... 225
Figure 120 – Vibration target mounted on diffractometer ..... 226
Figure 121 – Vibration test looking at Diffractometer ..... 227
Figure 122 – Detector stage to Beryllium Window ..... 228
Figure 123 – Vertical vibration tests at different heights ..... 229
Figure 124 – Vertical vibration tests of detector stage and main table ..... 230
Figure 125 – Vertical vibration tests of detector stage ..... 230
Figure 126 – Internal air temperature of enclosure ..... 233

Figure 127 – External air temperature in metrology lab ..... 234
Figure 128 – External temperature of experimental hall ..... 235
Figure 129 – Comparison of internal and external temperatures ..... 235
Figure 130 – B16 Hutch temperature ..... 236
Figure 131 – Vibration test with 2 aluminium plates and granite block ..... 237
Figure 132– Screen shot of vertical vibrations during test. ..... 238
Figure 133 – Screen shot of horizontal vibrations during test. ..... 239
Figure 134– Vertical vibration. ..... 239
Figure 135– Horizontal vibrations. ..... 239
Figure 136– Data sheet Vertical Transmissibility for a CM-255 ..... 240
Figure 137– Measured vertical transmissibility. ..... 240
Figure 138– Data sheet Horizontal Transmissibility for a CM-255 ..... 241
Figure 139– Measured horizontal transmissibility. ..... 241
Figure 140 – MinusK platform ..... 243
Figure 141 – MinusK vibration test results ..... 244

## List of tables

Table 1– Recent Synchrotrons ..... 2
Table 2 - Low expansion glass ceramics ..... 34
Table 3 – CTE of machineable ceramics ..... 34
Table 4 - 36% nickel/iron alloys ..... 35
Table 5 - Metal Matrix Composites available from Advanced Metal Composites Ltd ..... 37
Table 6 - CTE of some Carbon fibre yarns ..... 39
Table 7 - CTE of Silicon Carbide ..... 40
Table 8 - CTE of Granite ..... 44
Table 9 – Phase change materials ..... 47
Table 10 - Melting point of some Paraffins ..... 49
Table 11 - Water chiller pressure pulse reduction results ..... 58
Table 12 - Thermal mass of common materials ..... 61
Table 13 - Examples of thermal insulation materials ..... 64
Table 14 – Control loop parameters ..... 73
Table 15 – Ziegler-Nichols parameters ..... 75
Table 16 – Tyreus-Luyben parameters ..... 76
Table 17 - Thermocouple materials ..... 82
Table 18 - Resistance values for thermister and RTD's ..... 85
Table 19 – Sources of vibration ..... 88
Table 20 – Vibration criteria ..... 90
Table 21 – 1/3 band analysis frequency bands ..... 91
Table 22 – Loss factors for some materials ..... 100
Table 23 – Noise level in db(A) fans on ..... 106
Table 24 – Noise level in db(A) fans off ..... 107
Table 25 – Recommended sound levels ..... 107
Table 26 – General noise levels ..... 108
Table 27 - Acoustic impedance of some materials ..... 110

Table 28 - Reflection coefficients at some material interfaces ..... 110
Table 29 - Example Micro perforated panel parameters ..... 111
Table 30 - ISO 8573-1:2001 Compressed air quality class ..... 132
Table 31 – ABEC ratings for bearings ..... 134
Table 32 – ABMA Grades up to 20 only ..... 134
Table 33 – Materials used in flexures ..... 142
Table 34 – Sony laser scale types ..... 145
Table 35- Sony laser scale BL series versions ..... 145
Table 36 – Barometer specification ..... 156
Table 37 – RLU10 wavelength stability ..... 160
Table 38 – Measurement uncertainty ..... 166
Table 39 – Frequency modes of vibration ..... 200
Table 40 – Summary of attocube tests ..... 219
Table 41 – Vibration sensors ..... 238

## Abbreviations

| | |
|---|---|
| APS | Advanced Photon Source |
| Be | Beryllium |
| CERN | European Organization for Nuclear Research |
| CTE | Coefficient of thermal expansion |
| ESRF | European Synchrotron Radiation facility |
| FWHM | Full Width Half Maximum |
| KB | KirkPatrick- Baez |
| Li | Lithium |
| PC | Personal Computer |
| PCM | Phase change materials |
| PMMA | Poly methyl methacrylate |
| SDE | Sub divisional errors |

# Chapter 1. Introduction

## 1.1 Synchrotrons

### 1.1.1 History

In 1947 it was discovered that when charged atomic particles are accelerated in a cyclotron, parasitic radiation was emitted (F Elder). At first this was a nuisance but then it was found that this radiation could be used to perform many ground breaking experiments. Particle accelerators are now constructed solely to generate this radiation and these accelerators are called synchrotrons. Radiation generated by synchrotrons enables experiments to be carried out in many areas of research including structural biology, physics, chemistry, materials science, engineering, earth and environmental sciences (Munro, 1997).

### 1.1.2 How synchrotrons work

Synchrotrons circulate a beam of high energy electrons through a vacuum tube in a circular orbit. The electrons are guided by magnets and their energy is maintained by an RF cavity. Intense electromagnetic radiation is emitted by the electron when subjected to a force by a magnetic field. The wavelength of the radiation emitted depends upon the magnetic field strength, the rate of change in field strength and electron energy. This emitted radiation is the used to perform experiments. The advantages of a synchrotron are as follows:

- The photon intensities are high, this enables data to be collected quickly and weak interactions studied.
- The energy of the radiation can be varied continuously so that energy scanning experiments can be performed.
- The energy of the radiation can cover a wide range from a few electron volts (vacuum ultra violet) to hundreds of Kilo electron volts (hard X-rays).
- The source size is small.

- The beams have low divergence.

A summary of some recently constructed synchrotrons is shown in Table 1.

| Synchrotron Name | Country | Electron Energy (GeV) | Circumference of storage ring (m) | Year of first operation |
|---|---|---|---|---|
| Swiss Light Source | Switzerland | 2.4 | 288 | June 2001 |
| Soleil | France | 2.75 | 354 | May 2006 |
| Diamond | UK | 3 | 561 | Jan 2007 |
| Australian Synchrotron | Australia | 3 | 216 | July 2007 |
| Shanghai | China | 3.5 | 432 | April 2009 |
| Alba | Spain | 3 | 268 | In construction |

**Table 1– Recent Synchrotrons**

The radiation is generated by the electrons and is emitted in the direction of travel. The radiation travels down the beamline, which is tangential to the storage ring. The beamline contains devices for modifying the radiation such as slitting the beam size, focussing the beam, rejection of unwanted energies, holding and orientating the sample and housing detectors. The sample station is usually towards the end of the beamline and is generally about 40-50m from the source.

## 1.2 Diamond Light source

Diamond Light Source is the UK's national synchrotron science facility, located at the Harwell Science and Innovation Campus in Oxfordshire. Diamond has 19 fully operational beamlines, 8 beamlines in design and construction, approval to design 4 beamlines and develop proposals for one more beamline. As well as new beamlines, there is a programme of continuous improvements and upgrades of existing beamlines to take advantage in developments in new experimental techniques, new solid state detectors and more complex sample environments.

To maintain Diamonds ability to carry out cutting edge research it is important that the latest technology is used to support the underlying science research. There is a great deal of interest in carrying out scientific research at the nanometre scale and it is

recognised that modern 3rd generation synchrotrons with high intensities and low emittance X-ray beams can play a crucial role in this. Other world class synchrotrons such as NLS2, ESRF, PETRA 3 and the APS are building nano focus beamlines and developing expertise in this area.

Diamond has been very involved in the development and testing of state of the art X-ray focussing optics and has a world class facility for testing long grazing incidence X-ray mirrors (S Alcock, 2010). The ability to build and operate nano focus beamlines is seen as an essential progression. To a certain extent this has already started. A dedicated test beamline, at Diamond, called B16 Test beamline, is used to test new devices and techniques (Sawhney, 2009). Many recent experiments on B16 have been using state of the art focusing optics and beams of 160nm have been obtained. The techniques developed on B16 have been applied on the I18 Microfocus Spectroscopy beamline where a 70nm sized beam has been produced.

One future beamline will be required to focus to nanometre sized beams and in addition some beamlines, such as I22 Non crystalline diffraction beamline, have experiments that would benefit from nanometre focussed beams. There are also developments in experimental techniques. Of particular interest is the technique of Coherent diffraction. In this technique a small spot size is not produced but scanning of the sample across the unfocussed coherent X-ray beam at nano metre resolution is critical. To be able to satisfy future potential demand it is recognised that the Technical Division at Diamond should be able to design and build systems that are suitable for nano metre focus beamlines.

## 1.3 Hard X- ray applications

Low energy X-rays are easily absorbed by atmospheric air and so experiments must be performed in vacuum. In vacuum nano focus systems have the advantages of being more thermally stable but there are severe restrictions on the sample environments that can be used. This thesis only looks at systems that are suitable for in air operation with hard X-rays.

## 1.4 Requirements for nanometre precision mechanics

Although the divergence is small, the radiation beam does expand. Long grazing incidence primary mirrors are often used to either collimate or focus the beam onto the sample or an intermediate focus spot. These primary mirrors are often located to give modest focussing (1:1 to 3:1).

For some micro focus beamlines a second set of focussing optics is used. These image the intermediate source generated by the primary mirrors to produce a smaller beam size at the sample. In some cases primary mirrors are not used and only a final short focal length final focussing system is used.

In either case the distance between the final focussing optics and the sample must be very short if large demagnification is required.

Synchrotron beamlines are heavily used by a wide variety of users. These users are allocated limited beamtime for their experiment which can be from a week down to half a day. Beamlines are therefore designed to produce extremely high quality data but that is easy to use and highly reliable.

Stable, easy to use and precise mechanics are essential to manipulate the focussing optics, sample and detectors.

Recent developments in optics have enabled smaller beam sizes to be obtained and beam dimensions of below 10nm have now been obtained. (H Mimuraa, 2011) There is however a big challenge to produce beamlines that can routinely carry out experiments with beam sizes of the order of 10's nm.

## 1.5 Aims and Objectives

The aim of the research is to examine the engineering difficulties and challenges in building an experiment station suitable for nano focus experiments, suggest solutions and make recommendations for further work.

The objectives of the research are as follows:

- To determine what are the technical problems to be addressed.
- To highlight what are the current technologies.
- To review trends in current research.
- Carry out some test and development.
- Make recommendations in any changes of design methodology or technology that Diamond Light Source should adopt in the future.

## 1.6 Scope of the dissertation

### 1.6.1 Specification

The specification of this thesis is to identify equipment, techniques and materials that can be used to develop future beamlines at Diamond to achieve repeatable sub 100nm focussed hard-x-rays, stable over a few hours.

### 1.6.2 To determine what are the technical problems to be addressed

The methods of focussing X-rays will be reviewed and the experimental requirements for a nano focus experimental station will be discussed. This will include detector integration, sample positioning, alignment and calibration.

### 1.6.3 To highlight what are the current technologies

Current technologies in the field of motion stability and positioning will be examined and in particular what is being adopted in other ultra precision areas such as astronomy and wafer fabrication plants.

### 1.6.4 To review trends in current research

The thesis will review current research though the following methods:

- Review of published material in journals and conference proceedings.
- Discussions with manufacturers.
- Discussions and visits to other synchrotrons and research organisations.
- Attendance at conferences, seminars and open meetings.

### 1.6.5 To carry out some test and development

A range of tests were carried out on components and ideas that may be suitable for incorporation into a nano focus end station.

### 1.6.6 To make recommendations in any changes of design methodology or technology that Diamond Light Source should adopt in the future

The staff in the Technical Division at Diamond Light Source currently design, build and test experiment stations for micros focus beamlines. This thesis will examine what changes are required to progress from micro focus to nano focus. Issues that will be discussed include

- The use of low thermal expansion materials; their effect on design, manufacturing time, cost and design flexibility.
- The use of active and passive systems to improve position stability.
- The selection of higher specification commercial components, their integration and testing.
- What design methods can be adopted to reduce design time but increase performance.
- What research and development should be monitored and when should it be adapted.

# Chapter 2. Scientific requirements and challenges

## 2.1 Science at the nanometre scale.

Over the past few years there has been a explosion of research and interest in so called nano technology. This covers a wide range of science and technology. New electronic devices are being developed with ever smaller features and the demand for higher storage density is leading to developments in the understanding of magnetism at the nanometre scale. Nano particles are being developed which will deliver cancer gene therapy drugs to specific parts of the body. A better understanding of fluid flow at the nano metre scale is essential for development of a wide range of miniaturised diagnostic devices. Toxicology of nano particles is a big area of research as the behaviour of nano particles can be very different from micron sized particles.

## 2.2 Nano beamlines

With the ability to produce high intensity photons with wavelengths at the sub nanometre level, synchrotrons are seen as an essential part in materials research at the nano metre level. Some world leading synchrotrons are building hard X-ray beamlines suitable for research at the nanometre level.

### 2.2.1 APS

At the Advanced Photon Source (APS) at Argonne National Lab USA Beamline 26ID has been built by the Center for Nano Materials. The beamline is built for scanning microscopies with 30nm spatial resolution with additional full-field microscopy capacities. The instrument operates in the energy range of 3-30keV. The instrument aims for a wide field of applications based on its high sensitivity to elemental composition, crystallographic phase, and strain when applied at this length scale.

### 2.2.2 Soleil

The Soleil synchtron, located outside Paris, has a new beamline called Nanoscopium. Nanoscopium aims for diffraction and spectroscopy on the micro- and nano-length scale. A long straight section will host two canted undulators providing beam for a

micro/nano scanning microscopy station and for tomography. For scanning microscopy it is planned to use an 20mm period undulator insertion device in a modified straight layout, similar to I13 at Diamond. A pre-focusing mirror will be used to generate a secondary source (at 38m distance) and the beam will be further de-magnified with a Kirkpatrick Baez mirror system located about 80m from the source.

### 2.2.3 ESRF

The ESRF are undergoing a major upgrade and some of the beamlines are being upgraded suitable for nano research. The requirements for science at the nanometre scale has been examined by the staff at the European Synchrotron Radiation facility (ESRF) and has been incorporated into their upgrade programme. The scientific requirements came from the European White Book on Fundamental Research in Materials. They identified the following keys areas:

- Single objects at surfaces and interfaces, such as in microelectronic devices and magnetic nano dots.
- Soft condensed matter and biological systems such as microfluidics; toxicology of nano particles; nano materials and nano devices for therapeutics and drug delivery systems.
- Hard materials including nanocrystallisation.

The type and size of materials can be wide ranging and there is also the requirement to study these materials in environmental chambers such as high or low temperatures, high pressure, wet cells, in vacuum or in air.

Beamline ID13 may be counted to be one of the first upgraded beamlines at the ESRF. The beamline has been operational since 2008. Originally designed to perform SAXS experiments recently a new extension has been built annex to the main ring building. This is a station where the coherent diffraction results have been reported claiming a 10nm spatial resolution. Beamline ID22 NINA will have two branches: nano-scale imaging (NI) and nano-scale analysis (NA). The NI branch aims for a spatial resolution of <20nm, but at fixed wavelengths without spectroscopic capability. The priority for

the NA branch is XAS spectra over 1000 eV with signal to noise sufficient for structural analysis. It will not achieve a spatial resolution better than 1µm.

### 2.2.4 NSLSII

NSLS II is a synchrotron which is currently being built at the Brookhaven National Lab in the USA. This will include two hard X-ray nanobeamlines for submicron resolution X-ray spectroscopy, with a target beamsize from 1 micron to below 100 nm and a non-scanning beamline hard X-ray nanoprobe with an ultimate target beamsize of 1 nm. The latter will use multi-layer Laue lenses which are being developed at Brookhaven.

### 2.2.5 PETRA III

At Petra III in Hamburg the Hard X-ray Micro/Nano-Probe beamline P06 will provide advanced visualisation by micro/nano analysis using different X-ray techniques: X-ray fluorescence (XRF), X-ray absorption spectroscopy (XAS), X-ray diffraction (XRD), imaging (absorption, phase contrast) and various tomographies. Use will also be made of the high degree of coherence of the beam.

### 2.2.6 Spring 8

The synchrotron Spring 8 in Japan has beamline BL20XU. This beamline is used for a wide range of experiments: microbeam, scanning microscopy, imaging microscopy, holography, phase-contrast micro-tomography, interferometry, ultra-small angle scattering, etc. An in-vacuum undulator and a DCM deliver light up to 113 keV to two hutches: at 80m and at 245m from the source. The second station is in a Medical Imaging Centre. This beamline has been used in the past to test new optics and minimal spot sizes (FZP <100nm in 2002 and more recently nano-focus with KB mirror systems) have been achieved there. In addition, the spring-8 synchrotron and Ritsumeikan University have established a centre for synchrotron radiation nanoscience and their research fields are nano-characterisation and Analysis and Nanofabrication. Spring 8 also has a 1Km long beam line which is used to create small, fully coherent beams.

### 2.2.7 ANKA

The team at the ANKA synchrotron in Germany are working in the field of Nano and micro-technology which has included investigating the quantum size effects in Bismuth nano wires, development of polymer X-ray lenses using deep X-ray lithography, manufacture of micro gears with heights from 100µm to 3mm and research into the crystal structure of large paramagnetic polynuclear metal aggregates. The high resolution beamline NANO is under construction at a superconducting undulator source. NANO is dedicated to high resolution X-ray diffraction and surface / interface scattering with the focus on in-situ and ex-situ structural characterization of thin films and multilayers (amorphous, polycrystalline or single crystalline) of metals, oxides, polymers, composites and magnetic systems.

### 2.2.8 Diamond

Diamond have a test beamline which is used for development and testing of new devices and experimental methods. This has been used to test many new types of focussing optics and has been able to produce beam sizes of about 160nm. Some of the systems tested at B16 have been used on the I18 Micro diffraction beam line where beam sizes of 70nm have been produced. Diamond are currently commissioning a double beam line called I13- X-ray Imaging and Coherence. This beamline is 250m long and allows both direct imaging and coherence experiments. Another long length beamline, I14 Hard X-ray nano probe is currently in the early stages of design.

## 2.3 Focussing optics

An essential part of any nano focus beamline are the focussing optics. There are a number of focussing systems available, each of which has advantages and disadvantages over the others. These use diffraction, refraction or reflection effects to focus the X-rays.

### 2.3.1 Kirkpatrick-Baez mirrors

X-rays are can be reflected from dense polished surfaces at low grazing incidences. In the Kirkpatrick-Baez (KB) scheme two elliptical mirrors set perpendicular to each other are used to focus a beam in two directions. The main technical challenge to achieving

nano focussed beams is fabricating perfectly elliptical surfaces with figure error of much less than 1µRad and surface roughness of the order of Angstroms. X-rays can be reflected from a dense polished surface at very small angles so mirrors tend to be long and narrow. A shorter mirror will collect less photons so intensities are less, so the design is a compromise. Focussing distances from the final mirror must be at least half the mirror length and so final focusing mirrors have tended to be of the order of 100-300mm long. This means that the focussing optic assembly is of the order of 300-700mm in total length. The mirrors are mechanically bent to produce an elliptical shape by applying different bending moments at each end of the mirror. Motions are also required to move the mirrors into the beam.

The smallest spot size achievable is determined by the diffraction limit which is the ratio of radiation wavelength to numerical aperture. At the moment this has never been achieved because the mirror polishing has not been good enough. At the ESRF they have used a 170mm and 92mm long mirror pair (Figure 1) to produce a beam of 86 x 83nm (Hignette, 2005).They have used a multilayer on the first mirror to provide energy selection so a normal Double Crystal Monochromator is not required.

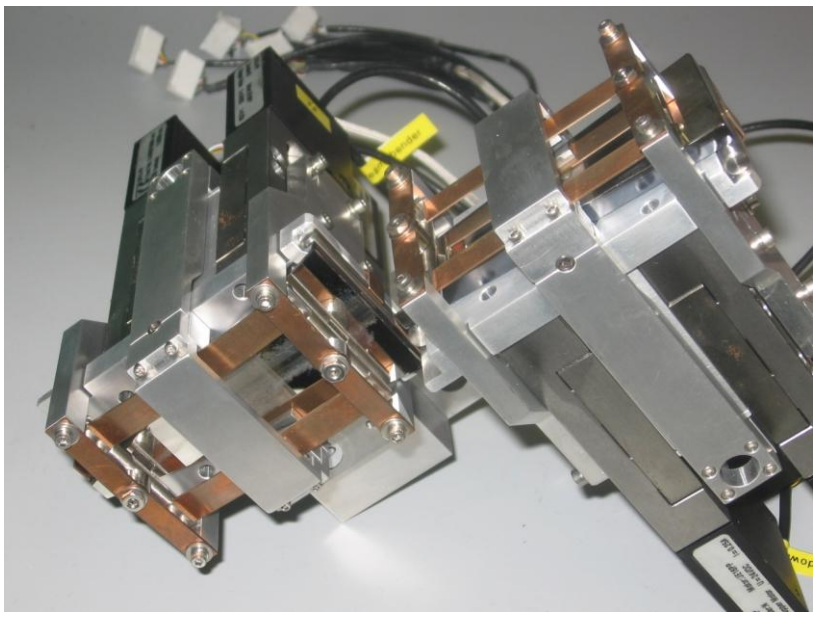

**Figure 1 – KB Mirror system**

KB mirror systems are widely used as focussing optics for both microfocussing and nano focussing optics. Recent developments in polishing mirrors using numerically controlled local wet etching (Yamamura, 2008), and elastic emission machining have enabled so called super polished mirrors to be fabricated and these have been used to produce beams of 25 x 30nm at the spring-8 1 Km long beam line (Mimura, 2009) and to 1nm using multilayer coated mirrors (H Mimuraa, 2011)

A variation of the KB mirror system is the Montel system. Here the two elliptical mirrors are positioned side by side and perpendicular to each other. This arrangement enables shorter focussing distances and the system is more compact. Recent tests using this type of mirror have achieved a spot of 150nm (L Wenjun, 2010). The team at Argonne believe 40nm is possible with improved mirror quality, thermal and mechanical stability of the focusing system.

### 2.3.2 Refractive lenses

#### 2.3.2.1 2D beryllium lenses

An X-ray lens is composed of one or more thin concave lenslets lined up in a linear array. Although the focussing effect of one lenslet is small, by adding many, up to 100, a focal spot can be obtained at reasonable working distances down to about 0.1m. The focal distance f for an X-ray lens array is given by the thin lens limit as:

$$f = \frac{R}{2N\delta}$$

Where R is the lenslet radius, N is the number of lenslets and δ is the index of refraction. To minimise absorption of X-rays, lens material is comprised of low atomic number materials such as Li, Be, Al, Mylar and PMMA. The most common materials are Beryllium and Aluminium.

The lenslets are mounted in a precise alignment frame sometimes located in small sealed enclosure so that the lenslets can be operated in a partial vacuum or an inert atmosphere of Helium.

The enclosure can then be mounted on a motorised stage. The alignment frame often has a set of secondary holes that are parallel to the lens axis and this is used to align the lenses to the beam. The motorised stage therefore needs to have pitch, rotation, vertical and transverse motions. This type of lens has been developed by the physics department at Aachen University in collaboration with the ESRF.

A typical beryllium lens assembly with a 1m focal length has 117 lenslets for focusing 20KeV and has an effective Diameter of 557µm. 2D lenses are extensively used for micro-focussing optics but not so much for nano-focussing.

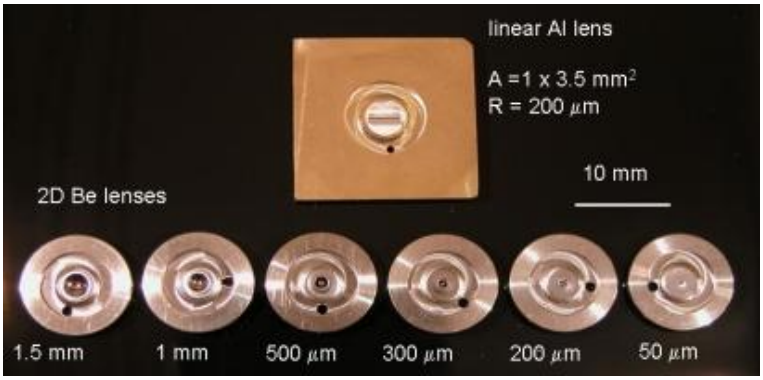


**Figure 2- 2D lenses produced at Aachen**

**(www.physik.rwth-aachen.de)**

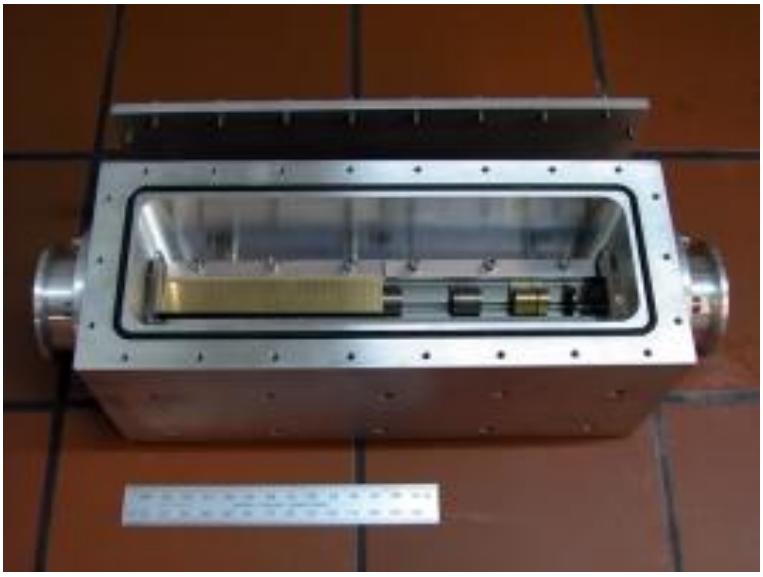

**Figure 3 - lens holder 1D lenses**

**(physik.rwth-aachen 1, 2012)**

To produce focussed beams of below 100nm with 2D lenses the beamline would need to be extremely long. To generate sub 100nm spots on normal beamlines of the order of 30-60m in length the lenslets would need to have an extremely small radius of curvature and this is not possible with the 2D lenses. An alternative approach is to use micro-fabrication techniques to generate planar lenses in Silicon. The Aachen group (C Schroer, 2003) have developed planar parabolic lenses and using two lenses in crossed geometry a microbeam of 380nm x 210nm at 25KeV was generated at 42m from the source in an experiment at the Swiss Light Source, and now routinely used for Petra's P06 nanoprobe beamline.

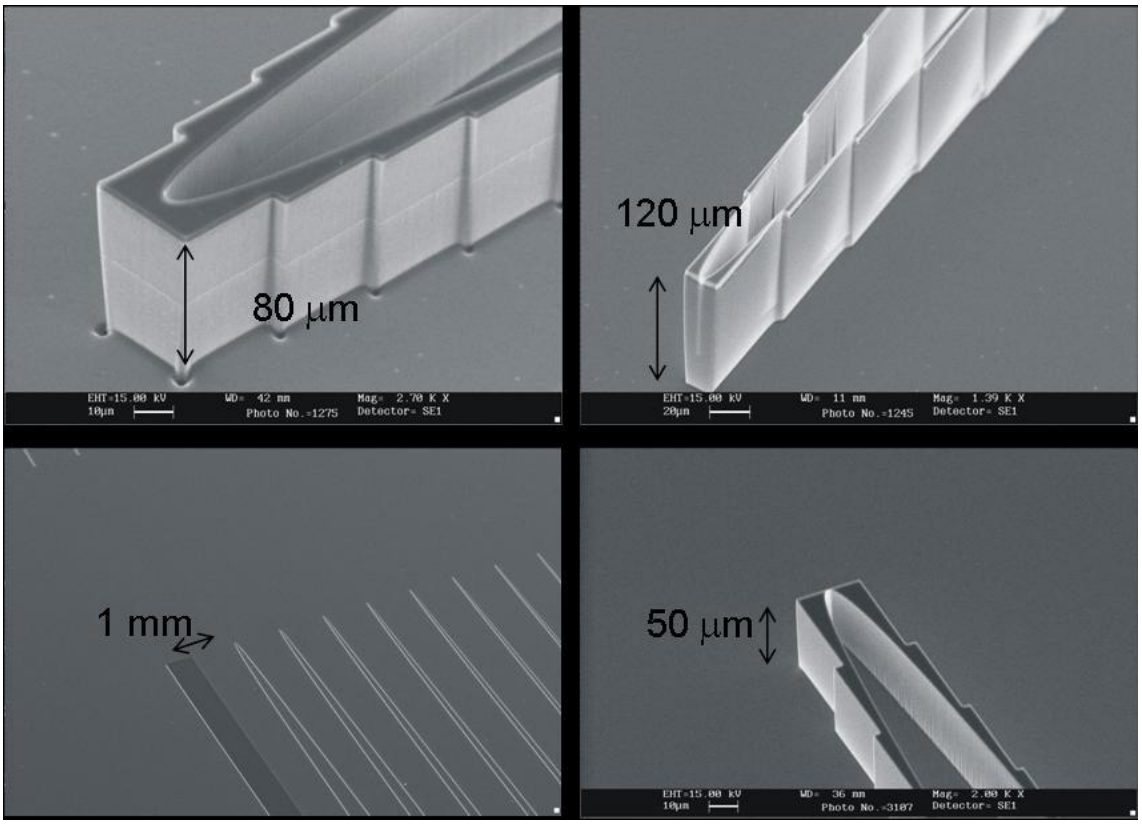


**Figure 4 - Silicon cuniform lenses**

**(diamond, 2012)**

Another type of 1D lens has been developed at Diamond and are kinoform lenses manufactured from Germanium and Silicon (Alianelli, et al., 2009). These provide low absorbtion and give a large effective aperture.

### 2.3.3 Fresnel Zone plates

A fresnel zone plate consists of a substrate such as silicon or silicon nitride, overlaid with a radiation absorbing material such as gold or tantalum. The gold or tantalum is removed by electron beam writing a resist and then etched to produce a series of concentric rings. The spacing between the rings reduces as the diameter increases such that the distance to the focus point is a wavelength every second ring. The zone plate acts as a diffraction grating and if the spacing between gold rings is correct constructive and destructive interference occurs so that the X-rays are focussed at a point.

For high energies the absorber material should be thick but as the separation between rings is small this gives high aspect ratios and these are difficult to fabricate. The separation also reduces as the diameter increase and so the problems in creating very small resolutions limit the outer diameter.

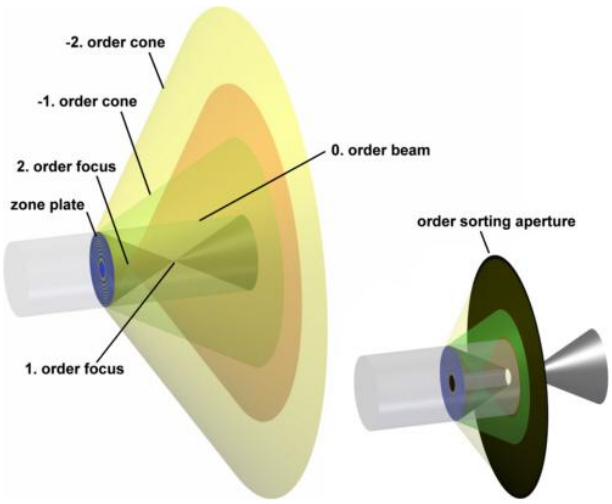


**Figure 5 - Fresnel zone plate and Order sorting aperture**

**(x-ray-optics 1, 2012)**

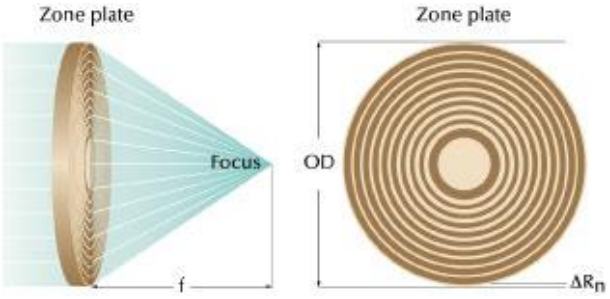


**Figure 6 - Schematic of a Fresnel zone plate**

**(xradia, 2012)**

One issue with zone plates is the problem that if the phase of the X-ray at the outermost zones is not in phase with that hitting the central zones then destructive interference occurs and this limits the efficiency of the zone plate. A measure of this is the coherence length and this should be larger than the zone plate aperture. Despite the difficulties in making zone plates, particularly for higher energies, zone plates are still the most commonly used system for producing nano focus beams.

### 2.3.4 Multi layer laue lenses

A team at Argonne, who have now moved to Brookhaven National Laboratory are developing multilayer laue lens which have the potential to focus to below 1nm (Kang, 2006). These are 1 D structures so 2 lenses are required to produce a 2D focussed spot. The lenses are produced by 1,000s of alternate layers of $WSi_2$ and Si layers. The work is continuing and some test work has been done at the B16 Test beamline at Diamond by the team from Brookhaven. The focussing distances are very small, a few mms and so both lenses, an order sorting aperture and the sample need to be close together complete with suitable holders and devices for alignment and sample scanning.

### 2.3.5 Capillary tubes

Tapered glass capillaries have been used in conjunction with other focussing mirrors to produce 50nm spatial resolution.

In mono capillary optics X-rays are guided in a single glass capillary by total internal reflection. The inner side of the mono capillary has an elliptical or parabolic geometry. The source is located at one of the two focal points of the ellipse. The light is

redirected to the second focal point in case of the elliptical geometry and is collimated in case of the parabolic geometry. Focusing an incoming beam parallel to the optical axis is also possible. In both cases the light undergoes a single reflection at the inner side of the mono capillary.

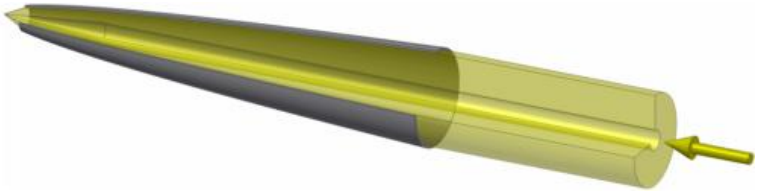

**Figure 7- Mono capillary tube**

**(x-ray-optics 2, 2012)**

Tapered capillary optics consists of a slightly conical tube with very smooth inner surface. The maximum cone angle is limited by the maximum angle of total internal reflection for the material and photon energy used. The incoming light is reflected one or more times at the inner surface of the tube, mostly by total external reflection in a glass capillary, but other materials would be fine as well. There is no precise focus point, more like a line of increased intensity along the optical axis. These optics are simple, but have the disadvantage of providing very small working distances and do not have any imaging qualities.

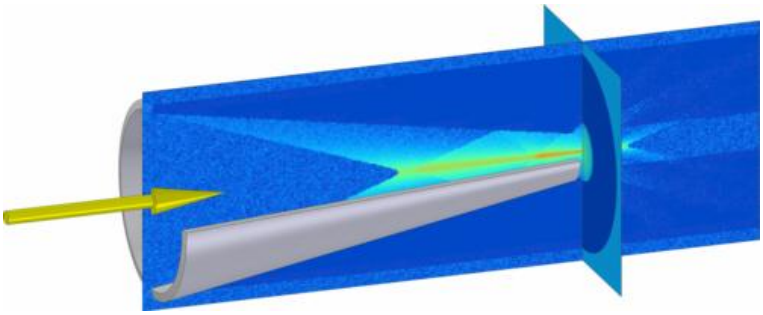

**Figure 8 - Tapered capillary tube**

**(x-ray-optics 3, 2012)**

### 2.3.6 Waveguides

If light material is deposited on a heavy material X-rays can penetrate the light layer but be reflected by the heavy layer, if the angles are below the critical angle. When the

X-rays leave the surface of the waveguide the beam is focussed. Some have developed Beryllium/ Molybdenum waveguides (A Lagomarsino, 2002) and a team at the Institut für Röntgenphysik at the Universität Göttingen have fabricated using electron-beam lithography polymethyl methacrylate (PMMA) coated silicon waveguides with a cross section of 30 × 70-nm cross section and 4-mm length. These provide fully coherent beams but the working distances are extremely small. Though they have been used for a few specific experiments they are unlikely to be used as a routine optics on a nano focussing beamline.

### 2.3.7 Diffraction limit

The minimum focussing size is limited by diffraction effects. The diffraction limit is defined by the Raleigh criteria which for a circular aperture is

$\Theta = 1.22 \times \lambda / D$

$\lambda$ is the wavelength and D is the Aperture.

The resolution for a Zone plate with a focal length of 50mm an aperture of 100µm with a 50µm source at 50m at 10KeV.

$\lambda$ = hc/E, h = planks constant 4.135 x10-$^{15}$eV/s, c = speed of light in a vacuum 3 x10$^{8}$ m/s.

$\lambda$ = 4.13510-$^{15}$ x 3 x 10$^{8}$ / 10,000 = 0.12nm

Diffraction limited size (d1) = 1.22 x $\lambda$ x f / (2 x D) = 1.22 x 0.12nm x 50 x 10-$^{3}$/(2 x 100 x 10$^{-6)}$ =36nm

Image size (d2) = 50 µm x 50 x10$^{-3}$/50 = 50nm

Diffraction limited image = = = 61nm

### 2.3.8 Summary of focussing optics

There is a wide variety of focussing optics available. Some, such as zone plates are small and need to be moved by small actuators and some such as KB mirrors require much larger actuators. However in most cases adjustment in pitch , yaw, vertical and

two horizontal directions will be required. In the case of 1D focussing systems there will need to be systems for both lenses and the order sorting aperture. Devices with very short focal lengths will offer limited space for the adjustment mechanics and sample environments. The choice of focussing optics will depend upon the experimental technique adopted, source distance, beamline length, source characteristics and sample environment.

## 2.4 Types of experiments suitable for nano focus

### 2.4.1 Nano diffraction

X-ray diffraction usually uses large beams which give structural information that is the average over many polycrystal grains. But with high intensity, small sized beams information such as the local lattice structure, crystal orientation, grain morphology and strain tensor can now be obtained over local microstructures. Examples of some recent diffraction experiments are as follows

- X-ray Nanodiffraction on a Single SiGe Quantum Dot inside a Functioning Field-Effect Transistor. (Hrauda, 2011)
- High-sensitivity strain mapping around epitaxial oxide nanostructures using scanning X-ray nanodiffraction (Tao Sun1, 2011)

Beamline ID13 at the ESRF is currently being upgraded to be able to perform micro and nano-diffraction. The nano hutch is located 100m from the source. it consists of a granite structure and gantry systems with a vertical axis goniometer stage, 2D detector and the option to change optics using a removable optics support system. The environment is temperature controlled to ±0.05 °C over 8 hours. (C Riekel, 2010). Nano diffraction beamlines are in operation at 26-ID-C at the APS and are also being built at ANKA, DESY and Diamond (I14).

### 2.4.2 Micro fluorescence

When a material is exposed to X-rays the material can eject an electron from a low orbit. An electron from a higher orbit then fills the gap and the loss of energy is released as a photon. Thus the material emits a photon who's energy is characteristic

of the atom. This is called fluorescence. Induced X-ray fluorescence reveals the spatial distribution of individual elements in a sample. In energy dispersive analysis a detector is used which produces pulses of which the voltages are proportional to the energy of the detected photon. These are often mounted at about 90 degrees to the beam axis and the distance from the detector head to the sample is usually variable.

Examples of detectors are as follows

- Bruker SOL-XE Li-drifter silicon drift sensor Cooling using a peltier
- Ortec Germanium detector cooled by Liquid Nitrogen
- SII Nano Technology INC. Vortex –EX, Silicon drift detector using peltier cooling

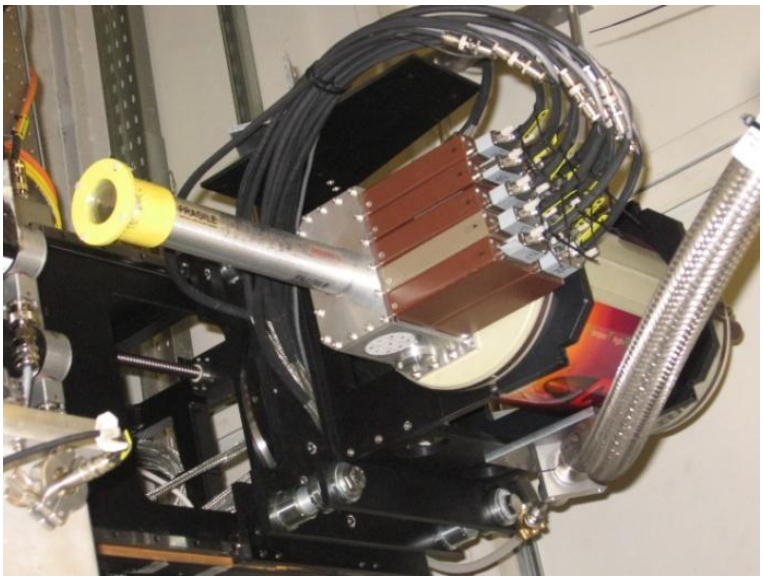

**Figure 9 - Mulit element germanium detector used at B18 Core spectroscopy beamline at Diamond**

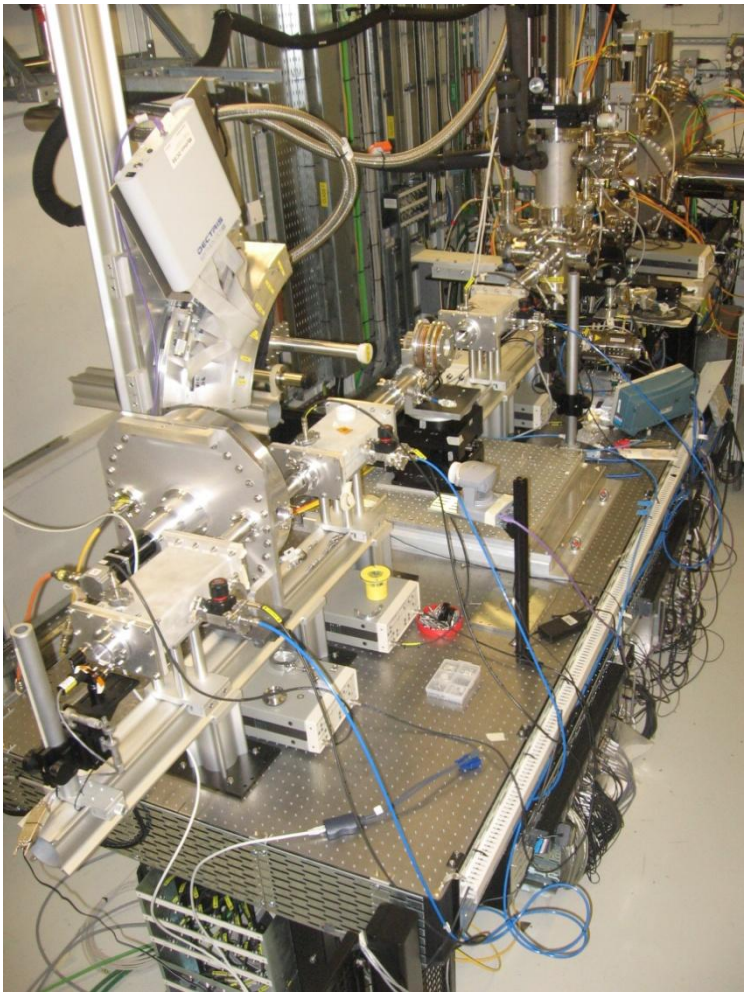

**Figure 10 – Example of fluorescence experiments**

An example of a fluorescence experiment is the High-resolution nanoprobe X-ray fluorescence characterization of heterogeneous calcium and heavy metal distributions in alkali-activated fly ash (J Provis, 2009).

### 2.4.3 Transmisive imaging

An image can be obtained of a sample by illuminating the sample with a large sized beam of X-rays and then using camera with a fluorescent screen. For small sized beams another method is to scan the image and then record the intensity of the X-rays after transmission through the sample and hence an absorption map can be obtained. To do this an intensity detector is required with a large dynamic range. This should be situated as close to the sample as possible.

### 2.4.4 Phase contrast imaging

Traditional X-ray imaging produces an image that shows the absorption of the X-ray source as it scans a sample. Phase contrast imaging uses a spatially coherent beam and a high resolution detector. As the sample is scanned across the beam different regions of the sample refract the X-ray beam and they undergo a phase shift and hence create constructive and destructive interference. These patterns enable high contrast imaging of the interfaces within the sample. The detectors do need to be a long way from the sample and the beam does need to be coherent and so this usually needs a long beamline. Phase contrast imaging is especially well suited for imaging soft matter or biological samples which no not provide much absorption contrast.

## 2.5 Technical challenges for a sub 100nm beam experiment station

### 2.5.1 Focussing distance

The beam size produced by a focussing optic is dependent upon the source size, distance of the optic from the source and the focussing distance. Synchrotrons like Diamond have most of the beamlines contained within the main building with distances from the source of about 40-50m. At Diamond there is space to build two longer length beamlines up to 300m long, and one of these called I13 is currently in construction. The source size for a Bending magnets beamline at Diamond is about 50µm(V) whereas on an insertion device beamline such as I13 the source size is 20µm. This means that to produce a 10nm spot on B16 at 50m the focussing distance needs to be about 10mm whereas on I13, because of the smaller source size and longer beamline length the focussing distance can be as much as 150mm. This makes is much easier to fit in sample holders and order sorting apertures.

For ID lenses and Multilayer laue lenses, two lenses must be fitted as well as the Order sorting aperture within the focussing distance. The focussing distance will also dependent upon the energy elected. So when changing energy the relative positions of the optics, Order sorting aperture and sample must be changed.

The laue and 1D lenses also need to be adjusted relative to the beam in pitch and yaw, as well as height and horizontally across the beam. The requirement for small focussing devices such as 2D lenses is for precise alignment motions within a small operating envelope.

### 2.5.2 Positional stability

Because of the small spot size the number of photons hitting the sample is small and so to collect enough data many experiments will require exposure time ranging from seconds to hours. If the relative position of the sample to the focussing optics is not stable then the beam will move out of focus or different areas of the sample will be illuminated during the experiment. In addition if the sample is vibrating relative to the focussing optics then a blurring of the focussed spot will occur with loss of resolution.

Lack of position stability due to vibrations or long term drift is therefore critical, but not all motions are critical. For example. A beamline consists of a fixed source a focussing optic and sample. For a beamline with a focussing optic at 50m from the source and producing a 100nm beam then the focussing distance is only 100mm from a 50µm source size. If the focussing optic and the sample are linked together, then any vertical motion relative to the source has almost no effect on the focussed beam spot size. In fact the focussing optic and sample have to move over 1m vertically to produce a 10% change in focus spot size! What is more important is the relative vertical motion between the focussing optic and sample, where 10nm motion would produce 10% change in spot size. It is therefore essential that the focussing optic and sample are as rigidly coupled together as possible to prevent relative motion.

### 2.5.3 Sample alignment

The sample will need to be positioned so that the required area of interest is being hit by the X-ray beam. For micro focus beams a common technique is to place a radiography paper at the sample stage and expose it to X-rays, the paper goes dark where it exposed. A camera with a microscope objective is then adjusted so that the cross hairs are aligned onto the centre of the dark spot on the paper. The paper is removed and the sample fitted. The sample is then moved until the area of interest is

on the cross hairs. For nano focus experiments this technique is not possible, the smallest feature visible using visible optics is at best 250nm and so to get any form of visible spot the beam would need to be defocused.

A simple method is to scan the sample and look for a characteristic signal of a feature that is near the centre of interest and then do a series of scanning experiments around that area.

An alternative would be to use a Atomic force microscope to identify the area of interest and measure the coordinates relative to a well defined object on the sample or its holder.

A method employed by Meyerheim (H Meyerheim, 2009) is to use an AFM tip aligned on the sample. The focussed X-ray beam is scanned across the sample and the X-ray signal of the nano objects is recorded resulting in a positional 2D map of the structures. When the X-ray beam hits the AFM tip, photoelectrons are emitted inducing a photocurrent which is simultaneously recorded, facilitating the alignment.

At the APS an Olympus LEXT confocal laser scanning microscope is being used (Beitra & Watari, 2010). This has resolution down to 120nm.

### 2.5.4 Sample scanning

The sample will need to be moved across the focussed beam. A common procedure is to implement an automatic programme that moves the sample to a position, opens the shutter to expose the sample, collects data from the detectors, closes the shutter and then moves the sample to the next position. Data can then be collected quickly and a defined area of the sample tested automatically. The time taken to do a single sample depends upon the exposure time, number of position and the time taken to move and settle the sample at its new position. Users will require the option of determining the step size moved by the sample and this may be very small. The stage used for the sample therefore needs to be able to move in very small steps both vertically and horizontally with a minimum of time. In addition the sample stage should be very stable so that the sample is not moving during an exposure. Many nano focus

optics collected and focus very few photons and so the exposure time can be much larger than micro focus experiments.

### 2.5.5 User sample mounting

There a wide range of samples that users will bring to a beamline, sometimes these will be pre-mounted on a sample holder, other times they will need to be mounted at the beamline. Some users will test samples at a variety of beamlines and so there can be a desire to have a common mounting system for similar beamlines and experiments. Much beam time can be lost in adapting sample holders and mounting samples so it is important that the user is aware of the mounting arrangements before they come to do the experiments. Important information is for example the nominal beam height from the sample holder base and the space volume available for the sample.

### 2.5.6 Detector integration

The type of detector, its orientation and position is dependent upon the experimental technique adopted. Some of the detectors can be physically quite large, some users will require detectors to be moved either during a scanning experiments or between experiments. The movement can be changing the distance from the sample to the detector, usually along the beam axis, or by changing the angle of the detector face to the beam axis. In many cases experiments will require multiple detectors to be used. The users will therefore want an experimental station where detectors can be changed easily and their position adjusted remotely. Generally the stability and positional accuracy for the detector is not as critical as the relationship between focussing optics and sample.

### 2.5.7 Alignment and diagnostics

Alignment is not a simple task and unless a logical alignment procedure is adopted much time can be wasted in finding the beam and optimising the shape and focal point.

Often the first stage is to remove any final focussing optics from the beam, opening up the beam defining slits and checking that an X-ray beam is present. A fluorescent screen imaged by a camera can be used. The visual image then gives confirmation of the beam and shows its shape. The beam size and position is defined by a set of slits and these are then adjusted to give the correct size.

When X-ray lenses are used the assembly often has an alignment hole offset from the lens axis. The lens assembly is then brought into the beam and moved until the alignment hole is positioned to allow the X-ray beam to pass through. The lens assembly is then adjusted in pitch and yaw until a perfectly round image of maximum size is produced. The X-rays lens is then translated by a defined amount and the X-ray lenses should then be aligned with the X-ray beam.

The focussed beam is then too small to be seen by a normal screen and camera. A fluorescent screen and high magnification microscope can then be used such as that built by the company Optique Peter. The resolution is limited by the effective pixel size of the camera and the grain size of the fluorescent screen material.

The problem is then to find the focal point. If the microscope system is suitable this can be moved along the optic axis until the minimum spot size is found. If the beam is too small another method is to scan the beam with a gold wire mounted on a high resolution stage, measure the x ray absorption and hence determine the beam size.

Here a cross hair made from gold wire is scanned across the beam and the beam intensity is measured after the wire. As the wire traverses the beam the intensity will reduce to zero. By differentiating the signal a measurement of the beam size can be obtained. This is often quoted as the Full Width half Maximum (FWHM). A computer programme can be implemented that performs a scan, measures the FWHM and then increments the detector along the beam axis and then repeats the scan, and then the position with the smallest FWHM is the focal point.

This procedure thus requires a fluorescent screen and camera, a wire scanning device and an intensity detector. These have to be moved into and out of the beam and be

able to be positioned at the focal point which is where the sample would be. The wire also needs to be mounted on a precision scanning stage that can be moved both vertically and horizontally. If the beam size is 100nm then the step size for the wire needs to be at most 10nm. Instead of a gold wire a lithographic structure can be used..

At the ESRF beam size measurement is performed using a 38 nm thick gold layer sputtered on a polished vitreous carbon substrate. A 3 micron wide structure with Gaussian shape obtained by ion milling of the gold layer leaves a gold wire, which can be detected by fluorescence. At 9 mradS (0.5°) grazing incidence with respect to the carbon substrate, no reflection occurs from the carbon and the gold structure equivalent width of 26 nm (3,000 x sin 0.5). Both thickness and width of the wire combine into an equivalent wire with a FWHM of 45 nm. The gold nanowire is mounted on a lever based translation mechanism actuated by a stepping motor, with mean increments of 10 nm. The fluorescence signal is acquired by a silicon drift detector. Selecting the energy ranges of the gold *L*-edges, the response of the carbon substrate is negligible.

It is therefore important that the components can be removed fully from the X-ray beam so that a non focussed X-ray beam can be detected. This may require relatively large travel ranges. The focal point will be where the sample is located and by changing energy the focal length will vary and so the focussing optics will need to be moved along the axis. This again may require quite large movements

At the sample position a wire scanner with intensity detector, imaging camera and sample station will need to be exchanged and this will again require large travel motions with finer motions required of nm resolution in both horizontal and vertical directions.

### 2.5.8 Sample mounting and sample changing

Samples come in a variety of shapes and sizes. Protein crystallography samples are often mounted on a wire loop attached to a standard magnetic holder such as the Hampton mount. These are held in a carousel inside a liquid nitrogen dewar to

maintain their crystalline state. A small robot arm is then used to remove the samples from the dewar and place them onto the stage on the beam axis.

**Figure 11 – Hampton Research mount**

**(hamptonresearch, 2012)**

In some earth science and solid state physics research samples are tested at very high pressures. This can be done using a diamond anvil cell. Here the sample is mounted between two diamonds which are pushed together by a screw thread system.

For nano focus beamline one of the problems is the limited space. To produce small beam sizes the final focussing element has to have a short focal length and if zone plates are used an order sorting aperture has to be positioned between the sample and the zone plate. This reduces the space further. In some cases the size of the sample mount will limit the amount of demagnification possible. The sample and its mount must be also be very rigid to prevent movement. Clamped or magnetic chuck solutions will be required in most cases and so the use of small mounts with M1, M1.6 and M2 screws is expected to become normal. Magnetic fields from sample holders may however create problems for some experiments so this may have to be taken into account.

With limited space changing samples becomes an issue. The user must be able to remove the sample but without damaging or affecting the position of the focussing optics. One option is to have an automatic sample changer. This could be a

manipulator that can replace the sample using a pneumatic or motorised set of fingers that are mounted on an arm that is moved on a motorised stage. The user could mount a set of samples on a carousel that could be placed so that the manipulator can change samples quickly. In addition the temperature stability may be affected by the user gaining access to the sample area so again a remote controlled sample changer will help maintain thermal stability.

For remote placement of samples a pneumatic or magnetic chuck will be required. The sample mount could be on a kinematic mount to aid placement, many kinematic mounts are relatively large so a micro kinematic mount may be required. Hardened steel or carbide balls and cylinders are often used, such as from Bal-tec. The smallest cylinders available from Bal-tec are 4.7mm diameter. For precise location the kinematic mount should be preloaded but if this is a strong permanent magnet then the force to pull off the sample mount would be large and subject the sample mount stages and manipulator to large forces, applying any sort of holding down screw system would be difficult. An alternative would be a pneumatic clamp. Small pneumatic pin type cylinders are available but a compressed air supply would be required and the compressed air lines will be difficult to manage in a small space. Clippard Instrument Laboratory Inc manufacture sub miniature cylinders, an example is the SM-2, this has a bore of 4mm and a stroke of 6mm but is still 19mm long. MC produce a pneumatic actuator, type CJP, with a bore of 6mm,stroke of 5mm and length 16mm.

An electromagnet is another possibility as long as it could be made compact enough. Shape memory alloys can also be used as actuators, in this case heating the alloy using ohmic heating can change the material from one crystal structure to another and its shape changes, this could then act as a device to lock the sample stage into position. NiTinol (54%Ni, 46%Ti), is one example of a shape memory alloy and this has a transition temperature in the range 20-30°C at which point it changes phase from Martensitic to Austenitic. The problem with this is that to operate the device heat

must be applied and this does not help with thermal stability. Another alternative would be to use a voice coil actuator to operate a holding down clamp.

### 2.5.9 Integration into existing beamlines

A nano focus system could be designed into the beamline at the start but it would also be desirable to upgrade existing beamlines to be able to perform nano focus experiments when required. The question about when this is required is an important issue. Not all experiments require very small beam sizes so it would be desirable for the nano focus equipment to be portable and easily installed and removed.

To prevent accidental radiation exposure to staff, synchrotrons have a well defined safety system. This system includes the requirement for an experiment hutch to be searched by a single person. To ensure the search is thorough a series of search buttons are located around the hutch and these must be pressed in a specific order within a certain time during the hutch search. There is therefore a desire that equipment is designed so that there are no hidden spaces which cannot be searched easily and thoroughly. A nano focus end station should therefore not be fully enclosed with internal volumes large enough for a person to hide and escape detection.

To install equipment with the experimental hutches many are fitted with removable roof sections so that equipment can be lowered in with a large overhead crane. Once the roof panels are removed some of the ventilation equipment may need to be removed and indeed the removable roof sections may not be in the same position as the desired position for the nano focus end station. Access should therefore be assumed to be via the doors which for an experimental station normally include a set of double leaf doors. This restricts the width of a nano focus station to be about 1.2m wide. Most experimental hutches have a crane which is either 500Kg or 1 Tonne. This can then be used to lift the nano end station into position. The end station will have a significant number of motorised axis, some beamline will have spare stepper motor motion axis complete with controllers but the nano focus end station may be fitted with other types of actuator such as piezos and linear motors. The end station should

therefore come complete with its own controllers for all the axis including position encoders.

Beamlines are cramped and there is not often any space to fit a complete new end station. The nano focus end station will often have to be fitted into an existing station. Some components could be removed but often the support structure such as a granite table or diffractometer cannot be removed. This means that the nano focus end station needs to be low in height so that it can sit on an existing station.

Each beamline will have its own range of detectors which may have its own mounting system. Some detectors can be borrowed from other beamlines but these will also need to be positioned and may be adjusted remotely. Diagnostic devices such as a wire scanner and camera system will also need to be provided along with their controllers.

# Chapter 3. Thermal stability

## 3.1 Thermal stability issues

Experiments may often be performed with exposure times of some hours. The position of the X-ray beam on the sample could change because of changes in temperature and the subsequent motion because of thermal expansion of the supporting structure. This section examines some methods of counteracting these effects.

## 3.2 Low thermal expansion materials

Using materials with low coefficient of thermal expansion (CTE) can help reduce the effects of temperature variation upon positional stability. Aluminium alloy 6082 is a commonly used material and has CTE of 25 x $10^{-6}$ /K. For a temperature change of 0.01° C over a length of 300mm, the change in length would be 0.01 x 300 x $10^{-3}$m x 25 x $10^{-6}$ = 75nm. For positioning 1nm sized beams, this variation is considerable even with good temperature stabilisation. So changing to low CTE materials may be beneficial. Some low CTE materials are discussed below.

### 3.2.1 Glass ceramics

There are a number of glass ceramics such as Zerodur TM (Schott), Clearceram-Z TM (Ohara corporation) and ULE $^{TM}$ (Corning). Manufacturers offer different grades with CTE's ranging from 0 ± 0.10 x $10^{-6}$ /K to 0 ± 0.02 x $10^{-6}$ /K in the temperature range 0° to 50°C. These materials are typically used for optical instrument mirrors as they can be cast into large slabs and polished to a high level of flatness with no grain structure. The Hubble space telescope primary mirror, as an example, is 2.4m in diameter and is constructed of Corning ULE in a honeycomb shape and weighs 826Kg.

Although these special low thermal expansion glasses are often used for optical mirrors, they are not ideal for most precision engineering parts. The material is expensive, has low stiffness, easy to chip or break and has a long lead time for large pieces. The materials are usually ground to shape but can sometimes be machined using water jet cutting techniques. Parts can also be joined together to form more

complex parts by diffusion bonding techniques. However these processes are still slow and very difficult and so the resultant parts are expensive.

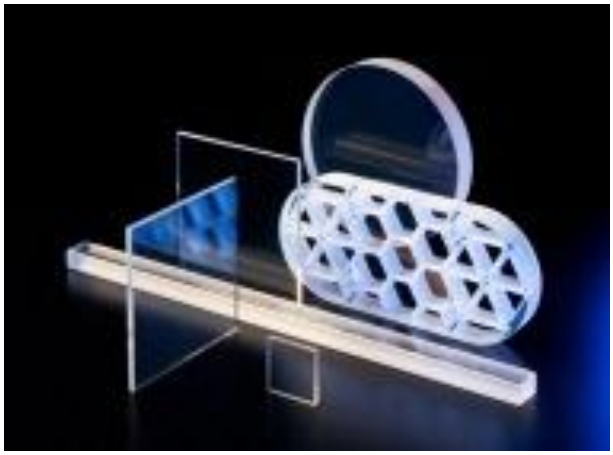

**Figure 12– Water jet cut Corning ULE parts**

**(oharacorp, 2012)**

Glass ceramics are also used for high accuracy linear encoder scales. Numerik Jena offer encoder scales manufactured from Robax ™ . Robax ™ is manufactured by Schott glass and has a quoted CTE of $0 \pm 0.5 \times 10^{-6}$ /K between 20 and 700°C. It is available in sheet form 3mm or 5mm thick.

Heidenhain offers a Zerodur ™ scale, this can be clamped and secured with silicon adhesive or be cemented to a special steel carrier.

Sony corporation manufactures an encoder system called “laser Scale” and this uses a scale made from Neoceram ™ which is produced by Nippon Electric Glass. Neocearm™ is offered in three grades, N-0 (Transparent), N-11 (White) and GC-190 (Semi transparent black). N-0 has CTE of $-0.04 \times 10^{-6}$ /K between 0 and 50 °C.

Renishaw offer a glass encoder scale but this is not a low expansion glass as the CTE is $8.5 \times 10^{-6}$ /K.

| Trade Name | Manufacturer |
|---|---|
| Zerodur | Schott Glass |
| Robax | Schott Glass |
| Clearceram | Ohara corporation |
| ULE | Corning |
| Neoceram | Nippon Electric Glass |

**Table 2 - Low expansion glass ceramics**

There are a range of machine able glass ceramics such as Macor® (Corning) and Shapal M Soft ®(Tokuyama Soda), generic machinable Aluminium Nitride and Duratec 750. They are not very low CTE materials but they are lower than most metals.

| Trade Name | CTE (x $10^{-6}$ /K) |
|---|---|
| Macor | 7.4 |
| Shapal M Soft | 4.4 |
| Machinable Aluminium Nitride | 4.5 |
| Duratec 750 | 6.6 |

**Table 3 – CTE of machineable ceramics**

Macor® and Shapal® is manufactured in slabs of about 300mm x 300mm x 50mm and costs of the order of £8,000 per slab. Shapal® does have a much higher thermal conductivity than Macor®. 1.5 W/mK and 90 W/mK respectively.

### 3.2.2 Sialon

Sialons are ceramic alloys based on silicon, aluminium, oxygen and nitrogen. They are mainly used where strength and wear resistance is required at high temperatures. Some Sialons have been developed with low CTE and high stiffness. These can be machined before sintering. S140 Sialon (Krosaki Harima) has a CTE of 1.3 x $10^{-6}$ /K at 23°C. Sialons can be machined in the green state to a near net shape before sintering, they can also be bonded to each other by a silver brazing method.

### 3.2.3 36% Nickel iron alloys

An iron alloy with a low coefficient of thermal expansion was invented in 1896 by Charles Edouard Guillaume. It was named “invar” because of its “invariable effect”. A number of companies produce a low CTE alloy with about 36% nickel. Each company has trademarked their own name for this alloy.

| **Trademarked Name** | **Manufacturer** |
|---|---|
| Invar 36 & super Invar 32-5 | Carpenter Technology Corp |
| Pernifer 36 | ThseenKrupp-VDM |
| Invar, Inovar, Microvar & Inovco | Arcelor Mittal |
| Nilo 36 | Special Metals Corporation |

**Table 4 - 36% nickel/iron alloys**

These alloys are designed to have a zero CTE at 20°C with the CTE increasing above this temperature. Typical quoted values are between 0.6 and 1.4 x $10^{-6}$ /K between 20 and 100°C. Super Invar which is manufactured by Carpenter Technology has a coefficient which increases at a lower rate than Invar 36 ™, as shown in Figure 13. Heat treatment is required to obtain the best stability from these alloys.

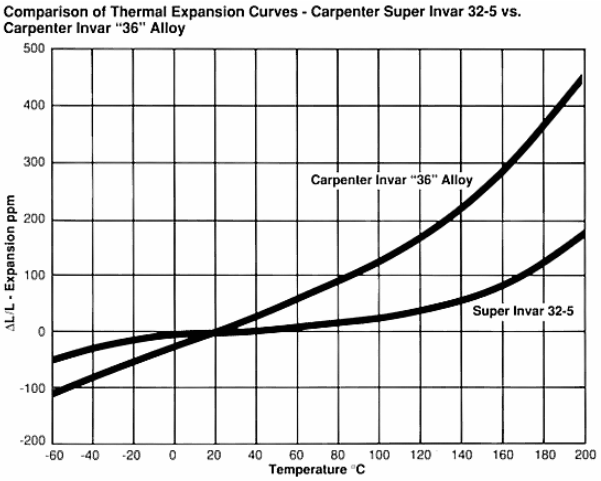


**Figure 13–CTE of Invar™ and Super Invar™**

**(hightemp, 2012 )**

Renishaw offer some of their encoder scales manufactured from a 36% nickel alloy and quote a CTE of 0.6 x $10^{-6}$ /K between 0 and 30°C.

### 3.2.4 Metal matrix composites

Metal matrix composites consist of continuous or discontinuous fibres, whiskers or particles embedded in a metal. These materials offer enhanced properties, such as higher fatigue strength and low weight or increased wear resistance or higher elevated temperature strength. Initially the aerospace industry were the main driving force behind their development, but these materials are now being used in automotive parts and for thermal management of electronics.

Manufacture of these materials is by a variety of methods including casting, powder metallurgy or diffusion bonding. The demand for metal matrix composites with low thermal expansion seems to only come from the space industry. The high-gain antenna boom for the Hubble space telescope, for example, was made with a diffusion bonded sheet of P100 graphite fibers embedded in 6061 Aluminium. The quoted CTE in one direction was -0.49 x $10^{-6}$ /K.

Each application has required the optimisation of different parameters and so materials tend to be developed for each specific application. Therefore, there are not many Metal Matrix Composites readily available as stock materials. However Advanced Metal Composites at Farnborough do offer the some materials from stock as listed in Table 5.

| Material Type | AMC Grade | CTE (x $10^{-6}$ /K) | General properties |
|---|---|---|---|
| Silicon Carbide Particle Reinforced Aluminium Alloy | AMC225XE | 15.5 | high tensile modulus |
| Silicon Carbide Particle Reinforced Aluminium Alloy | AMC640XE | 13.4 | good static and fatigue strengths |
| Silicon Carbide Particle Reinforced Aluminium Alloy | AMC217XE | 16.8 | high tensile modulus, good strength and fatigue strengths well in excess of high performance aluminium alloys, whilst retaining good ductility and formability |
| Boron Carbide Particle Reinforced Aluminium Alloy | AMC220BC | Not specified | high tensile modulus |
| Aluminium-Silicon Alloy | AMC4632 | 16.1 | excellent fatigue resistance at ambient and elevated temperatures |
| Aluminium Alloy | Calidus XM | 20 | High strength and fatigue performance at elevated temperatures |
| TiB2 Particle reinforced steel | Dynamis | Not specified | High hardness and good wear performance |

**Table 5 - Metal Matrix Composites available from Advanced Metal Composites Ltd**

There is limited availability of metal matrix composites and no commercially available materials with low thermal expansion. In Volume 3 of Comprehensive Composite materials, published by pergammon press in 2000, the section on metal matrix composites concludes as follows “It has been suggested that the thermal expansion of composites could be tuned within a wide range by proper tailoring of the mutual

arrangement of matrix, reinforcement and porosity, Experimental demonstration of this concept remains to be given."

### 3.2.5 Carbon fibre composites

Carbon fibre composites consist of a matrix of carbon fibres embedded in a resin matrix. The long length carbon fibres have a high tensile strength in tension and when supported in a resin a very lightweight, stiff and strong structure can be manufactured. The resultant material is isotropic with its mechanical and thermal properties depending upon many factors such as resin type; fibre orientation; fibre diameter and resin to fibre ratio.

The CTE of carbon fibres is both low and negative, but resins have a large positive coefficient. By manufacturing composites with a specific fibre size, direction and resin ratio a material with low CTE can be produced.

The most common resins are Polyesters, Vinyl esters and epoxies but there many others including cyanate esters which are primarily used in the aerospace industry.

The carbon fibres themselves are produced by controlled oxidation, carbonisation and graphitisation of carbon rich organic precursors which are already in fibre form. The most common precursor is polyacrylonitrile (PAN), because it gives the best carbon fibre properties, but fibres can also be made from pitch or cellulose. The fibres can be produced with high tensile strength or high tensile modulus or with properties between the extremes. Carbon fibre composite is often supplied as pre-pregs. These are sheets of fibres already impregnated with resin, they are stored cold and are soft so they can be placed over a mould or former. The pre-pregs can be supplied with the fibres laid in a single direction, multidirectional, short chopped fibres or woven in a variety of patterns. After placing into a mould they are often vacuum bagged to consolidate the fibres and resins layers and then baked in an oven to cure the resin.

The main manufacturers of fibres are Toray, Toho-Tenax, Mitubishi-Rayon, Hexcel and Cytec. Weavers include Sigmatex and Formax. Prepreg production companies include Hexcel, Cytec, ACG, SP Gurit and Amber Composites.

| Material | CTE (x $10^{-6}$/K) |
|---|---|
| Toho-Tenax HTA Yarn | -0.1 |
| Toray Carbon Fiber T300 Yarn | -0.41 |
| Mitsubishi Rayon Grafil 34-70 | +0.5 |
| Mitsubishi Rayon Pyrofil HS40 | -0.5 |

**Table 6 - CTE of some Carbon fibre yarns**

Manufacturing a carbon fibre composite with very low CTE is not easy and high thermal expansion rates may still be present orthogonal to the main fibre direction. The CTE is heavily dependent on many variables and due to variability in the manufacturing process the actual measured coefficient could differ significantly from zero. This can be overcome by making a large batch and then only selecting the good ones, or measuring a first stage material and then adding a second layer modified to compensate for any residual expansion in the first stage. There has been some work on optimising the design of composite tubes to reduce the variability in the CTE by selecting the fibre angle for both single ply and angle ply laminates.

Performance Composites Ltd produced a composite tube for Diamond Light Source with an unusual layout consisting of alternate layers of stainless steel foil and axially aligned high modulus fibres and resin to produce a tube with a CTE of $-0.43 \times 10^{-6}$ /K along its length. The company are however very secretive over the exact ratios and material specifications. The company are currently are supposed to be commercially active but seem to be verging on termination.

CarbonVision GmbH manufacture carbon fibre and epoxy resin composite breadboards. These have a lateral CTE of $2.5 \times 10^{-6}$ /K. Carbon tubes Ltd manufacture carbon fibre tube from pre-impregnated resins. They sell tubes which have zero coefficient of thermal expansion but this has not been tested so they do not know if this is true. They believe that the important issue is to select a high modulus fibre that has the strength to resist the thermal expansion forces generated by the expansion of the resin. It is proposed to test some of their tubes in collaboration with them.

### 3.2.6 Silicon carbide

Newport Spectra Physics have produced a range of positioning systems using silicon carbide which are designed for high speed processing of silicon wafers. Silicon carbide is very difficult to machine and has to be machined using grinding and vibration assisted diamond cutting tools. Newport have developed a bonding procedure where standard sections of silicon carbide can be bonded together to form complex mechanisms. They also use dense silicon carbide which can be polished to create an optical surface. Laser encoders can then be used which reflect off the reflective silicon carbide and so separate mirrors of different thermal properties are avoided. Newport Spectra Physics are using the stiff, low density silicon carbide to reduce the moving mass, increase acceleration times and decrease settling times primarily for the wafer processing industry.

The assemblies are manufactured using a range of standard thickness plates and rectangular box sections. Each surface is then ground flat before joining using an adhesive. Control of the adhesive thickness is important to ensure long term stability and stiffness. The limited availability of materials and complex joining processes and machining means that assemblies can take a long time to manufacture (20 weeks ) and are expensive.

| Material | CTE (x $10^{-6}$ /K) |
|---|---|
| SIC R (99% SiC) | 4.8 |
| SiC N (66%SiC, 33% Si3N4) | 4.4 |
| SiC-Si (85% SiC, 15% Si) | 4 |
| Dense SiC (100% SiC) | 4 |

**Table 7 - CTE of Silicon Carbide**

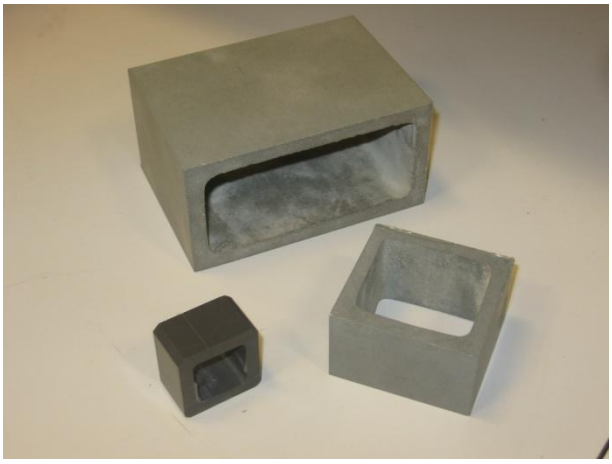

**Figure 14–Examples of Silicon Carbide section from Newport Spectra Physics**

Other companies such as IBS Precision Engineering are also using silicon carbide for parts for a metrology machine. There are many suppliers of Silicon carbide for high wear components but there are fewer making silicon carbide for metrology components.

CoorsTek Inc do offer components in Silicon Carbide. They have a number of grades manufactured in different ways, these include:

- Silicon Carbide using high temperature chemical vapour deposition.
- Reaction Bonded Silicon Carbide formed by casting, dry pressing or isostatic pressing
- Direct sintered Silicon Carbide formed by casting, dry pressing and isostatic pressing
- Graphite loaded direct sintered Silicon Carbide formed by casting, dry pressing and isostatic pressing

The direct sintered process allows a lower cost forming method and sizes up to 900mm x 1900mm can be produced in near net shape.

Boostec have manufactured parts for space optical instruments and have now been taken over by Mersen. I have been told by Mersen UK that they can only supply material as 25mm x 25mm box section but other sources say that Mersen can supply

other forms. This discrepancy may be due to lack of information within the company during the recent period of change of ownership.

Saint-Gobain manufacture a range of Silicon Carbide called Hexaloy, this includes Hexaloy SA, Hexaloy SP, Hexaloy SE and Hexaloy SG, these products seem to be aimed at high temperature applications.

Trex Enterprises have manufactured mirrors up to 1.5m in diameter using a high purity chemical vapour composite process.

Microplan offer a SiSiC in rectangular form called SDK SiC. This could be manufactured by Showa Denko KK or Shoko co ltd but information is sketchy.

AGC Ceramics also produce SiC but these seems to be thin materials used for solar cells.

### 3.2.7 Nexcera

Krosaki Harima Corporation have developed a very low thermal expansion coefficient cordierite based polycrystalline ceramic called Nexcera. Its CTE is $0\pm 0.03 \times 10^{-6}$/K at 20°C. It has a low density, high stiffness and can be manufactured into complex shapes by machining in its green state before sintering. It is however, like many ceramics, rather brittle and care must be taken when attaching any components not to cause stress concentrations. The material a mixture of Silicon, Aluminium and magnesium Oxides which when in dust form can cause irritation of the respiratory tract.

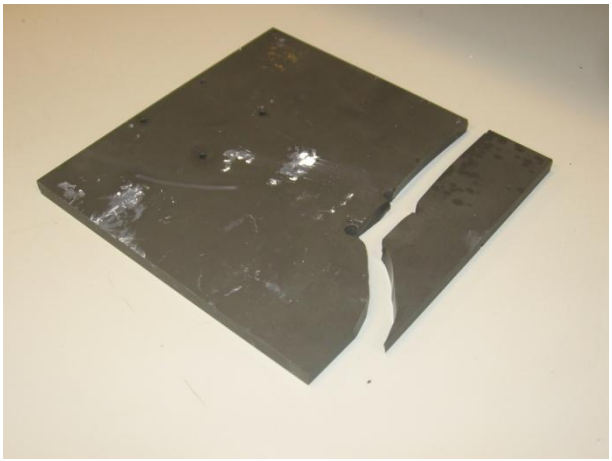

**Figure 15–Broken slab of Nexcera**

### 3.2.8 Ceramic composites

There has been work done on developing a wide range of exotic materials with low thermal expansion. Examples of which include Alumina reinforced eucryptite ceramics and (Garcia-Moreno O. , 2011) Sn doped silica glass (Kawata, 2006). These materials may offer low thermal expansion but are probably expensive.

### 3.2.9 Granite

Granite is often used as the base for precision stages. Although granite does not have a very low CTE its use as a large rectangular mass provides a large thermal mass which if housed within a temperature controlled environment will reduce the effect of the temperature oscillations generated by a normal air conditioning system.

The best granites for stable systems are fine grained black granites. These contain no crystalline quartz and little mica. They have lower porosity, lower moisture absorption, higher strength and lower thermal expansion than grey or pink granites.

Polymer granites are also available. These are a mixture of granite aggregates mixed with an epoxy resin. Granitek Ltd produce a polymer granite called Granitek 100 and Rockwell Automation produce Anocast™. The claimed advantage over natural granite is the good vibration damping properties. Their CTE is however worse than natural granite.

Botech NV use two granites from South Africa which are called Impala and African Black. Precision Granite Corp use Academy Black granite and sierra white granite. Standridge Granite corp use a black granite mined in California. Tmmtstone have quarrys in China and offer Jinnan black, Taishan Black and Taishan black diamond. Microplan use African Black and Blue Lanhelin from France.

| **Granite Grade** | **CTE (x $10^{-6}$ /K)** |
|---|---|
| Impala | 5 – 6 |
| African Black | 4 – 7 |
| Academy black | 6.9 |
| Sierra White | 7.5 |
| Jinnan Black | 4.61 |
| Taishan Black | 3.91 |
| Taishan Black Diamond | 5.9 |
| Blue Lanhelin | 7.4 |
| Granitek 110 & 100 | 11-13 |
| Anocast™ | 16.9 |

**Table 8 - CTE of Granite**

Dr Frank Wardle is working with ITP Group, a manufacturer of coordinate measuring machines to develop a range of air bearing stages made entirely from granite. These have a new type of micro pocketed air bearing system that offers increased stiffness over other air bearings.

### 3.2.10 Titanium

Titanium alloys are light weight and very strong. Grade 5 is the most common alloy and is known as Ti6Al4V. Some manufacturers such as Mad City labs Inc manufacture some of their nano stages in Titanium alloy. The CTE of 8.6 x $10^{-6}$ /K is lower than stainless steel and the higher strength and lower density can reduce the system total mass and so increase resonant frequency.

### 3.2.11 Aluminium Alloys

Commonly used wrought alloys such as 6082 have a large CTE of 23.1 x $10^{-6}$ /K. There are however some casting alloys which have lower CTE. For example LM29 (AL-Si23Cu1Mg1Ni1) has a CTE of 16.5 x $10^{-6}$ /K.

RSP technology have developed a melt spinning process with ultra fast cooling which has enabled them to produce very fine grained alloys with even lower CTE. Their Alloy RSA-443 (ALSi40) has a CTE of 13.1 x $10^{-6}$ /K and their RSA-473 (AlSi70) which is still in development has a CTE of 7.0 x $10^{-6}$ /K.

### 3.2.12 Summary of low CTE materials

Using low CTE materials offers improved thermal stability but at a cost. Experimental end stations are subjected to hard use by a wide range of users and materials that could easily chip or crack could be problematic. Experimental requirements always seem to be changing with new detectors being used, different sample environments and different experiment techniques. The ability to modify parts easily using conventional techniques offers distinct advantages.

Natural granite for a base remains a good choice and the ability to integrate granite air bearing stages offers many advantages.

For machined parts an effort should be made to move away from Aluminium Alloys to low thermal expansion materials, better would be carbon steel, best would be one of the 36% Iron alloys. At the moment costs are high, but if more use was made of these alloys the cost may come down particularly if one machinist could be selected as the supplier of choice.

Reaction bonded silicon carbide looks an interesting material but is very difficult to modify after manufacture.

For structural components an optimised carbon fiber /resin composite tube could be possible. Joining tubes into complex frames can be done using cast aluminium clamps or by bonding using wet layer up techniques. Wet lay up would however prevent easy

modifications. There are however problems in finding suppliers to develop suitable tubes and the variability of the manufacturing process still makes the material expensive. The recent availability of optical breadboards in low CTE carbon fibre is encouraging.

| **Material** | **CTE ( x $10^{-6}$ /K)** |
|---|---|
| Low expansion glass | 0 ± 0.02 |
| Nixcera Ceramic | 0± 0.03 |
| 36% Nickel iron alloys | 0.6 to 1.4 |
| Carbon fibre composites | 0.43 to 20 |
| Black Granite | 3.9 to 7 |
| Silicon Carbide | 4 to 4.8 |
| Carbon steel (0.1 – 0.2%C) | 8.3 |
| Titanium (Ti6Al4V) | 8.6 |
| Polymer Granite | 11 to 16.9 |
| Stainless steel (18% Cr, 8% Ni) | 11.5 |
| Aluminium Alloys | 16.5 - 23 |

**Figure 16– Summary of CTE of some materials**

## 3.3 Phase change materials

A typical air conditioning system can only control the ambient temperature within a range, the range may be small but there is still a variation. This error is due to limited resolution of the sensors, turbulent air flows, time varying conditions and imperfect control loop with time delay. When the air temperature is high thermal energy is transferred into the critical components and when the air temperature is lower thermal energy is removed. The thermal transfer depends upon the convection coefficient and the resultant temperature change depends upon the thermal mass of the critical components which is the product of the mass and the specific heat capacity of the material.

The apparent thermal mass would be increased if the material changed phase. The heat energy required would then include the latent heat of fusion as well and so for a constant heat input the resultant temperature change would be less.

The increased energy storage due to the latent heat is significant compared to the heat capacity of water. The energy absorbed by water for a 1°C temperature change = 1°C x 4.187 kJ/KgK = 4.187 KJ/Kg, but the energy absorbed by a Salt (S21) due to Latent heat alone is 229 KJ/Kg, over 50 times the sensible heat capacity.

There has been a lot of work in developing materials with different phase change temperatures for thermal energy storage and recovery applications. These materials are given the generic name of phase change materials (PCM) and can be divided into two groups, Organic compounds and Salt Based products.

A review of phase change materials was carried out in 2003 (Zalb, 2003) and in this review materials with a phase change temperature near 22°C are given in Table 9.

| **Type** | **Compound** | **Melting temperature (°C)** |
|---|---|---|
| Inorganic | $KF.4H_2O$ | 25.8 |
| Inorganic | $Mn(NO_3)2.6H_2O$ | 25.8 |
| Organic | Polyglycol E600 | 22 |
| Organic | Paraffin $C_{13}$-$C_{24}$ | 22-24 |
| Fatty Acids | Capric-Lauric acid (45-55%) | 21 |
| Fatty acids | Dimethyly sabacate | 21 |

**Table 9 – Phase change materials**

### 3.3.1 Salt based PCMs

A common salt product is Glauber's Salt (Sodium sulphate decahydrate, $Na_2SO_4.10H_20$). This normally freezes at 32.4 °C. Lower freezing temperatures can be obtained by mixing with other salts.

Salt products were the first type of PCM to be investigated for energy recovery systems, but they do have a few problems. They are corrosive, unstable, prone to

super-cooling and improper re-solidification. Some of these effects can be reduced by the use of thickening agents and nucleating agents.

An example is a mixture of 45:55 capric-lauric acid which has a phase change temperature at 21°C and a latent heat of 143 KJ/Kg.

There are a number of manufacturers of phase change materials including Phase Change Material Products Ltd, Climator Sweden AB, Rubitherm Technolgies GmbH, Cristopia Energy Systems and PCM Energy P.Ltd (TEAPPCM).

Phase Change Material Products Ltd offer a range of salt solutions with phase change temperatures ranging from 7 to 117 °C. Salt S21 for example has a phase change temperature of 21°C, a density of 1480 Kg/$m^3$ and a heat capacity of 150 KJ/Kg and a latent heat of 222 MJ/$m^3$.

Pure material has a single phase change temperature, but impure materials, unless forming a perfect eutectic have a 2 phase stage where solidification or melting occurs over a range of temperatures and may be different in the cooling or heating phase. As an example Rubitherm RT21 from Rubitherm Technologies GmbH is an organic paraffin based materials and has a melting temperature in the range 18-23 °C and a freezing temperature in the range 22 – 19 °C.

### 3.3.2 Organic PCMs

Organic Phase Change Materials are more stable, they melt congruently, super cooling is not a significant problem but they are flammable, odorous and do change volume considerably.

Polyethylene Glycols are a family of water soluble linear polymers formed by the addition reaction of ethylene oxide. Each polyethylene Glycol is designated by a number that represent its average molecular weight. Polyethylene Glycol 600 has a range of molecular weights from 570 -630. A number of manufacturers have their own product. Huntsman for example, has a product called POGOL 600 which has a quoted freezing temperature of 20-25°C. BASF's equivalent is Pluracol E600.

**Paraffin is a generic term for straight chain Alkanes with the formulae $C_nH_{(2n+2)}$. The melting melting points of some paraffins are given in**

Table 10.

n-Heptadecane looks an attractive PCM with a melting temperature of 22°C, a specific heat capacity of 22KJ/Kg.K , a density of 0.7783 g/ml and a latent heat of fusion of 240 KJ/Kg. But does expand by 14% on solidification, is flammable and has a rather poor thermal conductivity of 0.14 W/mK. 99.9% pure n-Heptadecane is available from Alfa Aesar at a cost of £228 per 500g.

| Carbon Number | Formula | Name | Melting point (° C) |
|---|---|---|---|
| C(16) | $C_{16}H_{34}$ | n-Hexadecane | 18 |
| C(17) | $C_{17}H_{36}$ | n-Heptadecane | 22 |
| C(18) | $C_{18}H_{38}$ | n-Octadecane | 28 |

**Table 10 - Melting point of some Paraffins**

### 3.3.3 Embedded PCMs

Many suppliers offer products that are sealed within easily handled containers. Rubitherm offer organic or a salt based material sealed within 450mm x 300mm aluminium panels of 10mm, 15mm or 25mm thickness.

There has been some work on developing phase change materials that can be imbedded in building materials such as concrete and plaster board. (Kelly) (Harlan, Mackay, & Vale) (Quanying, Lisha, & Chen, 2010)

DuPont have a product called Energain which is a 40% Copolymer: 60% Paraffin wax sandwiched between aluminium plates. BASF have a product called Smartboard which is a drylined gypsum based board impregnated with a paraffin droplets micro encapsulated, Dorkens product is called Delta-cool 24.

There has also been some work on impregnating phase change material within metallic foams. (S Krishnan, Suresh, & Garimella, 2008)

### 3.3.4 Conclusion

Phase change materials potentially offer a way of improving thermal stability particular n-Heptadecane which has a phase change temperature of 22°C. Work does need to be done on how it is contained and good heat transfer obtained.

## 3.4 Minimisation of internal air

Access to the experiment is often required by the user. This could be to change samples, adjust or move detectors or change focussing optics. Easy access is therefore required and so if a thermal barrier is fitted this does need to be fitted with removable lids, doors or removable access panels. When access is required then the air within the enclosure will be exchanged partially with air from outside the enclosure and the internal parts could change temperature both during the period when the doors are removed and during the period after until the air temperature equalizes with the temperature of the internal components.

This effect could be reduced if the volume of air that could be exchanged is reduced to the minimum. To do this the internal volume should be filled as much as possible. This could create problems with accessibility, space needs to be maintained for moving components and the material must not block or affect the scattering of atomic particles or radiation which is part of the experiment. However, these in fill pieces could be removed as part of the removable door, lid or panel or they could form an integral part of the equipment especially where access is not required.

A design approach could be to move away from designing the equipment as a set of plates bolted together to form a support structure for components and think more of a solid block that has been machined away only where necessary for the fitting of components, allowing line of sight and providing access. This could then be manufactured as a casting. This would then reduce the internal air volume to the minimum.

## 3.5 Minimisation of heat load variation

### 3.5.1 2 phase stepper motors

The position of detectors, samples , focussing systems and the like are adjusted using a variety of methods including DC motors, stepper motors, piezo actuators and pneumatic actuators. The most common is the 2 phase stepper motor driving a lead screw via a gearbox.

Initially at Diamond these motors were controlled using either Smart Drive or Stogra amplifier boards. The stepper motor amplifier card provides the pulsed signals to drive the stepper motor coils. The current output is limited by the amplifier card. The Smart Drive DM28/6 for example is limited to 2A RMS and 2.8A peak.

The motor when operating consumes electricity and this is converted into kinetic energy, noise energy or thermal energy. The greatest energy loss is thermal energy within the motor windings, this energy is conducted away through the base or shaft or is transferred to the surrounding air. The conduction path to the air is generally poor and stepper motors typically operate hot and in some cases will need guarding. This transfer of heat is a particular problem for motors in vacuum which are often fitted with monitoring thermocouples within the windings.

In many cases motors are only used occasionally and so for long periods of time the motor is not driven. However in many cases the motors cannot be powered off otherwise the device may move because of gravity or vacuum forces back driving the motor. It may be possible to provide the motor with a reduced current which is insufficient to turn the motor but is sufficient to prevent back driving. Both Smart Drive and Stogra amplifier cards reduce the current to 50% when the motor is stopped and for the stogra amplifier this feature can be switched off.

A 2 phase stepper motor can be operated in a number of scenarios as follows

- Motor not energised, no electrical power
- Motor energised at 50% power and not moving

- Motor energised at full power and not moving
- Motor energised at full power and moving.

The energy absorbed by the motor varies with each operating condition. When the motor changes from one operating mode to another the thermal load will change and so it will take time for the motor and its immediate surroundings to reach a stable temperature. This may take some time. Then, if the motor mode is again changed, even for a short period there again can be a long stabilisation time. There is a difference between the power consumed when stationary and when accelerating but this difference is less when the motor is energised at full power.

There is therefore an argument that for critical applications motors should be kept at a constant operating mode, they should never be de-energised and the amplifiers should not be set so that the power is reduced to 50% when the motor is stopped. It is almost a case that the motor windings should be maintained at a constant temperature and active means could be provided to ensure this. This could be by providing a small heating circuit or controlling the loss of heat by using a peltier controller or a cooling fan that is controlled by the winding temperature measurements.

The current motor controller used at Diamond is the Delta Tau Geobrick. A variation of this is now being introduced which has a smaller transformer providing 24 rather than 48V, this is being introduced for applications where smaller low power stepper motors are used. Currently the Geobrick has no reduced power option although this could be done with a small software programme.

### 3.5.2 Pneumatic actuators

In some cases detectors need to be moved from either in the beam or out of the beam and require no remote control adjustment of position. For pneumatic operation it is important to think about where the exhaust air is discharged to. The compressed air will not be either at a constant temperature or be the same as the air near the experiment. If the air from the solenoid is exhausted locally then the air temperature will be affected. The air must be therefore be discharged some way away. Frequent

operation of a pneumatic cylinder could mean that the cylinder is being fed by compressed air that is hotter or colder than the local air and the actuator body may change temperature. A vessel that can act as a heat exchanger to equalise the compressed air and ambient air temperatures could be considered.

### 3.5.3 Lighting

Many experimental hutches are provided with lighting that can be switched on and off by the user. Sometimes it is necessary for lights to be fully off such as when viewing any fluorescent screen images on a camera. When samples are changed or detectors adjusted the user often wants plenty of lighting to give good visibility. The problem is that switching lights changes the conditions. The heat from the lights is mainly transferred to the ambient air which is then taken away by the air conditioning system, this does have an effect on local temperature distributions. In addition there is a transfer of energy by radiation and this is absorbed by critical components. Some components are manufactured from Aluminium which has been anodised black and these will respond faster than natural anodised components to any change in ambient light radiation.

### 3.5.4 Conclusions

For critical applications the 2 phase stepper motors should be operated at constant heatload and the option for operating the motor at 50% current when the motor stops should be disabled. Exhaust air from pneumatic actuators should be exhaust far away from critical components. Aluminium anodised components should be natural rather than black.

## 3.6 Thermal expansion compensation

The effect of thermal expansion can be compensated for by mixing materials of different coefficients of thermal expansion (CTE). An example is a triangular structure, with the base of one material and the two legs as another material pin jointed. If the base is made of Aluminium with CTE of 25 x $10^{-6}$ /K and the legs are stainless steel with a CTE of 11 x $10^{-6}$ /K, then for an increase in temperature the legs will grow less than the change in base length. The angle will decrease and the apex height will not be as

great as for a uniform material triangle. A zero height change will occur if the triangle angle has an initial angle of 74.35°.

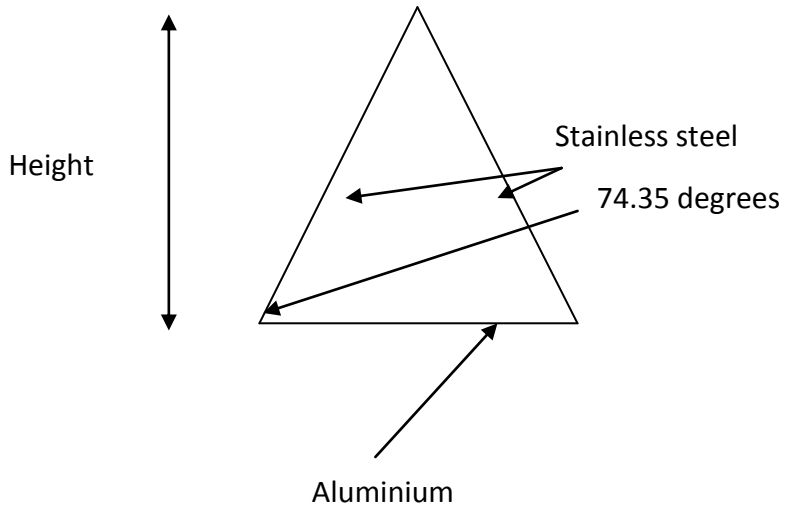


**Figure 17– Expansion compensated triangle**

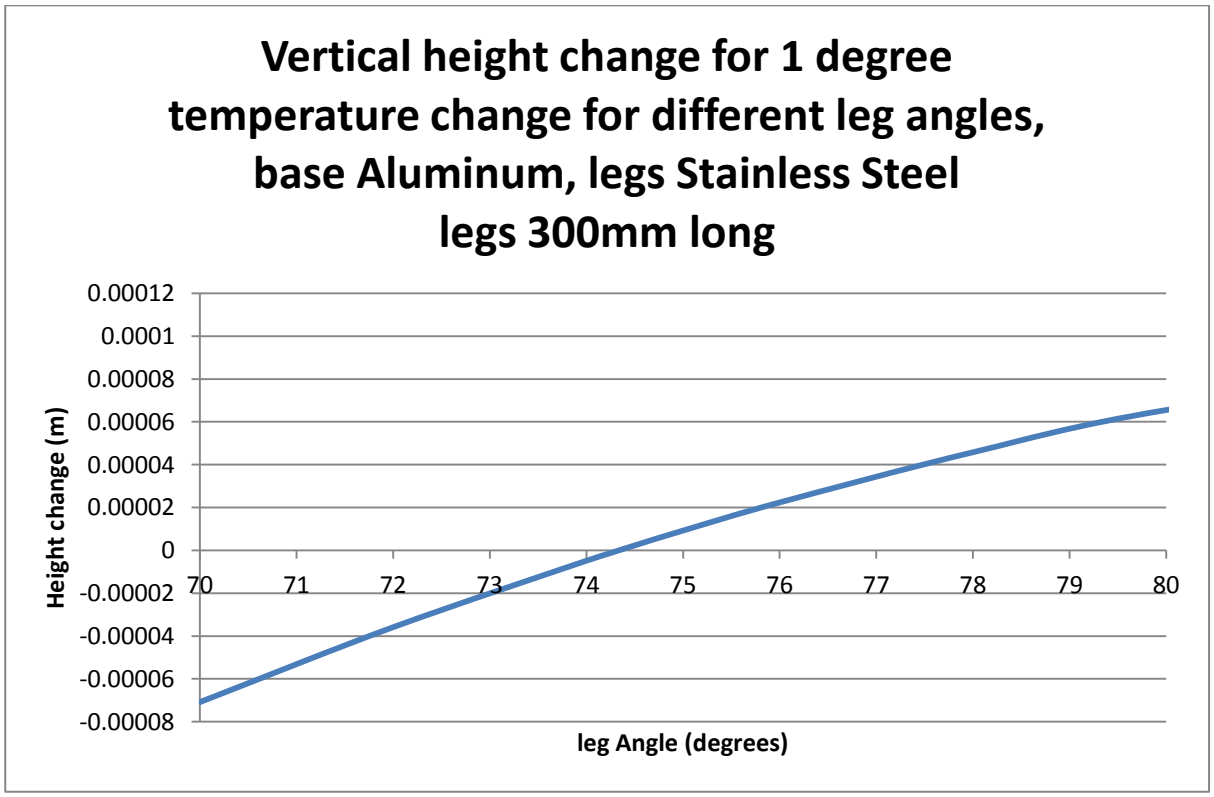


**Figure 18– Plot of vertical height change vs leg angle**

## 3.7 Thermal centre

In some circumstances it is possible to ensure that an important feature does not change position with temperature by placing it at the thermal centre. The concept is to design the system so that there is a single point which does not change position with change in temperature. This relies on understanding the thermal loads, conductivity and mechanical constraints, but this can be done using FEA. An important issue is allowing the system to expand and contract in a reproducible and controlled way, and this requires the use of sliding joints or flexures.

Kinematic mounts are very useful feature but they need to be manufactured of suitably hard materials to withstand the applied loads without excessive deformation at the contacts.

## 3.8 Minimisation of heat loads

In theory it does not matter if the heat loads to a critical component are large or small, the important issue is that the loads remain constant and the cooling conditions remain constant. The problem is that small changes in large heat loads produce a higher temperature change and this results in higher position change due to thermal expansion. Within the critical area the best solution is to minimise the total heat load. This can be done using the following approaches

- Replace the component with a lower heat load device
- Reduce the heat load by using higher efficiency mechanics
- Provide mechanical springs or counterbalance weights so that motors require less energy and are balanced in both directions.
- Move the high heat load parts away from the critical area
- Replace 2 phase stepper motors by pneumatic actuators where possible

An example of moving the heat load away from the critical area is with a Fluorescence Detector. Here the detector has a 100mm long nozzle and the high heat load electronics is on the back face. In this case the critical components are located within a temperature controlled box and a hole is provided through which the detector nozzle

fits. The detector is then close enough to the sample but the high heat load electronics are out of the critical area.

Another example is where an experiment requires the use of 2 different detectors which need to be exchanged remotely, here a stepper motor solution is replaced by a pneumatic actuator.

## 3.9 Reduce stabilisation time

During an experiment there will be disturbances to any thermal equilibrium that has been reached. These disturbances will include: change of power load on motors when samples, detectors or optics are adjusted; change of air if the enclosure is opened to change samples, detector or optics. These changes will result in drifting of position of the sample, optics and detectors until thermal equilibrium is returned. It is important that thermal equilibrium is returned as soon as possible.

The methods of doing this are as follows

- Reduce the necessity of opening the chamber by having remote sample changing system
- Maximise the thermal mass
- Maximise the use of materials with good thermal conductivity
- Actively cool with good thermal conductivity connections components which have variable heat loads.
- Actively heat components with variable heat loads to maintain constant heat load
- Reduce the volume of air displaced when the chamber is opened.
- Use low thermal conductivity materials to isolate critical components.

## 3.10 Active temperature stabilisation methods

The temperature of critical components could be stabilised by providing an active cooling or heating system with a controller.

### 3.10.1 Laboratory water circulator

Laboratory water baths are used extensively to maintain close temperature control of laboratory processes. These water baths consists of a bath and integrated controller or an independent unit that circulates controlled temperature water to an external process. Examples of manufacturers are as follows:

- Grant Instruments
- Julabo
- Lauda
- Haake
- Thermo electron
- huber

The systems that circulate water to an external process consist of a pump, water heater/chiller, temperature sensor, controller and water tank. The pump needs to be sized to give the correct flow rate against the process pressure drop.

An example of a circulator is the Grant GP200K immersion thermostat , this has an integral pump able to deliver 21 L/min at a maximum pressure of 460 mbar. For higher pressures a vertical turbine pump can be fitted, this can deliver up to 12 L/min at a maximum pressure of 1650 mbar. The thermostat has a display resolution 0.01°C and can use an external PT1000 for temperature monitoring.

One of the problems of water circulators are that the pumps can give rise to vibrations which are transmitted to the critical components. This is critical for nano focus systems.

### 3.10.2 Pressure pulse reduction system

Pressure pulses were seen from a grant water chiller fitted with a VTP2 vertical turbine pump. The chiller was used to cool the crystal from a Double Crystal Monochromator but analysis of the signal showed vibrations at 48.2 and 96.6Hz. To reduce this problem a pressure pulse reduction system was designed and fitted. The reduction in vibration was as shown in Table 11.

| Frequency (Hz) | % of signal without pressure reduction | % of signal with pressure reduction |
|---|---|---|
| 48.2 | 1 | 0.2 |
| 96.6 | 3.55 | 0.6 |

**Table 11 - Water chiller pressure pulse reduction results**

The pressure reduction system consisted of a vessel fitted between the pump and crystal. The vessel has a large area neoprene diaphragm that could expand as the water pressure pulsed.

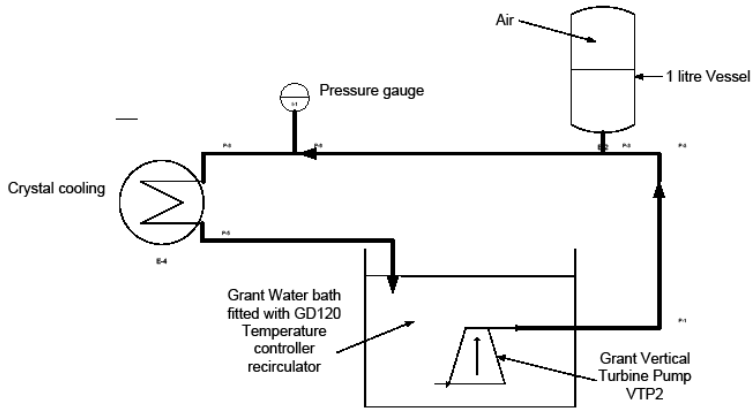


**Figure 19- Pressure pot circuit**


**Figure 20- Pressure pot**

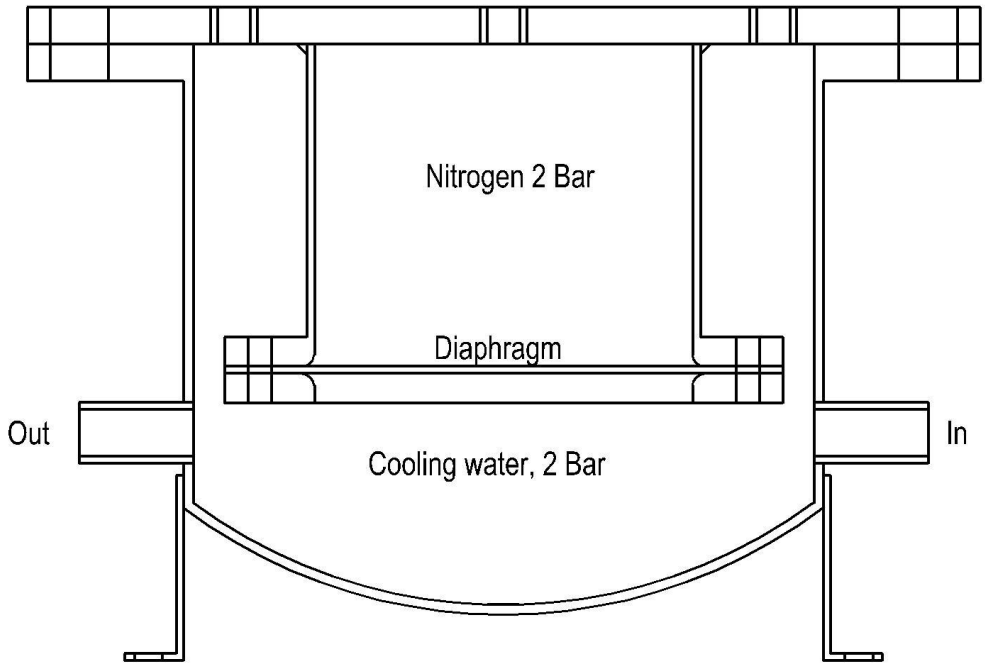


**Figure 21- Sketch of pressure pot**

The temperature control is limited as the water temperature is only controlled at one point. The resolution is limited to 0.01°C and temperature stability is generally 0.05 to 0.01 °C.

### 3.10.3 Peltier to water exchanger

Another method is to use a water cooling pipework that is connected to the critical components via a peltier controlled heat exchanger. The water temperature does not need to be closely temperature controlled as the water is only used as a thermal sink. The temperature is controlled by the peltier which pushes heat energy into or out of the water. One advantage is that there can be many peltiers on the one water circuit and so the temperature at many points can be controlled. The possible problem of water pressure pulses is however still present

### 3.10.4 Peltier to air exchanger

Peltiers can be fitted with a fan and finned heat exchanger. This approach eliminates the problem of water pressure pulses and allows the temperature to be controlled at as many locations as peltiers are fitted. A number of such systems have been developed for the control of critical scientific instruments, or lithography systems. (Higuschi.S & DeBra.D, 2006) Pulse width modulated controllers can then be used for each peltier. An enclosure suitable for nano focus mechanics has been tested using this approach. Details of this and the test results are given on Page 232.

### 3.10.5 Thermal mass

Materials with a high thermal mass will help reduce the change in temperature of the critical items when the external temperature is oscillating. Thermal mass is the product of specific heat capacity, density and volume. For a constant volume component then the thermal mass of different engineering materials is given in Table 12.

| **Material** | **Specific heat capacity (sp) (J/gK)** | **Density (G) ($g/cm^3$)** | **Thermal mass (Sp x G)** |
|---|---|---|---|
| Water | 4.186 | 1.0 | 4.18 |
| Mild steel | 0.49 | 7.85 | 3.84 |
| Stainless steel | 0.47 | 7.99 | 3.75 |
| Copper | 0.379 | 8.92 | 3.38 |
| Inconel 600 | 0.40 | 8.43 | 3.37 |
| Brass | 0.387 | 8.4 | 3.25 |
| Silicon Carbide | 1.0 | 3.21 | 3.21 |
| Aluminium | 0.880 | 2.7 | 2.37 |
| Titanium Ti6AL4V | 0.527 | 4.5 | 2.37 |
| Granite, Natural | 0.750 | 2.7 | 2.02 |
| Granite, polymer | 0.84 | 2.3 | 1.93 |

**Table 12 - Thermal mass of common materials**

To reduce the temperature change of the critical components the thermal mass should be maximised. Water is a very good thermal mass so one solution could be to use stainless steel tanks filled with water. The issue of possible leakage and evaporation loss would however need to be carefully considered. Natural granite is not as high a thermal mass as mild steel but large blocks of granite can be used as a base and is cheaper than the equivalent mass of mild steel.

### 3.10.6 Reduction of heat transfer from ambient air

Reduction in the energy transfer from the ambient environment can be accomplished by adding thermal insulation or by reducing surface area.

## 3.11 Thermal insulation

There are a number of materials suitable for thermal insulation at ambient temperatures. This includes foams, plastics, wools and stagnant air.

Foams are made by forming gas bubbles in a plastic mixture, with the use of a blowing agent. There are two basic types of foam. Flexible foams have an open cell structure and can be produced in both high and low densities. Applications include cushioning for furniture and automobiles, mattresses and pillows. Rigid foams are highly cross-linked polymers with a closed cell structure that prevents gas movement. Their main application is as insulation for buildings, refrigerators and freezers. Foams can be manufactured from many materials such as Neoprene, Polyethylene, Polypropylene, Nitrile rubber and Silicon. Foams can be supplied with adhesive backing and faced with protective foils and Fire retardant foams are also available.

There is a range of insulators called microporous insulators. These are based on inorganic oxides, primarily silica. They are claimed to have lower thermal conductivity than still air by reducing heat transfer by conduction, convection and radiation. The oxides have very low thermal conductivity, the microporous structure reduces the contact between air molecules and opacifiers are added to reduce thermal radiation. It can be supplied in various forms including board, panels and vacuum sealed in laminated film. Manufacturers include the following:

- Microtherm
- Unifrax
- Morgan thermal ceramics
- Zircar ceramics

Microporus insulation is primarily used for high temperature applications and where a requirement for minimal insulation thickness is required.

A common insulator used in buildings is mineral wool. This is a general term that includes materials made from mineral fibres, ceramic fibres and fibreglass. These products are cheap, have low flammability but they can irritate the eyes, skin and respiratory tract. Prolonged exposure can lead to harmful effects and some types are considered carcinogenic.

Natural fibres such as Sheep and flax wool are becoming more popular as an insulator. Wool has a crimped form which both traps air and prevents long term settling. These are typically manufactured in rolls or slabs suitable for house insulation applications with thicknesses of at least 75mm.

Super wool is an insulator manufactured by Morgan Thermal Ceramics and is a patented fibrous material that can be supplied as blanket, board, paper and felt forms. These are suitable for high temperature applications.

Expanded Polystyrene can be extruded or moulded. It is a rigid and tough closed cell foam made from pre-expanded polystyrene beads.

Extruded closed cell polystyrene foam is sold under the trademark of Styrofoam by Dow chemical. It has low thermal conductivity and improved surface roughness. It can be hot wire cut from thickness from 5mm to 150mm. According to EN 13501-1:2003 (Fire classification of construction products and building elements) Polystyrene is Class E which is defined as : Product may quickly lead to a flash over situation, possibly within the first two minutes of the reference scenario test.

| Material | Grade | Manufacturer | Thermal conductivity (W/mK) |
|---|---|---|---|
| Silica microporus | Microtherm board | Microtherm | 0.02 |
| Mineral wool | Rockwool roll | Rockwool | 0.044 |
| Sheep wool | Thermafleece TF35 | Thermafleece | 0.035 |
| Still air | | | 0.024 |
| Neoprene foam | | | 0.054 |
| Polyethylene, closed cell | TF30LPE | Copex Microcellular | 0.034 |
| Nitrile rubber foam | Kaiflex ST | Kaimann GmbH | 0.036 |
| Silicone foam | BISCO BF-1000 | Rogers corporation | 0.06 |
| Alkaline earth composition fibers | Superwool | Thermal ceramics | 0.05 |
| Expanded Polystyrene | Styrofoam SP-X | Dow Chemicals | 0.026 |

**Table 13 - Examples of thermal insulation materials**

For nano focus applications, high temperature resistance is not required and space is not critical. Materials that are easy to cut to shape, adhere to metal surfaces, have low flammability and produce low levels of dust would be ideal. A closed cell cross linked polyethylene foam with one side faced with aluminium and one side with adhesive tape will meet this requirement.

The flammability of plastics are often tested using the procedure outlined in UL94 which is now harmonized with IEC 60707, 60695-11-10 and 60695-11-20 and ISO 9772 and 9773. The UL94 grades applicable to foams are HF-1, HF2 and HBF. Polyethylene foam is available in grade HF-1.

## 3.12 Reduction in surface area

Often structures are manufactured as plates bolted together. This makes the structure cheap, easy to modify and can be stiff. It does however, give a large ratio of surface area to volume. An improved design would be to use solid blocks rather than plates and this approach could be satisfied using granite. Another approach would be to

create sealed volumes which could be filled with materials such as dry sand, water or phase change material, this could be done using plates. Water would require good sealing, probably fully welded stainless steel, but dry sand could be used for bolted structures. Open steel framed structures could be improved by fitting thin plates on the external surfaces but the internals would need to be filled with insulation material to prevent heat transfer by convection. The ideal shape for structures and components would be a sphere but a more practical approach is a cube.

## 3.13 Temperature control through air heat exchange

If we are trying to maintain very high levels of temperature stability the aim would be to maintain a very small temperature difference between the structure and the air flowing over the structure.

We would also be interested in maintaining a low air velocity so that the sample is not disturbed by air flows. The ideal would be if natural convection would be adequate.

### 3.13.1 Natural convection

Convective Heat transfer

$Q = A\,h\,(T - T_\infty)$

$T_\infty$ is the temperature of the fluid far away from the plate

T is the temperature of the solid surface

h is the convection coefficient

Q is the heat flux, A is the surface area

For pure natural convection

$Nu = f(Gr, Pr)$

Nu is the Nusselt number

Gr is the Grashof number, this is a dimensionless number which is the ratio of buoyancy forces to viscous forces

for a vertical flat plate

v is the kinematic viscosity (15.11 x $10^{-6}$ at 20°C)

g is acceleration due to gravity (9.81msec$^{-2}$)

Pr is the Prandtl number (0.713 for air at 20° C)

β is the volumetric thermal expansion ( 3.4 x $10^{-3}$)

α is the thermal diffusivity.

L is the length

K is the thermal conductivity

For an isothermal, vertical plate in natural convection the experimental data approximates to

So for a vertical plate of height 300mm, length 500mm with a temperature difference of 0.001 °C the heat transfer will be

Gr = 9.81 x 3.4 x $10^{-3}$ x 0.001 x $0.3^3$ / $(15.11 \times 10\text{-}6)^2$ = 3,944

$$\frac{\text{———————}}{\text{———————}} \quad \frac{}{\text{——}} = 4.47$$

$Q = A\ h\ (T-T\infty)$

$= \frac{}{\text{——}}\ (T-T\infty)$

$= 0.3 \times 0.5 \times 4.47 \times 0.0257 \times 0.001 / 0.3 = 57\ \mu W$

By comparison a temperature difference of 0.01° C the heat transfer would be

$$\frac{\text{———————}}{\text{———————}} \quad \frac{}{\text{——}} = 7.32$$

$Q = 0.3 \times 0.5 \times 7.32 \times 0.0257 \times 0.01 / 0.3 = 940\ \mu W$

This shows that that natural convection would not produce enough heat transfer for such a small plate.

### 3.13.2 Forced Convection

Re is the Reynolds number = V L / v

Over a plate fully Turbulent flow at $1 \times 10^6$ so for a 0.5m long plate the flow is not fully turbulent unless the air flow is greater than

$V = 1 \times 10^6 \times 15.11 \times 10^{-6} / 0.5 = 30$ m/sec

For fully laminar flow at Re < $3 \times 10^5$

The air velocity V < $3 \times 10^5 \times 15.11 \times 10^{-6}$ / 0.5 < 9 m/sec

At 0.1 m/sec

Re = 3,309

Nu = 0.664 $Re^{1/2}$ $Pr^{1/3}$

Nu = 34

Q = 0.3 x 0.5 x 34 x 0.0257 x 0.01/ 0.3 = 436 µW

Fully turbulent flow is not reached until long distances, but if the flow is re-circulated with many turbulent enhancing features then turbulent conditions could be forced.

If fully turbulent conditions can be realised then

Re = $1 \times 10^6$

Nu = 0.664 $Re^{1/2}$ $Pr^{1/3}$

Nu = 590

Q = 0.3 x 0.5 x 590 x 0.0257 x 0.01/ 0.3 = 0.07 W

This would still mean that 100 plates would be required to transfer 7 watts of heat from the air.

### 3.13.3 Temperature stability using air flow

These results show that heat transfer by air across a boundary with a very small temperature difference is poor. The prime heat transfer route from nano focus components within an enclosure must therefore be by thermal conduction.

## 3.14 Separate metrology frame

Most instruments combine the actuators and measuring systems into one integrated assembly. But there is an argument for separating the measurement system from the

main frame. Actuators generate forces, vibration and heat and this can be transmitted through the main frame of the assembly to the supporting floor or other base structure and cause instability. If the metrology was measured against a separate metrology frame rather than the main frame then these effects would be reduced. The metrology frame could be simpler and be manufactured from a more costly material to give improved stability.

## 3.15 Improvements in hutch temperature control

### 3.15.1 Improvement of temperature control of hutches at the ESRF

At the ESRF they are investigating improved thermal stability at the sample by improving the hutch temperature stability. A simulation was performed and this was compared against 2 years data which included temperature, atmospheric pressure, lighting, door state, human presence, electrical power consumption, air velocity and water valve state. Proposals include insulating the walls and roof with 50mm thick Rockwell, extracting air at the four lower corners of the hutch, providing a textile membrane over the roof, reduction of air leakages to less than 10%, extraction directly above electronic racks and providing an insulated porch entrance. (Baker, Marion, Zhang, Marchial, Mackrill, & Favier, 2010)

### 3.15.2 Improvements of temperature control at Diamond

#### 3.15.2.1 Description of the current system used at Diamond

The air within the B16 Experiment hutch is re-circulated through 2 water cooled fan coil chillers. These units do not provide any heating or humidity control, they only chill the air. Both units are identical and comprise of 4 sections.

**Figure 22 – Hutch roof mounted air chiller and fan**

Section 1 is a disposable filter, Section 2 is a pleated filter, Section 3 is the water cooling coil with a duty of 4.98KW and Section 4 comprises of 3 fans running simultaneously providing 0.505$m^3$/sec of air at 100Pa differential pressure. The two units are located at opposite ends of the hutch. Each unit blows chilled air into a long blue fibre sock mounted in the roof. This sock allows air to permeate through the sock skin along its length and so provide a low velocity even distribution of cooled air.

**Figure 23 - B16 Hutch showing air distribution socks**

The fan coil units are fed from a Diamond Central chilled water supply ring main. A single spur feeds the B16 Beamline and feeds all the fan coil units on the beamline. This spur then breaks into separate feeds for each room. The spur for the experiments hutch is controlled by a single 3 port valve. The spur then splits after the valve into 2 parallel lines that supply each of the two cooling coils.


**Figure 24 – Location of 3 port valve outside the hutch**

The control system is a cascade PI +PID loop. The room temperature is measured using a Nickel 1000Ω RTD sensor and this is compared against the set point. This generates a secondary set point. The average temperature from the two fans is compared against the secondary set point and this controls the position of a 3 port valve on the chilled water supply.

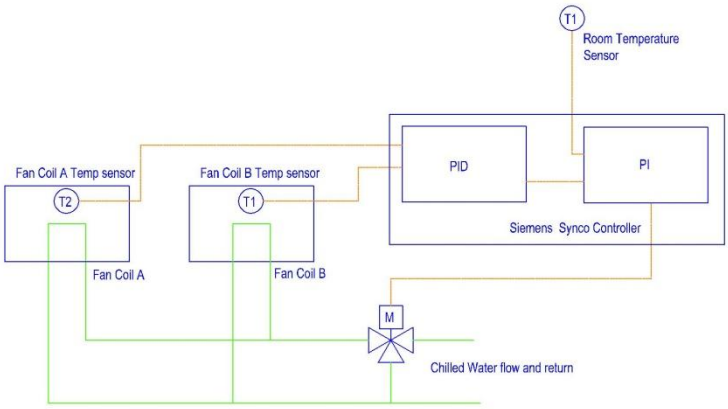


**Figure 25 Hutch air temperature control schematic**


**Figure 26 – Air temperature control panel**

### 3.15.2.2 Controller

The controller is a Siemens Synco 200 range type RLU210. This unit has 1 control loop and can have 3 Universal inputs, 1 Digital input and 1 analogue output. The controller comes with a range of ready programmed standard applications. This unit has been set up to run application A07(ADB005LU1HQ) , which is a programme suitable for “supply air temperature control with chilled water cooling coil” and includes a cascade control.

A cascade control comprises of two control loops, the first loop is generally a fast acting loop which produces a control variable for the second loop.

The temperature of the hutch appeared to have a very wide range and showed an almost 24 hour cycle. A re-tuning of the control system was carried out.

The control original loop settings are listed in Table 14.

| Parameter | Function | Original value |
|---|---|---|
| ROOM XP | Proportional function | 2 |
| ROOM TN | Integration component | 20.00 |
| SU MAX | Absolute high of the supply air temperature | 35 |
| SU MIN | Absolute low of the supply air temperature | 14 |
| SU DMIN | Low temperature difference limit control between the present room temperature and the supply air temperature | 50 |
| SU DMAX | High temperature difference limit control between the present room temperature and the supply air temperature | 50 |
| SEQ4 XP | Proportional function. | 30 |
| SEQ4 TN | Integration function. | 3 |
| SEQ4 TV | Differential function | 00.00 |
| TIMEOUT | | 00.00 |

**Table 14 – Control loop parameters**

The control system is based on a cascade system with an inner loop and an outer loop. The outer loop compares the set point and the room temperature sensor to produce a value for the air inlet temperature. This has a proportional and Integral action. The inner loop uses the inlet air demand and the inlet air temperature sensor to control the motorised 3 port valve. This has a proportional, integral and differential action.

The room Temperature sensor is a Nickel 1000Ω RTD Sensor. This gives a 0.5% resistance change from 20 to 21°C. The 3 port valve is a Siemens Modulating control valve with magnetic actuators, 1:1000 resolution, Fast positioning time <2 second, with Position feedback. This can be set to linear or equal percentage.

To do the tuning the outer loop was disabled. This was done by setting X3 as a Digital Input, setting X3 to Cascade On in the Control Loop. Then X3 and B were linked with a jumper wire. A temperature sensor was located at the exit from the fans on one of the fan units. The Integral and Differential factors were set to zero and then a step input of 2°C was demanded. The temperature at the fan outlet was then recorded at 1 second intervals.

The tuning procedure was to increase the gain until oscillation was constant and then to use the Ziegler-Nichols method to determine the new proportional, integral and differential parameters. The gain when oscillation started is the ultimate gain $K_u$. The period of oscillation is $P_u$. The Ziegler-Nichols tuning rules aim for a quarter-amplitude damping response. With quarter-amplitude damping, the process variable oscillates around the set point after a set point change or disturbance. The oscillation dies out at a rate in which each successive peak is one-quarter the amplitude of the previous peak.

The Siemens controller uses a function called Xp which is called the proportional band. Proportional band = 100/gain. So that the controller output = error x 100 / proportional band. For the Siemens controller the proportional band (XP) unit is °Kelvin (K). So for a XP setting of 5K a 1°C error will produce a controller output of 20. At a XP value of 10K the controller output would be reduced to 5. The Xp value was decreased until oscillation was constant. See Figure 27. Constant oscillation occurred at a Xp value of 0.7K and the cycle time was 150 seconds.

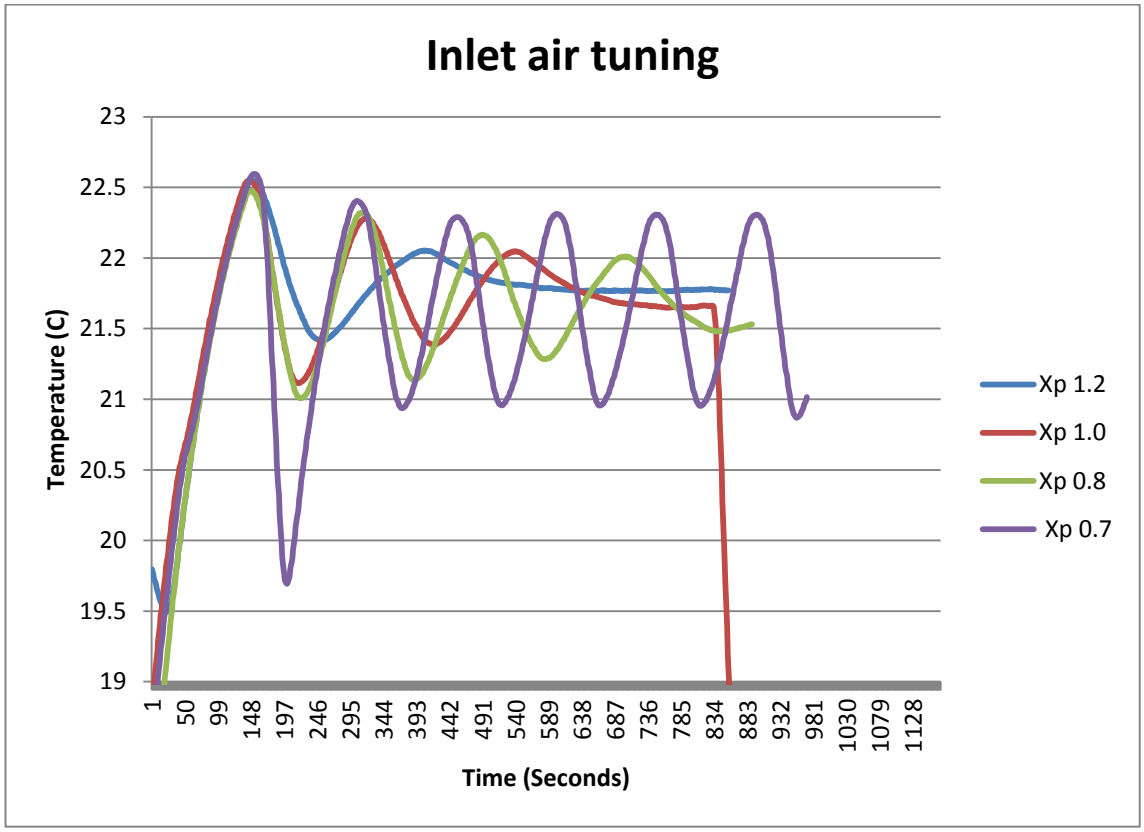


**Figure 27 – Temperature profiles for different Xp values**

Using Kp=1/Ku of 1/0.7 and $T_d$ = 150 seconds

The new tuning parameters using the Ziegler-Nichols method are shown in Table 15.

| | **$K_c$** | **$t_i$** | **$T_d$** |
|---|---|---|---|
| Ziegler-Nichols | 0.6 $K_u$ | $P_u/2$ | $P_u/8$ |
| | Kp = 1.2 | 1min 15 Sec | 19 seconds |

**Table 15 – Ziegler-Nichols parameters**

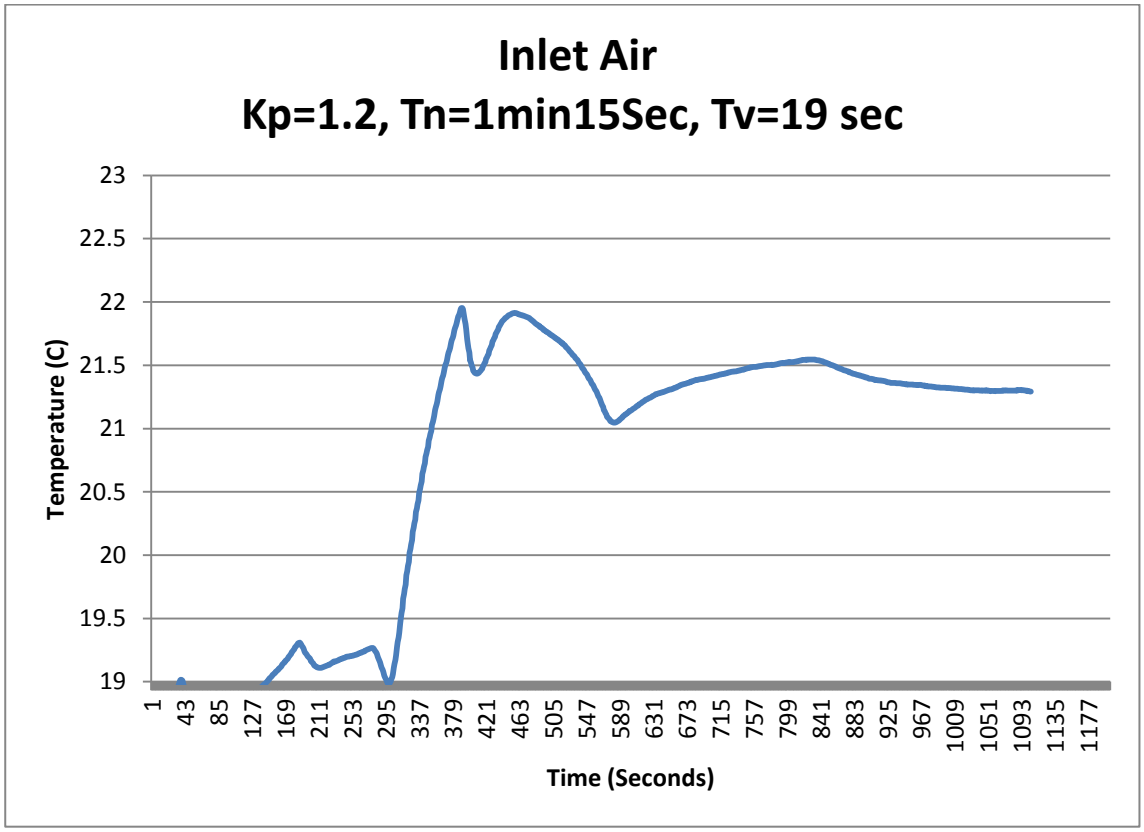


**Figure 28 – Tuning result with Zeigler-Nichols parameters**

The controller was reprogrammed and again a 2°C step demand was made and the temperature profile plotted. This seemed to show a rather aggressive proportional factor so an alternative tuning parameter based on Tyreus-Luyben was tried.

The tuning parameters using the Tyreus-Luyben method are shown in Table 16.

| | **$K_c$** | **$t_i$** | **$T_d$** |
|---|---|---|---|
| Tyreus-Luyben | $K_u/2.1$ | 2.2 $P_u$ | $P_u/6.3$ |
| | Kp = 1.5 | 5 min 30 sec | 24 sec |

**Table 16 – Tyreus-Luyben parameters**

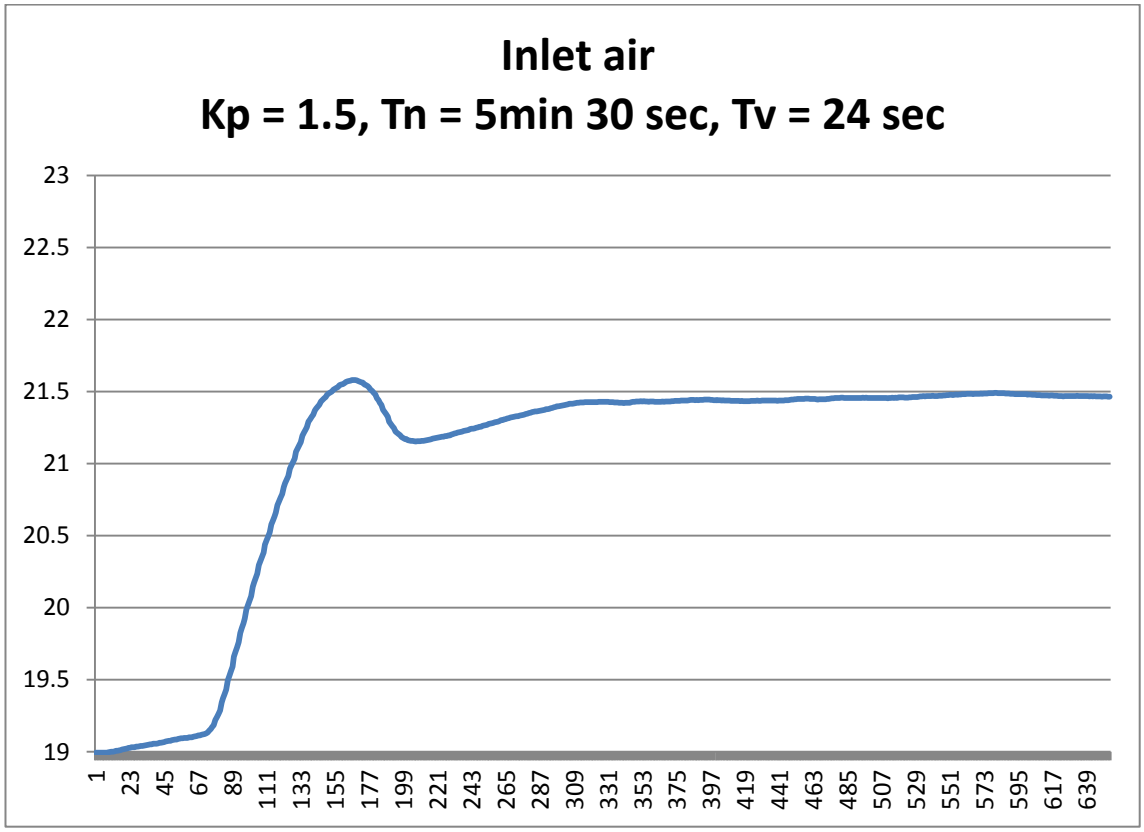


**Figure 29 – Tuning results with Tyreus-Luyben parameters**

This seemed to give a very good result and so a long term stability test was performed over 24 hours. This however showed very marked periods of instability. The reasons for this was not clear.

The water temperature seemed to be constant and the control valve can operate quickly. The control valve characteristic can be set as either equal percentage of linear control. The factory setting was equal percentage, this means that flow capacity increases exponentially with valve travel, so equal increments produce an equal percentage change in the flow. This was changed to linear, this required a larger Xp value, but otherwise did not seem to make any difference to the frequency of the spikes. The Xp value was further increased.

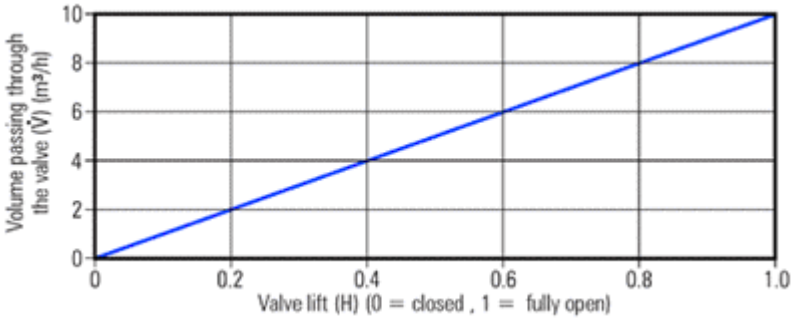


**Figure 30 – Linear valve characteristic**

**(spiraxsarco 1, 2012)**

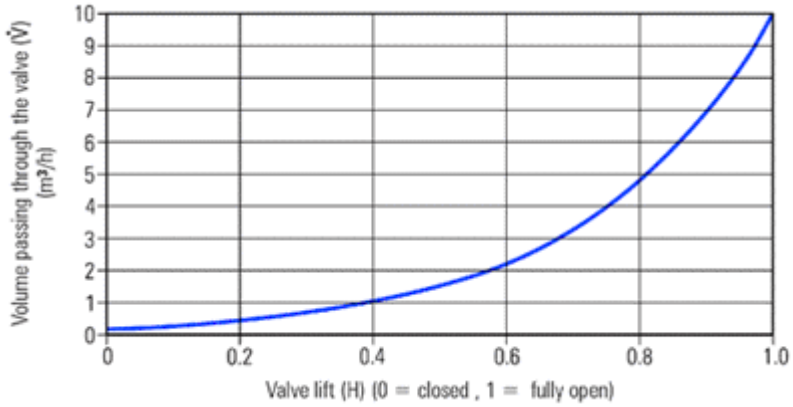


**Figure 31 – Equal percentage valve characteristic**

**(spiraxsarco 2, 2012)**

Tuning is continuing with the aim to eliminate the wild fluctuations and produce stable temperatures within ± 0.2°C.

These tests show that changing the PID parameters can have a big effect on the hutch temperature stability. And it is essential that Diamond staff have the competence and equipment to do this quickly and effectively. A data logger is essential in order to do the tuning and as well as temperatures it would be useful to be able to monitor water temperature, valve position and the input signals from the air temperature sensor and the fan coil outlet temperature sensors. Tuning can only be carried out when the hutch is not being used and so needs to be during shutdowns.

### 3.15.3 Figure of merit

The distortion due to heat load is not just affected by the thermal expansion but other thermal properties such as thermal conductivity. If heat can be transported throughout the material more evenly then the peak temperatures are reduced and the peak distortions reduced.

Newport Spectra Physics use a figure of merit which they call Geometrical Precision when comparing materials. This figure of merit = Thermal conductivity / (thermal expansion x Specific Heat capacity x Density).

An FEA analysis was performed on a block of material with a heat load applied at one end and cooled on two faces on the lower face. The maximum deflection was calculated for materials similar to aluminium but with different coefficients of thermal expansion and different thermal conductivity. The block has nominal dimensions of 200 x 50 x 100mm.

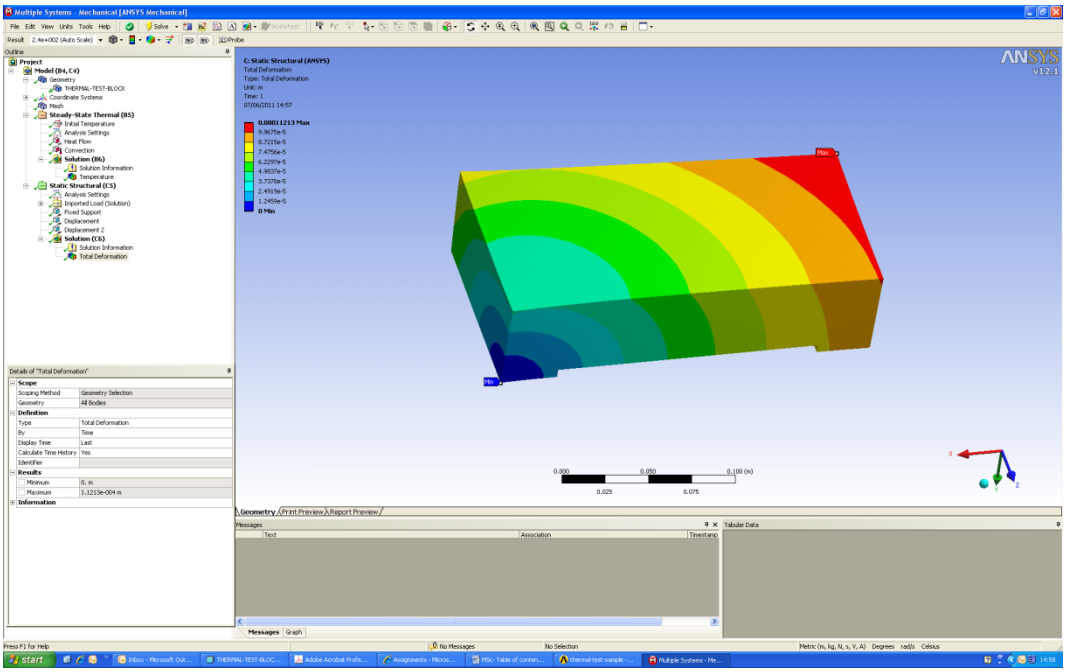


**Figure 32 –Temperature distribution of block**

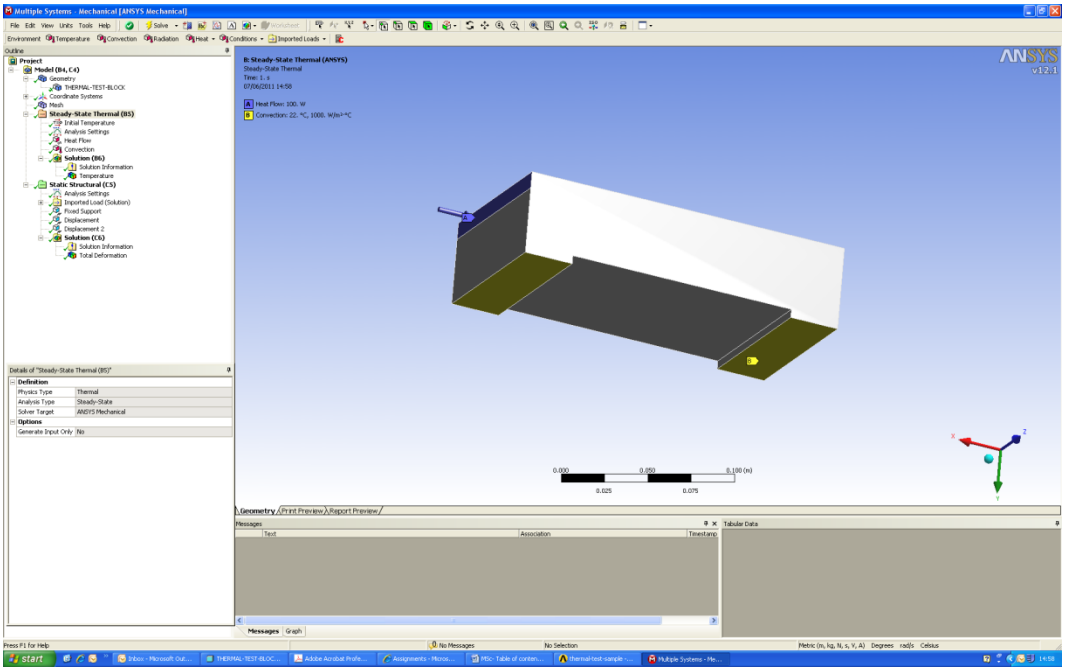

**Figure 33 – Location of constraints of block**

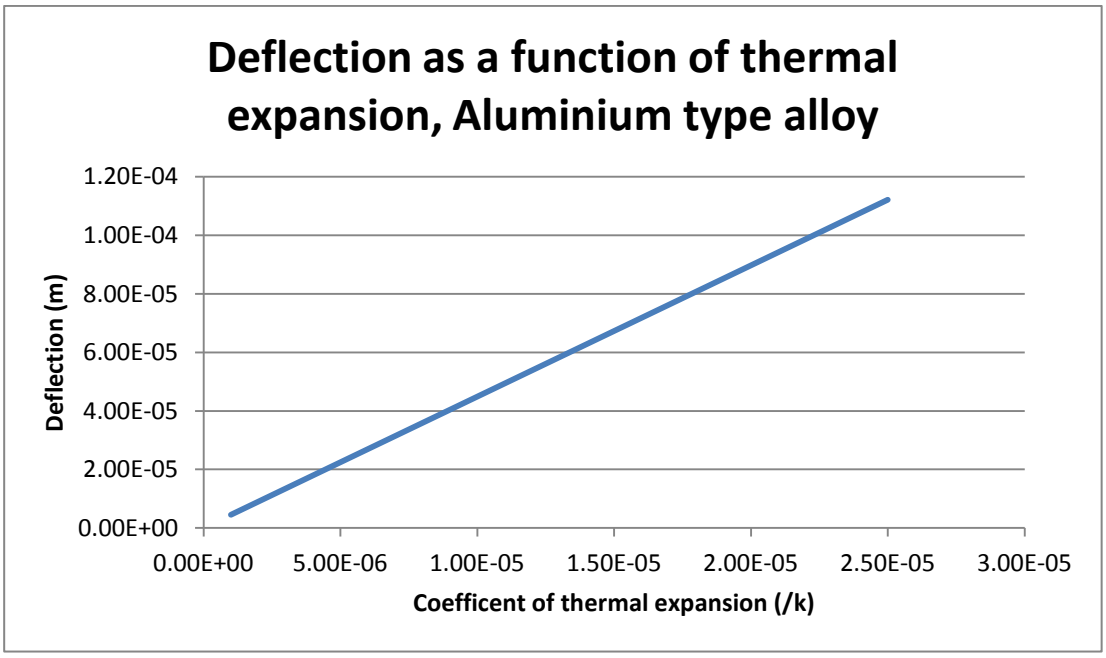


**Figure 34 – Deflection of Aluminium as a function of thermal expansion**

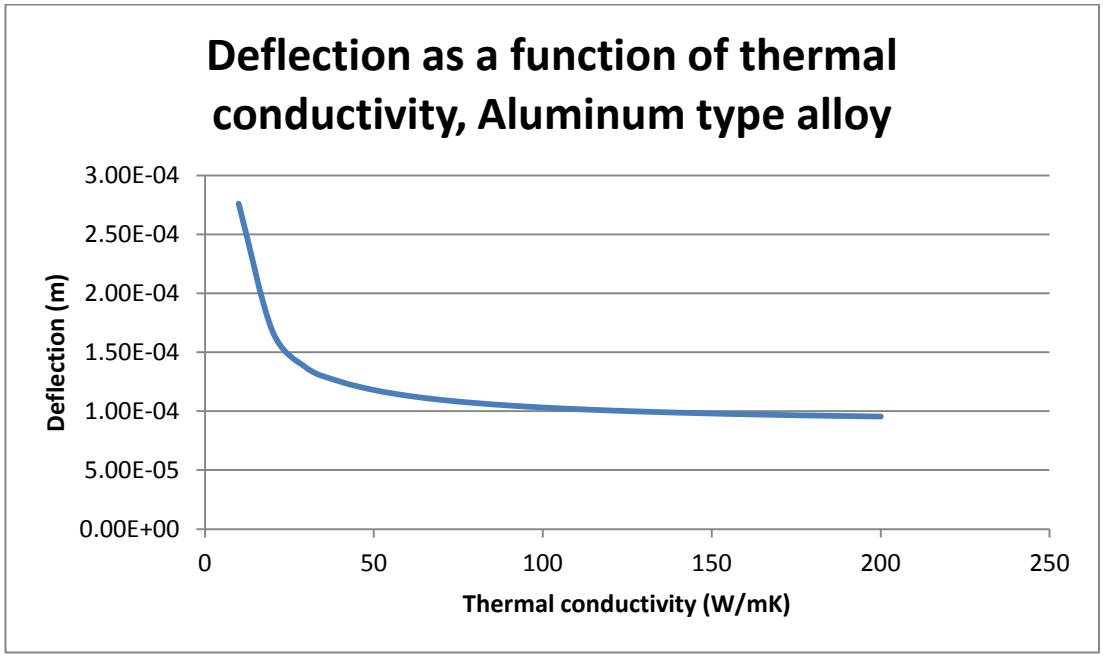


**Figure 35 – Deflection of Aluminium a a function of thermal conductivity**

The results show that as expected the deflection increase linearly with the change in coefficient of thermal expansion. The increase in thermal conductivity does show a reduction in deflection but this is far from linear. There is a sudden decrease and then a very small improvement. This shows that thermal conductivity will help but taking a simple ratio can be misleading. The results are dependent upon the shape of the component, the heat load and cooling details and the method of constraining the component.

## 3.16 Temperature measurement

The common methods of measuring temperature are Thermocouples, Resistance thermometers, thermisters and silicon diodes. The advantages and disadvantages of these devices are considered below.

### 3.16.1 Thermocouples

In 1826 Thomas Seebeck discovered that if two wires of different materials are joined at each end and there is a temperature difference between the two junctions then a small current will flow. This effect is called the Seebeck effect and such a device is called a thermocouple. There are many types of thermocouples using a variety of

dissimilar metals. Each type of thermocouple has different characteristics, some are suitable for cryogenic temperatures, some very high temperatures.

| Type | Material A | Material B | Temperature range (°C) |
|---|---|---|---|
| J | Iron | 55% Copper- 45% Nickel (Constantan) | 0 to 750 |
| T | Copper | 55% Copper- 45% Nickel (Constantan) | -250 to 350 |
| K | Nickel-10% Chromium (Chromel) | Nickel- 2% Aluminium (Alumel) | -200 to 1250 |
| E | Nickel- 10% Chromium (Chromel) | 55% Copper- 45% Nickel (Constantan) | -200 to 350 |
| N | Nickel 14.2% Chromium -1.4% Silicon | Nickel- 4.4% Silicon 0.1% Magnesium | -270 to 1300 |
| S | Platinum- 10% Rhodium | Platinum | 0 to 1450 |
| R | Platinum- 13% Rhodium | Rhodium | 0 to 1450 |
| B | Platinum- 30% Rhodium | Platinum- 6% Rhodium | 0 to 1700 |
| C | 95%Tungsten- 5% Rhenium | 74%Tungsten- 26% Rhenium | Up to 2800 |
| L | Iron | Copper- Nickel | -200 to 900 |
| U | Copper | 55% Copper-45% Nickel (Constantan) | |

**Table 17 - Thermocouple materials**

Thermocouples are often used to measure temperatures on equipment that is some distance away and so to reduce the cost of cabling compensating or extension cable is often used. Extension cables exhibit the same voltage and temperature characteristics as thermocouple cable but over a limited temperature range. Compensation cables use a substitute material and exhibit similar voltage and temperature characteristics as thermocouples over a limited temperature range but are less accurate than extension cables.

The thermocouple can only detect a temperature difference between one junction and the other. The National Institute of Standards and Technology (NIST) thermocouple reference tables tabulate the voltage generated by different temperatures at the hot junction with the cold junction held at 0°C in an ice bath. Holding the cold junction at 0°C is not practical so a more practical solution is to measure the temperature at the cold junction with a thermister and then subtract the parasitic thermocouple contribution. This process is called cold junction compensation.

In addition to the problem of cold junction compensation thermocouples have a number of other disadvantages. Because of the low voltages generated, Thermocouples are susceptible to noise from 50Hz mains so a low band 2Hz or 4Hz filter is usually applied. The voltage generated by a thermocouple is not linear and so some form of linearization must be performed. Thermocouples when used at high temperatures will age and so will appear to drift. The small voltage generated requires sensitive instrumentation and the accuracy is limited.

Thermocouples are available in three Tolerance classes. This is a measure of the error between the measured and true temperature. For a K type at room temperature class 1 is ±1.5°C, class 2 and 3 is ±2.5°C.

### 3.16.2 Resistance thermometers

The resistance thermometer is a device that measures the resistance across a device whose resistance varies with temperature. The most common type is a platinum resistor that has a resistance of 100 ohms at 0°C, called a PT100. These devices can have two, three or four wires. The best is a 4 wire device. In the 4 wire case 2 wires are used to measure the voltage drop across the resistor and 2 wires are used to supply the driving current. This eliminates any measurement of the resistance of the cables which connect to the resistor which may be much larger than 100 ohms and produce errors.

Resistance thermometers are also affected by electrical noise and so should be screened with one end grounded. The resistance change is also not linear with temperature.

Like thermocouples, resistance thermometers are manufactured to different tolerence grades. These are stated in IEC751 and are as follows; at 0°C Class A is 100 ±0.06 Ω, class B is 100 ±0.12 Ω, 1/3 DIN is 100±0.04 Ω and 1/10 DIN is 100 ±0.012 Ω. This equates to errors at 20°C as follows: Class A (±0.15 °C); class B (±0.3°C); 1/3 DIN (±0.1 °C) and 1/10 DIN (±0.03 °C).

There are also devices with resistance of 500 and 1,000Ω at 0°C called PT500 and PT1000 and devices that use nickel or copper instead of platinum.

There are two types, wire wound and thin film. The wire wound type are typically 1 to 5mm in diameter and 10 to 50mm long and wound around a glass or ceramic former. The other type are composed of a thin film deposited on a ceramic substrate. The thin film devices are smaller and give a faster response.

### 3.16.3 Thermisters

A thermister is a device whose resistance changes a large amount with a small change in temperature. There are two types, either a negative (NTC) or positive (PTC) resistance/temperature coefficient. PTC thermisters are manufactured from semiconductor material and NTC are manufactured from oxides of manganese, cobalt, copper and nickel.

PTC thermisters are of a switching type where the resistance rises suddenly at a critical temperature. This type of device is often used to sense when objects exceed a critical temperature. NTC thermisters are best suited for precision temperature measurement. Thermisters are non-linear and a third order approximation is required to convert the measured resistance to a temperature. This equation is called the Steinhart-Hart equation. The resistance of thermisters are much higher than traditional RTD's, the resistance of the connecting cables is proportionally less and so 2 wire connections to thermisters is usual, rather than the 3 or 4 wires required for

RTD's. Thermisters can also be made in smaller sizes than RTD's with faster response times Thermisters are more sensitive to RTD's. Table 18 shows the resistance values at 25 and 26° C for a thermister and two RTD's.

| Device Type | Resistance at 25 °C (Ω) | Resistance at 26°C (Ω) | % change |
|---|---|---|---|
| 10KΩ Thermister | 10,000 | 9,572 | 4.4 |
| PT100 | 109.73 | 110.12 | 0.35 |
| PT1000 | 1097.3 | 1101.2 | 0.35 |

**Table 18 - Resistance values for thermister and RTD's**

Thermisters will self heat and as the thermister changes temperature the resistance will change, there is therefore a settling time. A measure of this is the dissipation constant which is given by the manufacturers for each device. This is given in mW/°C, however this is usually for a device suspended by its leads in still air and may not be representative of its characteristics in its actual operating conditions.

## 3.17 Trends in current research and development

Low thermal expansion material development seem to be driven by the needs of many industries including semiconductor industry, astronomy , space science and electronic packaging. There is much research work published on novel ceramics (Poowancum, 2010) and composites (Garcia-Moreno, 2010). There seems to be less research into carbon fibre composites and this may because of their limited use at elevated temperatures. Thermal management of electronics is a big issue and much work is done on suitable materials (Sugimura, 2008). New forms of aluminium alloys embedded with fibres or whiskers are appearing which offer reduced thermal expansion.

Manufacturers of metrology equipment continue to use Granite with some parts in low thermal expansion ceramics and silicon carbide. Equipment for the semiconductor industry is also incorporating Silicon Carbide, in this case high throughput requires fast accelerations so high stiffness low density materials are gaining popularity.

Temperature control is important for precision metrology equipment and VUV lithography steppers but research in precision temperature control is not as extensive as low thermal expansion materials. However much use seems to be made of Peltier devices for fine control. (Heuberger, 2001).

There are a number of systems described using insulated boxes and peltier heat exchangers for precision temperature control and there are some patents on their use.

Phase change materials research is concentrated on their use for building energy recovery systems and research into their use for precision temperature control does not seem to be evident.

There are many types of thermal insulating materials for ambient use and development is primarily at materials suitable for non ambient conditions.

## 3.18 Recommendations to improve thermal stability

### 3.18.1 Materials

Move away from the general use of Aluminium Alloys to Carbon steel.

Consider the use of 36%Nickel/Iron alloys for critical components.

Develop a favoured supplier for machined items from 36% Nickel/Iron alloys to reduce costs.

Use low CTE encoder scales for critical applications.

Consider the use of Low CTE Carbon fibre breadboards where appropriate.

Investigate alternative suppliers of low CTE Carbon Fibre tube.

Expand the use of natural granite.

Monitor developments of phase change materials, particularly any research into materials suitable for metrology equipment including materials embedded in metallic foams.

Investigate if some organic PCM's could be used.

Agree a standard insulating foam for use at Diamond.

### 3.18.2 Design

Consider using block shapes where thermal mass is larger and the surface area to volume is lower.

Remove high heat load devices from the critical area as much as possible.

Isolate critical components with thermally insulated enclosures.

Replace high heat load generating components with lower heat generating devices.

Minimise internal air volumes.

Increased use of a separate metrology frame.

#### 3.18.2.1 Temperature control

Consider using peltier devices for high stability applications

Agree a standard peltier controller for use within Diamond

Investigate the electronics required to support thermister temperature monitoring instead of PT100s.

#### 3.18.2.2 Hutch temperature control

Implement a programme of data collection of hutch conditions.

Use 3D computational fluid dynamics software to model air flows and temperatures.

Investigate if any of the following could improve hutch stability:

- Adding thermal insulation on walls and roofs
- Reducing air leakage
- Adding porch

# Chapter 4. Vibration stability

## 4.1 Sources of vibration at Diamond

Vibrations are transmitted to components through the concrete floor. At Diamond measurements have shown that the major sources of vibration and their frequency are pumps and fans. Located on the same campus is the ISIS Pulsed neutron and muon Source and the magnets pulse at 50Hz and during ISIS operation these vibrations can be seen. In addition during periods of high wind the building resonates at 3 Hz.

| Source | Frequency (Hz) |
|---|---|
| Wind (Building) | 3 |
| Control and Instrumentation Area Air handling units | 16 & 18 |
| Demineralised Water pumps | 25.4 |
| ISIS Magnets | 50 |

**Table 19 – Sources of vibration**

The experimental hall floor is a reinforced concrete slab supported on concrete piles. The experimental hall is a separate slab to the slab that supports the building structure and cranes so that vibration transmission is reduced. Although the vibrations are small these are measurable and do affect beam stability.

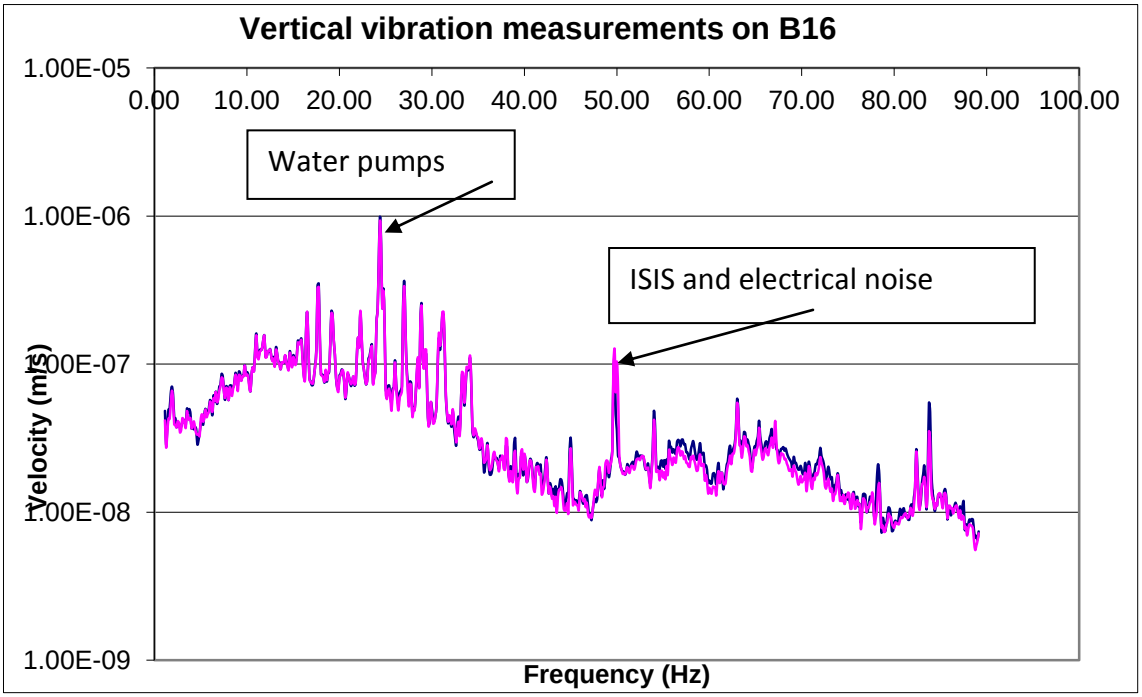


**Figure 36 – Vibration measurements on B16**

Measurements on B16 experiment hutch floor were carried out using HBA-L1 Ultra low frequency vibration gauges from the Institute of Engineering Mechanics, China Earthquake Administration. Dip switch 2 ON (Small velocity). Bandwidth 1 – 100 Hz. These were connected to a Data Physics Quattro signal analyser. These results show frequencies at approximately 16, 17, 19, 22, 24, 27, 28, 31, 34, 44, 50, 53, 63, 78 and 83 Hz

## 4.2 Vibration criteria

A vibration criteria has been established for facilities requiring low vibration environments. The VC criteria was developed in the 1980's (Amick, Gendreau, Busch, & Gordon, 2005) and was pushed by the USA Institute of Environmental Sciences and Technology. In the 1990's a further criteria, NIST-A was developed by the Advanced Measurement Laboratory at the U.S. National Institute of Standards and Technology (NIST). The NIST-A criteria differ from the VC criteria in that the NIST-A is a mixture of displacement and velocity, where the VC criteria are pure velocity. These criteria are shown in Table 20.

| Criteria | Definition |
|---|---|
| VC-A | 260µg between 4 and 8Hz<br>50 µm/s between 8 Hz and 80 Hz |
| VC-B | 130 µg between 4 Hz and 8 Hz<br>25 µm/s between 8 and 80 Hz |
| VC-C | 12.5 µm/s between 1 and 80 Hz |
| VC-D | 6.25 µm/s between 1 and 80 Hz |
| VC-E | 3.1 µm/s between 1 and 80 Hz |
| VC-F | 1.6 µm/s between 1 and 80 Hz |
| VC-G | 0.78 µm/s between 1 and 80 Hz |
| NIST-A | 0.025µm between 1 and 20Hz,<br>3.1µm/s between 20 and 100 Hz |

**Table 20 – Vibration criteria**

The vibration criteria is based upon 1/3 octave band analysis.

| Band No | Centre Frequency (Hz) | Lower frequency (Hz) | Upper Frequency (Hz) |
|---|---|---|---|
| 20 | 100 | 89.1 | 112 |
| 19 | 80 | 70.8 | 89.1 |
| 18 | 63 | 56.2 | 70.8 |
| 17 | 50 | 44.7 | 56.2 |
| 16 | 40 | 35.5 | 44.7 |
| 15 | 31.5 | 28.2 | 35.5 |
| 14 | 25 | 22.4 | 28.2 |
| 13 | 20 | 17.8 | 22.4 |
| 12 | 16 | 14.1 | 17.8 |
| 11 | 12.5 | 11.2 | 14.1 |
| 10 | 10 | 8.91 | 11.2 |

| | | | |
|---|---|---|---|
| 9 | 8 | 7.08 | 8.91 |
| 8 | 6.3 | 5.62 | 7.08 |
| 7 | 5 | 4.47 | 5.62 |
| 6 | 4 | 3.55 | 4.47 |
| 5 | 3.15 | 2.82 | 3.55 |
| 4 | 2.5 | 2.24 | 2.82 |
| 3 | 2 | 1.78 | 2.24 |
| 2 | 1.6 | 1.41 | 1.78 |
| 1 | 1.25 | 1.12 | 1.41 |

**Table 21 – 1/3 band analysis frequency bands**

Taking the measured results and then summing the measured values of each band gives the results shown in Figure 37. This shows that the floor vibrations just about meet the VC-D criteria.

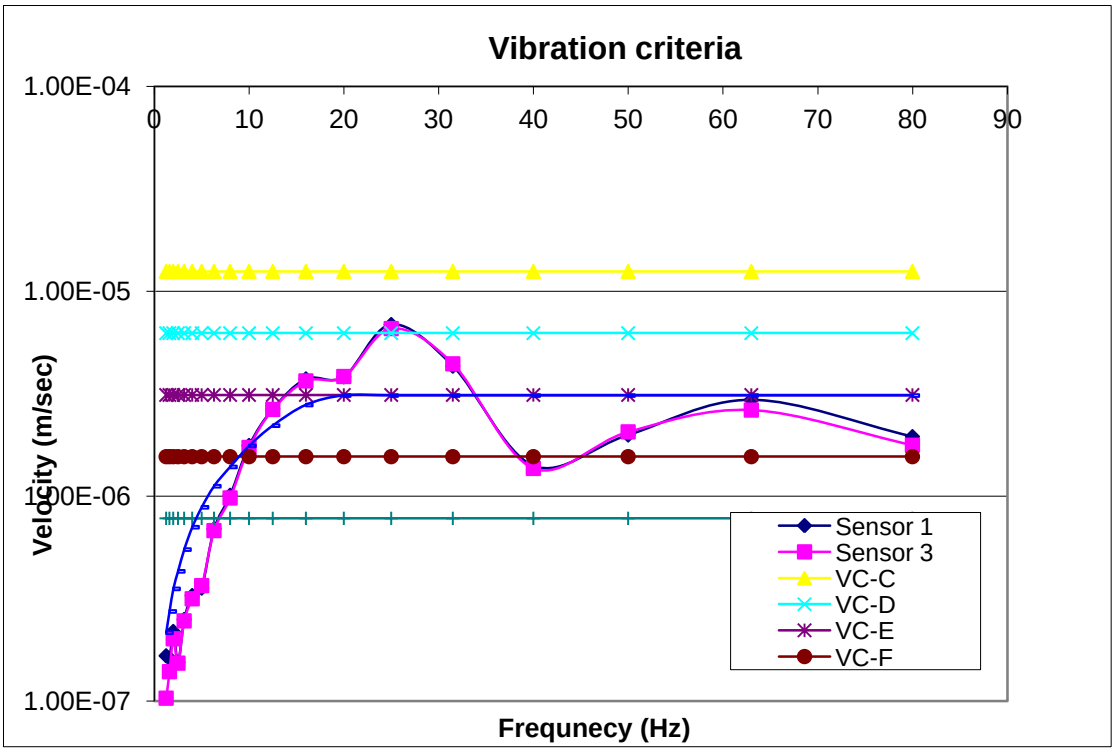


**Figure 37 – Vibration criteria**

The Deutsches Elektronen-Synchrotron publish measurements from other facilities and these are given is a Power Spectral Density over the range 0.02 to 80 Hz. Other methods used to compare sites are displacement rms with 15nm or less classifies as “quiet” and the rest as “noisy.

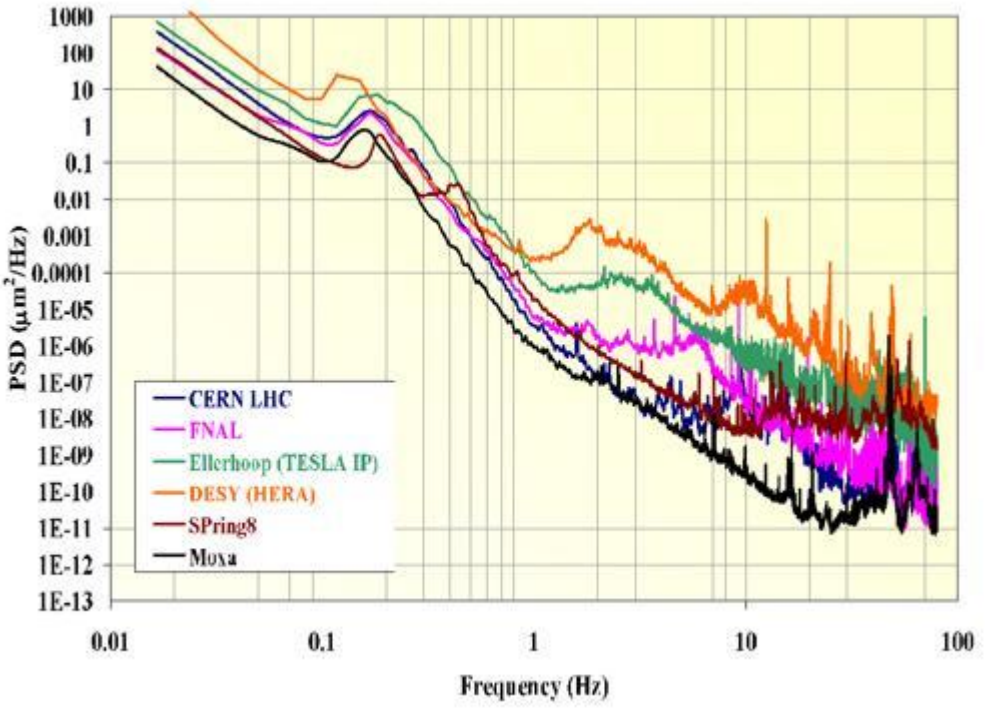


**Figure 38 Ground vibrations measured at various sites.**

(Desy, 2012)

## 4.3 Transmissibility and resonance

Vibrations from the floor are transmitted through supporting structures and will affect beam stability. The vibrations are often amplified by the supporting structure and if the resonant frequencies of the supports are at the same frequency the amplification can be quite large.

Vibration tests measuring displacement show that the displacements are low but at some frequencies they can be above 10nm. If the long term aim is to be able to focus

10nm sized beams then the ideal would be to have vibrations which are less than 10% of the focussed beam size, hence 1nm.

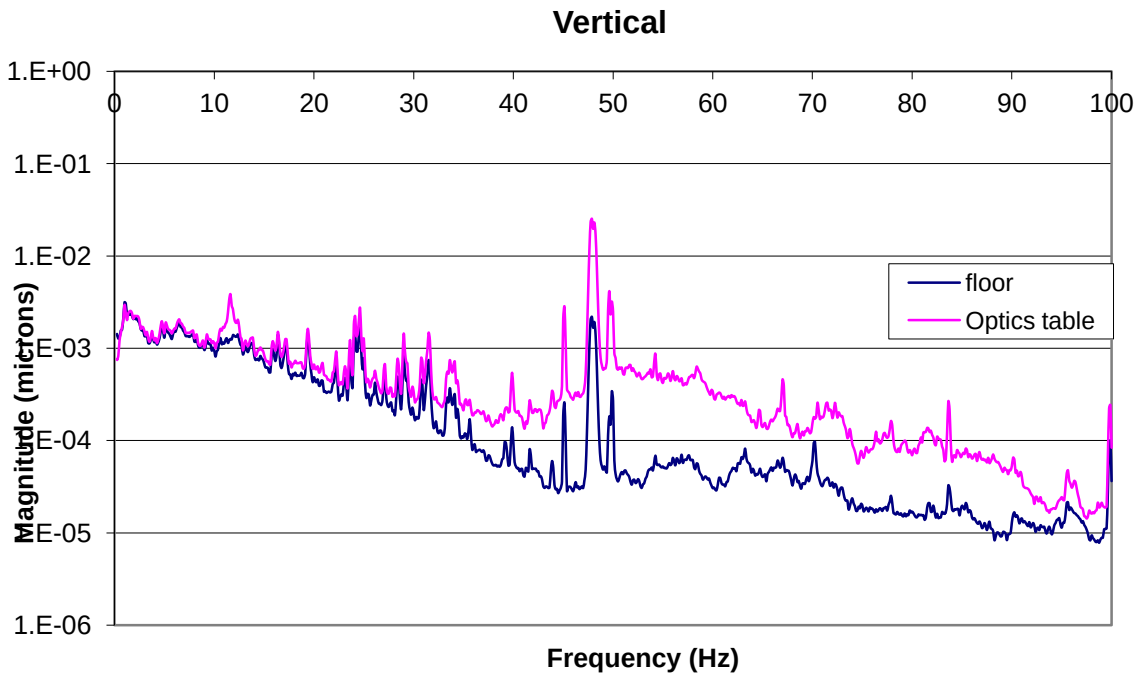


**Figure 39 – Vibration displacement measurements**

To achieve very low levels of vibration the following methods can be applied.

- Isolate using external passive means
- Isolate using external active means
- Internal passive damping
- Improve stiffness
- Reduction of vibration at source

## 4.4 External passive vibration isolation

### 4.4.1 Introduction

Traditional spring and damper arrangements are often used to provide vibration isolation. These systems however have a critical frequency at which resonance occurs. Below this critical frequency the transmissibility is unity and it is only well above the critical frequency that the transmissibility reduces. The critical frequency is related to

the mass and spring constant. To get critical frequencies below a few Hz the spring must be very soft and is not practical.

### 4.4.2 Minus K negative spring system.

Minus K Technology Inc, have developed a vibration isolation platform using negative stiffness springs. This is based upon a vertical spring and a weak flexure pivot with springs acting in an orthogonal direction. By matching the stiffness of these springs a net stiffness of close to zero can be obtained.

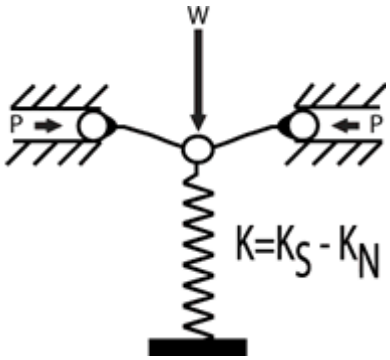


**Figure 40 – Negative stiffness spring**

**(minusk, 2012)**

Test results of a minus K bench top isolation system are presented in Appendix C.

### 4.4.3 Pneumatic isolators

Pneumatic isolators are a common method of supporting optical tables and isolating them from floor transmitted vibrations. The isolator consists of a reinforced rolling rubber diaphragm which forms a seal between a piston and an air reservoir. The pressure in the reservoir is controlled by a height control valve. These devices have a resonant frequency that is independent of the mass of the table. The load capacity is defined by the air pressure and area of the piston. The resonant frequency is approximately as :

ω0 resonant frequency,  is the gas constant, g is acceleration due to gravity, A is the piston area, V is the volume of the compressed gas reservoir.

These devices have limited horizontal isolation. Any changes in the load of the table such as motion of the payload or touching the pay load by users will lead to quite large motions. Although the table will return to its original position this is defined by quite a crude valve so its actual position may not be repeatable within a few millimetres.

Results of some tests of a small pneumatic isolator system are presented in appendix D

## 4.5 External active vibration isolation

### 4.5.1 Introduction

An active vibration isolation systems uses a sensor to detect vibration and then uses this signal to feedback to an actuation system which supports the table and corrects the table position to reduce the vibration. One of the critical issues is the suitability of the sensor. The sensor has to accurately measure vibrations down to low frequencies and also produce very low levels of noise.

Another issue is the actuator. This needs to produce large forces to provide accelerations of the table and operate with a high band width. Piezo actuators are one solution as they can produce relatively large forces, however to operate at high frequency the limitation can often be the electronics controller to provide sufficient current to drive the piezo. So piezos may only be suitable for low mass systems Another solution is to use voice coil actuators or Giant Magnetostrictive devices. Some ideas on a piezo operated anti vibration system based on distance feedback are presented in Appendix E.

### 4.5.2 Kolibri system from TNO

TNO Industrie en Techniek in The Netherlands have produced a system called Kolibri. To overcome the problem of a lack of a low frequency response sensor they have designed their own sensor which can measure down to 0.1Hz.  They claim that the motion of their table is 30x less than a passive table.

### 4.5.3 HWI Scientific Instruments

HWI manufacture small bench top systems suitable for Atomic Force Microscopes up to much larger systems. For the small systems they claim dynamic isolation between 0.7 to 1,000 Hz, with passive isolation beyond 1,000Hz. What is not certain is that for very low background vibrations is the sensor sensitive enough and indeed does the sensor generate more noise than the low vibrations that are to be counteracted?

The largest system is the AVI.600/LP which has a load capacity of 600Kg per individual unit. The dynamic range is 1.0 to 200Hz and purely passive beyond 200Hz.

### 4.5.4 Halcyonics GmbH

Bench top active vibration systems from Halcyonics are the Micro 40, 60 and 80 devices. The active bandwidth is 0.6 – 200Hz. Frequencies above this are isolated by the internal spring and damper passive isolation system. Load capacity is 100Kg

### 4.5.5 CERN Magnet isolation system

A team at CERN are designing a possible Compact Linear Collider which could be up to 48Km long. This linear accelerator would consist of 2,000 quadrupole magnets some of which would need move some tens of nm's every 20ms. Some initial tests have been done to incorporate an active vibration compensation system. The test used a Piezo actuator with a stroke of 25µm and a resolution of 0.1nm. The piezo included a capacitive position sensor. The sensor was a Guralp CMG-6T geophone with a frequency range of 0.03 to 100Hz. The controller was based on a National Instruments PXI-6289 card. Results on the test rig have shown a reduction in displacement of 3.5x at 1Hz during the day and a factor of 2x at night. (Collette, et al., 2010).

### 4.5.6 Giant Magnetostrictive Hybrid actuation system

There has been some work on building a vibration control systems using Giant Magnetostrictive actuators and pneumatic actuators in parallel. The tests showed that table accelerations were reduced by 10-15db in the 1-100Hz range. (Nakamuar, Nakayama, Yasuda, & Fujita, 2006)

## 4.6 Internal passive damping

### 4.6.1 Damping using shunted piezos

Piezos can be incorporated into structures and used to reduced vibrations. Due to the piezo effect some of the vibration energy in the structure can be transformed by the piezo material into electrical energy. This energy can then be dissipated through a shunt circuit. The most effective method is a tuned shunt incorporating an inductor, resistor and capacitor. Optimum damping is achieved by tuning the electrical resonance to the frequency mode to be damped. The problem is how to design the shunt circuit so that multi-modes are effectively damped (F Viana, 2008) and at low frequency the optimum inductance is very high. One solution is to use a synchronized switch damping circuit. (C Richard, 2000)

Physik Instruments have developed a range of so called patch piezos called DurAct™. The currently available sizes are 61mm x 35mm x 0.4 or 0.5 or 0.8mm thick. A larger range of sizes is being developed. The thicker DurAct can produce a blocking force of 775N. Another manufacturer is Mide Technology Corporation.

There is a great deal of research into using piezo devices as energy harvesting. These devices act like tuned dampers. Within the outer casing is thin strip of piezo material that is free to vibrate and generate a current. The piezos are tuned by adding mass to the tip. Currently these require significant accelerations (0.2g) to produce any useful energy but the development of cheaper electronics may allow the greater use of piezos for vibration damping at much lower levels. As an example, the electronic unit (EHE003) from Mide is designed to be used with two Volture™ piezos generating as low a voltage as 400mV. They are however still expensive with a single stack cost $300 and $60 for the electronics.


**Figure 41 – Volture piezo energy harvester**

**(Mide, 2012)**

### 4.6.2 Damping using visco elastic materials

Adhesive films or pads are available manufactured from energy dissipative visco-elastic material. The material properties are characterized by its shear modulus G and loss factor η. The stored energy is proportional to G and the fraction of stored energy dissipated by damping is proportional to η. These are vibration frequency and temperature dependant. At the APS vibration in the main synchrotron girders was reduced by using support plates consisting of 3 layers of 1.6mm thick stainless steel plates and 2 layers of VEM 0.15mm thick Anatrol-217. An example is a damping adhesive from Roush called RA218. This is a permanent pressure sensitive acrylic based adhesive formulated to have high damping for joining dissimilar materials. The graphs show the change in loss factor and shear modulus with increasing temperature and frequency.

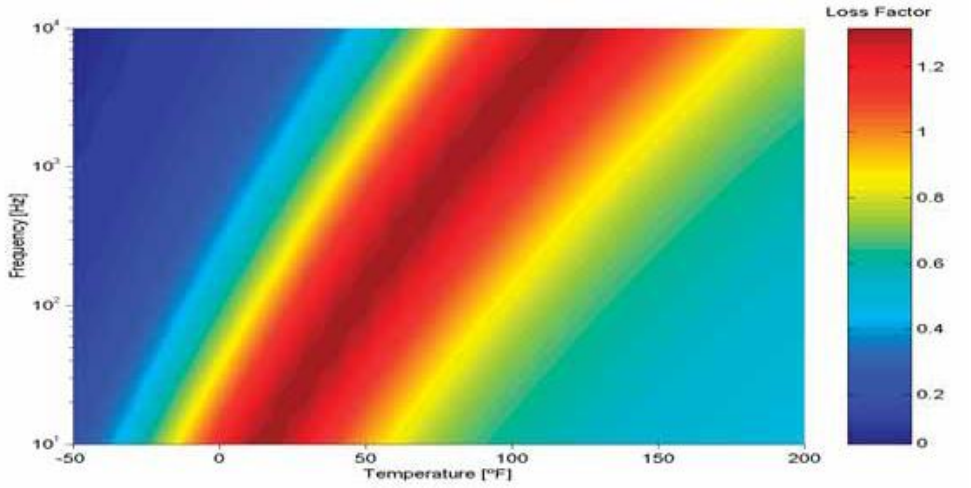


**Figure 42 – Loss factor of RA218 against temperature and frequency**

**(roush 1, 2012)**

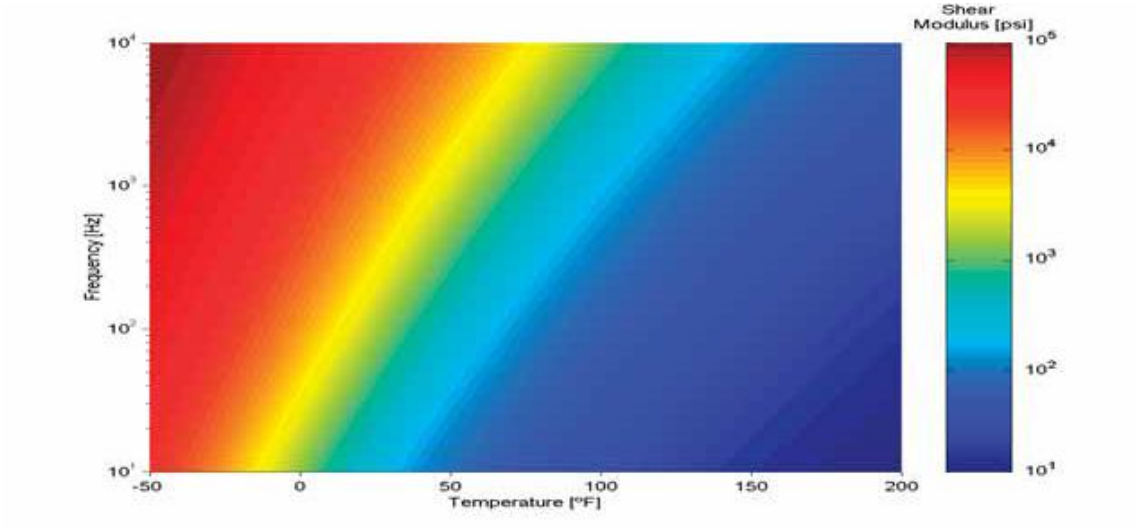


**Figure 43 – Shear modulus of RA218 against temperature and frequency**

**(roush 2, 2012)**

### 4.6.3 Constrained layer damping

Constrained layer damping (CLD) is a technique where layers of damping material are embedded into the structure or fixed to structure surface. It is important that the effective modulus of the CLD and structures effective modulus is matched and that the CLD material covers between 30-90% of the structure surface.

Effective modulus = thickness x modulus

An example of a suitable material is 3M Viscoelastic damping polymer 100 VHB adhesive transfer tapes 9460, 9469, 9473.

Constrained layer damping has been used at the Advanced Photon Source to reduce amplification of vibrations to the magnet girders. They have shown improvements of a factor of 4-6. (Mangra, Sharma, & Doose, 2000)

### 4.6.4 Structural damping

Structural or Hysteresis or hysteretic damping is the energy lost due to friction between molecules related to displacement during vibration. A measure of this lost energy is called the loss factor. The Loss factor is frequency dependant. Some manufacturer's data give the damping ratio rather than the loss factor. Loss factor $\eta$ = 2 x damping ratio $\xi$.

| Material | Loss factor |
|---|---|
| Aluminium | $0.3 – 10^{-5}$ |
| Lead | $5 – 30^{-2}$ |
| Lead with Antimony | $1 – 4^{-3}$ |
| Steel | $0.2 – 3^{-4}$ |
| Neoprene | 0.1 |
| Butyl rubber | 0.4 |
| ISODamp C-1002<br>EAR Speciality composites | 0.93 @ 10 Hz |

**Table 22 – Loss factors for some materials**

Polymer Granite (concrete) has been preferred over cast iron for precision machines such a lathes and milling machines. Some tests showed that composite samples, with weight fractions of about 80% of granite and 20% of epoxy, presented damping properties approximately three times greater than gray cast iron.

Paragon Manufacturing Inc, produce a sandwiched steel panels consisting of metal/plastic/metal which is available in steel or Aluminium.

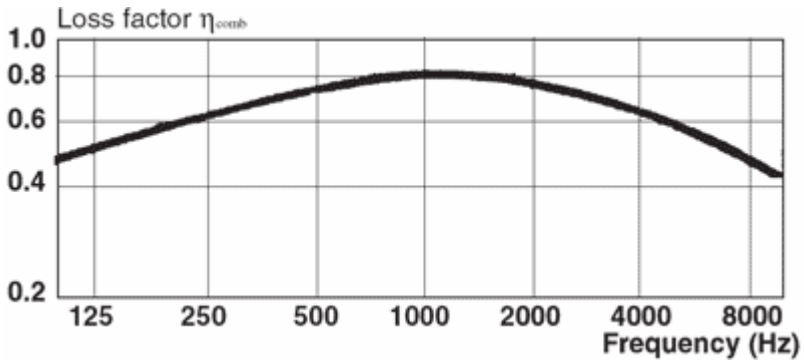


**Figure 44 – Loss factor of Paragon MPM**

**(noisedamp, 2012)**

Rubber anti-vibration mounts operate with hysteric damping. These mounts are often used for supporting devices such as fans and pumps that produce vibrations. It is important that the mount is correctly sized for the system to be supported. If the mount is overloaded the mount can compress completely and bottom out and so increase the stiffness of the mount. Rubber mounted systems will have a resonant

frequency at which point the transmissibility is greater than 1. In general the transmissibility does not reduce back to unity until the driving frequency is 1.4x the resonant frequency so it is important that the primary frequencies are well above this point. Elastomer mounts act as incompressible solids and so are manufactured into shapes that allow them to bulge under load. A useful indication of this is called the shape factor.

Shape factor = Area under load / Area free to bulge

A factor of between 0.5 and 1.0 has been found to be most suitable.

### 4.6.5 Tuned mass dampers

A tuned mass damper consists of a mass suspended by a spring and damper. CSA Engineering Inc sell small tuned mass dampers for machine supports. An example is the TMD05 which is 44mm in diameter, 36mm high and has an operating frequency range of 30-250Hz.

**Figure 45 – CSA Tuned mass damper**

**(csaengineering, 2012)**

Tuned mass dampers however only removes energy at specific frequencies and must be at least 3-10% of the structures mass.

### 4.6.6 Internal viscous damping

Internal viscous damping is a method of damping proposed by Slocum. This consists of damping beams located within the structure. A high viscous fluid, such as super high

viscosity silicone (GE Vascasil) is applied in the small gap between the damping beams and the structure. The damping beams are displaced from the structures neutral axis and so any bending creates a shear stress in the fluid and dissipates energy.

### 4.6.7 Damping using granular materials

Some suppliers use sand filled steel welded structures for some synchrotron components. But it is not apparent that this has been optimised. The damping does seem to be dependent upon the size, mass and type of granular material used and the damping is very frequency dependant. There has been some work on low mass polymer fills. (Park & Palumbo, 2009)

## 4.7 Vibration reduction at source

To reduce the possible electrical noise the original design of Diamond did not allow any electronic variable speed controls of motors. Motors operating common pumps and fans are therefore operating at exactly the same frequency (25.4 Hz) and so the vibration sources are at well defined frequencies. There may be opportunities for modifying the pump speed so that they are not all running at the same frequency and this may reduce the magnitude of the vibration source.

**Figure 46 – Water pump plinth and spring supports**

At diamond there are a large number of pumps for various cooling systems. These are mounted on inertia bases which are fixed to the floor via open coil springs. The coils springs are designed to isolate the vibrating pump from the floor. The pumps are connected to the pipes by flexible couplings and the pipes are suspended by hangars fitted with springs. Detailed measurements of each pump may be worthwhile, it may be found that the springs are not correctly sized or that some of the pumps are unbalanced or damaged. There may also be opportunities to use tuned mass dampers.

### 4.7.1 Summary

If the final focussing optics and the sample are rigidly mounted then in theory any vibrations will move all the components together. If the motion is true vertical or horizontal the effects on the focussed spot will be minimal because of the long distance to the source. Local pitch and yaw are however much more important. The problem is that the focussing optics and sample are not completely rigid. The mechanisms for moving and adjusting the components and the structures are to some extent flexible and so vibrations form the floor will affect the focussed spot.

One method is to make the system very rigid with resonant frequencies above 80Hz. This means using highly stiff actuators and supports. Bearings will be required to be very stiff and large force actuators will be required. Using this approach the vibration levels will never be better than the floor vibration levels.

A second approach is to use passive isolation devices. This could be done using rubber or pneumatic isolators. The problem with this is that the relationship between the final focussing optics and the source has to remain constant. Any disturbance to the system from either a moving mass or users changing samples will disturb this relationship and the system may not return to its original position. This solution is not seen as viable.

A third approach is to use active vibration control. Because of the active feedback this offers potential for a highly stable environment. There are still some issues. Are the sensors sensitive enough that there is a net reduction in vibration levels when the background vibration levels are very low? Can a system be designed so that is strong

enough to support the required mass and isolate from frequencies up to 100Hz? Most proprietary systems have passive isolation above 100Hz, can this be removed so that there is no variation in position over the long term?

It may be possible to use position feedback to a reference table for a pure active system. High speed FPGAs, capacitance sensors and high force actuators such as magnetostrictive or voice coil actuators could be a possible solution.

There are a number of ways to incorporate damping materials within the structure. Piezo patches look interesting but are currently not sensitive enough. Internal viscous damping could be incorporated into new structures but this is not an easy solution. Constrained layer damping has been used and this could be used on the main supports. Damping using granular materials is quite common for some steel fabrication supports but data on its effectiveness is sparse.

Reduction in source noise may benefit from further work. There is a proposal to operate the Demineralised water pumps at different frequencies but this would affect the cooling system performance so this is not being done yet. The use of tuned mass dampers could be investigated and the pump support system may not be fully optimised for the actual masses supported.

# Chapter 5. Acoustic stability

As well as vibrations transmitted through the floor, there are disturbances transmitted through the air as sound waves. Some experiment samples are very flexible and their position is affected by acoustic vibrations the main source of which is the air temperature control unit fans in the hutch ceiling.

## 5.1 Human ear response to sound

The human ear can detect noise intensities over a large range so a log scale is adopted called the Sound Intensity Level (SIL)

$SIL(db) = 10 \log10(I/I_{ref})$

The threshold of hearing ($I_{ref}$) is assigned the sound level of 0 decibels (0db) and is an intensity of $1 \times 10^{-12}$ W/m$^2$.

Another scale used is the sound pressure level (SPL)

$SPL = 20 \log10(P/P_{ref})$

The human ear does not respond equally well to all frequencies. So to better represent the perception of sound, filters are used. The A filter reduces the lower frequencies sounds and is used to represent perception of soft sounds at about 40db. The B filter approximates the ear for medium loud sounds. Filter C does not filter out as much low and high frequencies and approximates the ear at very high sound levels. It is used for traffic surveys and Filter D is used to measure aircraft flyovers.

Noise meters are fitted with selectable filters and will give a measurement of the Sound intensity level either as db(A), db(B), db(C) or db(D).

Db $LA_{eq}T$ is the equivalent continuous A-weighted sound pressure level having the same energy as a fluctuating sound over a specified time period T.

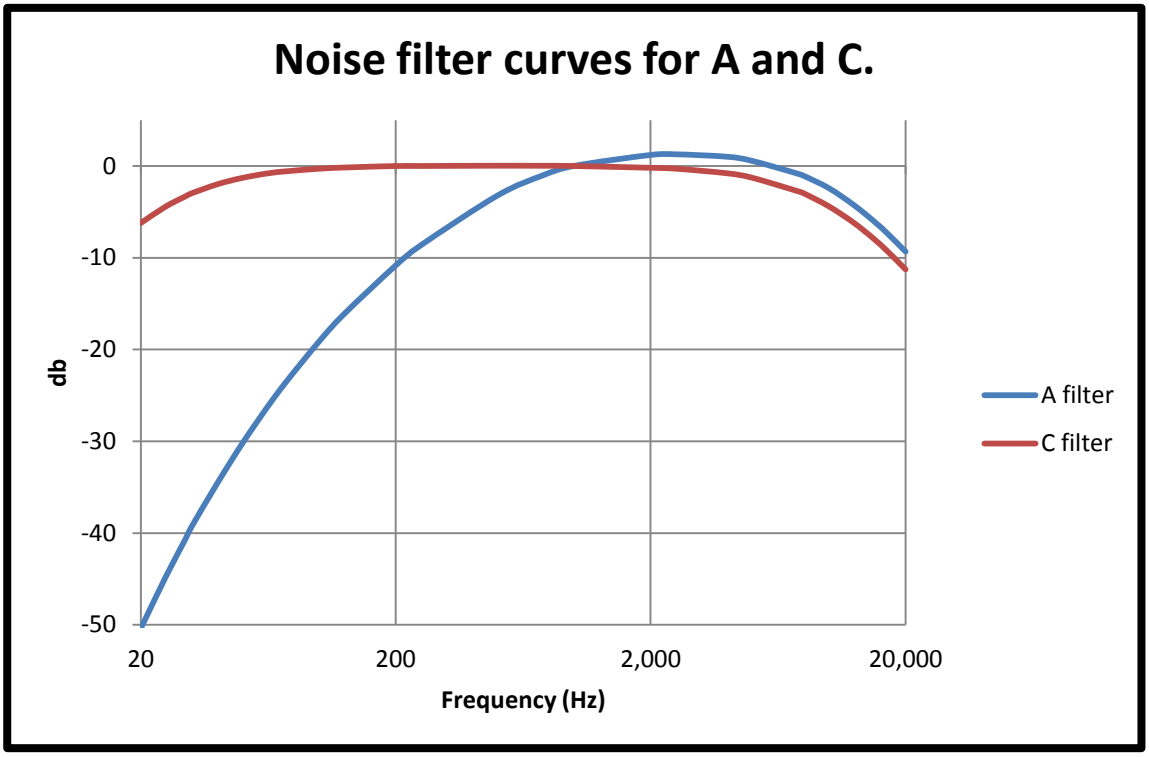


**Figure 47 - Graph of Sound filter response against frequency**

A measurement of the sound intensity within the B16 test beamline Experiments hutch was performed using a Dawe D-1422c Digital impulse sound level meter. The measurements were taken at a height of 1.4m above floor level at 1m intervals along either side of the equipment and for the conditions of 2 fans on, and no fans on. All measurements are db(A).

| Distance (m) | 1 | 2 | 3 | 4 | 5 | 6 | 7 | 8 | 9 | 10 |
|---|---|---|---|---|---|---|---|---|---|---|
| Far side | 61.7 | 61.3 | 61.2 | 61.2 | 60.6 | 60.4 | 60.7 | 60.2 | 60.3 | 60.5 |
| Control room side | 52.2 | 61.0 | 61.6 | 61.1 | 60.5 | 60.6 | 60.9 | 61.0 | 61.9 | 61.1 |

**Table 23 – Noise level in db(A) fans on**

| Distance (m) | 1 | 2 | 3 | 4 | 5 | 6 | 7 | 8 | 9 | 10 |
|---|---|---|---|---|---|---|---|---|---|---|
| Far side | 57.5 | 57.3 | 57.4 | 55.7 | 56.3 | 56.1 | 56.5 | 57.5 | 57.3 | 56.9 |
| Control room side | 56.2 | 55.0 | 56.3 | 55.0 | 54.5 | 54.2 | 56.5 | 56.5 | 58.3 | 59.6 |

**Table 24 – Noise level in db(A) fans off**

There were 4 major noise sources a vacuum pump, a local control rack and 2 fans. The pumps measured 65db(A) at 0.5m, the fans 62.8db(A) at 0.5m and the control rack 65.2 bd(A) at 0.5m.

The db(A) sound intensity measurements give a good indication of the perceived noise level to the human ear. This shows that the noise is equivalent to a noisy office.

BS8233 "Sound insulation and noise regulations for buildings – code of practice" proposes upper ambient noise limits for areas requiring reasonable conditions for study and work requiring concentration.

The sound measurements will vary over time so an average is used. This can lead to underestimation of noise levels which vary significantly with time but is a reasonable approach to office environments. The recommended sound levels given in BS8233 are Long term average when filtered through a type A filter.

| **Typical situation** | **Design range Db $LA_{eq}T$ (Good)** | **Design range Db $LA_{eq}T$ (Reasonable)** |
|---|---|---|
| Library, cellular office, museum | 40 | 50 |
| Staff room | 35 | 45 |
| Meeting room, executive office | 35 | 40 |

**Table 25 – Recommended sound levels**

This may not indicate the effect on delicate samples but it does show that the environment is relatively noisy when compared to other noise sources as shown in Table 26.

| Location | Approximate levels | Notes and critical levels |
|---|---|---|
| Quiet office | 40 – 50dB(A) | |
| Normal conversation at 1 metre | 60 - 70dB(A) | |
| Musical noise, Normal piano practice | 60 – 70dB(A) | |
| Loud radio | 80dB(A) | Lower Exposure Action Value @ 80dB(A) |
| Chamber music in a small auditorium | 85dB(A) | Upper Exposure Action Value @ 85dB(A) |
| Stadium football or rugby match | 87dB(A) | EXPOSURE LIMIT LEVEL @ 87dB(A) at the ear |
| Average personal stereo | 90dB(A) | |
| Symphony orchestra | 95dB(A) | |
| Some power tools (eg band saw) | 100dB(A) | |
| Rock band / outside broadcast music event or indoor concert | 120dB(A) | |
| Jet engine at 25 metres or outside broadcast motor racing event (pits or trackside) | 140dB(A) | Permanent damage, extreme discomfort |

**Table 26 – General noise levels**

This may not be the best environment for users who are setting up sensitive and difficult experiments where concentration is required. A reduction in ambient noise levels may be of benefit.

## 5.2 Sound effect on samples

The amount of energy transported past a given area per unit time is called the Intensity.

Intensity = Energy / ( time x area) usual units are Watts/$m^2$

This energy can be partially reflected and partially absorbed by the equipment. Detectors, stages and frames are of hard materials such as stainless steel, Aluminium or Granite and much of the energy will be reflected (see Section 5.3) . Any absorbed energy can induce vibrations, but as the energy is the sound waves is very small the effect on most components will be negligible.

Samples and very small objects such as zone plates may however be affected significantly and some users have found that the air conditioning systems need to be turned off when measuring fragile or poorly supported samples, although this may be due to air currents rather than airborne vibration.

## 5.3 Sound reflection coefficient

Sound will be reflected by a surface if the acoustic impedance is miss-matched.

The reflection coefficient = $(R_2-R_1) / (R_2 + R_1)$

Where $R_1$ and $R_2$ are the acoustic impedance of the materials at the boundary.

Acoustic impedance = Density x longitudinal velocity of sound in the medium.

| Medium | Density (Kg/m3) | Longitudinal velocity of sound (m/s) | Acoustic impedance (x $10^6$) |
|---|---|---|---|
| Air | 998 | 344 | 0.343 |
| Aluminium 2014-T4 | 2730 | 6380 | 17.4 |
| Mild steel | 7800 | 5900 | 46 |
| Lead | 11200 | 2200 | 24 .6 |
| Granite | 2750 | 6500 | 17.8 |
| Concrete | 2600 | 3100 | 8.06 |

**Table 27 - Acoustic impedance of some materials**

| Material boundary | Reflection coefficient |
|---|---|
| Air/concrete | 0.918 |
| Air/ Aluminium | 0.961 |
| Air / Granite | 0.962 |
| Air / Lead | 0.972 |
| Air / Steel | 0.985 |

**Table 28 - Reflection coefficients at some material interfaces**

Table 28 shows that the reflection coefficients for materials used in experiments hutch is very high.

## 5.4 Sound absorption

Materials can absorb sound by a number of ways including the following: Viscous losses as the pressure wave pumps air in and out of cavities in the absorber; Thermal elastic damping; Hemholz resonators; Vortex shedding and direct mechanical damping

The main methods of absorbing sound are by using Porous absorbers, perforated panel absorbers, slotted panels, Micro perforated panels and hemholz resonators.

### 5.4.1 Porous absorbers

Porous absorbers include open cell foams, carpets, fibrous mineral wools and glass fibres. These materials allow air to flow into the cellular structure where the sound energy is converted into heat. Sealing the surfaces prevents the air entering into the

structure and so reduces the sound absorption capacity. The material must also damp the energy.

### 5.4.2 Panel absorbers

Panel absorbers are non-rigid, no porous materials which are placed over an air space that vibrates in response to the pressure exerted by the adjacent air molecules. Panel absorbers are usually most efficient at absorbing low frequencies.

### 5.4.3 Resonators

Resonators absorb sound in a narrow frequency range. A resonator is an open ended container or void and the size of the opening, neck length and volume of trapped air govern the resonant frequency. A hemholz resonator is an example.

### 5.4.4 Micro perforated panel absorbers

These are panels with very small holes, typically less than 1.0mm in Diameter. They have the advantage that they can be made of any material such as metals and so can be no flammable, easy to keep clean and generate no particulate dust. (K Sakagami)

Some theoretical work has been done and the parameters of a panel can be determined. (Maa, 1998) The panels do however need to be thin so adequate support is required.

As an example, a general purpose absorber with an absorption band from 250 – 2,000 Hz would have the parameters listed in Table 29.

| Parameter | Value (mm) |
|---|---|
| D (hole diameter) | 0.144 |
| t (Panel thickness) | 0.144 |
| B (hole separation) | 1.77 |
| D (Cavity depth) | 64 |

**Table 29 - Example Micro perforated panel parameters**

RPG Inc manufacture a number of sound absorption products. Clearsorber™ is a transparent polycarbonate sheet designed to be placed in front of a glass panel. It is

available as a foil 0.1mm thick, 1m wide with 0.1mm diameter holes on 0.21mm centres and has been used an various projects including the British Museum Atrium.

RPG claim that If the perforations in a Helmholtz resonator are made sub-millimetre in diameter, they are comparable to the thickness of a boundary layer of air. As sound passes through these micro-perforations, sound absorption will occur due to viscous boundary layer effects in the perforations, as long as an air cavity is provided between the foil and the glass mounted behind it. It is then possible to achieve sound absorption without the need for additional porous material in the cavity behind the micro-perforated sheet, thus allowing the panel to be transparent or translucent

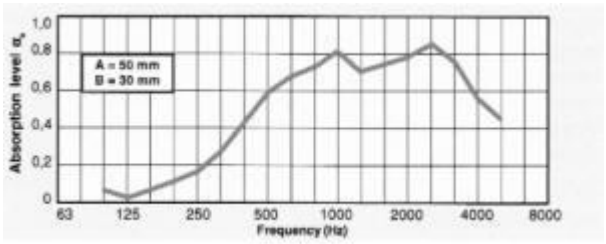


**Figure 48 - Absorption of Clearsorber™ micro perforated film**

**(rpginc 1, 2012)**

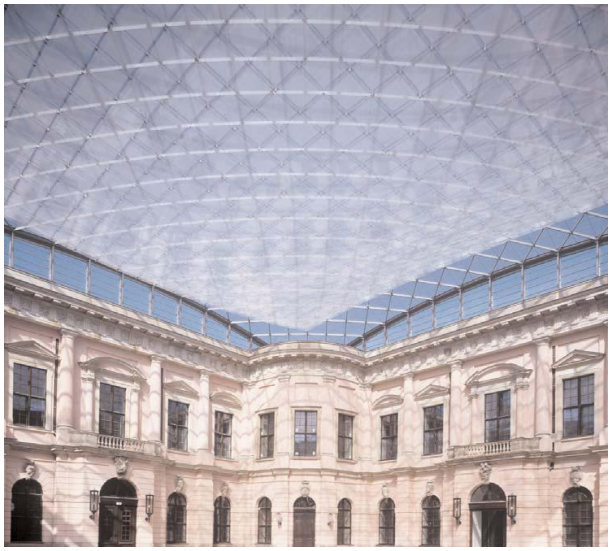

**Figure 49 - British museum Atrium**

**(rpginc 2, 2012)**

Another product from RPG is Clearsorber™ honeycomb which is a product consisting of two 1mm thick micro-perforated panels separated by a clear honeycomb. This is available in size in 19mm and 35mm thickness and sheet sizes of 2,500mm x 1,250mm.

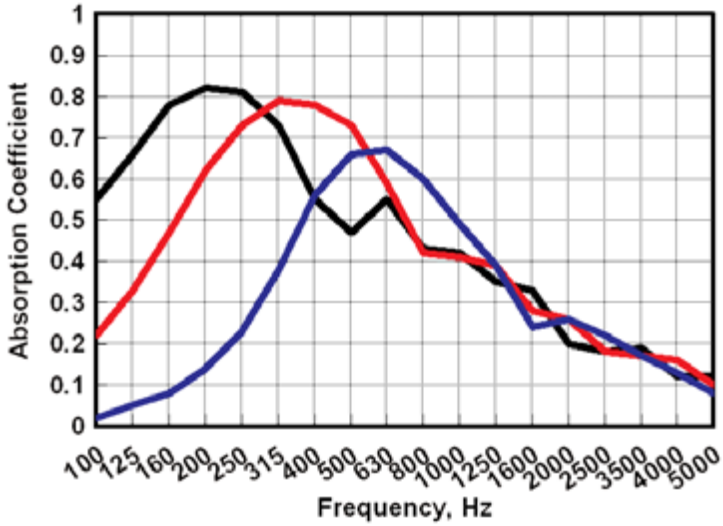


Absorption coefficient for a 1 mm Sheet with 5 mm spaced 0.5 mm holes and cavity depths of 2" (50 mm blue), 8" (200 mm red) and 16" (400 mm black).

**Figure 50 - Absorption of Clearsorber™ honeycomb**

**(rpginc 3, 2012)**

An another product is called Modex. This is designed for absorbing low frequency vibrations. It consists of a metal plate attached to a porous backing which acts as a damped spring.


**Figure 51 – Modex panel**

**(rpginc 4, 2012)**

Absorption is by the plate acting as a spring mass damper, the plates natural vibration modes being damped by the adhesive bond to the porous backing and absorption directly by the thick porous layer. The total thickness is about 100mm.

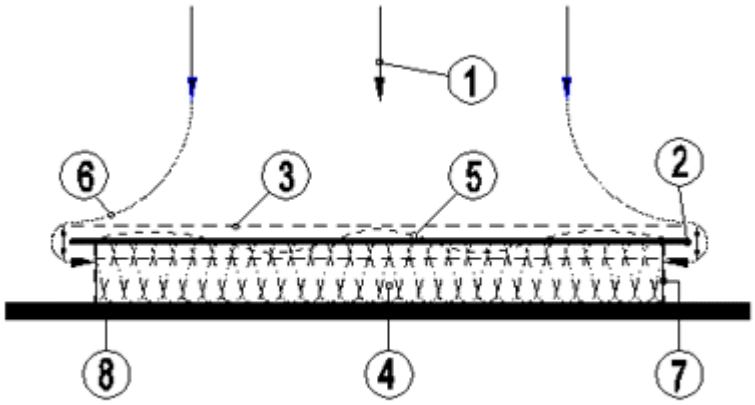


**Figure 52- Diagram of RPG Modex panel**

**(rpginc 5, 2012)**

## 5.5 Noise source frequency

The sound absorption of different products and materials are dependent upon frequency and so it is essential that an analysis of the major noise source frequencies is determined. A measurement was carried out using a Sure PG57 Microphone, linked to a Monacor amplifier and connected to a Textronix oscilloscope fitted with a FTT module. A Fourier transform of the noise found the following dominant frequencies.

Near the fans 29, 62, 96, 120, 146, 226 Hz

Near the electronic rack 50, 80, 100, 825 and 1630 Hz

## 5.6 Sound reduction

The main source of noise are the fans of the air temperature cooling system. The fans are located within the hutch rather than outside to reduce the size of openings through the lead shielding. There may be opportunities to reduce the noise generated by improving the fan housing stiffness or changing the supports or adding damping material to the casing.

The electronic rack was a single module for motion control called a Delta Tau Geobrick. This was surprisingly noisy with a high frequency. It may be possible to install this within an acoustic enclosure. The source of the noise should also be traced, it may be the internal re-circulating fans and these could be replaced with lower noise fans as are found on domestic computers.

## 5.7 Reverberation time

The reverberation time ($T_v$) is the time taken for the energy density to reduce to $1x10^{-6}$ of the initial value. It is often given the title $RT_{60}$ as the noise must reduce by 60db. This can be calculated by the following formulae

$T_v = 0.016\ V/a$

V is the room volume

a is the total absorption (total area x noise absorption coefficient)

This shows that reverberation time increase for larger rooms, a steel hutch with many metal surfaces it will have a poor absorption and so reverberation time for a typical experiments hutch is relatively long (0.3 seconds at 125 Hz).

Actual measurements of the reverberation time were conducted by Adrian James Acoustics limited and this showed reverberation time of over 2 seconds at 125Hz. This shows that the room is “boomy” which is tiring and tends to amplify low frequency noise. This long reverberation time reflects a very low noise absorption coefficient.

## 5.8 Room modes

Standing waves can be set up within rooms and these depend upon the size of the room. There are three main modes. Axial, Tangential and oblique.

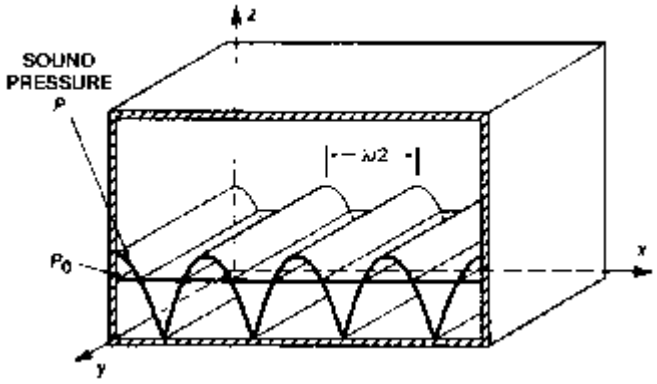


**Figure 53 - Axial room modes**

**(mcsquared 1, 2012)**

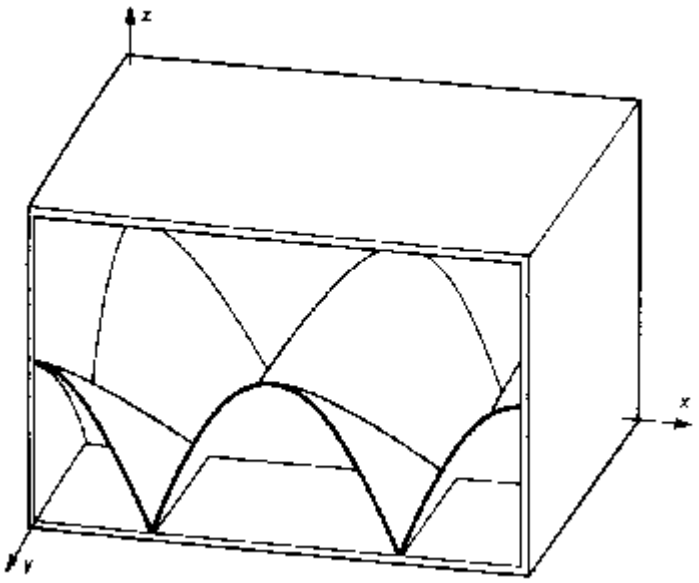


**Figure 54 - Tangential Room modes, ½ energy of axial modes**

**(mcsquared 2, 2012)**

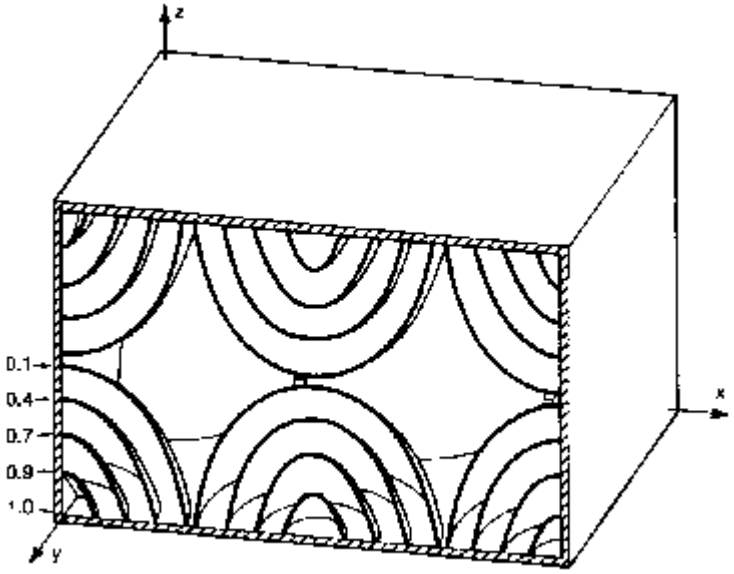


**Figure 55 - Oblique Room modes, ¼ energy of axial modes**

**(mcsquared 3, 2012)**

The B16 experiments hutch has dimensions of length 13.5m, width 4.6m, height 3.8m

The room modes can be calculated as follows:

Axial 12, 37, 42, 25, 74, 90, 38,112, 135, 50, 149, 181, 63, 186, 226, 76, 224, 271, 89, 261, 316, 101, 299, 362, 114, 336, 407 Hz

Tangential 39, 47, 58, 79, 94, 117, 118, 141, 176, 158, 188, 234 Hz

Oblique 60, 120, 180, 240, 300, 360, 420, 480, 540 Hz

This shows that there is no single room mode frequency and that a wide range of source frequencies could be poorly dissipated.

## 5.9 Acoustic vibration summary

The construction used to build experiments hutches provides little noise attenuation from the noise generated by internal cooling fans. Acoustic vibrations are not powerful enough to affect equipment but small fragile and poorly supported samples are affected. The ambient noise level could be considered high for an environment where users are expected to set up experiments which demand a high level of concentration and care. There are many new sound absorption materials and the micro perforated panels look particularly applicable because off their low flammability, easy clean surface, low dust generation and small thickness. Further work on examining the costs and effectiveness of various forms of noise attenuation panels is recommended.

It may also be prudent to consider noise attenuation in the initial design of new beamlines. Experience from B16 Test Beamline is that the dominant noise is from the air conditioning fans. The speed of the fans makes a big difference and if the cooling effectiveness is poor then the fans need to be operated at maximum speed which then creates the maximum noise levels. Reducing heat load would enable the fans to be operated at lower speeds. The dominant heat load is the ambient lighting (B16 experiments hutch is 24 x 70W = 1.68KW) so if more efficient lighting could be chosen this reduces the heat load and enables lower fan speeds to be selected and so reduces the noise.

# Chapter 6. Position control

## 6.1 Actuators

### 6.1.1 Stepper motors

Stepper motors are the most common type of actuator used in synchrotron beamline components. There are three types; variable reluctance, permanent magnet and hybrid.

The variable reluctance motors do not use a permanent magnet and so the rotor can move freely without any detent torque. These motors have low torque.

Permanent magnet motors are low speed, low torque with large step angles of 45 or 90 degrees.

Hybrid motors are constructed with multi tooth stator poles and a permanent magnet rotor. Standard motors have 200 rotor teeth and rotate at 1.8 degree step angles, but other configurations such as 0.36, 0.72, 0.9 and 3.6 degree steps are available.

#### 6.1.1.1 Unipolar and Bipolar motors

In a Unipolar scheme each coil has a center connection and so 6 or 8 leads are required. The centre connection is connected to a positive supply and the two ends are alternatively grounded to reverse the direction of the field. One set of windings are energised for positive direction and the other set are energised for the negative direction.

In a Bipolar scheme there is no center tap and so the winding is simpler with only 4 wires. In a Unipolar motor only half the windings are used at any one time. The space extra occupied by these additional windings means that Unipolar motors are not as efficient as Bipolar motors.

### 6.1.1.2 Series or parallel wound

In a Bipolar motor the full coil on each phase is used, each half coil can be connected in series or parallel. In series the motor gives high low speed torque but because of the high inductance the torque reduces rapidly with speed. To obtain the same low speed torque when operated in parallel the current must be increased by 40%. The lower inductance means that the torque reduces less rapidly with increased speed. To reduce the heat load generated in stepper motors it may be prudent to choose parallel wound motors.

### 6.1.1.3 2 phase or 5 phase

In a 2 phase motor the stator has 8 magnetic poles ( 4 per phase) and a 5 phase motor has 10 magnetic poles ( 2 per phase). This means that the rotor has to only move 1/10 of a tooth pitch to line up with the next phase as opposed to the 2 phase which requires a move of ¼ of a pitch. For a 50 tooth rotor this results in a 5 phase motor having 500 steps per revolution instead of 200 steps per revolution for the equivalent 2 phase motor. The 5 phase motor also gives lower torque ripple and lower vibration

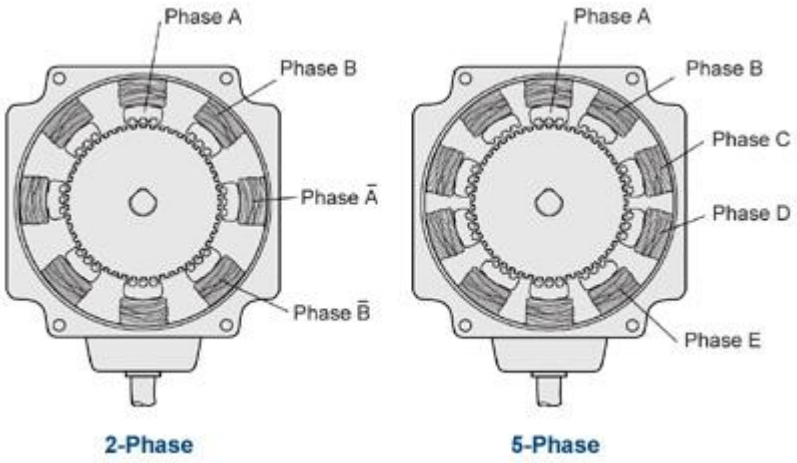


**Figure 56 – 2 and 5 phase motors**

(Oriental, 2012)

At Diamond the standard solution is to use 2 phase motors. Increased resolution is usually obtained by fitting a suitable reduction gearbox and this combined with micro-

stepping and small pitch lead screws easily gives sub micron incremental motion. The lower vibration levels of a 5 phase motor offer advantages and may be appropriate in some circumstances.

#### 6.1.1.4 Micro-stepping

Micro-step drives decrease the current to one phase while increasing the current to the next phase. This results in the motor taking smaller steps. Micro-stepping drives allow steps to be reduced by a factor of up to 250. Micro-stepping also reduces vibration and produces less noise. It must be remembered that if power is switched off the motor rotor will try to move until a tooth is fully aligned.

### 6.1.2 DC Motor

In a normal DC motor the permanent magnets are static and the rotating armature contains an electromagnet. To change the direction of the magnetic field of the armature the current is reversed as it spins and so the electrical contacts must allow constant rotation. These brushes wear out, limit the speed of the motor, create electrical sparking and limit the number of poles on the armature.

In a brushless DC motor the permanent magnets are on the inside and the electromagnets are on the outside. A more complicated controller is then required to charge up the electromagnets as the shaft turns. There can also be many more electromagnets on the stator and this gives more precise control. This type of motor eliminates the wear on the brushes, gives much higher speed, there is no sparking and less electrical noise.

The controller needs to know the stators position in order to determine how to energies the stator magnets and so some designs will use a hall effect sensor.

The bushless DC motor can give a much larger dynamic range of speed control when compared to a stepper motor and gives a more constant rotational speed. This can be very important when taking data constantly when moving.

### 6.1.3 Piezo actuators

Piezo electric actuators are available in a range of sizes and some are able to produce very large force or relatively large strokes. The most common form is a stack of active material which is pre-stressed. Typically a stack actuator can produce a zero load extension of 100's of µm. The displacement is roughly linear with applied voltage and there is hysteresis. There is also a degree of creep, so some sort of position feedback is usually required. Piezos can operate very fast and with sub nm incremental motion but the effective bandwidth is limited to about 1/3 of the resonant frequency.

$$\frac{\quad}{\quad}$$

M is the effective mass of the actuator, K is the stiffness.

Some manufacturers such as Cedrat Technologies, offer piezos which operate in a flexure that produces an amplification of the stroke. For example the V-APAXL 1000 has stroke of 1,050µm and a blocking force of 745N.

**Figure 57 – Cedrat amplified piezo actuator**

**(cedrat-technologies, 2012)**

Piezo actuators can be purchased as stand alone actuators or incorporated into stages. Companies such as Physik Instruments, npoint and Mad City labs offer stages with single or multiple degrees of freedom which incorporate position measuring systems to provide closed loop control.

### 6.1.4 Voice coil actuators

Voice coil actuators are in theory very simple devices consisting of a moving conductor and a fixed magnetic field. Voice coil actuators were originally used for speakers but are now used in many applications such as vibration testing shaker tables. The force on the conductor is proportional to the magnetic field.

Voice coil actuators have a number of advantages over other types of actuators. These include:

- Zero Hysteresis
- Higher acceleration rates than servo, and stepper motors, yet lower than can be achieved with piezoelectric
- Low heat generation.
- Direct Drive.
- Low Acoustic Noise
- Inexpensive relative to traditional servo motors.
- Long Life, Limited number of moving parts.
- High force, when compared to comparable stepper motors, and servomotors

Manufacturers of voice coil actuators include:

- SMAC
- Motran Industries Inc
- Cedrat
- Airex Corporation
- BEI Kimco
- Moticont

As an example a BEI Kimco LA16 housed voice coil actuator has a stroke of 6mm and a force of 60N in an assembly 40mm diameter and 46mm long.

SMAC manufacture a unit with an integral encoder with up to 0.1µm resolution. When used with the controller for force, position, acceleration and velocity can be programmed so that high accelerations and a soft stop can be set. The LCA25 unit for example has a stroke of 10mm accelerations up to 30G and measures only 25mm x 55mm x70mm.

### 6.1.5 Piezo slip/stick devices

These operate by using pairs of piezo crystals that alternately push against a rod or plate in a step wise manner so that the holder is pulled along the rod by the alternate actions of the piezos. There are a number of manufacturers of piezo stages operating on this slip/ stick principal. They include:

- Attocubes
- Physik Instruments
- Smaract GmbH
- Micos
- Physik instruments
- Nanomotion (eg HR1 motor)
- New scale technology (eg squiggle motor)
- New Focus (Newport spectra physics). (eg Pico motors)
- Piezo Motor AB (eg Piezo legs)
- Cedrat Technologies

**Figure 58 – New focus slip stick piezo actuator**

(newfocus, 2012)

Some can be equipped with encoders. Experience with non encoded attocubes are that the step distance depends upon the direction, load, frequency and voltage. It is very difficult to use such devices to perform any sort of scanning but they seem good for set and forget positioning. The stiffness is rather poor, and the parasitic motion can be quite large especially for some of the rotation devices. The pitch goniometer may also not be stable. They are however very small and produce a low heat load. Three attocube devices can be connected to one single controller which is quite large and does need to be close to the attocube. The controller can be operated by an RS232 signal. Some actuators are complete with small cross roller bearings which give large load capacities and reduced parasitic motion, some such as the Micos PP-22 and those produced by SmarAct GmbH come with integrated encoders. Some devices include an optical encoder which produces light, in some cases this light has affected nearby detectors and so this issue should be taken into account.

### 6.1.6 Linear motors

One type of linear motor has parallel magnetic tracks facing each other which are not moving. The moving part is supported by a bearing system and runs up and down the tracks. The moving part is ironless so there is no attractive force between it and the magnets. The moving part has a low mass coil winding often encapsulated in epoxy resin. Air cooling is often fitted.

Another type are the flat type linear motor which can be slotless ironless, slotless iron and slotted iron. The slotless iron less motor is a series of coils mounted in an aluminium base, the slotted type have the coils mounted on iron laminations and this increases the magnetic force. The slotted iron motors have an iron core and so have much generate greater forces. In both the slotted iron and slotless iron there is an attractive force between the moving part and the static part and these produces a varying force along the length called cogging. This can reduce the ability of the motor to provide fine incremental motion. Because linear motors are a direct drive there is no lead screw and so very high accelerations can be produced with very low noise or wear. The moving part does need to be supported by a separate bearing system and these can be cross roller bearings or air bearings. A position encoder is required as open loop control is not possible.

### 6.1.7 Giant Magnetostrictive actuators

Magnetostrictive materials convert magnetic energy into mechanical energy. Some materials were discovered in the 1970's that are capable of very large mechanical movements and these are termed Giant Magnetostrictive alloys. The most common material is Terfenol-D (Tb0.3Dy0.7Fe1.9) but there are others such as the Magnetic shape memory alloys NiMnGa. Actuators are commercially available. Cedrat Technologies for example produce the DMA XL which has a stroke of 100µm a maximum force of 21,000N and a maximum frequency of 1,000Hz. These devices are highly non linear and have large hysteresis so closed loop control is required.

### 6.1.8 Pneumatic actuators

Pneumatic actuators are commonly used for simple positioning where either the actuator is fully extended of fully contracted. They are cheap, can produce large forces, can operate faster than a motor and lead screw system and can be easily interlocked. They also generate little heat so for systems which require a simple operation they offer advantages. Many actuators have cushioned end stops and by using bleed valves on the inlet and outlet a smooth motion can be obtained. Actuators can be single acting or double acting. The double acting will have the same pressure pushing and

pulling so if the actuator is vertically mounted gravity will assist in the down motion and oppose up motion. With a constant air pressure the resultant speeds could be very different so for heavy loads a compensating spring should be used to even out the speeds.

### 6.1.9 Hydraulic actuators

Hydraulic actuators are commonly used where very large forces are required such as mechanical excavators. The hydraulic oil is pumped using a hand pump or an installed electric pump and high pressures, typically 10,000psi, are used. A solenoid valve is used to regulate the flow of oil into the actuator. These are often used for positioning control unlike the pneumatic actuators and a position sensor is required. Pneumatic solenoid valves dump the expelled air to atmosphere whereas on a hydraulic system the fluid is re-circulated. Seals are critical and any damage to the actuator rod or the seal can result in leakage of high pressure oil. Leakages are messy.


**Figure 59 – Hydraulic actuators**

**(enerpac, 2012)**

### 6.1.10 Magnetic Shape memory alloy actuators

Shape memory alloys that change shape have been around for some years. These are materials that change crystalline state when they are heated or cooled at the their specific transition temperature. There use in actuators has been limited because of the small length changes produced and the slow speed of response. A new type of shape

memory alloy has now been produced which elongates by up to 10% in a magnetic field (J Tellinen, 2002). Cycle times can about 1 mSec. These are not as fast as piezo actuators but they are small and may be used in the future.

## 6.2 Bearings

### 6.2.1 Aerostatic bearings (air bearings)

Air bearings are devices where air is fed to a small gap between two surfaces and the resulting pressure lifts one surface above the other to create a very low friction bearing.

Air bearings have been mainly used for very high spindles for machine tools, but they have also been used for linear motion. In rolling bearings the coefficient of static friction is greater than the coefficient of dynamic friction, when a motor turns a ball screw, the screw winds up to store the energy because of the high static friction, once the static friction is overcome the friction falls and the screw unwinds and so pushes the slide past its desired position. Because air bearings offer very low friction they offer the ability to move components with very small incremental motion and also with very high speeds. For nano focus  motion applications the issue with air bearings is static and dynamic stiffness and damping.

The rate at which air is supplied to the gap is controlled either by a series of orifices or by using a porus membrane. Often the orifices feed air into a set of grooves. As the air moves away from the grooves to the gap the pressure reduces and these pressure variations will depend upon the size and location of the orifices and grooves. In general the average pressure is about 50% of the air supply pressure.

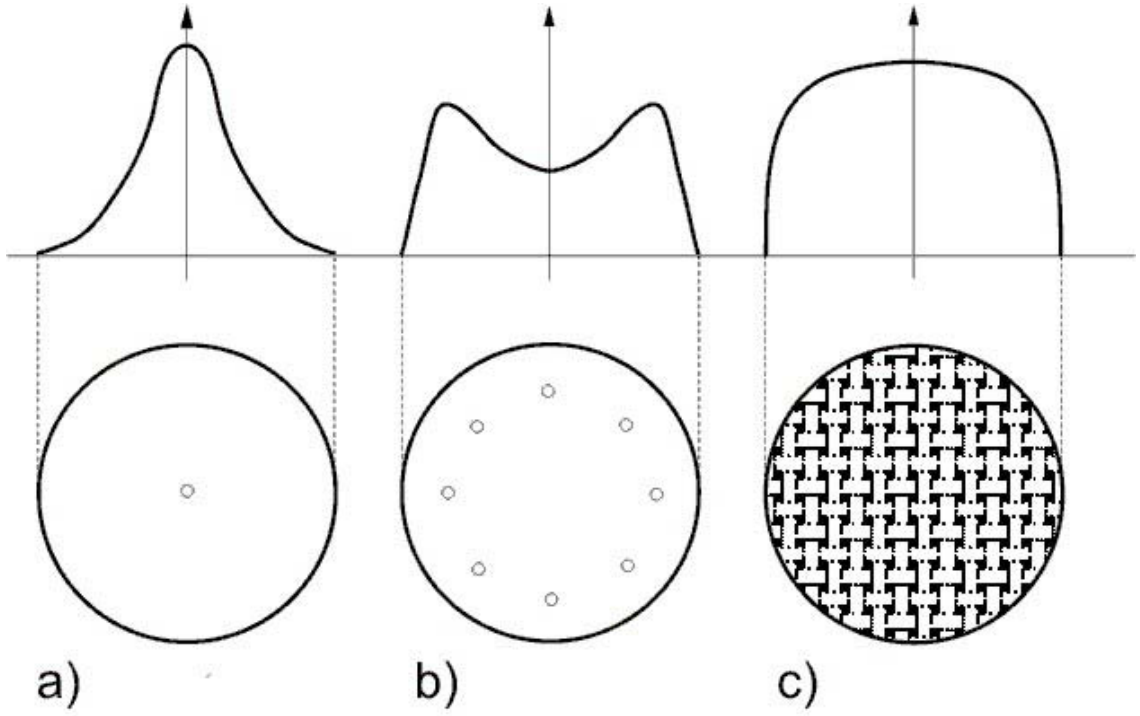


**Figure 60 - Pressure distribution of different orifice arrangements**

**(Uhlmann & Neumann, 2012)**

When the air supply is off the lift force is limited by the surface area of the grooves where for porous carbon bearings the lift force is applied across the complete area.

The stiffness of the air bearing can be increased by applying preload which reduces the ride height. Preload can be applied using mass, magnets, vacuum or opposing air bearings.

The stiffness of air bearings depends upon the air pressure, geometry, surface are and preload. An air bearing with a large surface area and large preload will have a much higher stiffness than small area bearings and low preload.

As an example a new way 200mm porous carbon bearing has a load capacity of 7,770N, a nominal ride height of 5 µm and a stiffness of 700 N/µm. But the ride height will vary with air pressure and load. A change is load of only 35 N will create a height change of 50nm and if the supply pressure changed by 1% change the ride height could

also change by 50nm. Tight control over the air pressure stability is required if ride height of an air bearing is critical. For applications where height is critical the air could be turned off and the gap allowed to reduce to a zero and then any fine motion could be performed using a piezo stage mounted on the air bearing stage. There has also been some work on developing air bearings with active feedback (Ro, Kim, Kwak, & Park, 2010) that varies the preload using electro magnets or by modifying the air pressure using a piezo actuator.

As air moves away from the orifices the air expands and so cools and this will cool the support structure which can result in a change of shape. As flow rate is a function of the cube of the gap there is a desire to have as small a gap as possible and gaps of the order of 3µm may be possible in the future. In addition by reducing air pressure the gap can be reduced. This creates a stiffer bearing as the improvement due to smaller gaps is greater than the losses due to lower pressure. Gap tolerance should be kept to below 10%, so suitable manufacturing methods will need to be selected.

#### 6.2.1.1 Dynamic stiffness

Because of the compressible nature of gas air bearings have poor dynamic stiffness. There has been work to improve this so that air bearings can be used for stages for micro milling machines. One method is to use a magnetic oil as squeeze film damping (F Wardle, 2010). In this case two rail are fitted to a linear air bearings system. The rails have semi-circular matched convex and concave profiles with a small gap between them. The gap is filled with magnetic oil which is held in place by a series of magnets fitted to the base of the rail. Test results show an increased dynamic stiffness of over 10x. In general damping can be increased by reducing the operating gap and increasing the bearing area.

#### 6.2.1.2 Air bearing suppliers

Manufacturers of linear air bearings include the following:

- AB Tech Inc
- New way

- Nelson Air Corp
- Air Bearing technology Inc
- Leuven air bearings
- ESS Mikromechanik GmbH

Some manufacturers offer complete liner air bearing stages and some offer complete stages with linear motors and encoders.

#### 6.2.1.3 Instability

Pneumatic hammer is a term given to a pneumatic instability when there is a delay between the bearing clearance change and the variation in pressure in the orifice pocket. If the clearance increases the pressure reduces, the gap then reduces, the pressure then increases and so the gap increases. This cycle then repeats. The pocket volume therefore needs to be kept small and a pocket to air gap volume ratio of 1:20 is recommended and for small gap sizes micron deep pockets are sometimes advocated.

#### 6.2.1.4 Air bearing design

There are many parameters that can affect air bearing performance and there are some papers giving rules of thumb, nomographs (Stout & Sweeney, 1984) or formulae for calculating such parameters as gap height, orifice diameter, air pressure, gap volume, pocket volume, preload and number of orifices to name but a few.

#### 6.2.1.5 Air quality for air bearings

As gaps become smaller the quality of the compressed air becomes even more important. As well as particles blocking orifices and gaps, oil and water vapour can create small droplets which will affect the gap size. New Wave bearings recommend Quality class 4 air but these requirements may become more stringent in future.

| Quality Class | Maximum No of particles 0.1 – 0.5µm | Maximum No of particles 0.5 – 1µm | Maximum No of particles 1 – 5µm | Dew point ( °C) | Total Oil (mg/m$^3$) |
|---|---|---|---|---|---|
| 1 | 100 | 1 | 0 | -70 | 0.01 |
| 2 | 100,000 | 1,000 | 10 | -40 | 0.1 |

| | | | | | |
|---|---|---|---|---|---|
| 3 | | 10,000 | 500 | -20 | 1 |
| 4 | | | 1,000 | +3 | 5 |
| 5 | | | 20,000 | +7 | |
| 6 | | | | +10 | |

**Table 30 - ISO 8573-1:2001 Compressed air quality class**

Local pneumatic regulators often include a particulate filter which is available in a range of filter sizes from 40µm to sub micron, however, particles may not be rounded and so long narrow particles can still penetrate filters. Water can be removed by air dryers or mechanical water separators and oil vapour can be removed using a Coalescing filter. This often consists of a glass fibre filter medium. The air travels through a tortuous path through the filter and by absorption, oil vapour coalesces into droplets of oil which run down into a bowl at the bottom of the filter. The oil is then drained of manually or automatically.

Supply pressure may also be non constant and have a beat frequency generated by the compressor. Addition volume such as accumulators may need to be fitted. The effect of sudden pressure fluctuations due to operation of other local pneumatic devices such as valves and actuators may also be a problem and so a separate circuit for air bearings may be sensible.

### 6.2.2 Hydrostatic bearings

Instead of using compressible gas such as air, incompressible fluids such as hydraulic oil and water can be used for a bearing. These devices offer much higher stiffness, 2,000N/µm as against 700 N/µm for an air bearing and for grinding and cutting machine applications offer improved wear resistance. The fluid is fed at high pressure from an external pump and as the fluid bleeds out of the gap it is collected in a drip tray and then filtered and re-circulated through the pump. (A Slocum, 1995)

### 6.2.3 Rotary stroke bearings

Rotary stroke bearings consist of a hardened precision ground shaft and a cylindrical sleeve, between which are a set of balls located in a housing. There are a number of manufacturers but some such as Mahr offer a precision range. In this case the sleeve

inner diameter, shaft diameter and ball size are matched to give the required loading. A high loading gives higher friction but greater stiffness. The shafts are manufactured from X155 CrVMo 12 1, 100 Cr 6 (1.3505) or 16 MnCr 5 (1.7131). The shaft is precision ground and lapped to ISO h3, Rz <1 µm., Roundness within 1/3 ISO-IT3, Straightness within 5 µm/100 mm, hardened to HRC 60–64/HV 720–815 and grade 5, sorting class P0 steel balls are used. The coefficient of friction depends upon the preload and can be between 0.001 and 0.008.

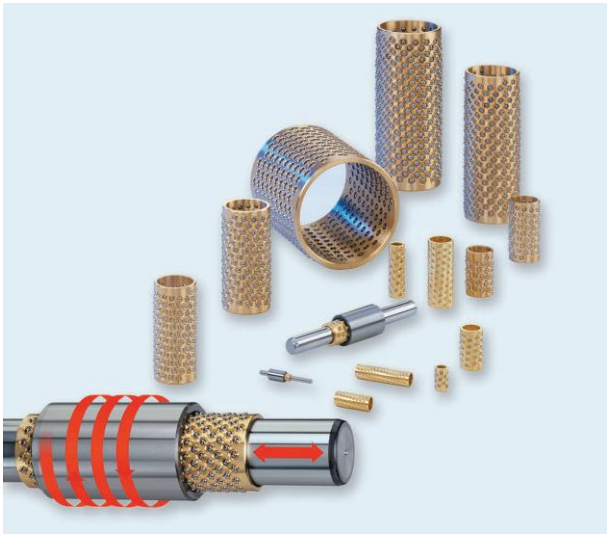

**Figure 61 – Rotary stroke bearing**

**(mahr, 2012)**

### 6.2.4 Roller bearings

Rotary bearings such as angular contact bearings are an important part of many precision actuators. There are a number of measurements of precision for such bearings such as ABEC. The Annular Bearing Engineers Committee (ABEC) of the Anti-friction bearing manufacturers association (AFBMA) has produced a standard for bearings which defines the tolerance of the inner and outer bores of bearings. Other standards are DIN 620 and ISO 492:2002.

| DIN 620 | ISO 492 | AFMBA |
|---|---|---|
| P0 | Class 0 | ABEC 1 |
| P6 | Class 6 | ABEC 3 |
| P5 | Class 5 | ABEC 5 |
| P4 | Class 4 | ABEC 7 |
| P2 | Class 2 | ABEC 9 |

**Table 31 – ABEC ratings for bearings**

As an example the outer mean diameter variation for an ABEC 1 ring less than 18mm Outside diameter is 0 to -7.5µm whereas an ABEC 9 ring is 0 to -2.5µm. ABEC 7 bearings are often classed as super precision and ABEC 9 as ultra precision. Super and ultra precision bearings are often employed in high speed spindles where any out of roundness variations in spindle bearings can produce unacceptable vibrations. Precision rotational assemblies are also highly dependant upon bearing to spindle fit, spindle accuracy and bearing preload.

The American Bearing Manufacturers Association grade have produced a grading for allowable variations in ball diameters and surface roughness. These are called ABMA grades.

| ABMA Grade | Allowable ball diameter variation (µm) | Deviation from spherical form (µm) | Lot Diameter variation (µm) | Surface roughness (µm) |
|---|---|---|---|---|
| 3 | 0.08 | 0.08 | 0.13 | 0.012 |
| 5 | 0.13 | 0.13 | 0.25 | 0.02 |
| 10 | 0.25 | 0.25 | 0.50 | 0.025 |
| 15 | 0.38 | 0.38 | 0.76 | 0.025 |
| 16 | 0.4 | 0.4 | 0.8 | 0.025 |
| 20 | 0.5 | 0.5 | 1.0 | 0.04 |

**Table 32 – ABMA Grades up to 20 only**

Precision balls can be manufactured in a range of materials. The most common is an air cooled high carbon chrome steel with manganese and Silicon. There are many designations for this type of steel such as AISI SAE 52100, 100Cr6, SUJ-2 and EN31B. There exact compositions vary slightly between specifications.

For corrosive environments a martensitic stainless steel 440c grade is used for ball bearings. Silicon Nitride is also used, one of their big advantages is that they are lighter and so for very high speed spindles the centrifugal forces are lower. Silicon Nitride is also harder, requires less lubrication and is electrically insulating. It also has a higher Youngs modulus than steel so that the load capacity is decreased because of the high hertzian stresses produced.

One of the drivers for materials development for bearings are to increase life times, particularly for high load or high speed applications. For nano motion applications these are not prime drivers where the speeds are slow and usage is very low with a high percentage of the time with the bearing in a stationary mode. For nanometre incremental motion the major issue would be any permanent deformation due to prolonged static loads. A chrome steel bearing material for these low speed applications is suitable.

### 6.2.5 Re-circulating ball bearings

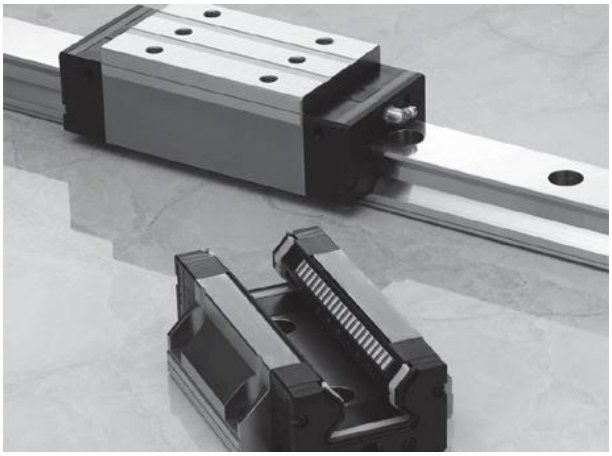

**Figure 62 – NSK Liner bearing**

**(nskeurope, 2012)**

There are a number of companies manufacturing re-circulating ball bearings such as THK and NSK. These include caged ball bearings, caged roller bearings and full ball type bearings. These can be supplied with different preloads. The effective of the preload is to make the bearing stiffer in the radial direction but this also increases the resistance and increased wear reduces the life. A typical medium preload is 10% of the basic dynamic load rating. Linear bearings can offer very high rigidity a NSK RA65BN for example has a rigidity of 4,444N per µm. The way that balls re-circulate is critical for high resolution motion and in some cases the point at which each ball leaves the loaded area to start its return path can be detected as a disturbance.

### 6.2.6 Linear crossed Roller bearings

Crossed –roller bearings do not include a re-circulating element and so in theory gives a smoother operation. The preload on the bearings is set during assembly and so this can give greater control or variability over a preloaded re-circulating ball bearing. The stroke lengths are only available in a limited range and the space constraints are rather different. In general cross roller bearings seem to be preferred for higher accuracy systems.

**Figure 63 – Linear crossed roller bearing**

### 6.2.7 Magnetic bearings

Magnetic bearings are used for very high speed spindles, flywheels and turbo blowers but there are some that can be used for linear systems (Peijnenburg, Vermeulen, & Eijk, 2006). An active magnetic bearing consists of an E shaped piece of SiFe with a coil wrapped around the center leg. A permanent magnet is also added to the centre leg to give a more linear response. A bridge is placed opposite the legs and the flux generated by the coil and permanent magnet generates an attractive force between the lags and the bridge. The current in the coil is then used to control the force. Active magnetic levitation systems are being developed for wafer positioning with 6 degree of freedom positioning and nm resolution. The feedback control to the magnets also offers high stiffness. These systems can also be used in vacuum. (Choi, Jeong, Gweon, & Kim, 2008)

## 6.3 Drives

### 6.3.1 Lead screws

A lead screw consists of a threaded shaft on which a threaded nut is fitted. The shafts usually have an ACME (General purpose, stub or centralizing) or ISO trapezoidal thread form , but some manufacturers offer a triangular thread. The nuts are bronze or plastic. The coefficient of friction is higher than a ball screw, they are usually less precise and less expensive. Some are available with anti-backlash nuts.

### 6.3.2 Ball screws

Ball screws consist of a gothic arch form of threaded shaft on which a ball housing moves. The ball housing holds a set of balls that engage on the thread on the shaft. The shaft thread can be rolled or for more precise applications precision ground. In some cases the balls re-circulate and this can offer reduced noise and lower friction. Ball screws are more expensive than lead screws but offer lower friction and increased accuracy.

**Figure 64 – Ball screw**

**(nskeurope, 2012)**

### 6.3.3 Satellite roller screws

Satellite roller screws are similar to ball screws but the load is transmitted by threaded rollers which have a large number of contact points. The static and dynamic load capacity is much larger and the effective pitch can be much smaller and so a separate gearbox may not be required. This type of device is manufactured by Rollvis Swiss and Nook Industries. As an example a rollvis RVR is available with a diameter from 8mm and pitch of 0.25mm up to diameter of 125mm and pitch of 5mm. By comparison the smallest pitch for an 8mm diameter THK ball screw is 1mm and a 25mm shaft is 20mm.

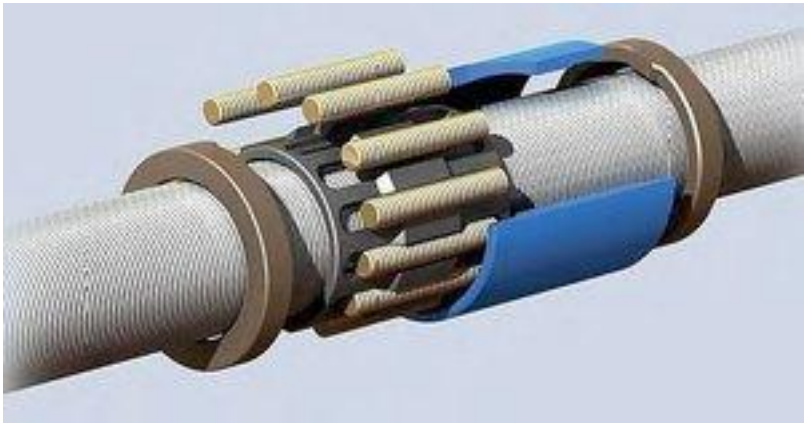

**Figure 65 - Rollvis Swiss satellite roller screw**

**(rollvis, 2012)**

The satellite roller screws are also available with preloaded nuts to eliminate backlash and increase rigidity.

### 6.3.4 Harmonic drive gearboxes

A Harmonic drive gear consists of a sun gear which drives a series of elastically deforming planet gears. The planet gears engage with a thin walled ring that has teeth on the inner and outer surfaces. The flex spine engages with an outer circular spine. The circular spline has two less teeth than the flex spline so as the flex spline rotates the outer spline moves by 2 teeth. Because of the elastic deformation about 30% of the teeth are engaged at any one time and so load capacities are large compared to normal planetary gear set with similar sized teeth. There is also zero backlash and high gearing ratios.

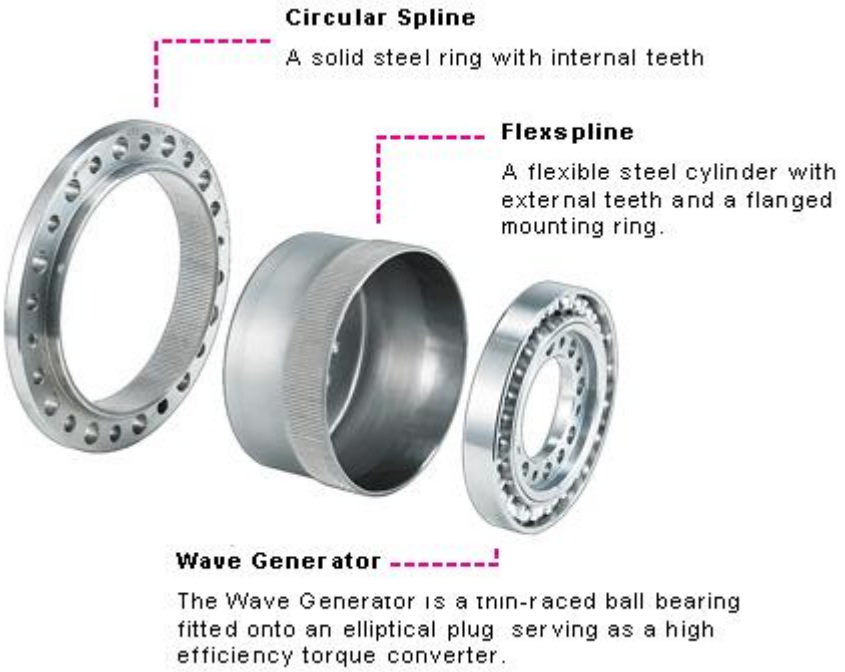


**Figure 66 - Harmonic drive**

**(harmonicdrive, 2012)**

Companies manufacturing these type of gearboxes include Harmonic Drive LLC and Micromotion Gmbh.

### 6.3.5 Low backlash gears

There are a number of gear systems that claim either low or zero backlash. The system developed by Maxon consists of pairs of planetary gears which are misaligned to each other by half a pitch and connected by a torsion spring so that the leading flank of one planetary gear is in contact with one flank of the centre wheel whilst the trailing flank of another gear is in contact with the other flank of the centre wheel.

**Figure 67- OTT anti backlash worm and wheel**

**(zahnrad-ott, 2012)**

Another type developed by OTT and Cone drives is a worm drive where the worm wheel is split into 2 parts that are sprung loaded against the flanks of the wheel.

Another product is called twin spin which has preloaded trochoidal reduction gears.

There is however no such thing as zero backlash. A drive system can be defined by its torsional stiffness and hysteresis loss and it is important that this information is obtained from the manufacturer or is measured so that the system performance can be evaluated.

### 6.3.6 Flexures

Flexures are a generic name for a hinge mechanism which relies only on the elastic property of materials to deflect, there is no sliding surfaces and so no friction and hence no lubricants are required. The operating range of flexures is limited but they offer very low hysteresis.

There are a number of designs including circular hinge, beam hinge and cross hinge. The use of precision wire eroding techniques has allowed complex flexures to be manufactured.

| | Grade | Trade Name of an example material |
|---|---|---|
| Steel | X220 CrVMo13 4 | Bohler K190 Microclean |
| Steel | X3NiCoMoTi18-9-5 | Bohler W720 VMR |
| Aluminium Alloy | AlZn5, 5MgCu | Perunal-215 |
| Aluminium Alloy | AlMgSi1 | Anticorodal 110 |
| Aluminium alloy 2014 | AlCuSiMn | Avional 660-662 |
| Aluminium alloy 7010 | EN AW-7010 | Contal |
| Titanium alloy | TTi6AlV4 | |
| Bronze C72900 | CuNi15Sn8 | CN8 |
| Aluminium Alloy | 6061-T6 | |

**Table 33 – Materials used in flexures**

Flexures are an important part of precision motion and their role is expected to increase. Generally flexures have limited deflections but this can sometimes be overcome by using quite complex designs with combinations of multiple beam hinges. Complex flexures can however have parts which have quite low natural vibration frequencies and it may be required to provide an additional constraint to prevent these low vibration modes. As flexure thicknesses become thinner surface finish becomes very important and of course machining tolerances reduce.

There are some suppliers of standard cross hinge flexures such as C-Flex, here the problem is accurate machining of the location feature.

## 6.4 Position feedback

### 6.4.1 Introduction

Position feedback is required to provide closed loop feedback. Types of device include optical scale encoders, laser interferometers, capacitive sensors, Eddy current sensors.

### 6.4.2 Incremental optical scale encoders

Optical scale encoders consist of a scale and a readhead. The readhead is positioned above the scale and uses optical methods to measure its position along the scale. They have the great advantage of being non contact with no hysteresis. There are a number

of manufacturers providing a range of both linear and rotary optical scale encoders suing different systems.

Optical linear scale encoder suppliers include the following

- Renishaw
- Heidenhain
- Sony
- Micro-E
- BEI Sensors
- Gurley Precision Instruments

The readhead of the encoder emits a light from a diode or laser and the light reflected form the scale is detected. The scale is graduated with alternate stripes. The readhead electronics measure the changes as the encoder travels along the scale. The scale therefore does not give an absolute position but can only measure how much it has moved. The position of the readhead relative to the encoder scale is important, and changes in readhead height and pitch need to be controlled. Some encoder systems are more sensitive to others, but in all cases systems to set the position of the encoder at the correct orientation and height need to be designed into the system.

#### 6.4.2.1 Reference Marks

To provide a zero position encoders will need a reference which to home to. Some systems offers reference marks which are separate components to be positioned as required, others are incorporating reference marks within the encoder scale, and sometimes the scale incorporates multiple reference marks so that homing can be accomplished with reduced distance travelled.

#### 6.4.2.2 Digital and analogue output

The analogue output consists of 2 1 volt peak to peak sine waves out of phase by 90 degrees, this is usually taken to an electronic interpolator that produces square wave digital pulses on 2 channels that are also out of phase by 90 degrees. By detecting if

phase A leads phase B or if phase B leads phase A the direction of travel can be determined and by counting the pulses the total distance moved is calculated.

#### 6.4.2.3 Interpolators

Interpolators are electronic modules that interpolate the sine waves and produce a digital signal. Interpolators are available at factors from 4 to 4,000.

#### 6.4.2.4 Renishaw

Renishaw offer a range of optical encoders. The most common is the RG2 and RG4 system. In this system the scale has either a 20um or 40 um pitch. In these systems an infra red led light is reflected form the scale and passed through a phase grating, this produces sinusoidal interference fringes. In the RG2 system the reflection is parallel to the scale, the RG4 reflects light at 90 degrees to the scale. The Sigum and Tonic system also uses an infra red LED but uses a different method to produce a sinusoidal signal, this system offers higher speeds and lower errors.

#### 6.4.2.5 Sony Laser Scale

The Sony laser scale has a semiconductor laser which passes through a polarized beam splitter which divides the beam into 2 portions. The split laser beam impinges on a hologram lattice in which a 550nm period pattern has been engraved on the glass surface.. The laser beam is diffracted and then reflected from a ¼ wave plate. The beam return to the hologram and then diffracted a second time.. The beam then returns to a detector and are combined. Since the two optical path are symmetrical in the left/right direction, the influences of atmospheric fluctuations and pressure changes are cancelled. The scale is made from a low CTE called NeoCeram and when combined with a 8,000x interpolator the laser scale has achieved a resolution of 17pm. The laser scale is offered in three types and the BL series is also offered in three versions.

| Model | | Signal wavelength | Minimum resolution |
|---|---|---|---|
| BL series | Transmissive integrated | 400nm | 50 pm |
| BH Series | Reflective | 250nm | 31.25 pm |
| BS Series | Transmissive | 138nm | 17.25pm |

**Table 34 – Sony laser scale types**

| Type | Low expansion scale | Power consumption | Measurement lengths available | Resolution (µm) | Readhead dimensions |
|---|---|---|---|---|---|
| BL55-RU | No | 600mA | 70- 1020 | 0.1/ 0.05 | 111 x 18 x 19 |
| BL55-RE | No | 600 | 60-1060 | 0.1/0.05 | 40 x 42 x 32 |
| BL55-NE | Yes (Neoceram) | 250 | 30- 420 | 0.1 | 25 x 18 x 21 |

**Table 35- Sony laser scale BL series versions**

#### 6.4.2.6 Heidenhain

Dr Johannes Heidenhain manufacture a range of position measuring systems. The most relavent for nano positioning is the Exposed linear incremental encoder type LIP. Heidenhain use 2 scanning systems, the imaging scanning with grating periods of between 10µm and 200µm and interferential scanning with graduations of 4µm or smaller which are used on the LIP systems.

As an example, the LIP 372 has a grating period of 0.512 µm and 32 fold interpolation factor gives a signal period of 32nm.

#### 6.4.2.7 Micro-E systems

Micro_E systems offer a range of linear encoders, an example is the Mercury II 6000. This has a broad alignment tolerance (stand off +/- 0.15mm and angular alignment ±2°,±1° ±1°). It has low power consumption eg MII 6000 power consumption is 0.9w of which 0.25w is for the sensor and offer 20 micron pitch 6mm wide tape scales with built in index and limit marks. The normal scale has a CTE 13ppm/°C and glass scales with a CTE 8ppm/°C but glass scales of near zero CTE glass are available as special.

(Type not specified). Mercury II 6000 resolution to 1.22nm with X16,384 interpolator and cyclical error +/- 30nm with tape scale, +/- 20nm with glass scale.

### 6.4.3 Absolute optical encoders

Absolute encoders operate in a similar way to incremental encoders but they can give an absolute position without having to home to a reference mark. These often have a non repeating bar code in the scale which is read by the readhead.

### 6.4.4 Laser interferometer encoders

#### 6.4.4.1 Michelson interferometers

Many laser encoders such as those made by SIOS and Renishaw are based upon a Michelson interferometer. A stabilised single frequency laser beam is generated and passed through a beam splitter. One parts of the beam exits the unit and is reflected back from a plane mirror or retro-reflector mounted on the part that is moving. The other part is reflected from a fixed mirror. Both beams return to the beam splitter and then combine and produce an interference pattern. The resolution is dependant upon the wavelength of light produced, but this can be substantially increased by using electronic interpolation factors.

The measurement is dependant upon the stability of the wavelength of the light so one of the key factors is having a highly stabilised light source. The other issue is that the wavelength of light depends upon the refractive index of air and this is affected by the pressure, temperature, humidity of $CO_2$ contents of the air. These affects can be compensated for using the Edlen formula. Laser interferometers are therefore equipped with detectors for measuring the conditions.

#### 6.4.4.2 SIOS

SIOS Meßtechnik Gmbh, produce a minature retroreflector interferometer. This has a measurement range up to 5m and a resolution of 0.1nm. SIOS also produce a triple beam device which can measure pitch and yaw as well as distance.

#### 6.4.4.3 Optodyne

Optodyne have developed a laser doppler displacement meter. It is polarization insensitive and so can use multiple reflections. This reduces the effect of air turbulence on the measurements. Light is frequency shifted by the motion of the retroreflector, a phase detector measures the phase variation.

#### 6.4.4.4 Renishaw

Renishaw produce a laser system called RLU10. This consists of a stabilised laser which is directed down a flexible waveguide to the interferometer head. The light is emitted from the interferometer head and reflected back by a plane mirror or retro-reflector.

The plane mirror offers higher resolution than the retro-reflector but it does mean that the mirror must always remain orthogonal to the incoming laser beam. The majority of the heat is generated by the laser supply electronics which can be mounted some way away from the interferometer head, but the head does also produce some heat. To overcome this problem a lower power head has recently been introduced.

The interferometer head is much bulkier than some of the optical laser scale heads and of course it needs a line of sight to a mirror or retroreflector. This is not too much of a problem for larger systems but when used to determine the position of small devices such as Attocube stages, then the bulk of the mirror is considerable.

#### 6.4.4.5 Attocube

Attocube produce a fiber based Fabry Perot interferometer. The space between the fiber probe and the sensor is called the cavity length. The laser light entering the cavity is modulated allowing the sensor to obtain two sinusoidal signals. This system offers 30pm resolution at cm range ,has a high tolerance on the angular alignment of the reflecting mirror and the sensor head is only 15mm diameter and 12mm deep. The FPS3010 unit has three sensing heads, has a maximum target velocity of 1m/sec, a working distance of 0 – 400mm and a resolution of 25pm and a repeatability of 2nm at 10mm working distance.

#### 6.4.4.6 Laser encoders for use on piezo stages

Slip stick piezo stages are pulsed devices were the voltage and frequency can be set at the controller. The amount of movement is dependent upon the loads and direction but the motion is by nature a pulsed motion with potentially very high velocities. These velocities may be too high for a laser interferometer to detect and loss of position information is possible. If laser encoders are to be used the bandwidth must be sufficiently higher than the stage velocity to prevent inaccuracy.

### 6.4.5 Capacitive sensors

In a capacitive position sensor, the electrified plate is the sensor surface and the second plate is the target. The voltage on the sensor is continuously changed and the amount of current required to change the voltage is measured. The change in capacitance varies with the gap and so the system can be used to measure small distances. Capacitive sensors have a limited measuring range of less than 1mm but can resolve down to 6nm. The sensor head can be very small, as an example the Lion Precision Sensor C6 is 5mm diameter and 15mm long. The target material must be conductive and changes in humidity will affect the dielectric constant and hence the capacitance.

### 6.4.6 Inductive (Eddy current) Sensors

A small coil can induce a current in a target surface and this current creates a magnetic field which opposes the field in the primary coil windings and changes the voltage across the coil. This effect can be used to create a distance measuring device. The range is limited but is much greater than capacitance gauges. For example the Lion Precision U50- probe has a range of 15mm and the U3 probe has a resolution of 20nm. Inductive sensors are not affected by nonconductive materials in the sensor to target gap and so are immune to dirt and dust. They do however depend upon the electrical resistance and magnetic permeability of the target and so the target materials are restricted to materials with low electrical resistance such as aluminium and copper.

# Chapter 7. Laser interferometer tests

## 7.1 Introduction

Measurement of distance is an essential part of any positioning system. The resolution of proprietary systems is often given but what are the errors, how can they be reduced and what is the uncertainty?

Tests on one such distance measuring system, in this case a Renishaw RLU10 fibre optic laser interferometer encoder were performed. This system was selected as it could be used for verify other motion devices including motor driven stages, piezo and slip stick piezo stages which may or may not have inbuilt feedback systems.

## 7.2 Test set up

A Renishaw laser encoder was set up inside a stabilised environment along with a humidity, atmospheric pressure and temperature sensors. The signals were collected by a National Instruments data acquisition system. The system is shown diagrammatically in Figure 68.

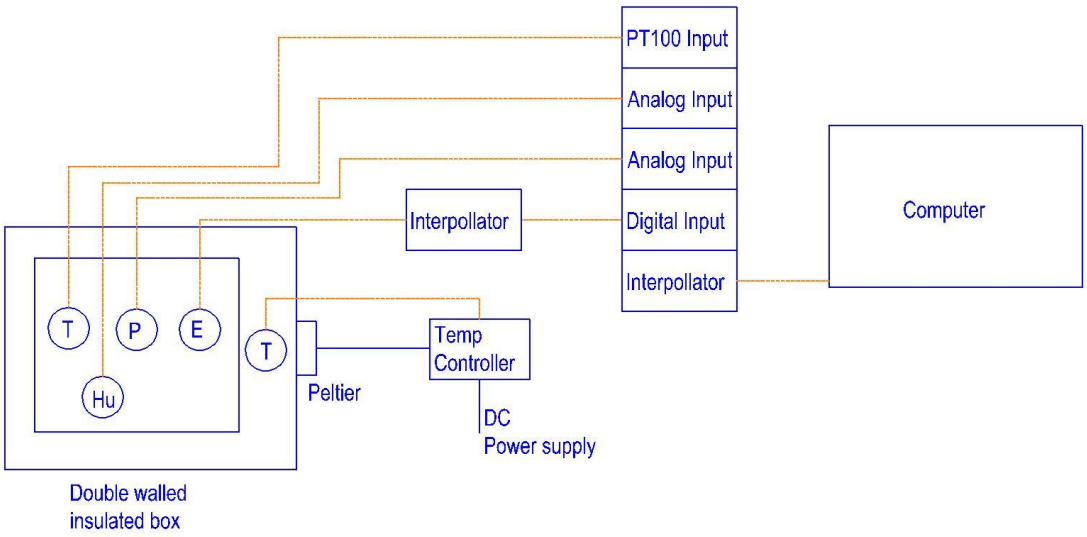


**Figure 68 – Signal collection scheme for the Laser interferometer tests**

### 7.2.1 Laser Encoder

The laser encoder consists of a RLU10 laser unit and a RLD 90° plane mirror detector head. The RLU10 is located outside the stabilised environment. The detector head is located within the stabilised environment and is connected to the RLU10 by a signal cable and a fibre optic cable. The laser beam is reflected back to the detector head by a plane 1 inch diameter mirror located 100mm from the detector head. The RLU laser unit provides a 1 volt peak to peak sine/cosine signal which is then connected to a REE0200A20B 200x interpolator which then outputs a RS-422A digital signal. The digital signal is then taken to a National Instruments 9472 digital input module located on a National instruments cRIO-9114 8 slot chassis.


**Figure 69 - Renishaw RLU10 laser unit**


**Figure 70– Renishaw detector head**

### 7.2.2 Encoder and mirror mount

The encoder is screwed down to a length of Silicon Carbide in the form of a box section 114mm wide, 58mm high, 300mm long, section thickness 7mm. The mirror is glued to a second piece of silicon carbide and this is also glued to the first section. The silicon carbide is stiff, has a lower coefficient of thermal expansion than aluminium or stainless steel.

### 7.2.3 Vibration reduction

The encoder, mirror and silicon carbide structure is supported on a 10BM-10 K-minus vibration isolated table. This is a mechanically sprung table using their patented negative spring technology. This has a vertical resonant frequency of only 0.5Hz

### 7.2.4 Temperature stability

The encoder structure and vibration isolated table are located within double skinned aluminium enclosure. The inner enclosure is Aluminium grade 6082, 16mm thick and the outer enclosure is made from Aluminium grade 1050A and is anodised black. Grade 1050A has a higher thermal conductivity than the normal 6082 grade. On the outer 4 sides are located four peltier heat pumps (Thermo Electric Devices THP33B) comprising of a peltier device, fan and finned heat exchanger. The external surfaces of the outer enclosure are insulated with 2 layers of 4mm thick thermal insulation (0.09 W/mK) and a layer of aluminium foil

**Figure 71 - Peltier heat pump**

A PT100 sensor is located on the inner surface of the outer enclosure opposite the peltier device. The PT100 is connected to a National Instruments 9217 4 channel analog input module. A lab view program is the used to control the peltier device in a

simple ON/OFF control in cooling mode only. The peltier power is switched using TTL relays which are controlled from a National Instruments 9472 Digital output module.

### 7.2.5 Pressure measurement

The pressure is measured using a Campbell Scientific CS100 Barometer which provides a voltage signal. The voltage is read by a National Instruments NI9206 Analogue input module.

### 7.2.6 Humidity measurement

Humidity is measured using a Vaisala HMP45AC Humidity and temperature probe. The voltage is read by a National Instruments NI9206 Analogue input module.

### 7.2.7 Location

The test was conducted within the vestibule of the Diamond Metrology Lab

### 7.2.8 Air turbulence

Turbulence of the air along the laser path was minimised by a simple silver foil shield.

### 7.2.9 Test procedure

#### 7.2.9.1 Data collection

The encoder, temperature, humidity and pressure signals were measured by the cRIO real time operating system at 10 mSec intervals. The data was then passed to a higher level lab view programme running on a PC. Here the data was filed at 1minute intervals.

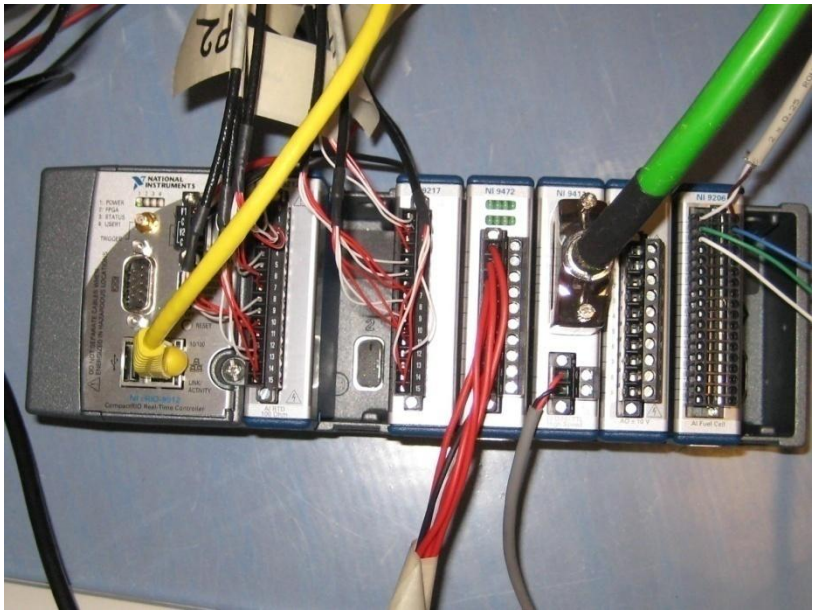

**Figure 72– National Instruments cRIO, back plane and C series modules**

#### 7.2.9.2 Peltier control

The peltier were controlled by the higher level lab view programme at an update rate of 200mSec.

#### 7.2.9.3 Test duration

Data was collected over at least an 8 hour period, the results were examined and then the test up was modified with the aim of improving long term stability. Opening the enclosure did result in change of temperature and this took many hours to stabilise.

#### 7.2.9.4 Data averaging

In these tests no data was averaged, all data was instantaneous data.

### 7.2.10 Sources of error

#### 7.2.10.1 Refractive index of air

The wavelength of the encoder laser beam will vary depending on the refractive index of the air that it travels through. There are 2 common equations, one developed by Ciddor and a version of the Edlen equation modified by Birch and Downs. These equations produce very similar results at ambient conditions. The refractive index varies with temperature, pressure, humidity and $CO_2$ concentration. The $CO_2$ concentration is often assumed to be constant at 450 ppm by volume. Renishaw give

the following factors that show the effect of temperature, pressure and humidity. These are based on the Ciddor or Edlen equations

0.96ppm/ °C, -0.27ppm/mbar, 0.0085ppm/%RH

#### 7.2.10.2 Temperature variation

The temperature of the air was measured using a PT100. The sensor should be as close as possible to the path of the laser through the air. The temperature may also vary along the length of the path. Keeping a short measuring distance will help. The interferometer head produces less than 2 watts but this may cause local heating of the air near the interferometer head. Even over short distance of about 50mm the temperature of the air can vary by about 0.2°C along the length of the laser path. The temperature difference does however seem to be constant.

The change in refractive index due to the change in air temperature can be compensated for. The uncertainty is estimated as follows

Limit of resolution of Temperature sensor, 0.003°C = 0.28nm (over 100mm)

Spatial variation in air temperature along beam path, 0.2°C

#### 7.2.10.3 Pressure variation

The pressure will vary depending upon atmospheric conditions, the building air handling system and opening and closing doors. The pressure was measured using a Campbell Scientific CS100 Barometer. This gave a linear voltage output of the range 600 to 1100 mbar at 0.05 and 2.5 volts respectively.

The equation to calculate the pressure from the voltage is then

P = 589.8mbar + Voltage x 204.08 mbar.

The quoted specifications for the Barometer are given in Table 36.

| | |
|---|---|
| Accuracy at 20°C | ±0.5mbar |
| linearity | ±0.4mbar |
| Resolution | ±0.1mbar |

**Table 36 – Barometer specification**

The voltage is read by a National Instruments NI9206 Analogue input module. This is a 16bit amplifier and Analogue to Digital converter. Over the input range ± 10V this gives a resolution of 0.3mV which equates to 0.06mbar. At a resolution of 0.1mbar then this equates to a variation in length over 100mm of

100mm x 0.1mbar x 0.27x $10^{-6}$ / mbar = 2.7 nm

In the test the pressure was measured at 200mSec intervals and a compensated encoder position was calculated. The compensated position was then recorded at 1 minute intervals. A test was conducted to determine the effect of pressure changes caused by opening a door. In this case the encoder position and pressure were recorded every 0.1 second and the internal door of the vestibule was opened 3 times.

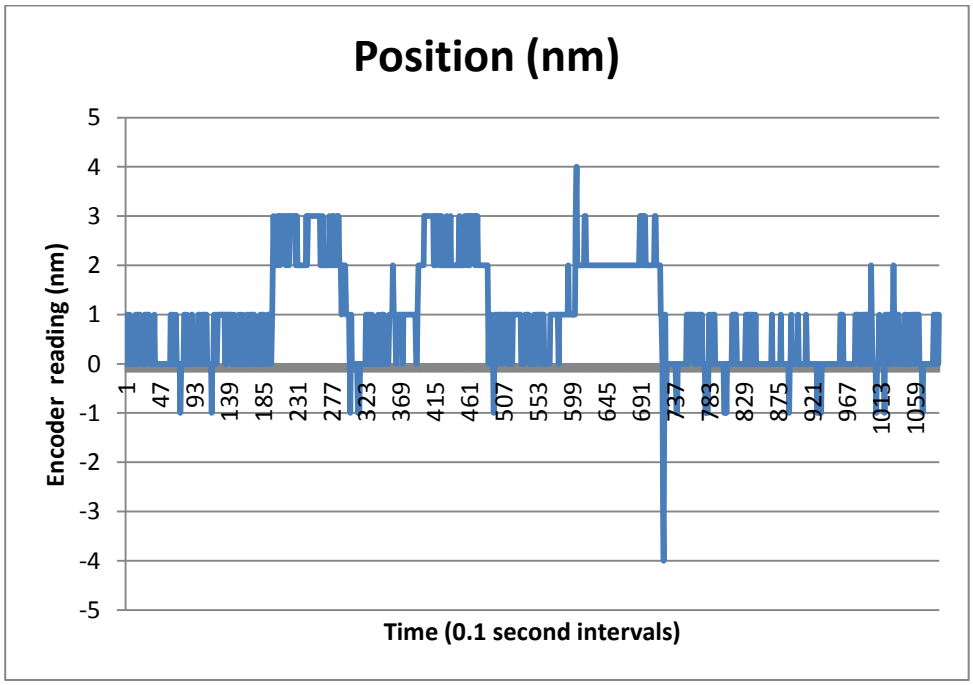


**Figure 73– Encoder position during door opening test**

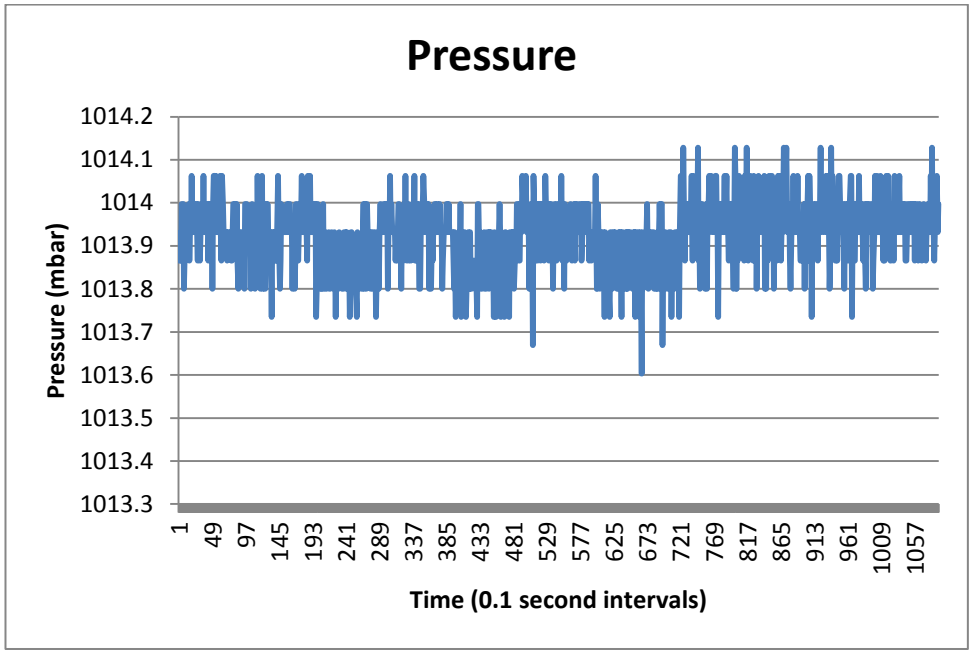


**Figure 74– Pressure reading during door opening test**

Figure 73 clearly shows the effect of the change in pressure on the encoder reading. The pressure in the room is maintained at 10 Pa (0.1mbar) above the external area. When the door is open the pressure reduces.

Figure 74 shows the pressure reading and the three periods when the pressure is reduced by about 0.1mbar.

The measured pressure drop and its change in encoder position match that predicted by the change in refractive index. A further test was done over an 8 hour period recording at minute intervals. Figure 75 shows the encoder reading and Figure 76 shows the pressure reading. This clearly shows a reduction of pressure as atmospheric high pressure moves away and a low pressure area arrives. The encoder reading shows an almost inverse effect. Taking into account the change in refractive index a pressure compensated position is shown in Figure 77.

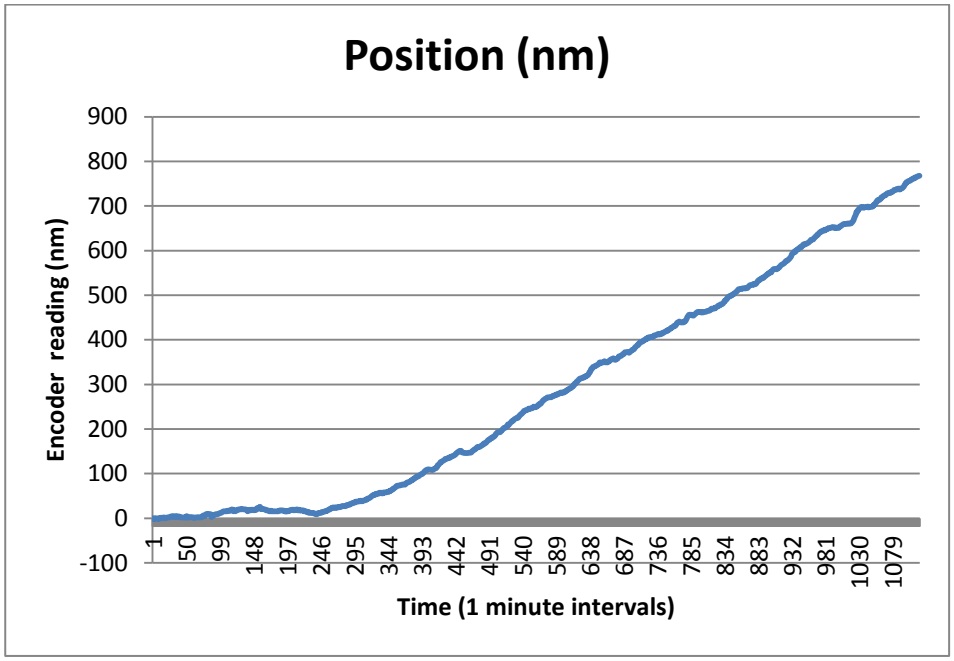


**Figure 75 - Measured position**

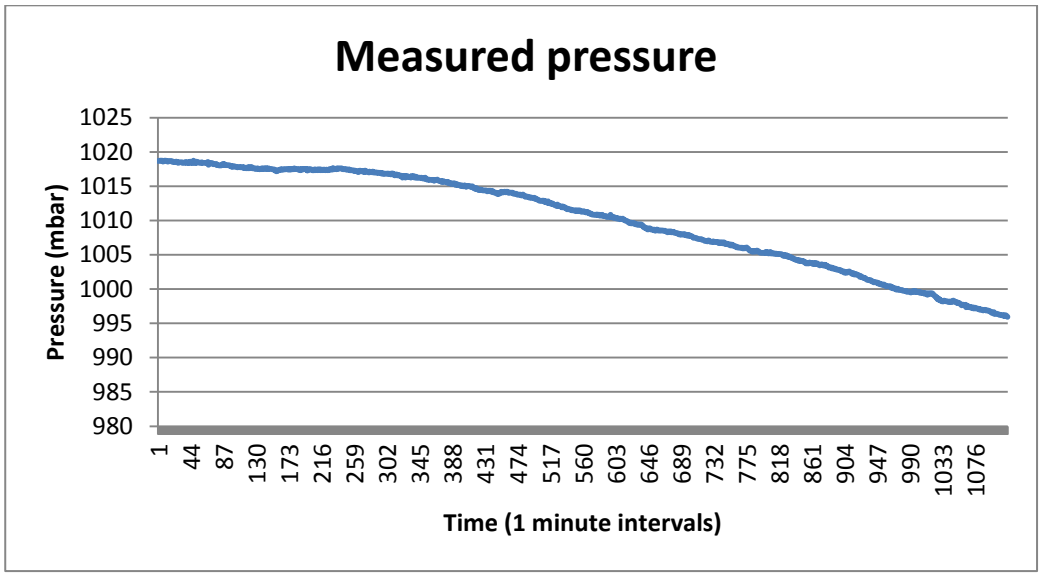


**Figure 76 - Measured pressure**

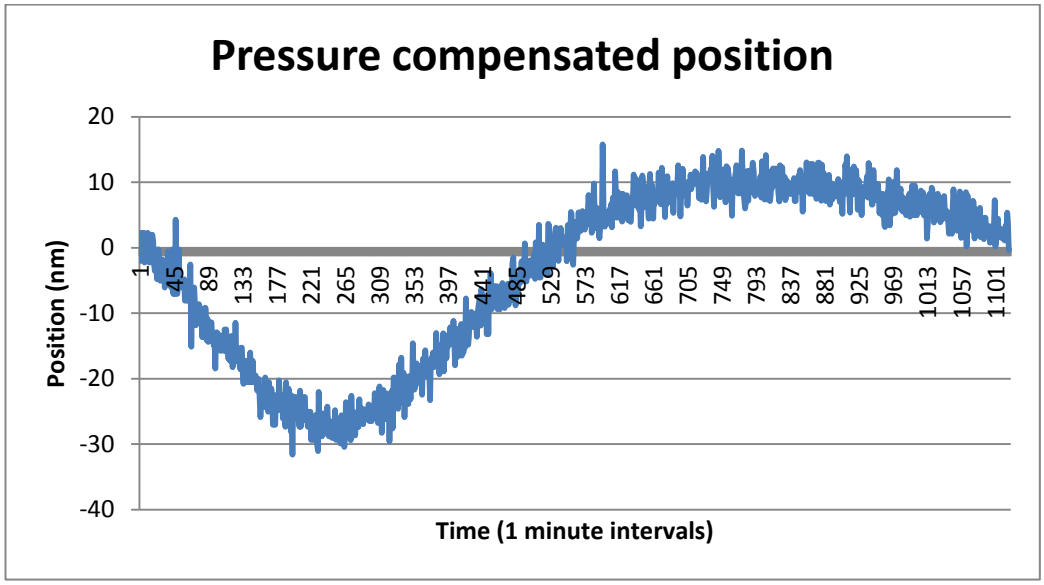


**Figure 77 - Pressure compensated position**

The effect of pressure on the refractive index can be compensated for up to the resolution of the pressure sensor which is 0.1 mbar (2.7nm)

Pressure compensated Position = Nominal - (P-P0) x $2.7 \times 10^{-7}$ x (Nominal position + Δx) +Δx

Where the nominal position is the distance from the mirror to the interferometer head at zero encoder counts, Δ x is the change in position from zero measured by the encoder, P0 is the nominal pressure in mbar and P is the measured pressure in mbar.

Figure 78 shows the pressure recorded over the first 50 minutes, the error bars show an error of ± 0.15mbar. A $2^{nd}$ order polynomial is fitted and 98% include the polynomial so a total uncertainty of ±0.15mbar at the ±2σ (95% confidence) seems reasonable

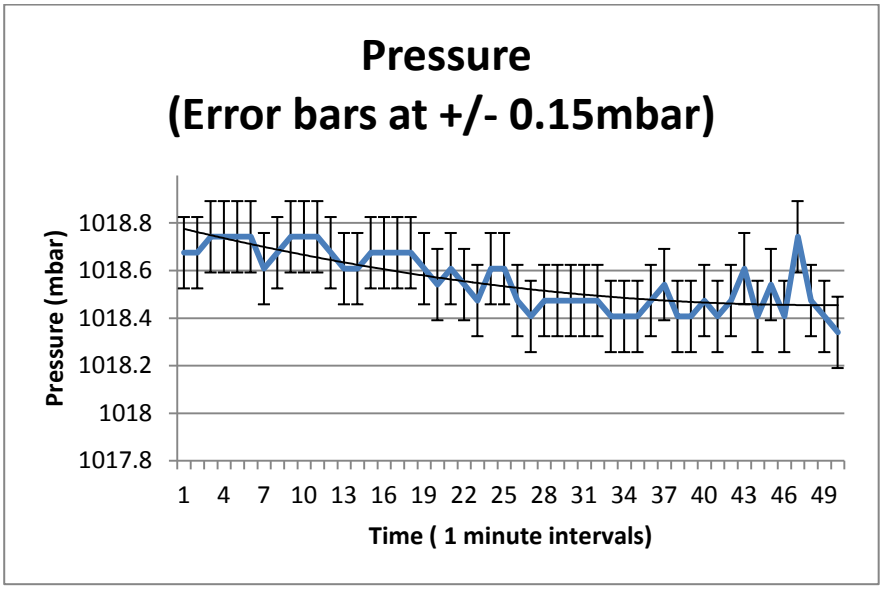


**Figure 78 - Pressure variation**

### 7.2.10.4 Humidity variation

Humidity is measured using a Vaisala HMP45AC Humidity and temperature probe. The output of the probe is from 0.008 to 1 volt DC over the range 0 to 100% relative humidity. The signal shows a resolution of +/- 1% RH. This equates to a length of

$0.0085 \times 10^{-6} \times 1 \times 100 \times 10^{-3} = 0.85\text{nm}$

### 7.2.10.5 Wavelength stability

The laser is stabilised but does vary with time. The quoted factors for the Renishaw RLU10 are as follows

| Variation in wavelength | Duration |
|---|---|
| ± 10 ppb | 1 minute |
| ± 0.05 ppm | 1 hour |
| ± 0.05 ppm | 8 hours |

**Table 37 – RLU10 wavelength stability**

Renishaw also produce the RLU20 unit and this has improved laser stabilisation. Over a 100mm measurement distance and 8 hour duration this would give an uncertainty of $\pm 0.05 \times 10^{-6} \times 100 \times 10^{-3} = \pm 5.0$nm

#### 7.2.10.6 Thermal drift coefficient of laser interferometer head

Renishaw quote <100nm/°C for the plane mirror interferometer. For an 11 hour test a variation in the support structure temperature of 0.003 °C was measured. This would give an uncertainty of $100 \times 10^{-9} \times 0.003$ C = 0.3nm

#### 7.2.10.7 Interpolator errors

The interpolator converts the analogue 1 volt peak to peak sine and cosine signal from the RLU10 unit to a RS-422A digital quadrature output and interpolates by a fixed factor between 4 and 4,000. In this case the interpolator was 200x.

The highest accuracy signal is obtained if the sine and cosine signal are in phase. If the sine and cosine signals are monitored on an oscilloscope a Lissajous Figure is obtained. For two sine waves out of phase by 90 degrees the lissajous figure is a circle. There are errors in the interpolator caused by DC offset, phase error and AC mismatch. These will then be observed as a lissajous figure which is either non circular or offset. These so called sub divisional errors (SDE) are cyclic and typically has a period of 158nm for a plane mirror interferometer. For the interpolator used the error is quoted a less than 50nm. At maximum rate of change then 1.61nm of length change corresponds to a measured length change of 0.78nm. The uncertainty caused by the cyclic error is a maximum of 1.61nm.

#### 7.2.10.8 Temperature measurements

The temperature is measured using 4 wire PT100 sensors connected to a National Instruments NI9217 Analog input module. The NI9217 has a noise rejection of 85 db at 50Hz and a resolution of 0.003°C when operated at less than 3.3Hz. The accuracy is 0.15 °C over the range -200 to 150 °C. However a higher level of resolution can be obtained if using the analog module to measure resistance and then convert the resistance to temperature in software.

The measured resistance is converted into a temperature reading using the following formulae.

$T_r = -R_0A + \sqrt{( R_0^2A^2 – 4R_0B(R_0-R_T))} / 2R_0B$

$R_0$=100, A = 3.908 x $10^{-3}$, B= -5.775 x $10^{-7}$

The uncertainty is assumed as 0.003°C

#### 7.2.10.9 Air turbulence

Convection currents within the box will create air turbulence, the effect on the beam measurement would be the change in refractive index caused by differential temperature. The beam is shielded by a foil and so no additional uncertainty has been added because of the air currents.

#### 7.2.10.10 Thermal expansion of supports

The mirror and encoder are mounted on silicon carbide structure. The distance between the encoder and mirror will vary with temperature. This is a real effect and should not be compensated for.

#### 7.2.10.11 Vibration

By supporting the encoder and mirror system on a rigid silicon carbide structure and then supporting this on an vibration isolated platform the effect of vibration has been minimised.

#### 7.2.10.12 Flatness of mirror

The mirror is not flat and so any change in position of the encoder over the surface of the mirror will show up as a length change. The laser beam diameter is however much larger than any change in position over the face of the mirror and so this effect is expected to be negligible.

#### 7.2.10.13 Electrical noise

Electrical noise can be categorised as follows

- Capacitive coupling caused by changing of electric fields

- Inductive coupling caused by changing magnetic fields
- Electromagnetic coupling caused by radiative signals
- Conductive circuits.

The electrical noise has been reduced as follows

- Encoder cable as a single shield
- The pressure gauge signal cable is a shielded twisted pair with shield grounded at one end.
- The humidity sensor signal cable is a shielded twisted pair.

## 7.3 Results

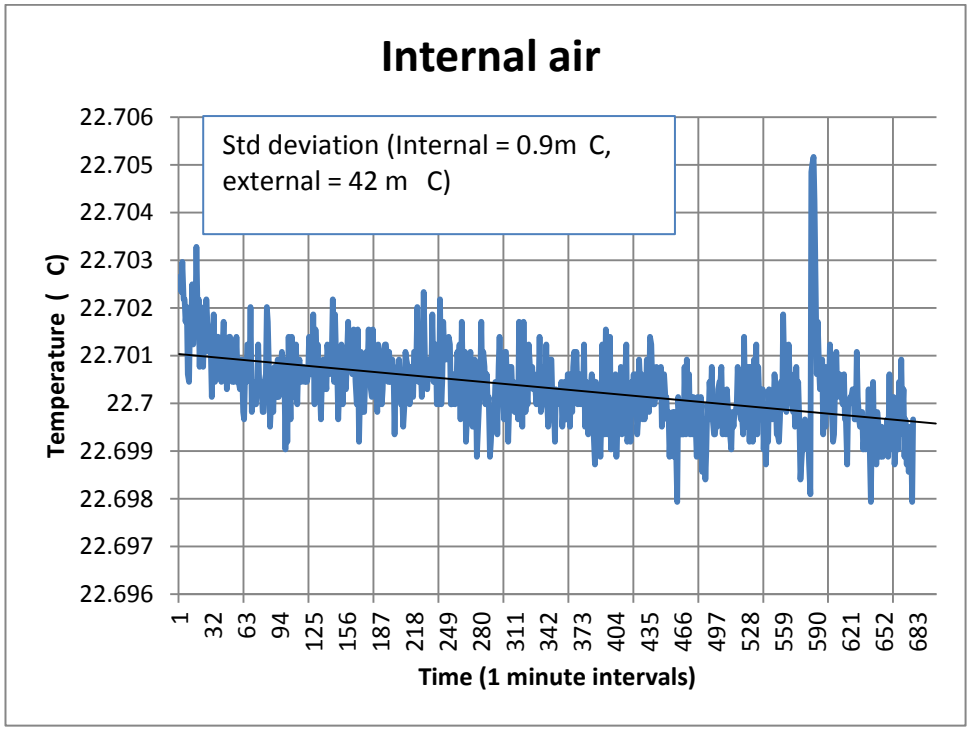


**Figure 79 – Temperature of air over a 11.5 hour period**

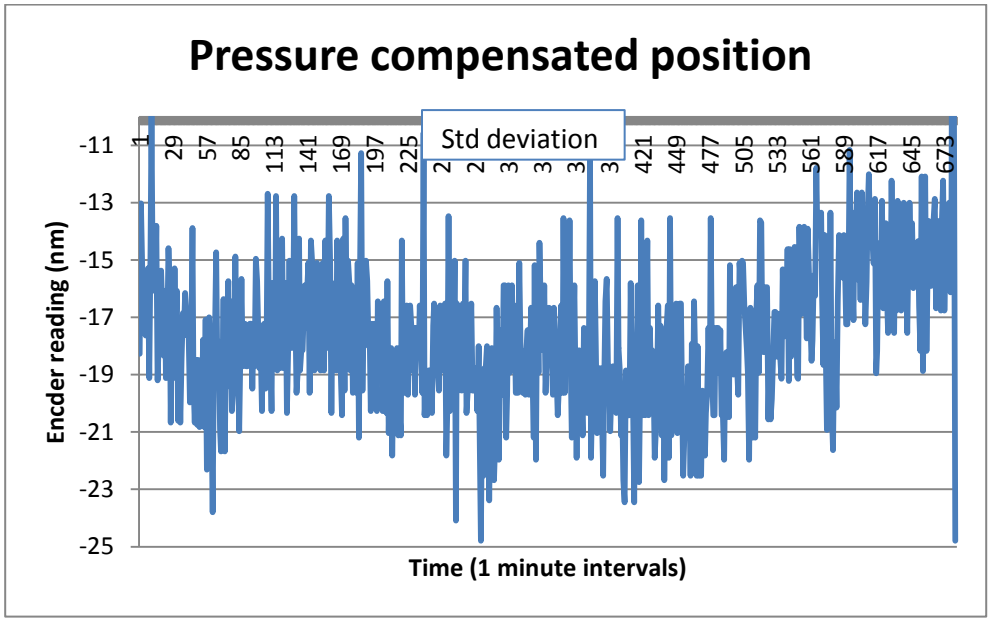


**Figure 80– Pressure compensated position over a 11.5 hour period**

The signal shown in Figure 80 has been compensated for pressure changes only. If the actual position only changes by 1nm the variation in signal gives an indication of the uncertainty. From these results the standard deviation of the pressure compensated position is 2.4nm. At an expanded uncertainty of 2 then this gives an uncertainty of +/- 4.8nm at 98% confidence.

## 7.4 Measurement Stability

If the measurement was perfect the distance between a fixed mirror and the laser encoder would be constant. The reason for a non constant signal have been identified as follows

- Changes in refractive index caused by pressure, humidity, temperature and CO2 content changes
- Wavelength stability
- Interferometer head thermal stability
- Interpolator error
- Thermal expansion of support structure
- Electrical noise
- Mirror flatness errors

- Limited resolution of pressure, humidity and temperature sensors
- Calculation and rounding errors

The resolution of the encoder is 0.78nm, so any physical change in distance below this level should result in a constant signal.

The following methods have been implemented to minimise the actual change in length. This includes

- Using low thermal expansion Silicon Carbide
- Maintaining good temperature stability
- Reducing the effect of vibrations by using a stiff structure on a vibration isolated platform

The effect of these is estimated to reduce the change in actual length to less than

$5 \times 10^{-6} \times 200 \times 10^{-3} \times 0.001 = 1\text{nm}$.

If the effects of actual length change are because of temperature changes then they should be gradual.

## 7.5 Measurement Uncertainty

An analysis of the uncertainty is given in Table 38.

| Symbol | Source of uncertainty | Value (nm) | Probability distribution | Divisor | ui |
|---|---|---|---|---|---|
| Rt | Refractive index – temperature resolution | 0.28 | Normal | 2 | 0.14 |
| Rp | Refractive index – pressure resolution | 4.05 | Normal | 2 | 2.02 |
| Rh | Refractive index – humidity resolution | 0.85 | Normal | 2 | 0.42 |
| Ws | Wavelength stability | ± 5.0 | rectangular | $\sqrt{3}$ | 2.89 |
| Ht | Interferometer head thermal stability | 0.3 | rectangular | $\sqrt{3}$ | 0.17 |
| Ie | Interpolator error | 1.61 | rectangular | $\sqrt{3}$ | 0.93 |
| u | Combined standard uncertainty | | normal | | 3.67 |
| U | Expanded Uncertainty | | Normal (k=2) | | 7.35 |

**Table 38 – Measurement uncertainty**

## 7.6 Discussion

The measurements over a 11.5 hour period gave an uncertainty of ± 4.8nm at 98% confidence, this compares with a theoretical uncertainty of ± 7.35nm. Considering that the results are only for 1 test then this comparison seems to show reasonable agreement. One of the main contributions to the uncertainty is the wavelength stability. Renishaw do offer a RLU20 with an enhanced wavelength stability. The wavelength stability of the RLU20 over an 8 hour period is ±20ppb as opposed to ±50ppb for the RLU10. The second major uncertainty is due to the pressure measurement and if the RLU20 is used this would be the major contribution. The Renishaw system is offered with a pressure compensation system and it would be interesting to know what the resolution and accuracy of their pressure sensor is.

Since these tests were conducted further improvements in short term stability have been achieved. This has been done by using a low thermal expansion ceramic instead

of the silicon carbide, but more importantly by changing the mirror support system. The mirror was glued but more stable results were achieved by spring loading the mirror against two stainless steel pins. In the short term, over 10's of minutes the system was stable to within one pulse (0.63nm).

The temperature within the enclosure took some time to stabilise because of the heat load from the RLU10 interferometer head. Renishaw now produce a lower heat load version which produces 0.14W rather than 2W.

## 7.7 Experience obtained

### 7.7.1 Local thermal stabilisation enclosure

To obtain good long term thermal stability of the optics and sample one concept is to provide a local enclosure. To test how practical this could be a temperature stabilised enclosure was constructed and used on B16 Test Beamline. The results are presented in Appendix F. The concept was to enclose the final focussing optics, the sample and some of the detectors within a temperature stabilised enclosure. In this case the optics used were zone plates with a focussing distance of about 100mm. A number of motorised stages were used to position the zone plates and the order sorting aperture and the sample. These included stepper motor stages from Newport Spectra Physics, a PI piezo stage and some translation, pitch, rotation and vertical motion attocubes. An intensity detector and a X ray camera were mounted on a pneumatic stage so that each could be exchanged remotely. The thermal enclosure was mounted on the optical table within the B16 Experiment hutch. Practical experience showed a number of issues.

The lids were quite heavy and quite onerous to remove on a regular basis, also because they were quite high, it was difficult to remove the lids easily. In future lighter hinged lids should be provided.

The time taken to obtain temperature stability was quite long, the motors produced a lot of heat and this increased the air temperature within the box, when the lid was removed the hot air escaped and it took a time for the fresh air to come up to temperature. The volume of air was too large and the heat load from the motors was high with no good thermal conductive path for efficient cooling.

The cables connecting the attocubes to their controller were very short so that the controllers had to be very close and this made access to the internals of the box even more difficult.

The experiments were conducted over a few days and the zone plates were frequently changed and this required changing of the focus distance. Access to move the components within the enclosure was difficult as the gross distance changes were manually made using a bread type of arrangement. In future these motions should be easily adjusted with a motorized stage which has a much larger range

The thickness of the box is quite considerable, about 50mm. This can be a problem with certain types of experiments were a large area detector is required to collect a wide angular fan of radiation. The sample station would need to be at the very end of the box as near the wall as possible and a circular aperture required to allow the radiation to reach the detector outside the enclosure. The aperture would need to be sealed with perhaps a double layer of Kapton to reduce heat transfer. This type of enclosure was probably not ideal for these type of diffraction experiments.

Fluorescence measurements can be done effectively, the detector is often located at 90 degrees to the beam and the detector usually has a long nozzle with the heat generating electronics situated further back. In this case a 30mm hole in the box allows the detector head to get close to the sample. This solution works well.

The temperature stabilisation using peltiers worked very well, the only source of vibration are the small fans on the heat exchanger. Space is required for the controllers and power supplies. Thermister temperature sensors gave very good resolution and enabled accurate setting of the set points for each peltier.

Some tests were done using granite blocks within the enclosure to increase the thermal mass. This gave some improvement but the heat transfer via air is poor when the temperature difference is so small. Thermal conduction must be seen as the prime heat transfer route.

The thermal enclosure offers benefits but can be quite restrictive and so should not be used unless the experiment cannot be performed without it.

One future experiment planned is to develop an X-ray interferometer. This has been attempted at Spring 8 but the thermal stability was identified as being critical and poor results were obtained because the thermal stability was not adequate. In this case the experiment was done in a rather simple enclosure. This is the type of experiment that would benefit from a thermal enclosure similar to that tested on B16. Over the next few months a new enclosure will be designed based upon lessons learned for the X ray diffractometer.

### 7.7.2 Hutch temperature controller settings

The hutch temperature control is known to be highly dependent upon the PID settings in the controller. Currently it is not possible to monitor the temperatures within the hutch and without such information accurate tuning and monitoring of performance is not possible. Work on tuning of the PID settings has been carried out on B16 and now new permanent data logging temperature sensors are being installed. It is proposed that all new beamlines be fitted with such sensors in critical hutches. In addition staff from the Facilities Management Group are being trained on how to tune the controllers.

### 7.7.3 Rigid coupling of optics to sample stage

A number of tests have been conducted on B16 using nano focus optics. In the early tests the optics were mounted on one tower stage system, the sample on another and the detector on a third. As beam sizes have reduced this has been found to be inadequate and vibration measuremenst with the Laser Vibrometer confirm this. Recent tests were conducted on a purpose built aluminium stiff frame system where the sample and optics were mounted on this common frame. This simple change has allowed beam sizes of 70nm to be produced on I18 Beamline and it has allowed the complete system to be easily moved between beamlines. Aluminium is not the ideal material but these type of experiments are often developed during the experimental period and changes are often required. Aluminium can be easily drilled with new holes to suit different arrangements. It can often be that the beamline scientist will take a hack saw to some parts to allow a new type of experiment to be conducted over a

weekend experiment run. Following these tests a new improved arrangement is being designed, this will use a similar frame concept but will be built in steel rather than aluminium. Once this has been tested a final arrangement probably using granite will be constructed as the final solution.

This concept of stiff coupling of the optics and sample stage is going to be applied to I14 Beamline. The original idea was to have separate granite slabs for the optics and sample stage, but this has been changed so that a longer and stiffer granite slab will support both.

### 7.7.4 Voice coil actuators

Motion solutions are often either stepper motor and lead screw or a pneumatic actuator. There are however many other choices and the voice coil actuators look particularly interesting. There are some new devices on the market that give high forces, large accelerations with integrated position feedback. These are being looked at for the use for a fast shutter system. In this case a small tungsten beam stop needs to be opened and closed with millisecond timing. The system is operated by a dedicated controller where the position, speed and acceleration can be controlled. We are discussing with the Diamond controls group how this can be integrated into our existing controls systems.

### 7.7.5 Slip stick piezo actuators

On B16 we have used attocube slip stick actuators but have found them unsatisfactory even when fitted with encoders. Recently we have tried a stage developed by MICOS USA which has cross roller bearings to give much higher load capacities. The footprint is small and the associated controller is physically small. These devices have shown to be very effective for linear travel and are being used for part of the 70nm experiment.

### 7.7.6 Pneumatic actuators

In a recent experiment on the B16 Test Beamline the motion of two small detectors located within a thermally stabilised enclosure were changed from stepper motor driven stages to pneumatic actuators. The pneumatic actuators were fitted with bleed

valves to prevent jolts but this was not perfect. The motions were vertical and no counterbalance spring was fitted so operation against gravity was smooth but when moving down the motion was a bit too sudden. The pneumatic actautors were used to reduce the heat load within the enclosure. This could be a solution if proper attention is made to reduce the jerk produced at the start and stop of the motion. There are however many advantages of going for a traditional motorised stage as the speed and accelerations can be better controlled and the end positions can be modified easily. Operation by pneumatic actuators, with balancing springs will be applied for smaller objects such as beam stops or filters rather than detectors.

### 7.7.7 Flexures

With the availability of local companies with precision wire eroding machines, suitable materials and the availability of FEA packages to engineers custom designed flexures are starting to become more common. The polychroamotor for I20 includes a number of flexures one of which provides a remote centre of rotation for twist correction in the crystal. Many piezo actuators are designed using flexure mechanisms and these have been used for scanning of samples. The use of flexures as already been used on beamlines and their use is expected to rise significantly in future.

### 7.7.8 Granite blocks

Granite has been used for structures because of its large thermal mass, long term stability and relatively low thermal expansion. Granite has been used for many projects at Diamond including the state of the art optical mirror measuring system located in the optical metrology lab. Polymer granites have also been used and their casting process offers more complex shapes to be produced, lead times can also be shorter. A polymer granite block has recently been installed for the I20 polychromator, in this case the final design could not be confirmed unto late in the project and a large cut out in the base was required to allow space for a detector arm bearing. A polymer granite solution was chosen. The mould tool was built, granite cast with inserts fitted, top surface ground and then inserts jig bored and system delivered in 6 weeks. It is expected that in future smaller systems will be built using granite.

### 7.7.9 Silicon Carbide

Silicon Carbide looks to be a very useful material but integrating the material into a design has proved to be difficult. One solution is to use standard sized shapes and then glue them into completed systems. The problem has been that to produce a structure with the correct features can result in a requirement to grind away lots of materials or have lots of small pieces bonded together. When compared to using solid metal the silicon carbide becomes more restrictive. Modification after delivery is almost impossible, machining can only be done using special machine tools and tapping threads can only be done using inserts. Despite much effort in developing some designs no progress has been made.

### 7.7.10 Low thermal expansion ceramics

Some tests have been done using a low thermal expansion ceramic called Nexcera. This has shown to be very thermally stable but integration and practical use is difficult. The material is only available ss simple sheets, it's brittle, expensive and has long delivery. More complex shapes can be produced but it is not seen as a practical material for use on a beam line.

### 7.7.11 Laser encoders

A lot of work has been done to gain practical experience with laser encoders. In theory they offer non contact distance measurement with sub nanometre resolution. One of the problems is compensation for pressure. The accuracy of the pressure measurement seems to define the available stability of the system, the use in vacuum would eliminate this problem. Stable readings over many hours at sub nanometre resolution have been achieved with the system mounted in a temperature stabilised environment, mounted on low thermal expansion materials and supported on a vibration isolated platform. In theory the laser system could be used to measure much closer to the position of the area of interest than say a scale encoder, but the system still needs to be fitted with relatively large mirrors or retro reflectors. For nano metre focussing systems the working distances are small and space for a zone plate, order sorting aperture and sample is very small and at this stage it is difficult to see how a

laser encoder system can be fitted. There are however new systems being developed some of which are much smaller and it may be that these systems can be fitted in the future, although they are expensive.

### 7.7.12 Capacitive sensors

Some capacitive sensors are currently being used. One use is to measure stage stiffness and the other is to measure thermal expansion of some prototype carbon fibre tubes. Capacitive sensors can offer nanometre resolution but the travel range is very limited. Experience with using these is at an early stage but it does seem that they are useful for such tests and because they are very small they could be incorporated into flexures easily. Commercial piezo stages often using capacitive sensors as feedback. They are however expensive and the issue of integrating the controllers into the Diamond controls systems needs to be addressed.

## 7.8 Exact constraint design

## 7.9 Introduction

At the nanometre level the influence of un defined forces becomes very import and exact constraint design should be adopted. As an example bolting two surfaces together is a common design principle but at the nanometre level this raises uncertainty in geometrical position. The two plates are not exactly flat so at which points are the plates making contact? This could vary depending upon the tightness of the bolts, the order in which the bolts are torque up, the level of friction between the plates, their bulk temperatures and the residual stresses from manufacturing. There are a number of concepts that should be adopted to ensure there is no uncertainty over position. These are outlined in this section.

## 7.10 Thermal expansion fixed point.

All materials will change shape with temperature. In the design a point must be identified which is where two parts are connected with no motion, all the other points should allow for differential thermal expansion. For example only one fixing could be a

counter sunk screw, the others should be flat headed to allow for differential movement and ideally be sprung loaded.

## 7.11 Fixing weak to strong

If two structures are bolted together which component deforms to match the other, if both structure have the same stiffness then the final shape is unknown. If a low stiffness component is fixed to a high stiffness component it then it is known which part will define the final shape.

## 7.12 Over-constrained motion

It is often that motion is defined by a pair of parallel linear bearings, but these are never parallel and there is some deformation in the rails in both vertical and horizontal directions. The design should allow a flexure so that one bearing is the master rail and the other is connected by a flexure so that it provides support but does not fight against the master rail.

## 7.13 Kinematic Mounts

Kinematic mounts are designed so that components can be removed and replaced with the maximum amount of reproducibility. There are a number of designs, materials and suppliers. These have been used for sample mounts on Beamline I15.

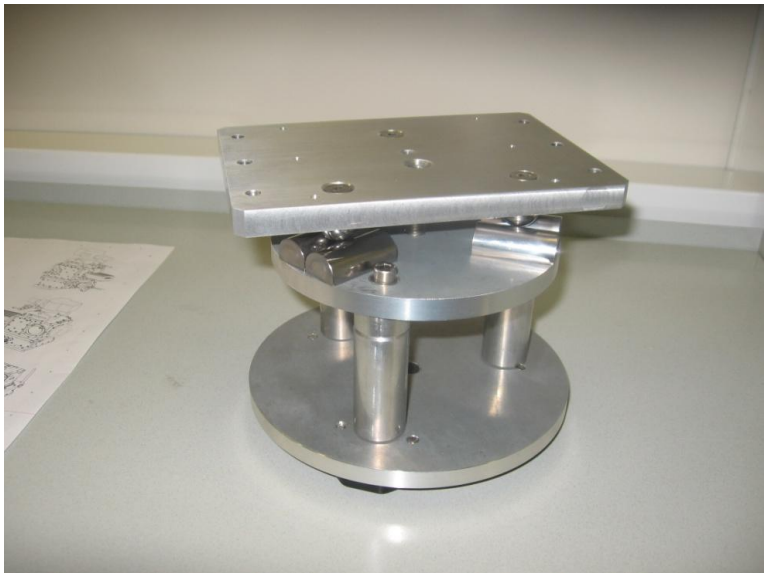

**Figure 81 – Example of a kinematic mounts**

### 7.13.1 Preload

One of the key features of a kinematic design is maintaining a constant preload. Highly loaded contact points will result in elastic deformation, to increase the reproducibility the contact points should be manufactured from very hard materials and the loading should be as reproducible as possible. This can be accomplished using permanent magnets, coils springs or disc spring washers. Plain bolts could be tightened with a torque wrench but the load is very dependent upon the coefficient of friction between the threads so this approach is not recommended.

### 7.13.2 Materials

Common materials include sapphire, chrome steel (52100), hardened stainless steel (404c) and Silicon Nitride. The most common is the chrome steel which can be produced with a good surface finish.

## 7.14 Experimental tests

A range of tests have been conducted by the author on equipment and ideas that may be suitable for incorporation into a system for a nano focus beamline.

Appendix A shows the results of some work on the Renishaw Laser interferometer. Diamond have almost exclusively used incremental optical scale encoders and had little experience of laser encoders. The tests conducted were to gain experience and attempt to characterise the uncertainty in position measuring. The tests clearly showed the problems of the influence of pressure, temperature and humidity on such devices and although the temperature can be controlled, atmospheric pressure will remain significant. These effects can be compensated but the sensitivity of the sensors becomes critical when measuring large distances with nanometre precision. Quoted resolutions look good on these devices but these tests showed that obtaining stable readings is very difficult and the influence of vibration, thermal stability, structure stiffness and electrical noise are key issues.

Appendix B is some work on an idea for a novel pyramidal structure using carbon fibre tubes. This gave some interesting results and showed the advantage of large diameter light weight, high stiffness carbon fibre tubes in a pyramid structure.

Some ideas for an active vibration platform based upon position measurement rather than velocity or acceleration is presented in Appendix C.

To counteract the effect of thermal expansion and low frequency vibration a piezo actuated adjustable length was developed and this is presented in Appendix D.

Some characterisation tests of an existing end station was carried out using a laser vibrometer. These results are presented in Appendix E.

It is recognised that thermal stability is an important issue and some work was done on developing a thermally stabilised environment. The objective was to obtain thermal stabilities of m°C over 24 hours but allow easy operation by the experiment users. The results of some tests are covered in Appendix F.

Some tests on passive vibration platforms are presented in Appendix G (Pneumatic isolators) and Appendix H (negative spring coefficient system).

# Chapter 8. Conclusions and recommendations for future Work

## 8.1 Summary of work conducted

In this thesis the requirements for an experimental end station suitable for focussing hard X-rays to below 100nm has been explained. A number of key mechanical issues have been identified which need to be addressed. The latest products have been reviewed and relevant research identified. Some tests have been conducted and concepts developed.

## 8.2 Main findings

In this thesis the challenges in producing sub 100nm sized hard X-ray beams have been examined. The different types of focussing optics have been reviewed and some types of experiments highlighted. The issues of thermal stability, vibration stability, acoustic noise and positional control have been discussed.

The main findings are as follows:

Changes in relative position due to thermal expansion is a substantial obstacle to generating stable beams during experiments and must be addressed.

A number of low coefficient of thermal expansion materials have been reviewed and some such as Invar ®, low thermal expansion glass scales and low thermal expansion carbon fibre composites should be used where appropriate.

The Temperature stability of the experiment environment has been improved by correct optimisation of the controller parameters.

Data collection on the environment temperatures has been improved so tuning can be carried out easily, trends observed and problems identified.

Local thermal enclosures have been shown to provide m°C stability and the use of these with peltier controllers can now be adopted for critical applications. Temperature monitoring systems are available with 0.001°C resolution and monitoring at this level has been shown to be required.

Phase change materials have been reviewed and a possible material identified which can help improve thermal stability.

A number of generic design changes have been identified which will help improve thermal stability, these include minimisation of air volumes, maximum use of thermal mass, CTE compensated designs and an approach to solid designs rather than open space frames.

Different types of temperature sensors have been reviewed and some recommendations given.

The final focussing optic and the sample stage must be mechanically closely coupled by sharing the same base structure. The base structure should be designed so that any floor transmitted vibrations produce motions of both the sample and focussing optics that are of equal magnitude and in phase in a pure translation motion. Couple pitch and yaw motion is highly detrimental and has to be minimised.

Some vibration isolated platforms have been tested.

A novel type of stiff support structure using triangulated carbon fibre has been analysed and tested.

A number of actuator and position detectors have been reviewed and some types not commonly used but which may offer advantages over currently used systems has been identified.

Extensive testing of a propriety laser interferometer has been carried out and an analysis of the uncertainty performed.

## 8.3 Recommendations

### 8.3.1 Thermal stability

In many cases experiments will require exposure times of many minutes or even hours and so drift due to non stable thermal conditions will reduce experimental data accuracy and resolution. Low thermal expansion materials have been examined and some methods of improving thermal stability discussed. The key recommendations are as follows

- Further effort should be made to find a supplier who can reliably manufacture low thermal expansion carbon fibre tubes.
- Equipment to accurately measure the thermal expansion coefficient of actual carbon fibre components needs to be obtained and a test procedure developed so that suppliers claims can be verified.
- Future designs should move away from aluminium alloys towards steels or granite and where appropriate 36%Nickel / Iron alloys such as Invar®.
- Phase change materials may offer a method to improve temperature stability and n-Heptadecane $C_{17}H_{36}$ incorporated into structures should be tested.
- A greater uses of large thermal mass blocks such as granite.
- Use of thermally insulated enclosures with active cooling using peltier devices.
- Install more temperature sensors within the experimental areas which can be reviewed by the beamline staff. These should be logged and have a resolution of 0.1°C or better.
- Review the temperature stability of all of the beamline hutches and change the PID settings if required.
- A robust methodology of establishing the optimum air conditioning system control parameters needs to be implemented.
- 0.001°C resolution thermistors should be used for monitoring in critical areas
- Remove any stepper motor controller programmes that reduce current when motor is stopped.
- Move large heat generating components away from the critical areas.

- Air flows around components will affect thermal stability and modelling of these using Computational fluid Dynamics software is likely to be required in the future. A review of the cost, ease of use and relevant functionality of the available packages is required.

### 8.3.2 Acoustic vibration

Acoustic vibration can affect very flexible samples and low frequency noise at even low levels can affect the concentration of staff setting up delicate and difficult experiments. There are many new types of sound absorber including micro perforated panels. A panel could be designed that would easily fit into a typical lead shielded hutch structure, this would make it easy to install on any beamlines at Diamond and Internationally. Further work on reducing noise by fitting a variety of sound absorbing panels should be carried out.

Incorporation of noise reducing materials in the design of control rooms should be included in future beamlines.

Higher efficiency lighting will reduce heat loads and allow fans to be operated at a lower speed, this will help reduce noise levels.

On occasions electronic racks need to installed in the experiment hutch, these produce quite high frequency noise. Where possible these should be enclosed in an acoustic cabinet. The source of noise from these racks should also be examined, it may be possible to replace the installed fans with lower noise devices as used on domestic computers.

### 8.3.3 Floor transmitted vibrations

Extensive work on the design of the Diamond building has resulted in very low levels of floor transmitted vibration. However vibration does exist which is significant at the micro and nano level. It may be possible to reduce the magnitude of the vibration sources by investigating the effectiveness of the pumps plinths and support systems.

Active vibration damping systems look interesting but sensor noise is critical for low vibration environments such as Diamond. The high load capacity devices such as that produced by Halcyonics GmbH may be appropriate but need testing to confirm suitability, particularly the amount of vibration in the pitch direction.

The work by CERN could also be applicable and this should be monitored. CERN do have regular meetings to discuss such issues and attendance at such future events may be sensible.

Piezo patches could offer benefit, and this technology should be monitored.

The increased use of constrained layer damping could be considered, particularly for vertical vibration damping. A standard solution could be developed which is applicable to the typical frame and granite structures use at diamond.

Sand filled steel structures are commonly used at Diamond but information on its effectiveness is scarce. A programme of testing and comparison would be useful.

Many component frames and bases are fixed to the floor via adjustable feet, in some cases they rely on self weight. There is some evidence that using self weight, even with granite is not sufficient and that hard bolting down helps reduce vibration. Some testing of this, looking at the variation in response when varying the preload could be of benefit.

### 8.3.4 Motion control

Air bearings look attractive but their stiffness is still much less than traditional cross roller or linear ball slides except for large surface area bearings with large preloads. For larger components such as complete systems mounted on granite slabs air bearings have advantages but their design is not easy. It is recommended that some standard solutions for large granite masses be developed.

Laser interferometers are still affected by changes in air temperature, pressure and humidity and even with compensation, the resolution and stability is limited. New

interferometers are being developed which are not affected by such change. These developments should be monitored and implemented if cost effective when available.

Voice coil actuators have not been used very much at Diamond but they offer some advantages of both speed of operation, long travel and programmable control of acceleration, velocity and distance.

There are a wide range of linear encoders and some of these offer very high levels of resolution such as the Sony Laser scale. For critical applications liner encoders with low thermal expansion scales and small grating periods adapted. More effort should be made to ensure the encoder is close to the line of action and at the point of critical measurement.

### 8.3.5 Keeping up to date with latest developments

#### 8.3.5.1 Conferences

The main conference for Engineers working in the Synchrotron field is the bi-annual MEDSI- Mechanical Engineering Design of Synchrotron Radiation Equipment and Instrumentation. There is also the bi-annual SRI- International Synchrotron Radiation Instrumentation conference but this tends to be very scientific experimentation orientated.

There are three main conferences for precision Engineering.

- EUSPEN – European Society for Precision Engineering and Nanotechnology
- ASPE - American Society for Precision Engineering
- ASPEN – Asian Society for Precision Engineering and Nanotechnology

The European conference covers a broad range including nano machining, space and astronomy developments, MEMS and semiconductor work. There has been very limited presentations on work directly related to synchrotrons but there is a lot of similarity with other industries and attendance at the last few EUSPEN events has been very useful in establishing contacts with engineers who have greater experience in areas such as flexures and active vibration control. There has also been some very

useful tutorials which form part of the conference. It is recommended that attendance at the EUSPEN should continue. The ASPE is similar to EUSPEN but on a much larger scale.

There is a conference called MNE, Micro and Nano engineering,this is an international conference on micro and nano fabrication and manufacturing using lithography and related techniques. It is probably not relevant.

There are also more specialised conferences such as the ISMA- International conference on Noise and Vibration Engineering and the International Conference on New Actuators. These would be of limited use as the conferences would cover such a wide range of research that very little would be of direct interest.

#### 8.3.5.2 Exhibitions

Most conferences have a exhibition attached and this a good way of meeting new suppliers. In the UK there is only one exhibition that could be useful and that is Micro Manufacturing Live UK exhibition. This has grown steadily, in 2010 it was in Coventry, but in 2011 it will be at the much larger venue of the NEC in Birmingham. Although very focussed on micro manufacturing there has been some useful contacts made and attendance at this annual event is recommended.

#### 8.3.5.3 Journals

The most relevant journal is Precision Engineering, this is issued 4 times per year and represents the three societies EUSPEN, ASPE and ASPEN. This should be circulated to all the Senior Mechanical Project Engineers working at Diamond. The International journal of Precision Engineering and Manufacturing is issued 6 times per year and should also be circulated on a trial basis.

The International Journal of Precision Technology (IJPTech) is published 4 times per year. This journal is mainly devoted to precision manufacturing but does include Hydrostatic bearings, tribology and metrology.

There is also a magazine called Micro Manufacture which is available free, this focuses in micro manufacture.

#### 8.3.5.4 Data bases

The most useful data bases are Science Direct and Scopus. These are available through the Rutherford Appleton Library but not all journals are available so that the full text cannot be viewed on every journal.

#### 8.3.5.5 Networking Events

There are a number of one off events where useful contacts can be made, this includes an event at the Royal Society in 2011, Ultra-precision engineering – from physics to manufacturing and an open day at the National Physical Laboratory at Teddington.

There is a UK government organisation initiative called the Nanotechnology-Knowledge Transfer Network. This is very much focussed on nano technology in its broadest sense but there are some specialised groups which may of interest such as the group working on Metrology and the Engineering and Optical group. It is worth monitoring the events page.

#### 8.3.5.6 University Liaison

There are a number of Universities that have departments doing research work in precision Engineering.

Brunel University have an Advanced Manufacturing and Enterprise Engineering dept led by Prof K Cheng. A particular interest of the group is Micro and Nano manufacturing where they are developing super precision micro milling machines and extremely high speed spindles.

Prof Derek Chetwynd at Warwick University is particularly interested in metrology of surfaces, small displacements and high-precision instrument systems. Also within the school of Engineering Dr Zhao is doing research into Energy Storage and phase change materials.

Cranfield University has a precision machining laboratory with micro-milling, diamond machining and precision grinding equipment. They have also recently started an MSc course called Ultra Precision Technologies and provide five day training courses in Precision Engineering.

The University of Huddersfield has established the Centre for Precision Technologies which acts as an umbrella for three sub groups. These are the Advanced Machining Technology Group, Surface Metrology Research Group and the Engineering Control and Machine Performance Group. Prof Xiangqian (Jane) Jiang is very much interested in surface metrology using optical methods and is working on a novel fibre interferometer which could applicable to nano motion control.

Cardiff University had a department well know for micro manufacture but the professor, Duc Pham, is moving to the University of Birmingham so this may change over the next year.

The Institute of Sound and Vibration Research at the University of Southampton has some very specific research activities but this does not seem to include any work in active vibration control for metrology equipment. However they do hold some short course such as the 3 day course on Vibration measurement and analysis.

Liaison with Universities look attractive but funding for Universities is difficult and there is pressure from University departments to joint fund a post doc as a method of collaboration. Any work with Universities must be seen as a long term commitment.

# References

A Lagomarsino, A. C. (2002). Advances in microdiffraction with x-ray waveguides. *Cryst Res Technology* , 757-769.

A Slocum, P. s. (1995). Design of a self-compensated, water-hydrostatic bearings. *Precision Engineering* , 173-185.

Alianelli, L., Sawhney, K., Tiwari, M., Dolnya, I., Stevens, R., Jenkins, D., et al. (2009). Germanium and silicon kinoform focussing lenses for hard x-rays. *International Conference on X-ray Microscopy.*

Amick, H., Gendreau, M., Busch, T., & Gordon, C. (2005). Evolving criteria for research facilities: 1 - Vibration. *SPIE ; Building for nanoscale Research and Beyond.* San Diego.

Baker, R., Marion, P., Zhang, L., Marchial, T., Mackrill, P., & Favier, F. (2010). Thermal stability optimization of the ESRF nano hutch. *MEDSI.* Oxford.

Beitra, L., & Watari, M. M. (2010). Confocal Microscope Alignment of Nanocrystals for Coherent diffraction imaging. *SRI 2009, 10TH INTERNATIONAL CONFERENCE ON RADIATION INSTRUMENTATION.*, (pp. 57-60). Melbourne.

Bilderback, D. H. (1994). Nanometer spatial resolution achieved in hard x-ray imaging and Laue diffraction experiments. *Science* , 201-203.

C Richard, D. G. (2000). Enhanced semi-passive damping using continuous switching of a piezoelectric device on an inductor. *Proc. SPIE*, (pp. 288-299).

C Riekel, M. B. (2010). Progress in micro- and nano-diffraction at the ESRF ID13. *Synchrotron Radiation in Polymer Science* .

C Schroer, e. a. (2003). Nanofocussing parabolic refractive x -ray lenses. *Applied phyics letters* , 1485 - 1487.

Choi, Y.-M., Jeong, J., Gweon, D.-G., & Kim, D. (2008). six degrees of freedom magnetic levitation stage using new active magnetic bearings. *ASPE Proceedings, Precision Mechanical Design and Mechatronics for Sub-50nm Semiconductor Equipment* . Berkeley.

Collette, C., Artoos, K., Kuzmin, A., Janssens, S., MSylte, Guinchard, M., et al. (2010). Active quadrupole stabilization for future linear particle colliders. *Nuclear Instruments and Methods on Physics Research A* .

F Elder, M. G. (n.d.). *Physics Review 71,829* .

F Viana, V. S. (2008). Multimodal Vibration Damping through Piezoelectric Patches and Optimal Resonant Shunt Circuits. *J. of the Braz. Soc. of Mech. Sci. & Eng* , 293-310.

F Wardle, C. B. (2010). Dynamic charchteristics of a direct-drive air-bearing slide system with squeeze film damping. *Int J Adv Manuf Technology* , 911-918.

Garcia-Moreno. (2010). Conventional sintering of LAS-SiC nanocomposites with very low thermal expansion coefficient. *JOURNAL OF THE EUROPEAN CERAMIC SOCIETY* , 3219-3225.

Garcia-Moreno, O. (2011). Alumina reinforced eucryptite ceramics:Very low thermal expansion material with improved mechanical properties. *Journal of the European Ceramic Society* , 1641-1648.

H Meyerheim, C. T. (2009). Wurtzite-type CoO-nanocrystals in ultrathin ZnCoO films. *Phys. Rev. Lett. 102, 156102* .

H Mimura (refB), T. i. (2011). One-dimensional sub-10-nm har dX-ra yfocusing usin glaterally graded multilayer mirror. *Nuclear Instruments and Methods in Physic sResearch A* .

H Mimuraa, T. K. (2011). One-dimensional sub-10-nm hard X-ray focusing using laterally graded multilayer mirror. *Nuclear Instruments and Methods in Physics*

*Research Section A: Accelerators, Spectrometers, Detectors and Associated Equipment* , S16-S18.

Harlan, A., Mackay, C., & Vale, B. *Phase Change Materials in Architecture.*

Heuberger. (2001). The extended surface forces apparatus. II. Precision temperature control. *REVIEW OF SCIENTIFIC INSTRUMENTS* , 3556-3560.

Hignette. (2005). Efficient sub 100nm focussing of hard X rays. *Review of Scientific Instruments* .

Higuschi.S, & DeBra.D. (2006). Active thermal control experiments for LISA ground verification testing. *Laser Interferometer Space Antenna- 6th International LISA symposium*, (pp. 194-198).

Hrauda, N. (2011). X-ray Nanodiffraction on a Single SiGe Quantum Dot inside a Functioning Field-Effect Transistor. *Nano Letters* , 2875-2880.

J Provis, V. R. (2009). High-resolution nanoprobe X-ray fluorescence characterization of heterogeneous calcium and heavy metal distributions in alkali-activated fly ash. *Langmuir* , 11897-904.

J Tellinen, I. S. (2002). Basic properties of magnetic shape memory actuators. *Actuator 2002.* Bremen.

K Sakagami, M. M. (n.d.). Application of microperforated panle absorbers to room interior surfaces.

Kang, H. (2006). Nanometer linear focussing of hard x rays by multilayer laue lens. *Physical Review Letters* .

Kawata, K. (2006). Novel low thermal expansion material for EUV application. *Proceeding of SPIE.*

Kelly, R. *Latent Heat storage in building materials.* CIBSE.

L Wenjun, e. a. (2010). Hard X-ray focussing with monetl mirror optics. *Nuclear instruemnst and Mathods in Physics Research A* .

Maa. (1998). Potential of microperforated panel absorber. *J Acoust Soc Am* , 2861-2866.

Mangra, D., Sharma, S., & Doose, C. (2000). Performace of the vibration damping pads in the APS storage ring. *International workshop on mechanical engineering of synchrotron radiation equipment and instrumentation.* Villigen.

Mimura, H. Y. (2009). Efficient focusing of hard x rays to 25 nm by a total reflection mirror. *Applied Physics Letters* .

Munro, I. (1997). Synchrotron Radiation Research in the UK. *Journal of Synchrotron Radiation* , 344-358.

Nakamuar, Y., Nakayama, M., Yasuda, M., & Fujita, T. (2006). Developemnt of active six-degree-of-freedom micr-vibration control system using hybrid actuators comprisiong air actuators and giant magnetostrictyive actuators. *Smart mater.Struct 15* , 113301142.

Park, J., & Palumbo, D. L. (2009). Damping of Structural Vibration using lighteweight granular materials. *Experimental Mechanics* , 697-705.

Peijnenburg, A., Vermeulen, J., & Eijk, J. v. (2006). Magnetic levitation systems compared to conventional bearing systems. *Microelectronic Engineering 83* , 1372-1375.

Poowancum. (2010). Development of Low-Thermal-Expansion Silicon Carbide/Zirconium Tungstate Porous Ceramics. *JOURNAL OF THE AMERICAN CERAMIC SOCIETY* , 2978-2980.

Quanying, Y., Lisha, A., & Chen, L. (2010). Thermal performance of shape-stabilized phase change paraffin wallboard. *International journal of Sustainable Energy* , 185-190.

Ro, S., Kim, S., Kwak, Y., & Park, C. H. (2010). A linear air bearing stage with active magnetic preloads for ultrprecise straight motion. *Precision Engineering* , 186-194.

S Alcock, K. S. (2010). Diamond-NOM: A non-contact profiler capable of characterizing optical figure error with sub-nanometre repeatability. *Nuclear Instruments and Methods in Physics Research Section A: Accelerators, Spectrometers, Detectors and Associated Equipment* , 224-228.

S Krishnan, Y. J., Suresh, V. S., & Garimella. (2008). Metal Foams as Passive Thermal Control Systems. *Theory and Applications of Transport in Porous Media* , 261-282.

Sawhney, K. (2009). A Test Beamline on Diamond Light Source. *SRI 2009, 10TH INTERNATIONAL CONFERENCE ON RADIATION INSTRUMENTATION*, (pp. 387-390). Melbourne.

Stout, K., & Sweeney, F. (1984). Design of aerostatic flat pad bearings using pocketed orifice restrictors. *Tribology International* .

Sugimura. (2008). New insulation material with flat-surface, low coefficient of thermal expansion, low-dielectric-loss for next generation semiconductor packages. *58TH ELECTRONIC COMPONENTS & TECHNOLOGY CONFERENCE* (pp. 747-752). Orlando: IEEE.

Tao Sun1, 2. Z. (2011). High-sensitivity strain mapping around epitaxial oxide nanostructures using scanning x-ray nanodiffraction. *Applied Physics Letters* .

Wardle, F., Bond, C., Wilson, C., Cheng, K., & Huo, D. (2010). Dynamic charcteristics of a direct-drive air-bearing slide system with squeeze film damping. *Int J Advnaced Manuf Technol* , 911-918.

Yamamura, K. (2008). Figuring of elliptical hard X-ray focusing mirror using 1-dimensional numerically controlled local wet etching. *Surface and Interface Analysis* , 1014-1018.

Yu-Tung Chen1, 2. T.-N. (2008). Full-field hard x-ray microscopy below30 nm: a challenging nanofabrication achievement. *Nanotechnology* .

Zalb, B. (2003). Review on thermal energy storage with phase change materials, heat transfer analysis and applications. *Applied Thermal Engineering* , 251-283.

**Image References**

Physic.rwth-achen 1, 2012,*2D lenses produced at Aachen*.[image online] Available at : www.physik.rwth-aachen.de/en/institutes/institute-iib/group-lengeler/?no_cache=1&sword_list[0]=xray [Accessed 3 February 2012]

Diamond, 2012, *Silicon cuniform lenses* .[image online] Available at : www.diamond.ac.uk/Home/Publications/newsletter/Spring10/thin_films.html[Accessed 3 February 2012]

X-ray-optics 1, 2012, *Fresnel zone plate and Order sorting aperture*.[image online] Available at : www.x-ray-optics.de/index.php?option=com_content&view=article&id=22&Itemid=125&lang=en [Accessed 3 February 2012]

Xradia, 2012, *Schematic of a Fresnel zone plate.*[image online] Available at : www.xradia.com/products/xray-optics/zone-plates.php[Accessed 3 February 2012]

x-ray optics 2, 2012, *Mono capillary tube.* [image online] Available at :www.x-ray-optics.de/index.php?option=com_content&view=article&id=45&Itemid=55&lang=en [Accessed 3 February 2012]

x-ray optics 3, 2012, *Tapered capillary tube.* [image online] Available at :www.x-ray-optics.de/index.php?option=com_content&view=article&id=45&Itemid=55&lang=en [Accessed 3 February 2012]

hamptonresearch, 2012, *Hampton Research mount.*[image online] Available at: www.hamptonresearch.com/product_detail.aspx?cid=19&sid=115&pid=337 [Accessed 3 February 2012]

Oharacorp, 2012, *Water jet cut Corning ULE parts* .[image online] Available at: www.oharacorp.com/pdf/ccz-combination.pdf[Accessed 3 February 2012]

hightemp, 2012,*CTE of Invar and super Invar.* [image online] Available at: www.hightempmetals.com/techdata/hitempSuperInvardata.php. [Accessed 7 February 2012]

Spiraxsarco 1, 2012, *Linear valve characteristic.* [image online] Available at: www.spiraxsarco.com/resources/steam-engineering-tutorials/control-hardware-el-pn-actuation/control-valve-characteristics.asp [Accessed 3 February 2012]

Spiraxsarco 2, 2012, *Equal percentage valve characteristic.* [image online] Available at: www.spiraxsarco.com/resources/steam-engineering-tutorials/control-hardware-el-pn-actuation/control-valve-characteristics.asp [Accessed 3 February 2012]

Desy, 2012, *Ground vibrations measured at various sites.* From " GROUND MOTION & COMPARISON OF VARIOUS SITES" by R. Amirikas, A. Bertolini, W. Bialowons, H. Ehrlichmann *, Deutsches Elektronen-Synchrotron DESY, 22603 Hamburg, Germany. Available http://vibration.desy.de/sites2009/site_ground-vibrations/content/e1454/e3974/e1475/infoboxContent1489/Nanobeam2005.pdf [Accessed 5 February 2012]

Minusk, 2012, *Negative stiffness spring.* [image online] Available at: www.minusk.com/content/technology/how-it-works_passive_vibration_isolatior.html [Accessed 3 February 2012]

Rousch 1, 2012, *Loss factor of RA218 against temperature and frequency.* [image online] Available at: www.roush.com/portals/1/downloads/products/RA218.pdf [Accessed 3 February 2012]

Rousch 2, 2012, *shear modulus of RA218 against temperature and frequency.* [image online] Available at: www.roush.com/portals/1/downloads/products/RA218.pdf [Accessed 3 February 2012]

Noisedamp, 2012, *Loss factor of Paragon MPM.* [image online] Available at: www.noisedamp.com/acoustic-properties.aspx [Accessed 3 February 2012]

Mide, 2012, *Volture piezo energy harvester*. [image online] Available at: www.mide.com/products/volture/volture_catalog.php#peh [Accessed 5 February 2012]

Csaengineering, 2012, *CSA Tuned mass damper.* [image online] Available at: www.csaengineering.com/products-services/tuned-mass-dampers-absorbers/ [Accessed 3 February 2012]

Rpginc 1, 2012, *Absorption of Clearsorber™ micro perforated film.* [image online] Available at: www.rpginc.com/products/clearsorberf/Clearsorber_Foil.pdf [Accessed 3 February 2012]

Rpginc 2, 2012, *British museum Atrium.* [image online] Available at: www.rpginc.com/products/clearsorberf/Clearsorber_Foil.pdf [Accessed 3 February 2012]

Rpginc 3, 2012, *Absorption of Clearsorber™ honeycomb.* [image online] Available at: www.rpginc.com/download/Brochures/Clearsorber%20Brochure.pdf [Accessed 3 February 2012]

Rpginc 4, 2012, *Modex panel.* [image online] Available at: http://www.rpginc.com/products/modexplate/index.htm [Accessed 3 February 2012]

Rpginc 5, 2012, Diagram of RPG *Modex panel.* [image online] Available at: http://www.rpginc.com/products/modexplate/index.htm [Accessed 3 February 2012]

Mcsquared 1, 2012, *Axial room modes.* [image online] Available at: www.mcsquared.com/metricmodes.htm [Accessed 3 February 2012]

Mcsquared 2, 2012, *Tangential room modes, 1/2 energy axial modes.* [image online] Available at: www.mcsquared.com/metricmodes.htm [Accessed 3 February 2012]

Mcsquared 3, 2012, *Oblique room modes, 1/4 energy axial modes.* [image online] Available at: www.mcsquared.com/metricmodes.htm [Accessed 3 February 2012]

Oriental, 2012, 2 and 5 phase motors. [image online] Available www.orientalmotor.com/technology/articles/2phase-v-5phase.html [Accessed 5 February 2012]

Newfocus, 2012, *New focus slip stick piezo actuator*, [image online] Available http://search.newport.com/?q=*&x2=sku&q2=8301NF [Accessed 5 February 2012]

Cedrat-technologies, 2012, *Cedrat amplified piezo actuator.* [image online] Available at:www.cedrat-technologies.com/fileadmin/user_upload/cedrat_groupe/Mechatronic_products/Piezo_actuators_electronics/APAs/Amplified_Piezoelectric_Actuators.pdf [Accessed 3 February 2012]

Enerpac, 2012, *Hydraulic actuators.* [image online] Available: www.enerpac.com/en/product/526 [Accessed 3 February 2012]

Mahr, 2012, *Rotary stroke bearings.* [image online] Available: www.mahr.com/index.php?NodeID=29 [Accessed 3 February 2012]

Nskeurope, 2012, *NSK Linear bearing.* [image online] Available: www.nskeurope.com/cps/rde/xchg/eu_en/hs.xsl/linear-guides.html [Accessed 3 February 2012]

Nskeurope, 2012, *Ball screw.* [image online] Available: www.nskeurope.com/cps/rde/xchg/eu_en/hs.xsl/innovative-fss-series-low-cost-ball-screws-for-actuators-and-transfer-equipment.html [Accessed 3 February 2012]

rollvis, 2012, *Rollvis swiss satellite roller screw.* [image online] Available: www.rollvis.com/EN/product.htm [Accessed 3 February 2012]

Harmonicdrive, 2012, *Harmonic drive.* [image online] Available: www.harmonicdrive.de/english/the-company/gear-concept/components.html [Accessed 3 February 2012]

Uhlmann & Neumann, 2012, *Pressure distribution of different orifice arrangements*. From "Air bearings based on porous ceramic composites by E. Uhlmann, C. Neumann. Technische Universität Berlin, IWF, Pascalstr. 8-9, 10587 Berlin, Germany". Available: *http://conference.iproms.org/sites/conference.iproms.org/files/PID163597.pdf* [Accessed 5 February 2012]

Zahnrad-ott, 2012,*OTT anti backlash worm and wheel.* [image online] *www.zahnrad-ott.de/Zahnrad_Ott_E_09.pdf* [Accessed 3 February 2012]

Newport 1, 2012,*Data sheet vertical transmissibility for a CM-255*.[image online] Available:http://search.newport.com/?q=*&x2=sku&q2=CM-225 [Accessed 5 February 2012]

Newport 2, 2012, *Data sheet Horizontal transmissibility for a CM-255*.[image online]

Available: http://search.newport.com/?q=*&x2=sku&q2=CM-225

[Accessed 5 February 2012]

# Appendix A Development and testing of a carbon fibre pyramidal structure

## A.1 Introduction

A typical end station support structure consists of a steel fabricated support or a granite slab or a combination of both. Steel structures are usually rectangular in shape and have poor stiffness with low frequency modes of vibration particularly in the horizontal direction. Granite structures are heavy and are difficult to move and take a long time to manufacture.

A possible alternative approach is to use a light weight structure that is highly rigid, easily modified and could be easily moved to different beamlines. The concept was to produce a structure that is rigidly attached to the floor and a good stiffness in both the vertical and horizontal directions.

## A.2 Description

A design was developed using carbon fibre tubing, the problem was how to join the tubes together. The solution was to use standard aluminium tube clamps a this enabled many different angles and joints to be made and was easily adjusted. A carbon fibre tube was found that fitted the internal bore of the aluminium clamps. The tubes and purchased from Hardy Composites Ltd.

ANSYS finite element software package was used to investigate the behaviour of different designs.

The design started off with a simple 3 legged structure and then braces were added up to a 4 legged, 12 element braced structure. As a comparison a steel frame was analysed.

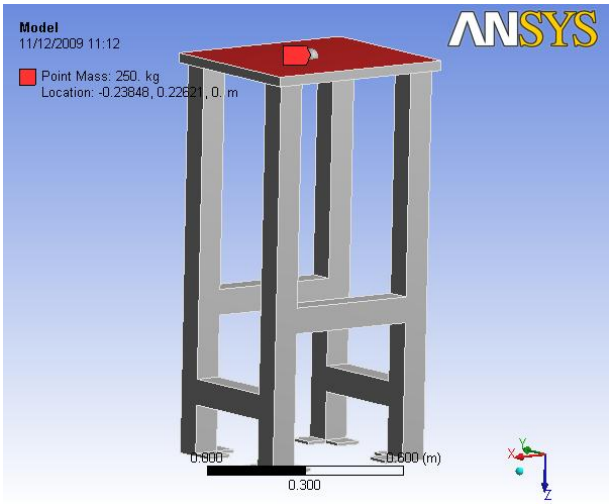


**Figure 82 – Simple steel fabrication**

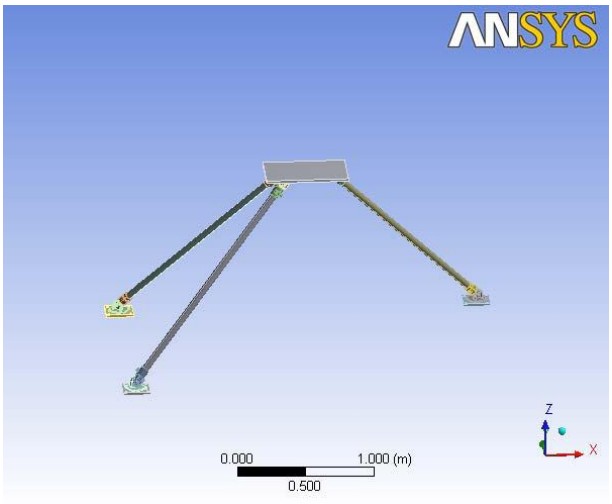


**Figure 83 – 3 legged structure**

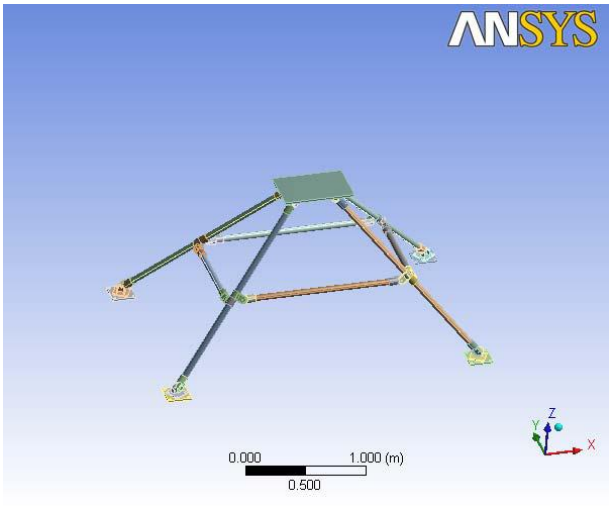


**Figure 84 – 4 legged, 4 brace structure**

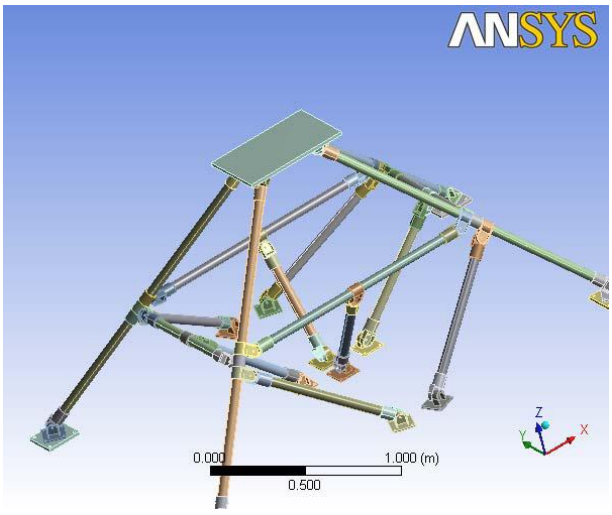


**Figure 85 – 4 legged, 12 brace structure**

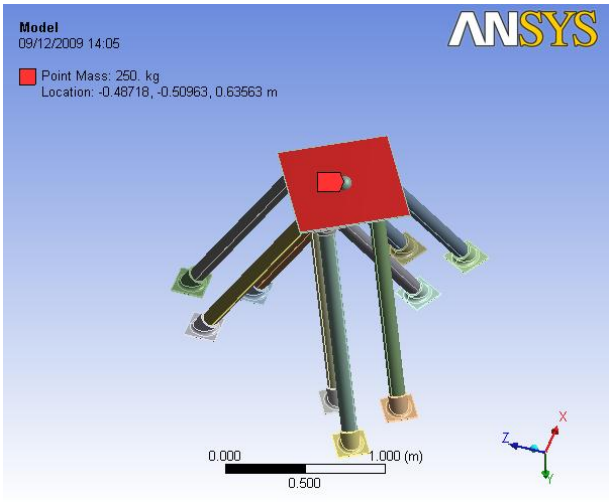


**Figure 86 – 3 legged, triple tripod structure**

## A.3 Analysis Results

The objective was to obtain resonant frequencies of above 80Hz with a supported load of 250Kg. As can be seen from Table 35, the steel frame had some lower modes below 80Hz. The 50mm carbon fibre tube sounded promising but the analysis showed that the frequencies were still low even without any supporting mass. Bracing was added and this made some improvement but not the significant improvement desired. A new design was then developed using 100mm diameter tube, with a three, 3 legged tripod nested closely together. This gave a substantial improvement with resonant frequencies above 80Hz even when loaded to 250Kg.

| **Modes** | **1** | **2** | **3** | **4** | **5** | **6** |
|---|---|---|---|---|---|---|
| Steel frame(250 Kg mass) | 22 | 27 | 86 | 181 | 279 | 309 |
| 3 legs | 29 | 35 | 40 | 59 | 65 | 73 |
| 4 leg, 4 brace | 33 | 36 | 37 | 61 | 66 | 72 |
| 4 leg, 8 brace | 41 | 46 | 61 | 64 | 73 | 96 |
| 4 leg 12 brace | 51 | 53 | 63 | 66 | 75 | 95 |
| 3 legged, triple tripod | 90 | 110 | 138 | 155 | 161 | 163 |
| 3 legged, triple tripod, 100mm dia tubes (250Kg mass) | 87 | 90 | 99 | 217 | 227 | 281 |

**Table 39 – Frequency modes of vibration**

## A.4 Actual test results

A 4 legged 8 braced structure was built and installed in the B16 test beamline experimental hutch. Vertical Vibration measuring devices were fixed to the floor, the base of the existing steel KOHZU table and the top platform of the end station. Measurements were taken over a 30 minute duration. The test was then repeated using horizontal measuring devices.

The tests were performed on a normal working day during a shutdown. A graph of vibration magnitude against frequency is shown for both Vertical and Horizontal tests.

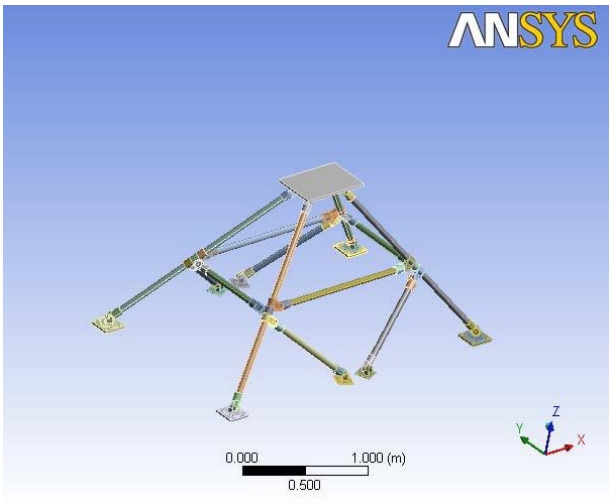


**Figure 87 – 4 legged, 8 brace structure**

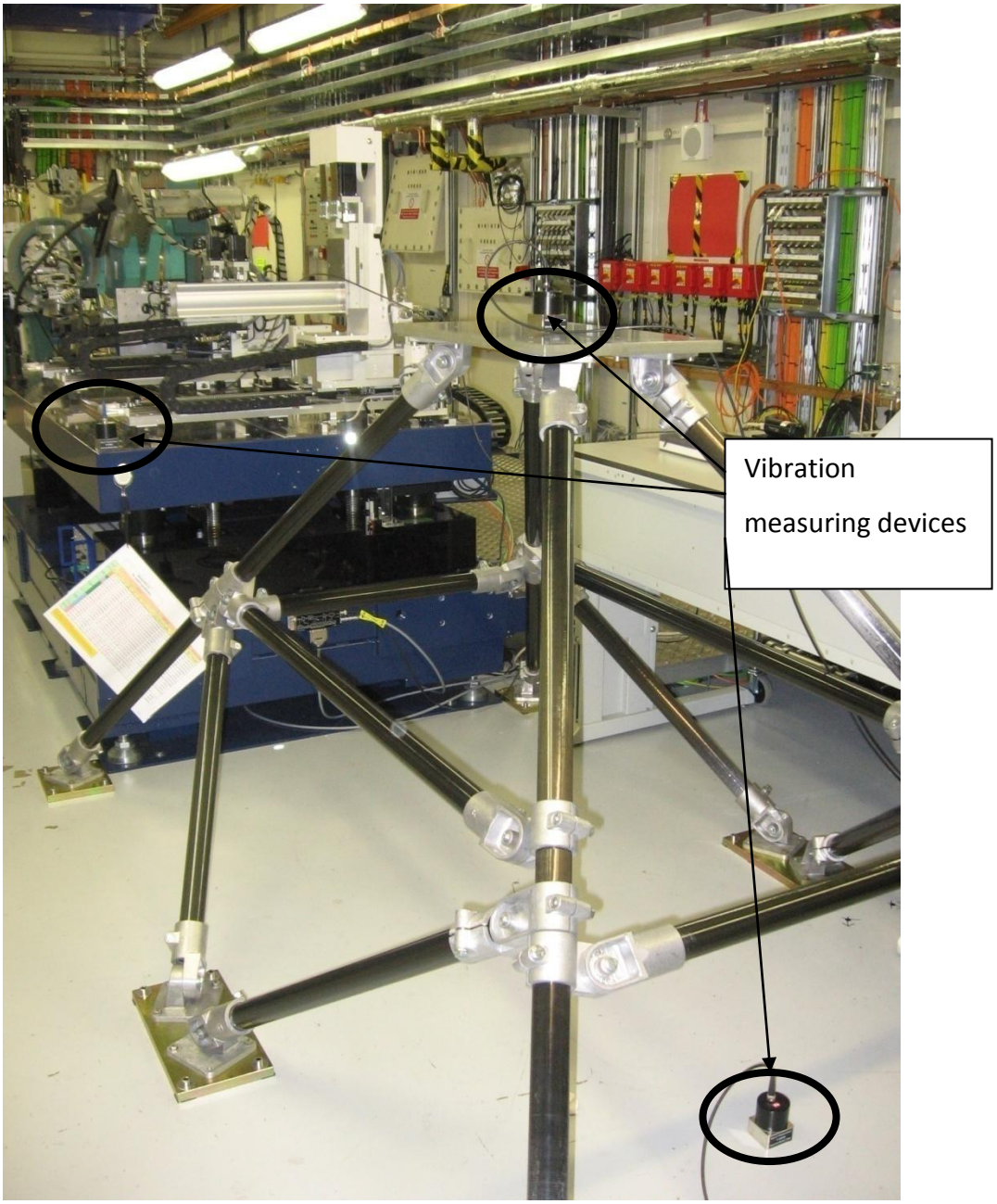


**Figure 88 – Testing of 4 legged structure**

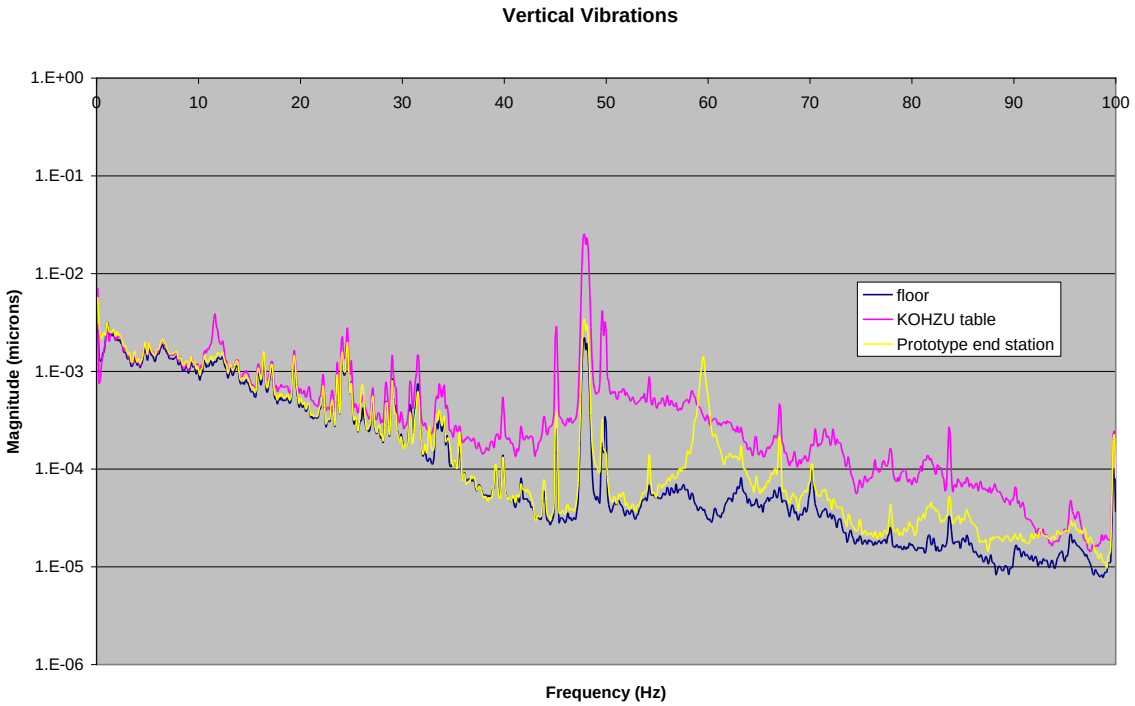


**Figure 89 – measured vertical vibrations of 4 legged structure**

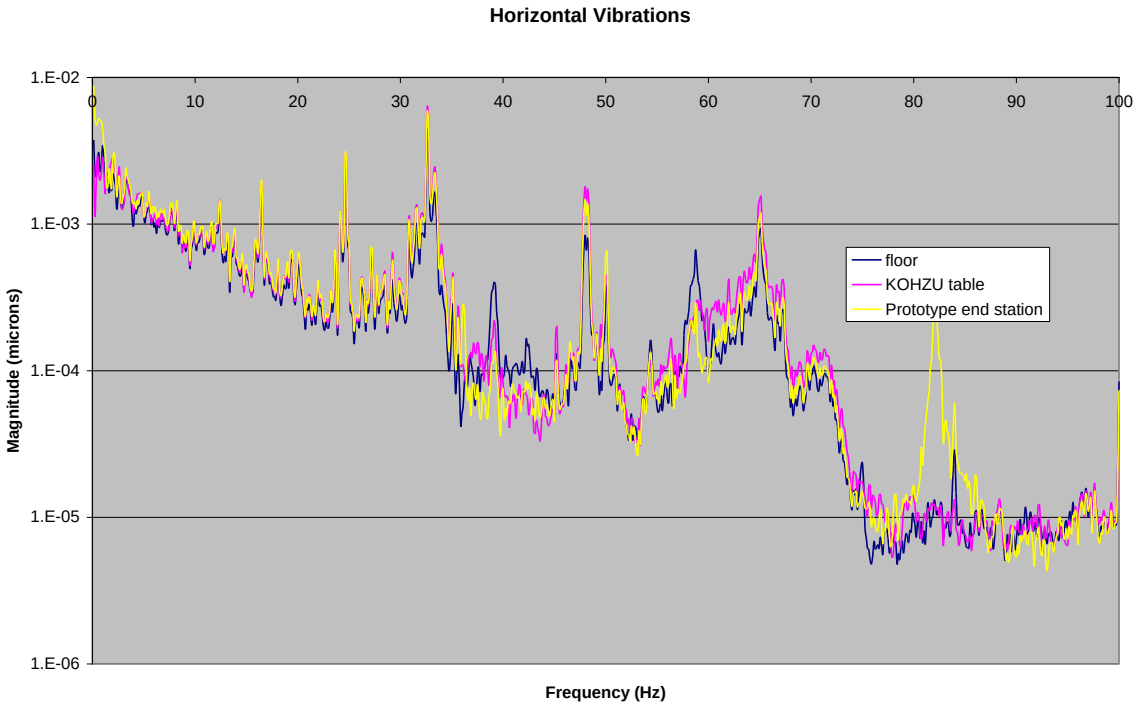


**Figure 90 – Measured horizontal vibrations of 4 legged structure**

## A.5 Discussion of results

### A.5.1 Vertical Vibrations

From 0 to 30 Hz all the results are similar but the KOHZU table does show an increased response at about 11Hz.

From 30Hz to 100Hz the KOHZU table is about a factor of 10 worse than the floor and prototype end station except at about 60Hz. Apart from the 60Hz resonance the prototype table shows good matching with the floor.

There is a marked vibration source at 48Hz. The prototype end station shows a low amplification of this but the KOHZU table amplifies this floor vibration by a factor of 10.

### A.5.2 Horizontal Vibrations

The horizontal vibration results are all very similar except the prototype end station shows a horizontal resonance at about 82Hz.

## A.6 Discussion

The ANSYS analysis predicted resonant frequencies at 41, 46, 61, 64, 73 and 96Hz and the actual measurements showed vertical and horizontal vibrations at 60 and 82Hz. The first and fifth mode is rolling, second and fourth is horizontal twisting, third is pitching and the sixth is vibration of a brace. The second and fourth mode have no vertical motion and all except the sixth mode have a horizontal components. The measured 60Hz could be the third mode but 82Hz vertical is not predicted.

The platform tested had a relatively small usable platform compared to the floor space occupied. Although it was lightweight and could be easily modified it was not that easy to move and did require bolting down to the floor using anchor bolts in 6 locations, each with 4 anchor bolts. Access to the platform was not that easy as the splayed legs prevented easy access. From a practical point of view the solution was not practicable. The modal frequencies were also quite low even with no mass. Some works was done on adding mass and improving the structure further and changing the top plate to a rigid box but the results were not encouraging.

The analysis of the 100mm diameter tripod was however very encouraging. The frequencies were high even with 250Kg supported mass and the footprint occupied by the supporting structure was relatively small. This type of structure looks promising particularly if large diameter carbon fibre tubes can be obtained with very low thermal expansion.

# Appendix B Active vibration system using positional feedback

## B.1 Introduction

One of the problems in using active vibration control is finding a suitable sensor. For environments with very low background vibration the sensor has to be extremely sensitive over the desired operating frequency range. The noise generated by the sensor itself must also be extremely low.

An alternative solution would be to use feedback from a distance measuring device with the distance measured to a passively isolated reference platform. If the reference platform had no devices which move and is isolated from any person touching it then it could remain very stable. As an example the MinusK negative spring platform gives good isolation at the required frequencies.

A working platform could then be mounted above the reference platform. This would be used to support the experimental equipment. It would be mounted on actuators to give six degrees of freedom and distance sensors would monitor the gap between the working platform and the reference platform.

## B.2 Sampling rate

If the magnitude of the vibration displacements is 100nm then assuming a sinusoidal motion sampling at 1,000 times the vibration frequency would give a incremental motion of 0.6nm. The sensor therefore needs to have a resolution of the order of 0.6nm and a system response at 1,000 x the desired isolation frequency. Assuming that the aim is to reduce vibrations up to 50Hz then this would demand an operating frequency of 50KHz.

The system would need to carry out some computation to calculate the required actuator driving signal, the ideal solution would be a programmable system where any proportional, integral and differential factors could be readily adjusted and any trigonometric factor included. The system selected is a National Instruments system

based on a stand alone unit with integrated processor and a backplane with FieLd programmable gate arrays.

## B.3 laser interferometer sensor

The initial concept was to use a laser interferometer such as that produced by Renishaw. The reflecting mirrors would be mounted on the reference platform and the laser head would be mounted on the working platform. Tests showed that this approach had a number of problems. Firstly the measurement is dependent upon the humidity, temperature and pressure of the air through which the laser passes. The temperature can be controlled but the pressure is more difficult, this could be done by isolating the system in a partial vacuum or having a purge gas which can produce an overpressure. The difficulty is then having to seal the environment and find a pressure controller that will give a constant pressure relative to absolute rather than ambient conditions.

The lasers are expensive and for a six degree of freedom system 6 heads would be required. The renishaw system has 2 heads so these would mean three units would be required. With a 200x interpolator the laser does have the required resolution of 0.79nm and has a sufficient update rate of 39KHz.

The output from the laser encoder is a 1v peak to peak signal, this was connected to a digital interpolator that converts the analogue signal into a A and B digital signal. The digital input was connected to a National Instruments 9411 card which was housed on the NI-9012 FPGA. A lab view programme was written to convert the digital signal into a distance measurement.

## B.4 Actuator

The Actuator chosen was a Physik Instruments PI1844.10. The calculated correction signal was produced by a National Instruments 9263 card, this connected to the PI Amplifier which then produced a driving voltage for the Piezo actuator. The driving voltage from the PI amplifier is limited by the capacitance.

Current = Capacitance v Voltage change x frequency

For a 300mA current, 6µF capacitance and operating frequency of 50KHz then the maximum voltage is only 1 Volt.

The piezo can produce 555N at 100 volts so at 1Volt the maximum force is 55N.

At a incremental motion of 0.6Nm at 50,000 Hz then the acceleration is 3m/sec.

At a maximum force of 55N then the allowable pay load is $55N/3mS^{-1}$ . = 18Kg.

## B.5 Number of degrees of freedom

Some active vibration systems operate with 6 degrees of freedom, but this may not be necessary. For an end station which house the final focussing optics and sample the effects of motion on the blurring of the focal sport vary dependent upon the type of motion. Pure roll for example will have no effect for a focussing system such as a set of 2D lenslets. Pure vertical and horizontal motion has much less effect because of the leverage of the long distance to the source. Of much greater significance is pitch and yaw motions.

A single actuator could be used for pitch, this could be linked to two vertical position sensors which are measuring the distance to the reference platform. If we are not concerned with vertical motion then subtracting the signal from the two sensors would give a pitch measurement which can then be used to drive the pitch actuator.

For Yaw motion a similar approach could be made with only two sensors and one actuator.

## B.6 Capacitive Sensor

An alternative to the laser interferometer is a capacitive sensor. A Lion Precision capacitive probe Type C23/C has a resolution of 0.4nm in its ultrafine range with a linearity of 1% and a range of 20µm, but its bandwidth is only 15KHz rather than the ideal 50KHz required.

# Appendix C Adjustable length platform

## C.1 Introduction

A concept for an adjustable length tripod is presented. This is based upon a 3 legged tripod in which each leg can be changed in length by using a piezo actuator. The original concept was that this platform could be used to compensate for thermal expansion and ground transmitted vibrations.

## C.2 Design

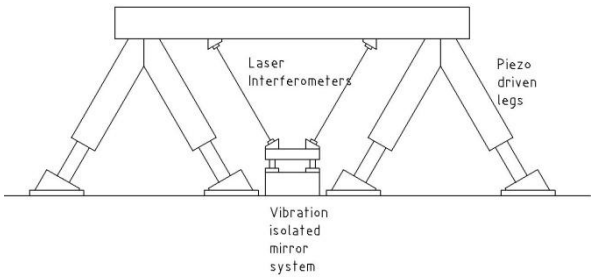


**Figure 91 – Design of adjustable length platform**

The concept is based on a tripod structure with each leg consisting of a rigid large diameter carbon fibre tube within which is a flexure allowing a change in length. The flexure was operated by a high voltage piezo actuator. The Flexure discs (150mm & 92mm Dia, 0.5mm thick) provides a stiff structure and low preload

**Figure 92 – Actuator leg**

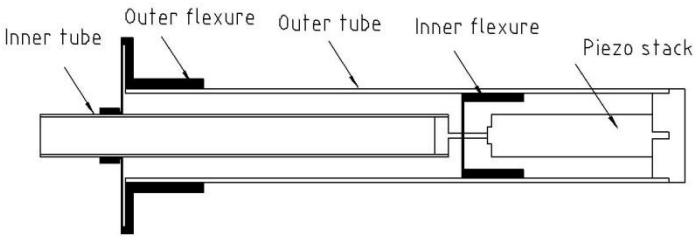


**Figure 93 – Schematic of actuator leg**

## C.3 Test results

A test was done with a single actuator. A Renishaw laser encoder Encoder with 0.79nm resolution was used to measure the distance and then this signal was used to provide a 16 bit resolution analogue output to control the voltage applied to the amplifier feeding a DC voltage to the piezo actuator. The control loop was implemented in a lab

view programme on a National Instruments USB based system. This was limited to an operating bandwidth of 40Hz.

**Figure 94- Actuator leg under test**

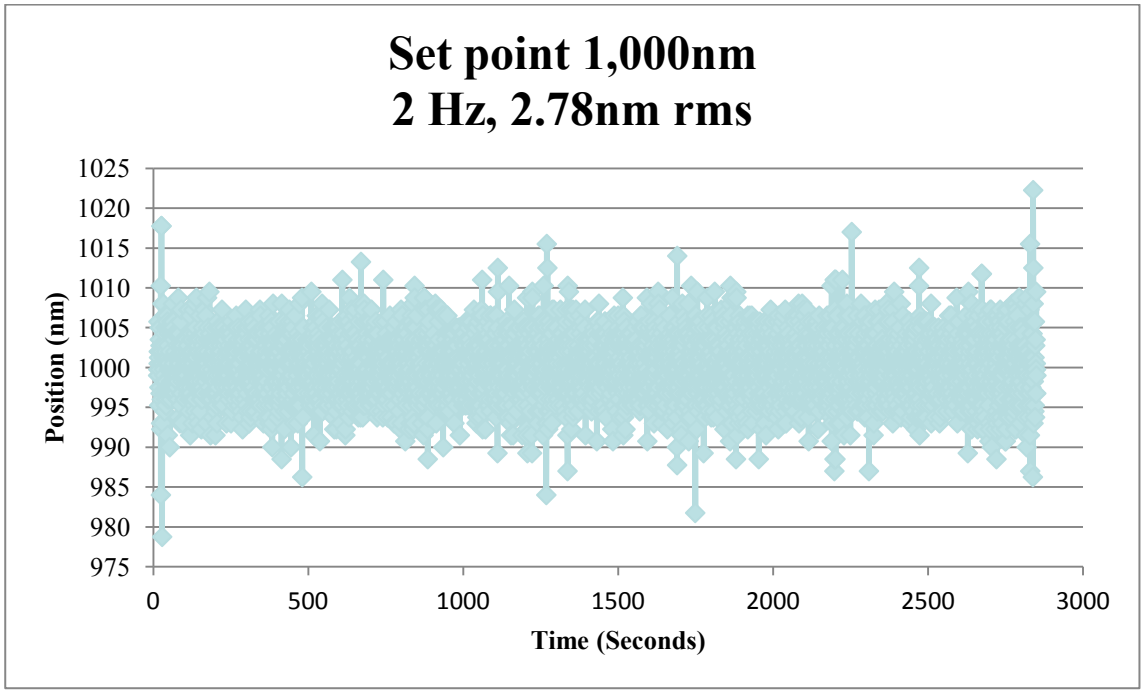


**Figure 95- Feedback results of actuator**

## C.4 Conclusion

The results showed a number of problems. Air movements increased the level of noise in the laser encoder and it did seem that background light levels also made a difference although this should not occur. The National instruments system was limited because it was using a USB connection between the modules and the programme running on the PC. The bandwidth could be increased substantially in moving to a field programmable gate array. The laser encoder is affected by temperature and pressure and so compensation is required.

The concept was reviewed by senior beam line scientists and the opinion was that a smaller system would be preferred so that it could be easier to integrate into existing beamlines.

# Appendix D Vibrometer tests

## D.1 Introduction

A series of tests were done using a Polytec vibrometer both in a laboratory and on the B16 Test Beamline. The aim of the tests was to look at the vibration stability of the main optical table in B16.

## D.2 Equipment

- Polytec vibrometer
- Honeycomb Optical table supported on pneumatic isolators
- Attocube positioning towers and ANC150 piezo step controller.

**Figure 96 – Polytec Vibromter**

## D.3 Settings

2Hz to 2KHz Frequency range, 3.2 seconds Sample time

## D.4 Test Results

## D.5 Rubber feet test

In this test the polytec vibrometer was attached to a 15mm thick aluminium plate via aluminium pads. The plate was then bolted down to the optical table. The target was an aluminium angle plate also bolted down to the same optical table. In another test the polytec vibrometer sat on the optical table supported on the rubber feet fitted to the base of the polytec vibrometer head. The purpose of the test was to determine if the rubber feet affected the results.

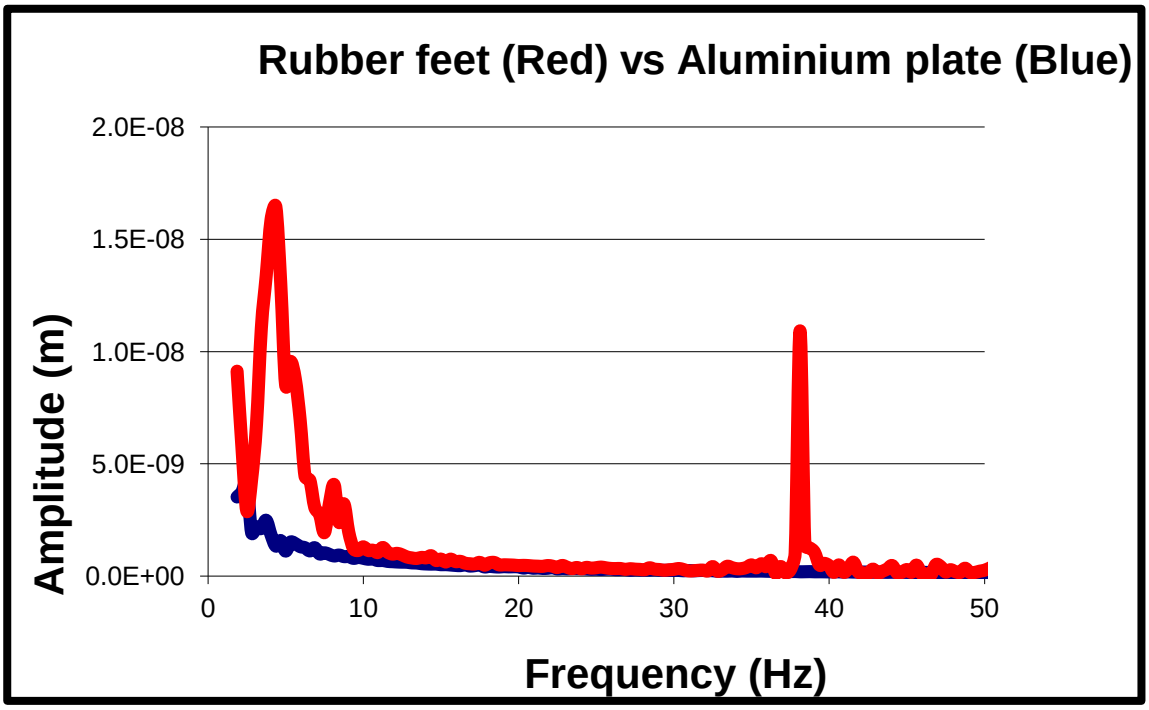


**Figure 97 – Vibrometer rubber feet test**

Figure 98 shows the comparison between the two tests. The rubber feet test gives much higher displacements at frequencies below 10Hz, but it also shows vibration at about 38Hz. This is shown more clearly in Figure 98.

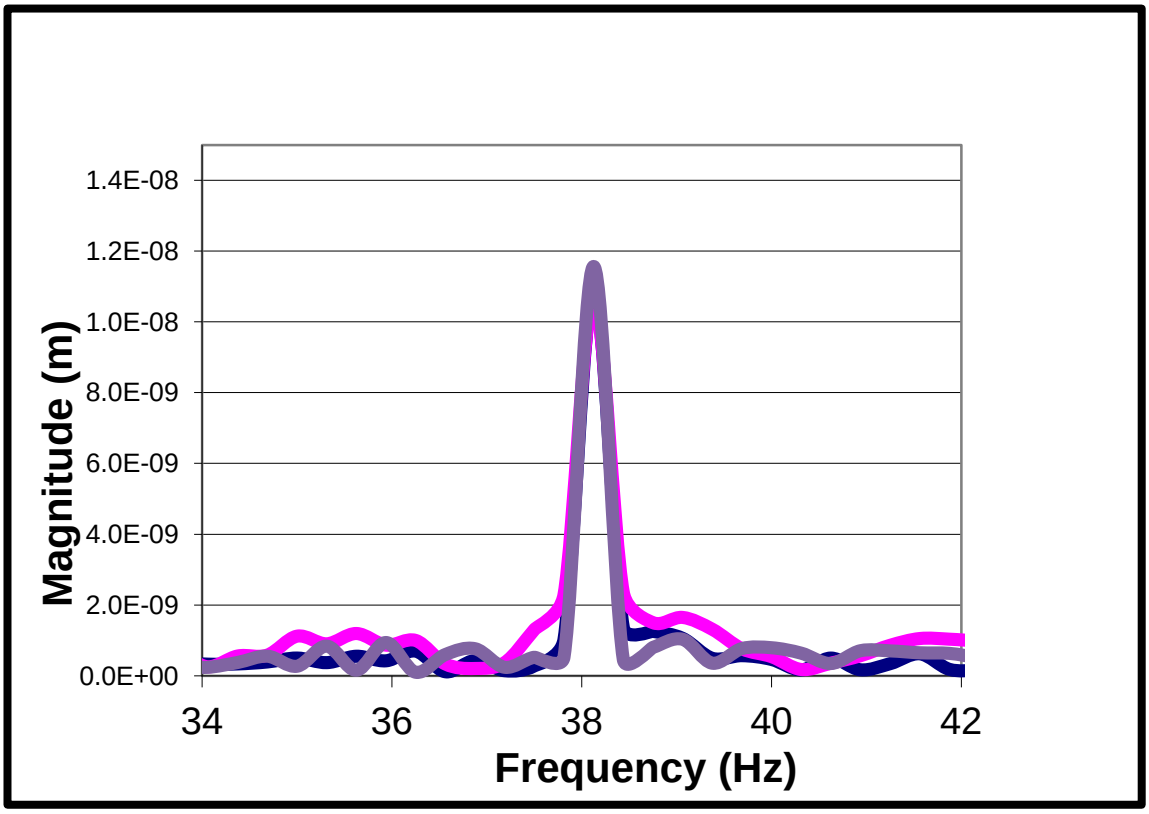


**Figure 98 - Vibrometer Test with rubber feet**

The conclusion was that the rubber feet provide flexibility which allows the vibrometer to move. In future all tests should be conducted with the polytec head firmly bolted to the solid aluminium plate via aluminium pads.

## D.6 Stationary Attocube test

An Attocube tower consisting of a vertical, x translation, rotation and 2 goniometer stages were bolted down to the optical table. In its stationary state the vibration was measured using the polytec vibrometer. The results are shown in Figure 99Figure 82.

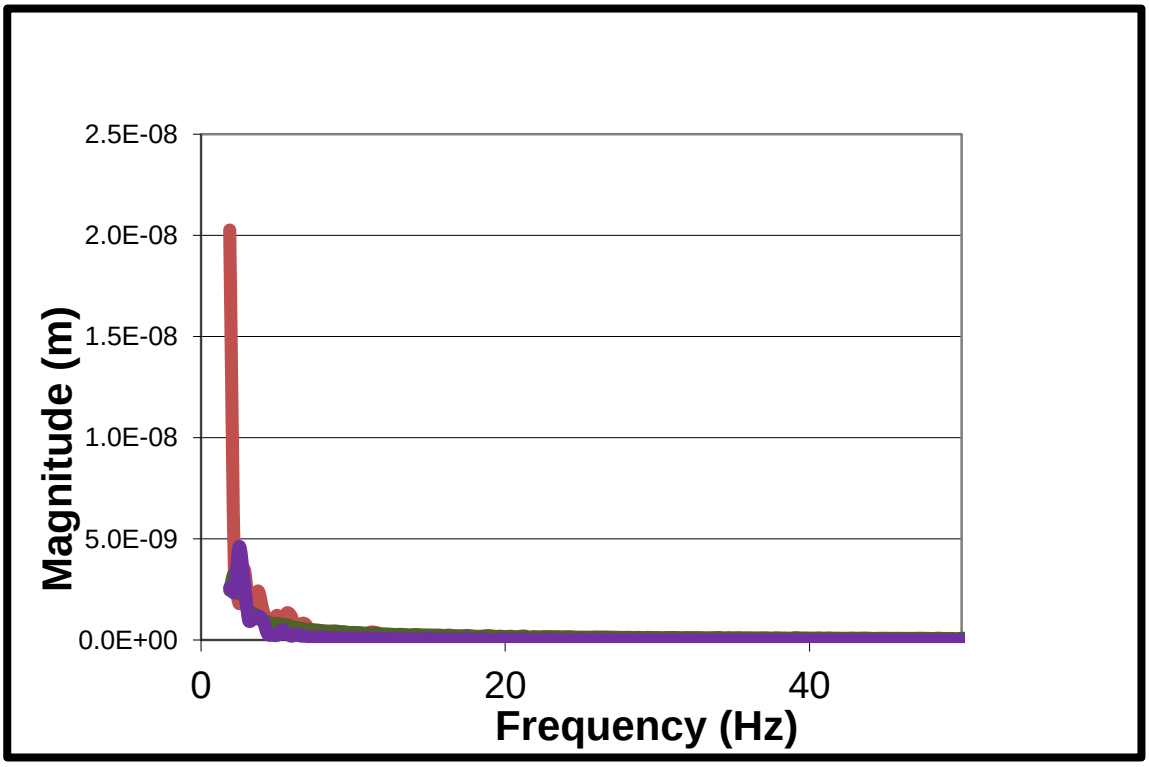


**Figure 99 - Stationary attocube**

The results show the tower is stable below 1 nm at frequencies above 10Hz. At lower frequencies there is some motion of perhaps up to 20nm.

## D.7 Attocube operational tests

The horizontal vibration of the attocube tower was measured when the vertical translation stage was operated at different frequencies and voltages.

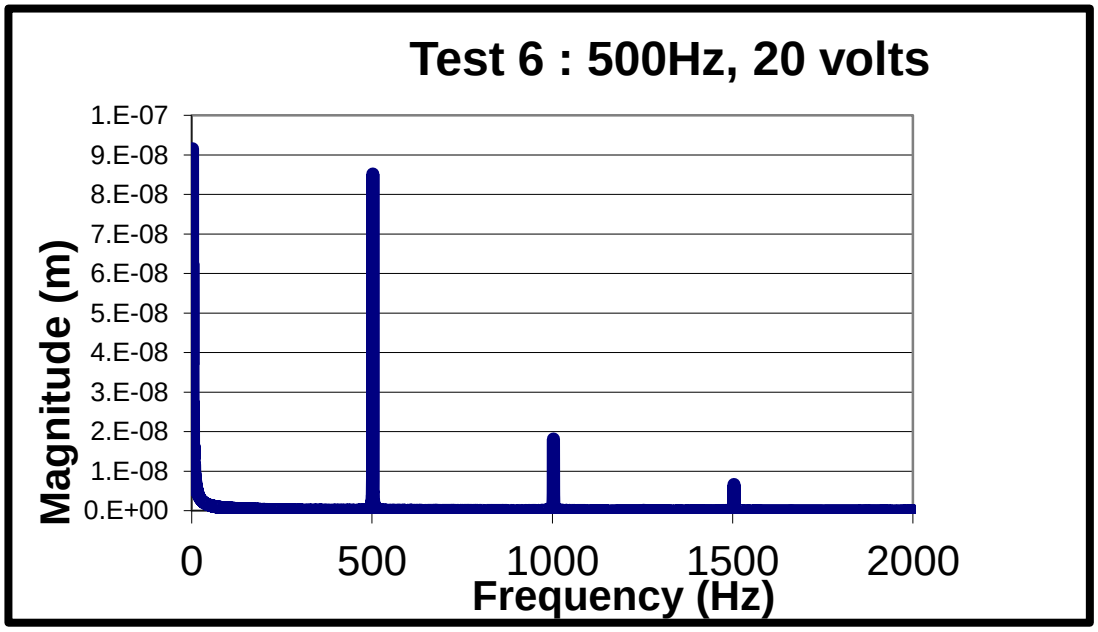


**Figure 100 - Attocube at 500Hz, 20 Volts**

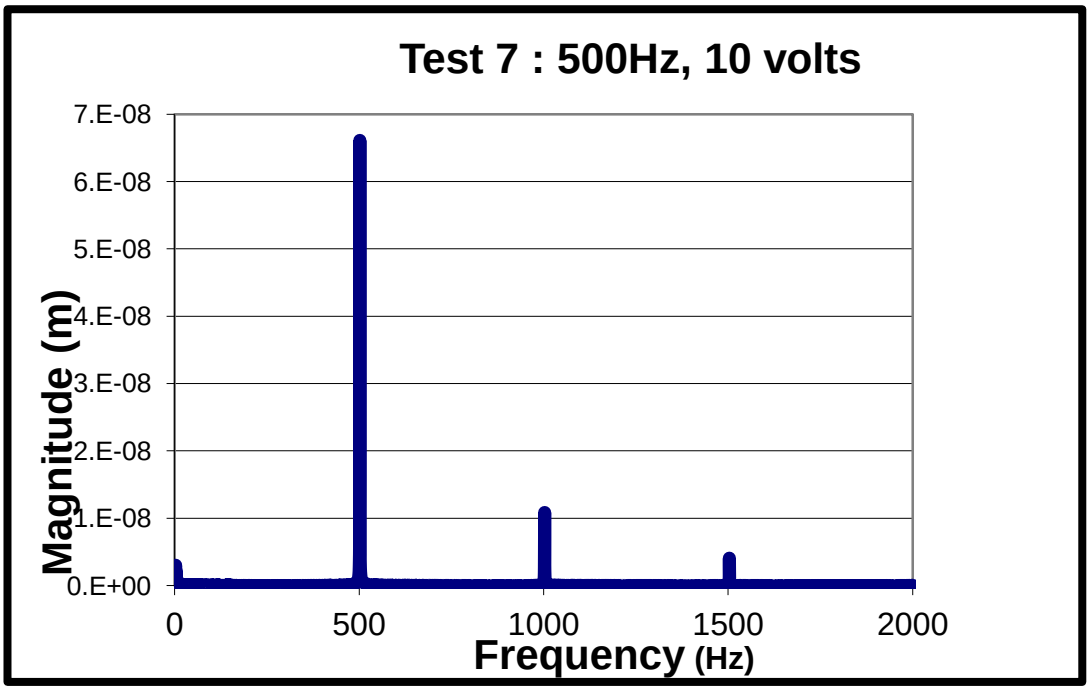


**Figure 101 - Attocube at 500Hz, 10 volts**

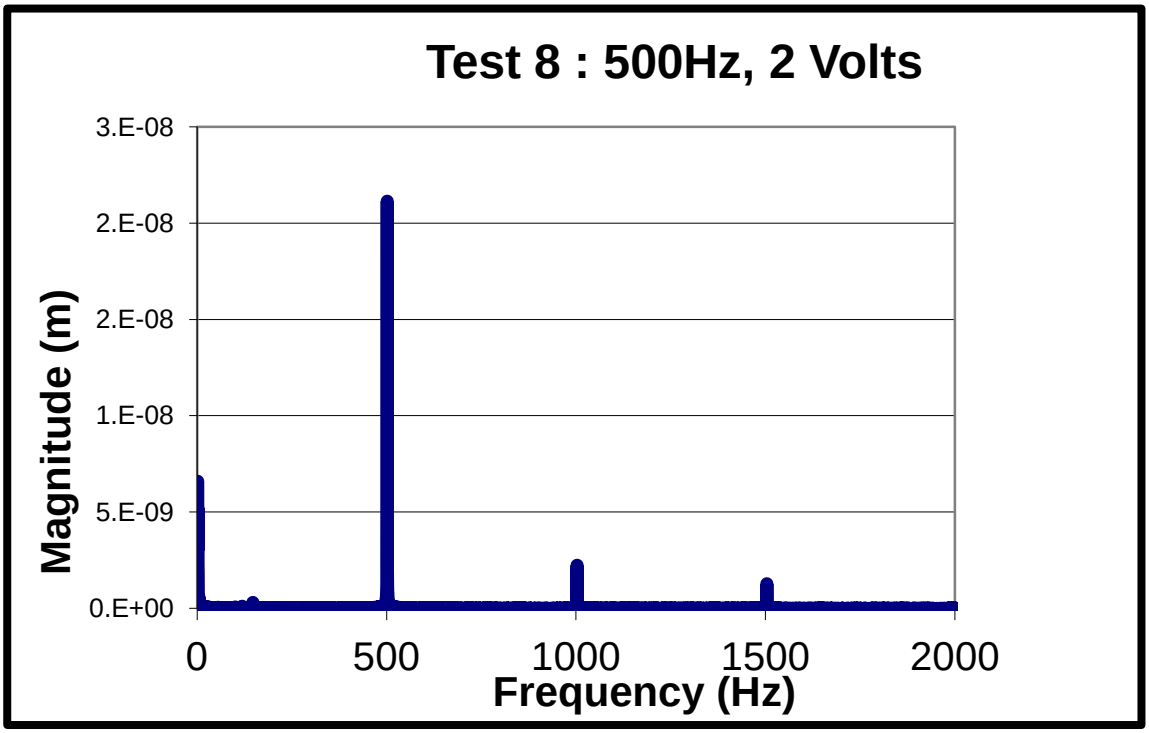


**Figure 102 – Attocube at 500Hz, 2 Volts**

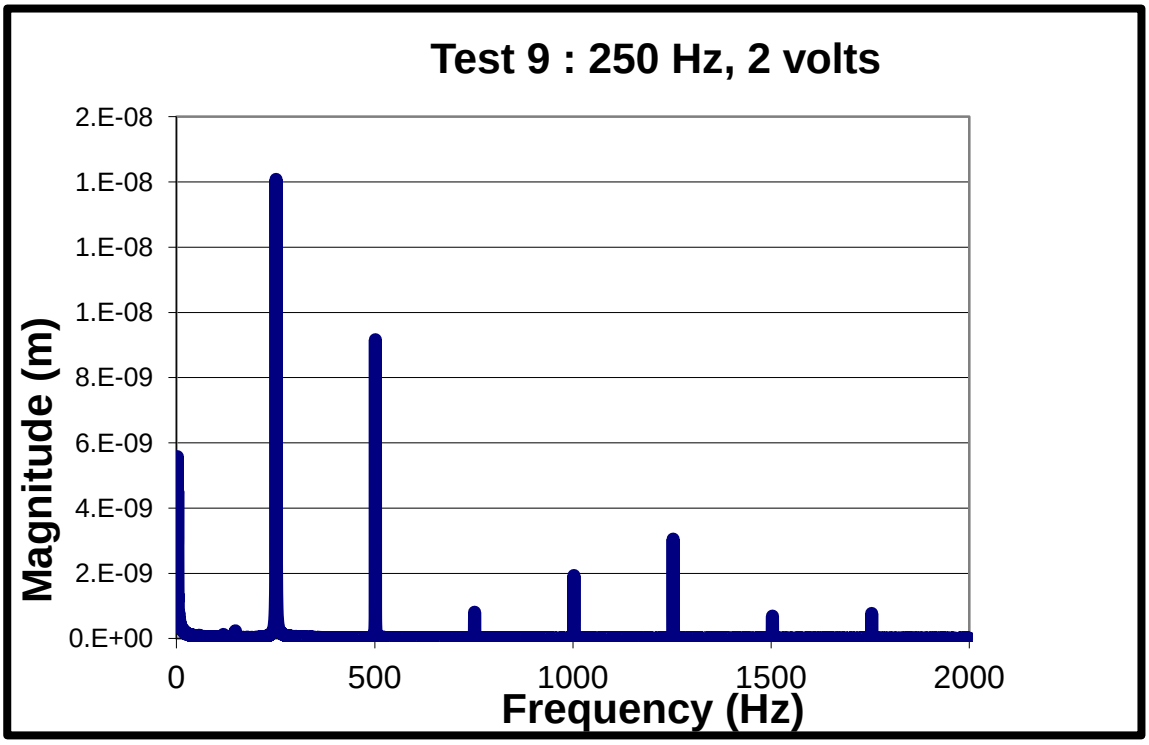


**Figure 103 – Attocube at 250Hz, 2 Volts**

These tests show that when driven vertically the attocube towers do vibrate horizontally. The magnitude increases with operating voltage.

| Test No | Frequency | Voltage | Magnitude at operating frequency |
|---|---|---|---|
| 6 | 500 Hz | 20 Volts | 86nm |
| 7 | 500 Hz | 10 Volts | 67nm |
| 8 | 500 Hz | 2 Volts | 21nm |
| 9 | 250 Hz | 2 Volts | 14nm |

**Table 40 – Summary of attocube tests**

## D.8 Most stable test

This test was in the most stable conditions. The Polytec was bolted to the optical table and the table supported on pneumatic isolators and the target also bolted to the table.

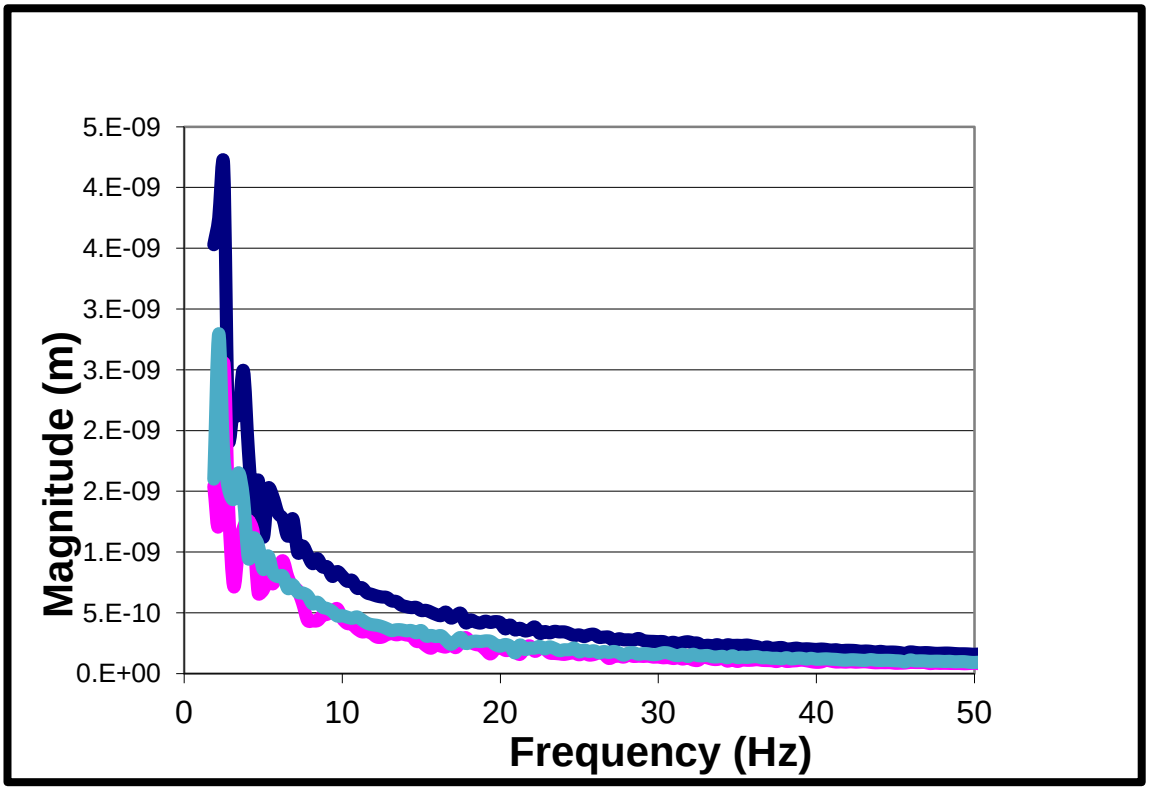


**Figure 104 – Most stable test**

The tests shows that even under best conditions there is still a movement of over 4nm at low frequencies. For sub 10nm spot size requirements then even this motion will

add error to the measurements. Can this be improved under these ideal conditions? Is the polytec accurate at these low frequencies?

## D.9 Conclusions of attocube tests

In future tests the polytec must NOT be resting on its own rubber feet. The detector should be bolted down via the aluminium feet.

When not operating, the attocube towers appears to be stable, although the tests were conducted on an isolated optical table. It may not however be suitable for holding optics generating beam sizes approaching 10nm

The polytec correctly measures vibrations at 250 and 500 Hz.

The attocube towers do vibrate horizontally when driven in a vertical direction. The magnitude of these movements depends upon the driving voltage. Even at low voltage the motion are much greater than 10nm. The attocube towers when driven by the current controller are NOT suitable as a wire scanner for measuring 10nm beam sizes.

There are large motions at low frequencies, the polytec does not seem to be able to measure frequencies much below 2Hz. An alternative measuring system for sub 10Hz measurements may be required to gain further understanding.

The pneumatically operated optical table in lab 86 does appear to remove the 10-15 and 25- 30Hz vibrations seen on the KOHZU table on B16 as measured in later tests

## D.10 Tests with vibrometer mounted on the detector stage

These tests were conducted with the vibrometer mounted on the detector stage and looking upstream towards the source in the Z direction.

**Figure 105 – Vibrometer mounted on detector stage**

Test 1 and 2 were looking at a right angled bracket mounted on the piezo stage of the diagnostics stage.

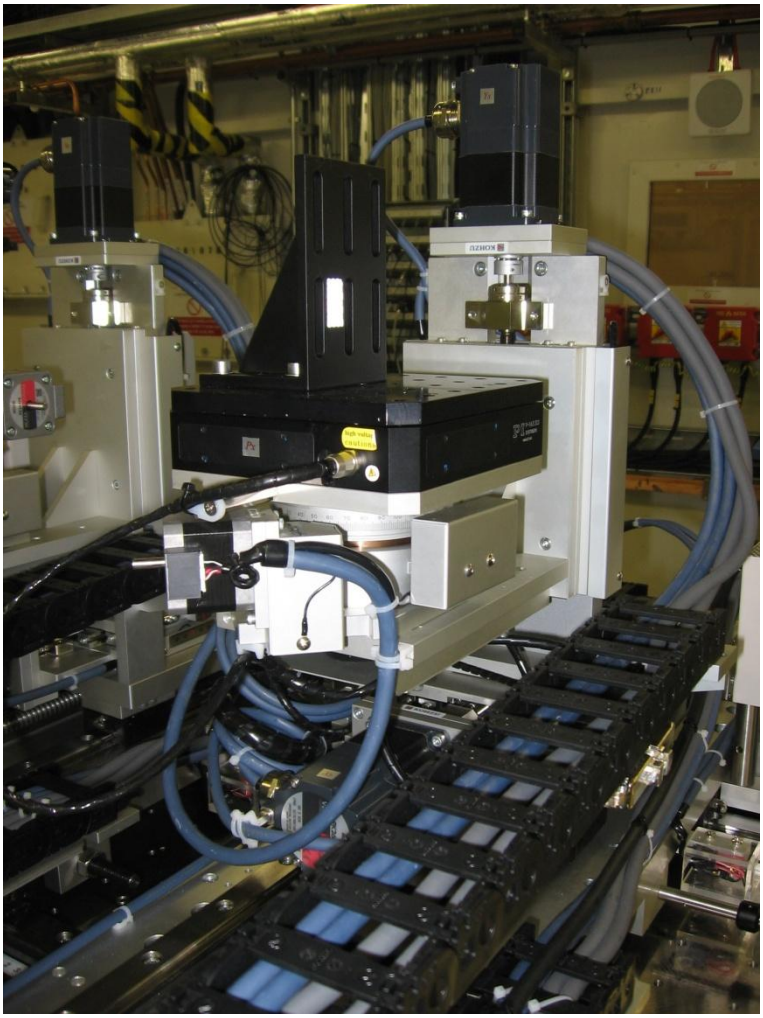

**Figure 106 – Vibration target mounted on diagnostics stage**

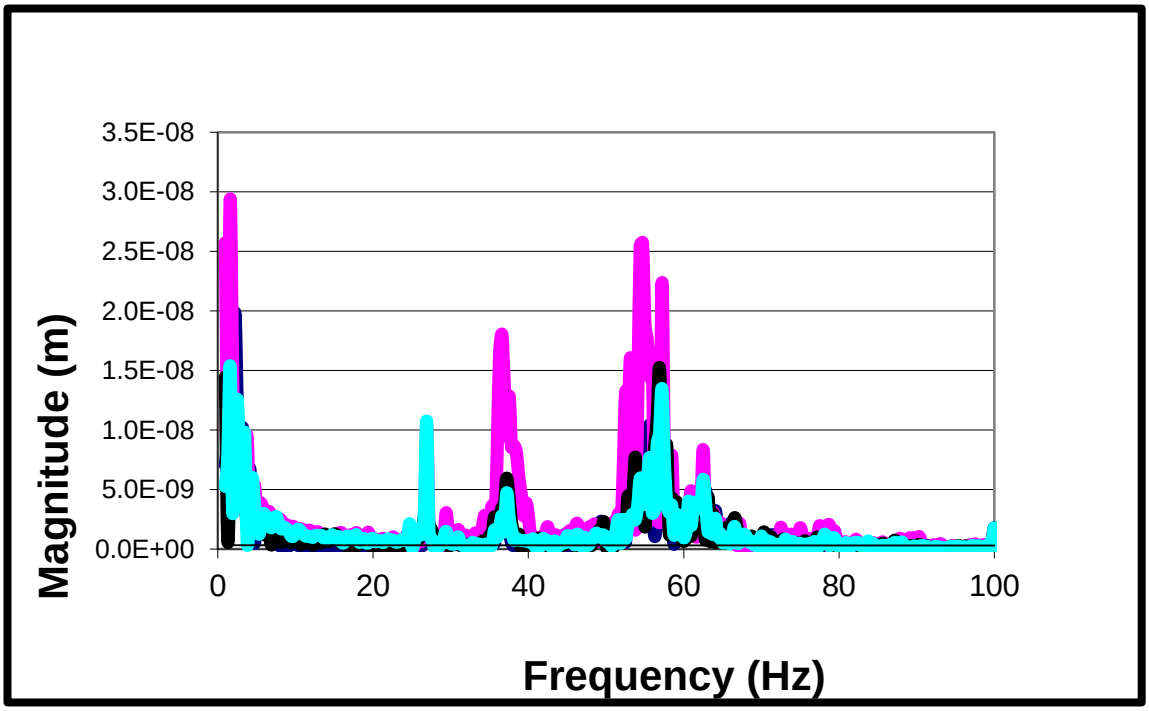


**Figure 107 – Vibration results between detector stage and diagnostics stage**

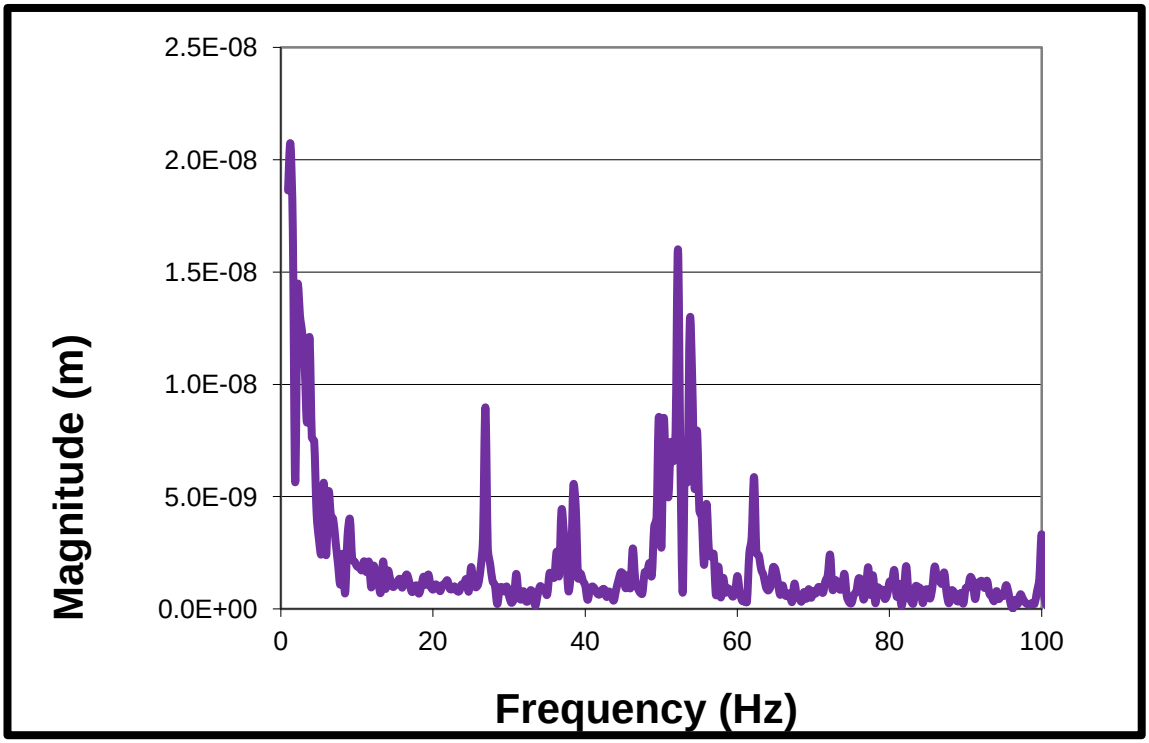


**Figure 108 – Vibration test with piezo stage at 5 volts**

Figure 107Figure 90 shows both tests. Figure 108Figure 92 shows much lower magnitude of vibrations at frequencies around 26, 38 and 54 Hz. This indicates that the piezo stage when not powered is less rigid. For sensitive tests the piezo should be powered or removed if not required. In this test only 1 axis had a voltage applied. If all three axis were powered then even less displacements may be measured.

In test 3 the bracket was moved to the optics stage.

This shows a similar spectrum to the diagnostics stage with the piezo at 5 volts.

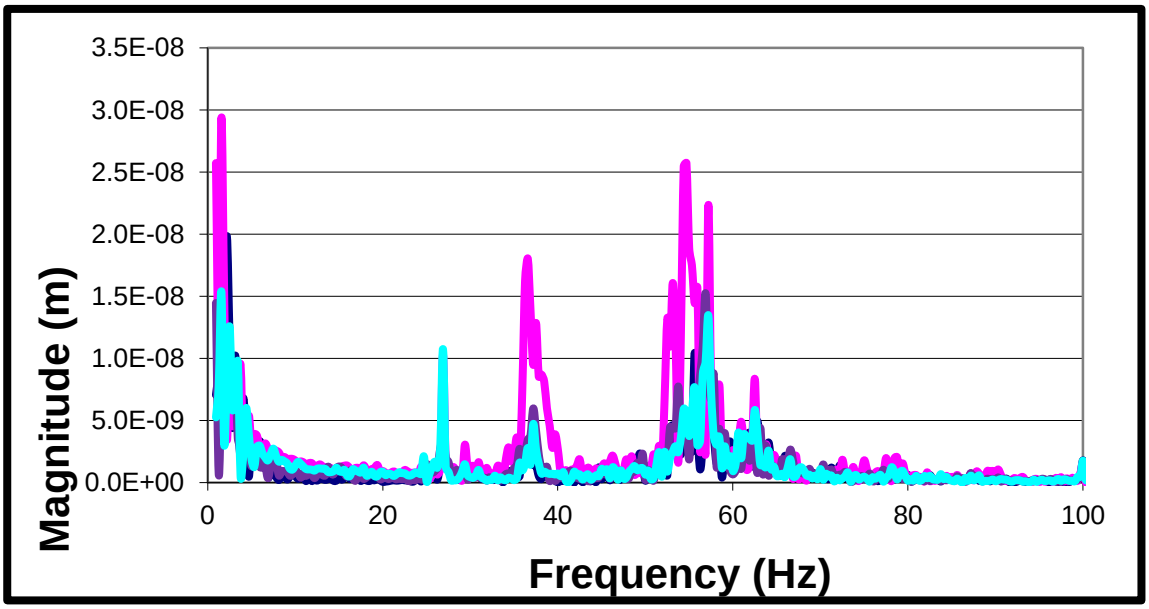


**Figure 109 – Vibration results between detector and optics stage (Test 3)**

Tests 4 and 5 were conducted with the Kohzu base at different heights. +140mm for test 4 and -40mm for test 5. There does not seem to be any significant difference.

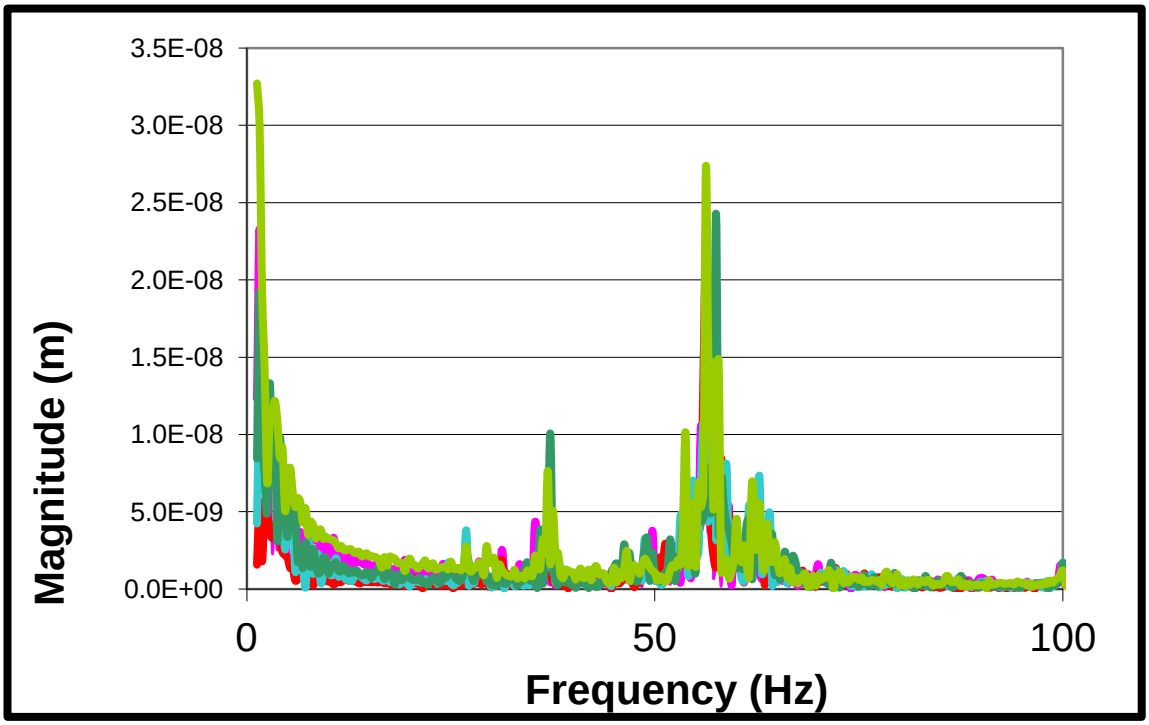


**Figure 110 – Vibration results between detector stage and optics stage at different heights (Test 4 & 5)**

Test 6 was looking at the diffractometer.

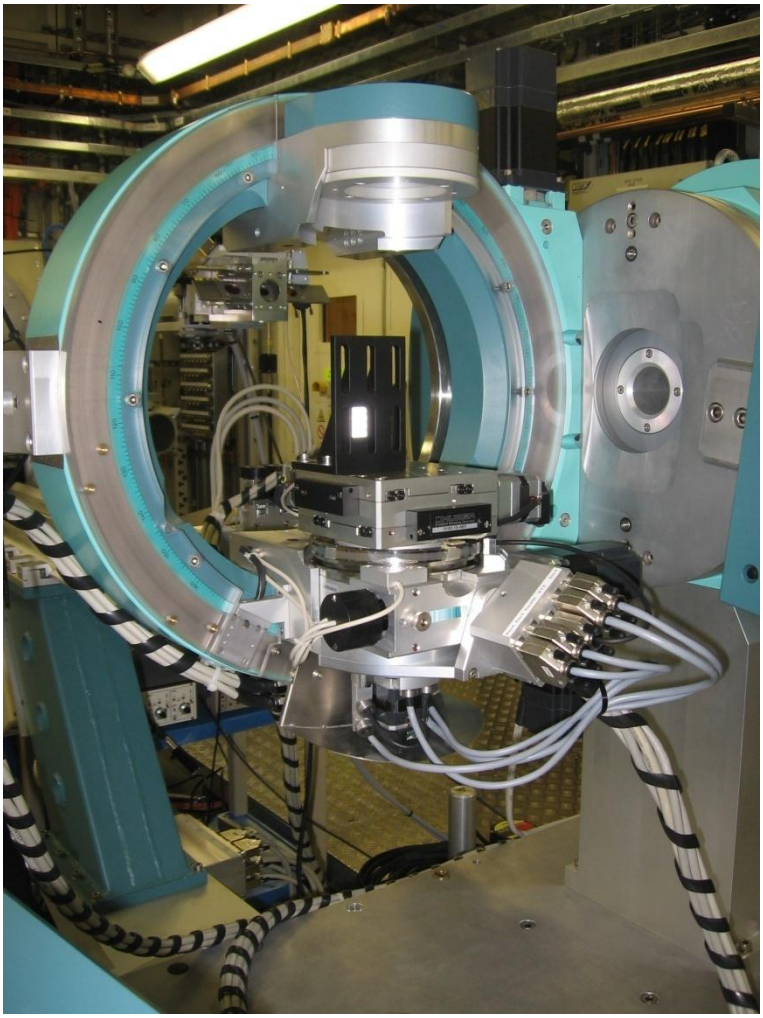

**Figure 111 – Vibration target mounted on diffractometer**

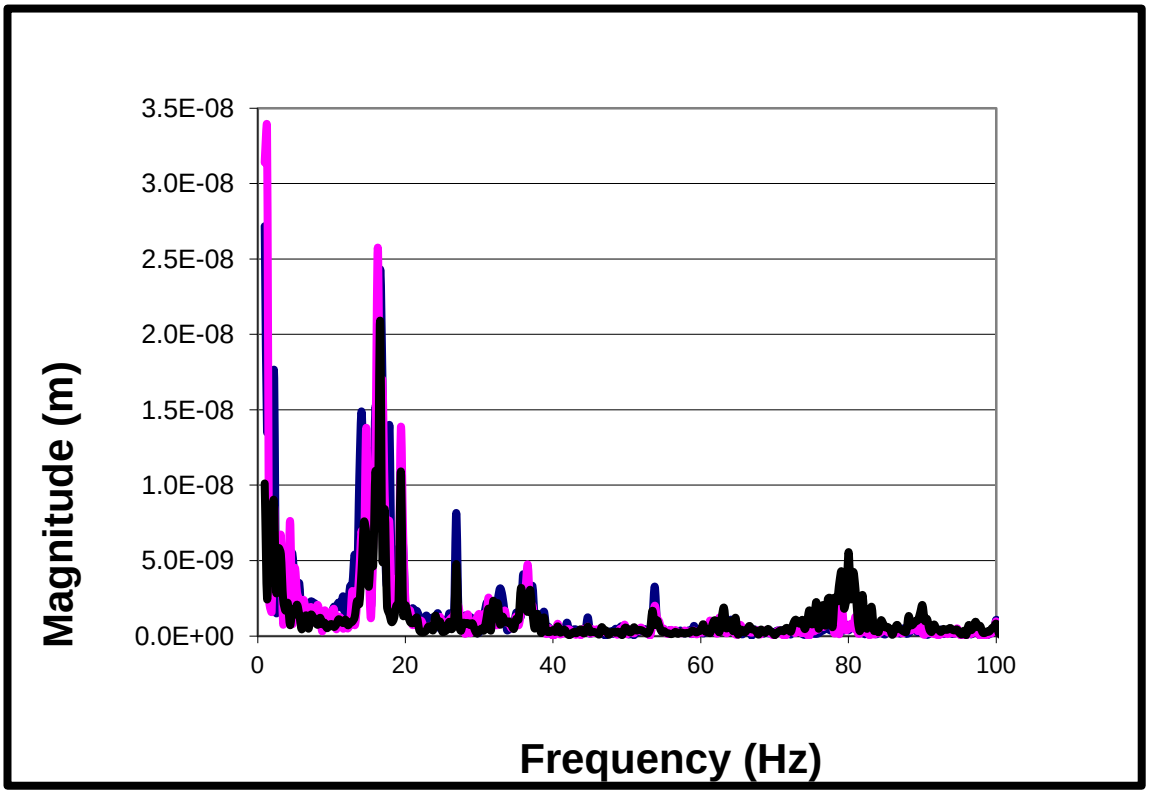


**Figure 112 – Vibration test looking at Diffractometer**

This shows that the motions at around 54Hz are between the optics stage and the detector stage. These seem to be absent from test 6. This indicates that the optics stage is moving at a frequency of around 54Hz. The tests show that relative motion along the beam direction between the detector stage and the diffractometer is relatively small at below 35nm. There is a resonance at around 15Hz. This indicates the complete KOHZU table and the Diffractometer base are moving at 15Hz as this is not present in the tests between stages of the KOHZU table.

## D.11 Test between detector stage and Beryllium Window

This test was with the vibrometer mounted on the detector stage looking at the fixed Berylium Window on Module 9. It shows the 15Hz motion but also a much larger motion at around 20Hz. This indicates that Module 9 is moving at around 20Hz in the direction of the beam

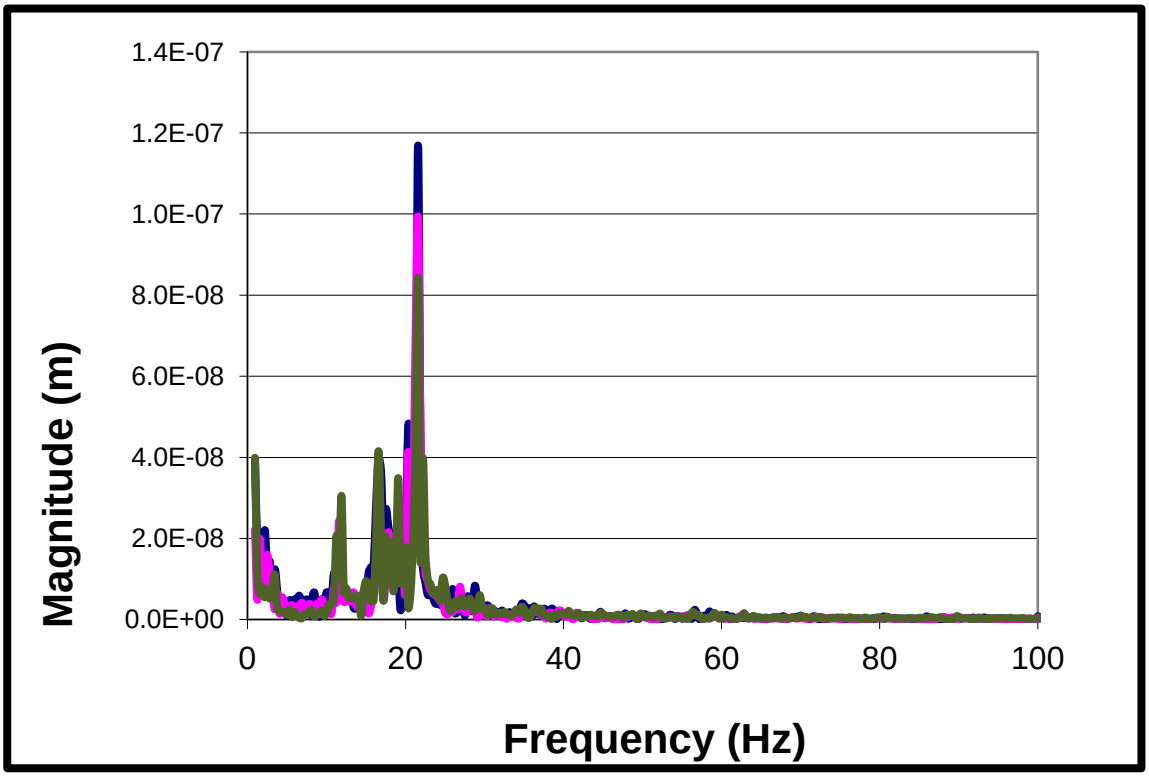


**Figure 113 – Detector stage to Beryllium Window**

## D.12 Vertical Test

4 tests were conducted with the polytec mounted vertically and pointing down.

Test 1 was with the polytec mounted on the optical table and pointing at the floor with the main jacks at the lowest position of -45mm

Test 2 was the same as test 1 but with the jacks raised to +145mm

Test 3 was with the polytec mounted on the detector stage and looking at the floor and test 4 was with the polytec again mounted on the detector stage but pointing at the top surface of the KOHZU table. Tests 3 and 4 were with the table at +145mm.

In each case 3 tests were conducted and the graphs below show the average for the three tests.

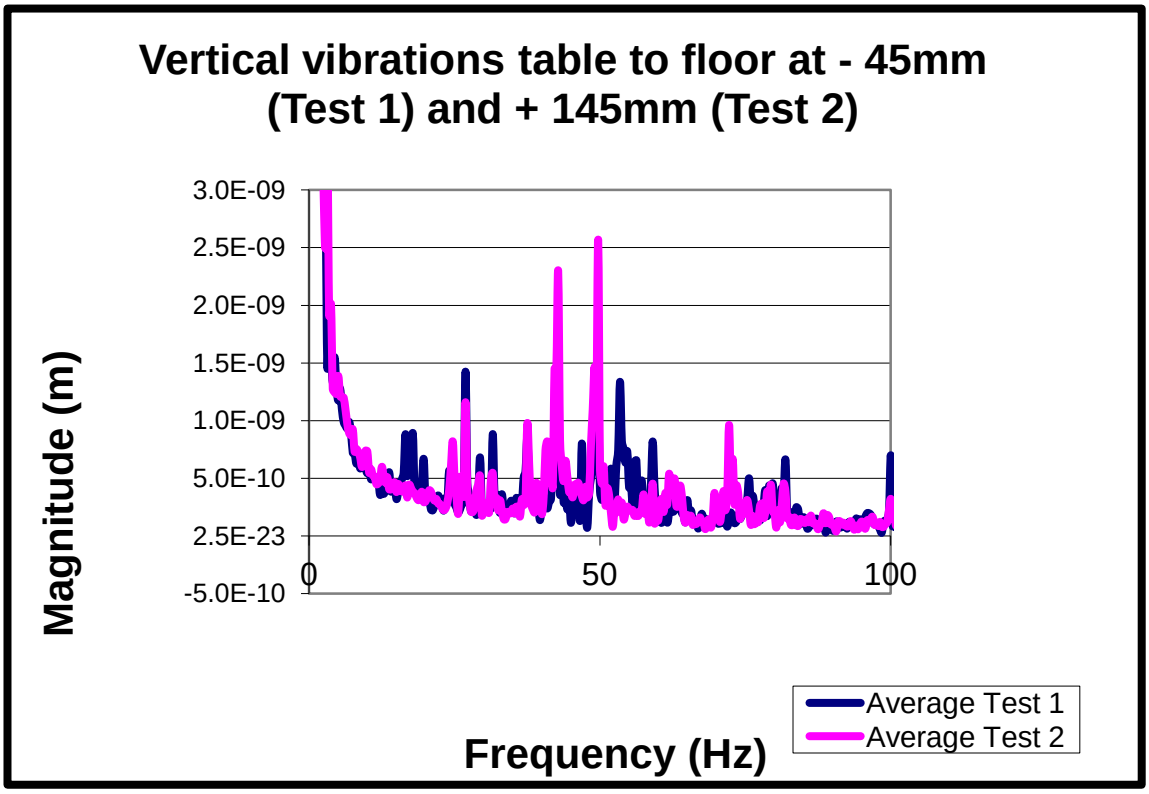


**Figure 114 – Vertical vibration tests at different heights**

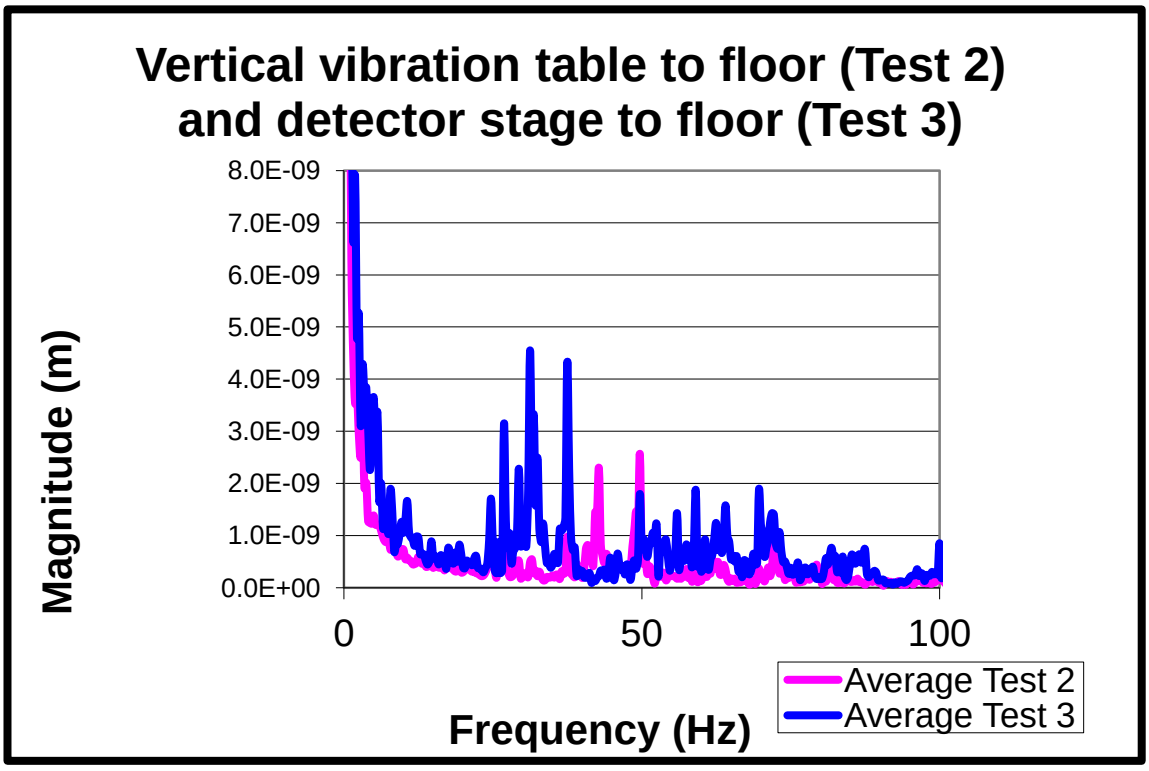

**Figure 115 – Vertical vibration tests of detector stage and main table**

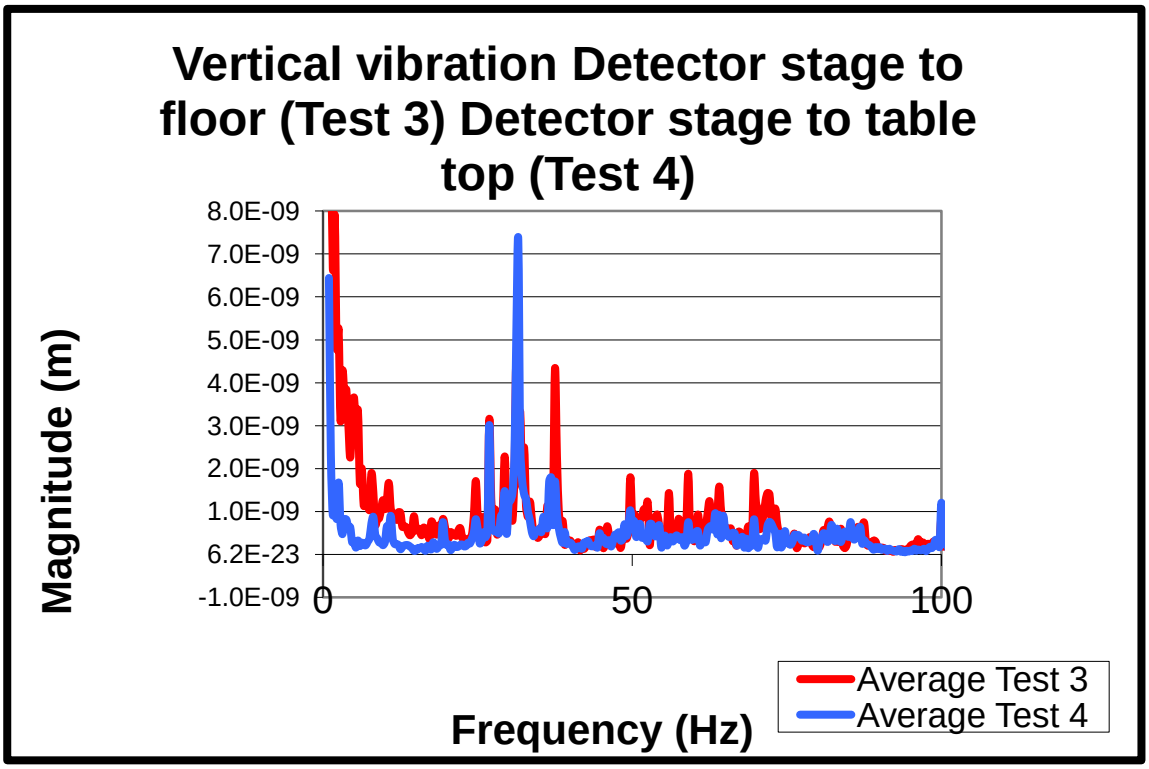


**Figure 116 – Vertical vibration tests of detector stage**

## D.13 Discussion of vertical motion results

Ignoring the motions at below 2Hz the vertical motions between the optical table and the floor are less than 3nm. The vibrations are worse when the table is raised to its highest level.

The detector stage is less stable than the optical table but the vertical motions are still less than 5nm relative to the floor.

The detector stage seems to have a vertical vibration mode at about 30Hz, but at other frequencies the relative vertical motion is below 3nm.

The motions below 2Hz appear to be large and so further tests with an interferometer that can measure motions accurately below 2Hz is required.

The vertical motions are significantly smaller than horizontal motions measured in previous tests.

The vertical motions of the optics and diagnostics stages could not be easily measured.

## D.14 Conclusion of Vibrometer tests on Optical table

For micro focus applications the table appears to be very good but is not ideal for a nano focus application. There are movements both vertically and horizontally between the three stages and between the stages and other components. Although these movements are small they are still significant at the nm scale. The polytec vibrometer is a good way of measuring vibrations, the beam size is small and it is a non contact method. Accurate measurement at below 2Hz however may not be very accurate.

# Appendix E Temperature stabilised enclosure tests

## E.1 Introduction

A temperature stabilised enclosure suitable for nano focus experiments was designed and tested. The Enclosure consisted of a double walled Aluminium alloy box. The inner box was manufactured from Aluminium Alloy Grade 5083. This has a better thermal conductivity than the standard Grade 6082. The internal volume was 568mm long, 360mm wide and 275mm high. The outer box was of Grade 6082. Both boxes were made from 16mm thick plate. There was a 10mm gap between the inner and outer box. The outer box was fitted with 4 integrated heat pump assemblies. These consist of a single 30w, 30mm peltier device, finned heat exchanger and a fan. The peltiers were controlled by a 4 stand alone temperature controllers. These were type PTC-CH series from Wavelength Electronics. The temperature sensors originally used used were 4 wire PT100 sensors but this was changed to Thermisters. The outer enclosure was fitted with 3 layers of 5mm thick neoprene sponge foam.

## E.2 Enclosure concept

The concept of the enclosure is that the heat pumps will maintain a constant temperature of the outer box at 4 locations. The temperature set should be the mid range of the expected external temperature. The thermal insulation reduces the heat gain or loss when the external temperature is higher or lower than the internal temperature. The inner box provides a high conductivity shield which surrounds the critical components and the air gap reduces conductivity but allows air to circulate and even out the temperature.

## E.3 Temperature measurement electronics

The temperature logging was carried out using 4 wire PT100 sensors connected to a National Instruments NI9217 Analog input module. The NI9217 has a noise rejection of 85 db at 50Hz and a resolution of 0.003°C when operated at less than 3.3Hz. The accuracy is 0.15 °C over the range -200 to 150 °C. However a higher level of resolution

can be obtained if using the analog module to measure resistance and then convert the resistance to temperature in software.

The measured resistance is converted into a temperature reading using the following formulae.

$T_r = -R_0A + \sqrt{( R_0^2A^2 - 4R_0B(R_0-R_T))} / 2R_0B$

$R_0$=100, A = $3.908 \times 10^{-3}$, B= $-5.775 \times 10^{-7}$

## E.4 Enclosure results

The best results were obtained within the Optics Metrology Lab where the surrounding temperature stability was within 0.1 C.

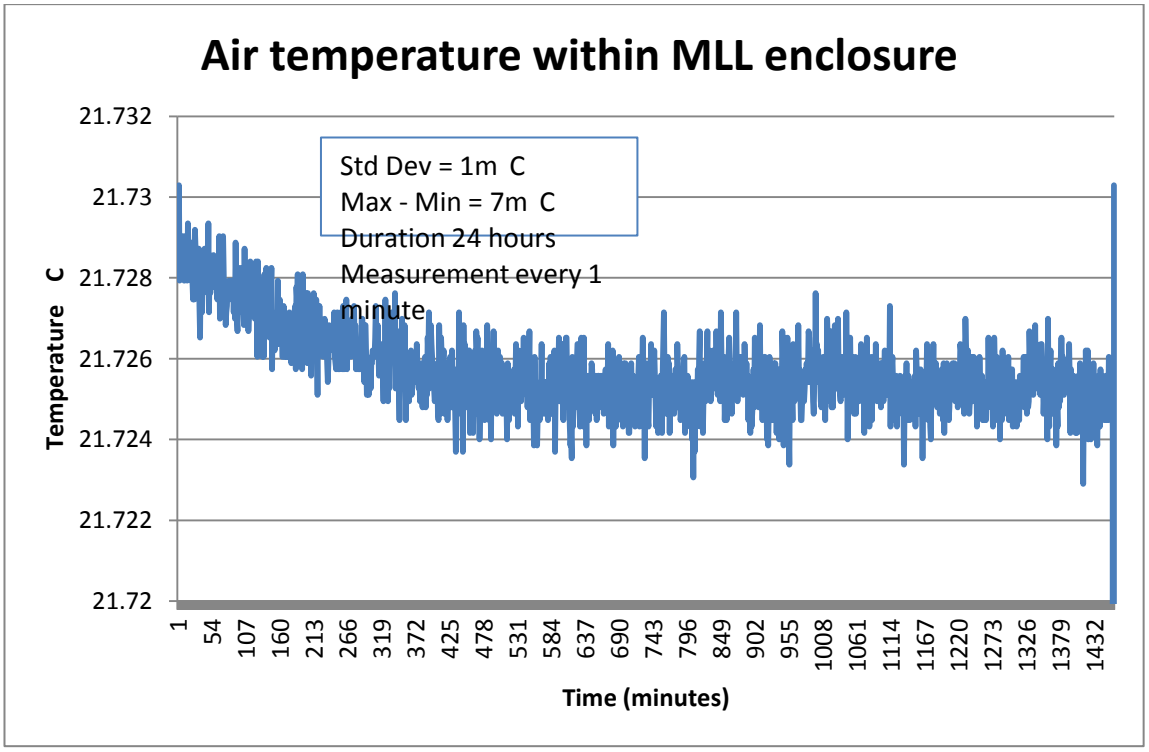


**Figure 117 – Internal air temperature of enclosure**

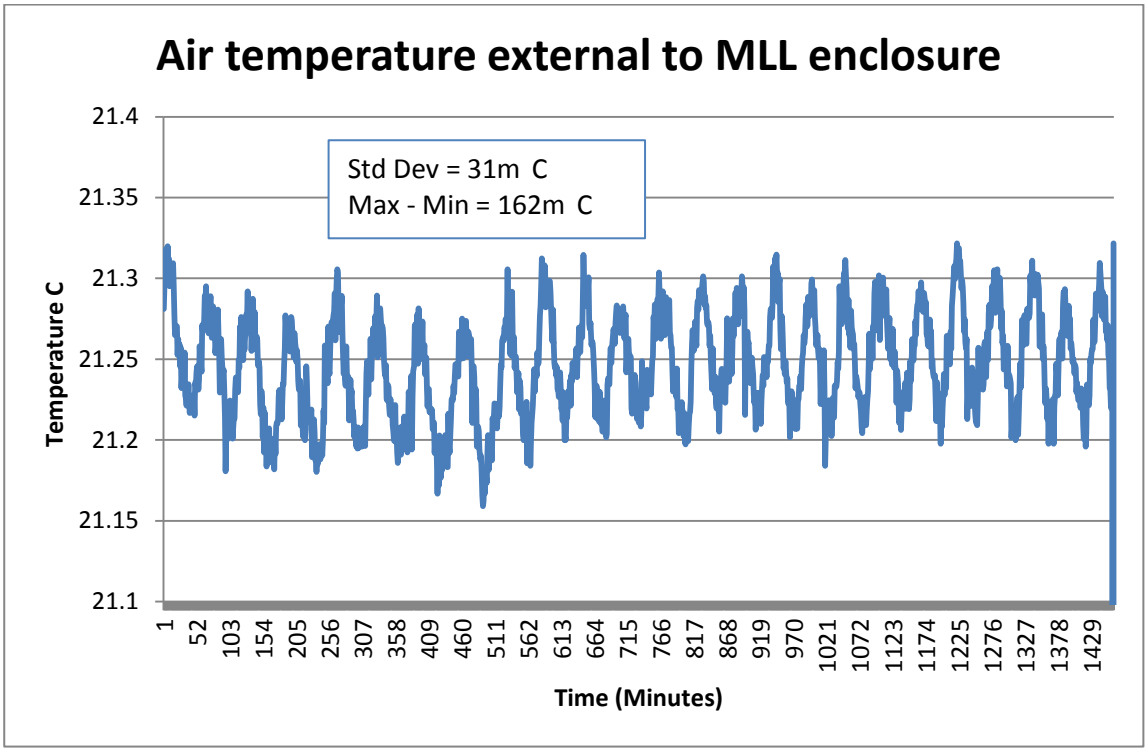


**Figure 118 – External air temperature in metrology lab**

The relatively high frequency saw tooth profile of the external temperatures helps to reduce the time for heat to be transferred through the insulation. The air conditioning system in the metrology lab is not representative of experimental hutches. A test was conducted in the experimental hall showed not only a larger temperature variation but a very long cycle time, as shown in Figure 119. This gave more time for heat to transfer through the insulation which is shown in Figure 120.

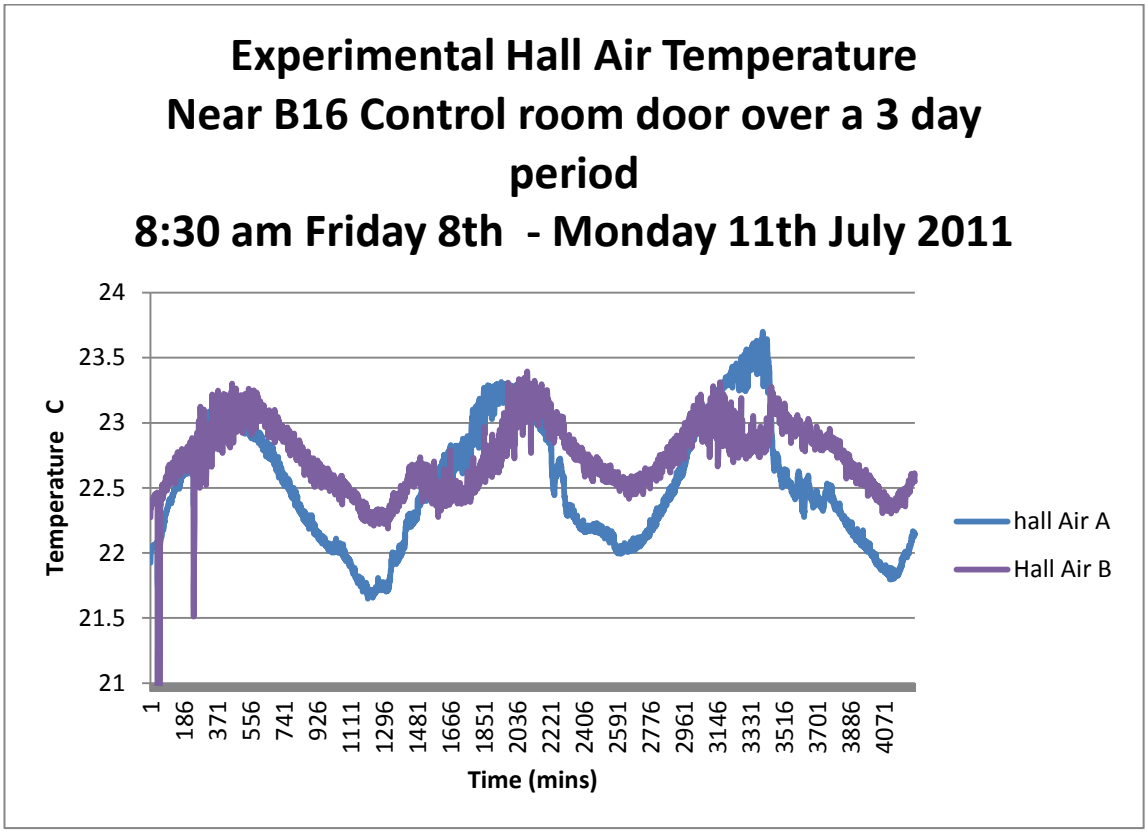


**Figure 119 – External temperature of experimental hall**

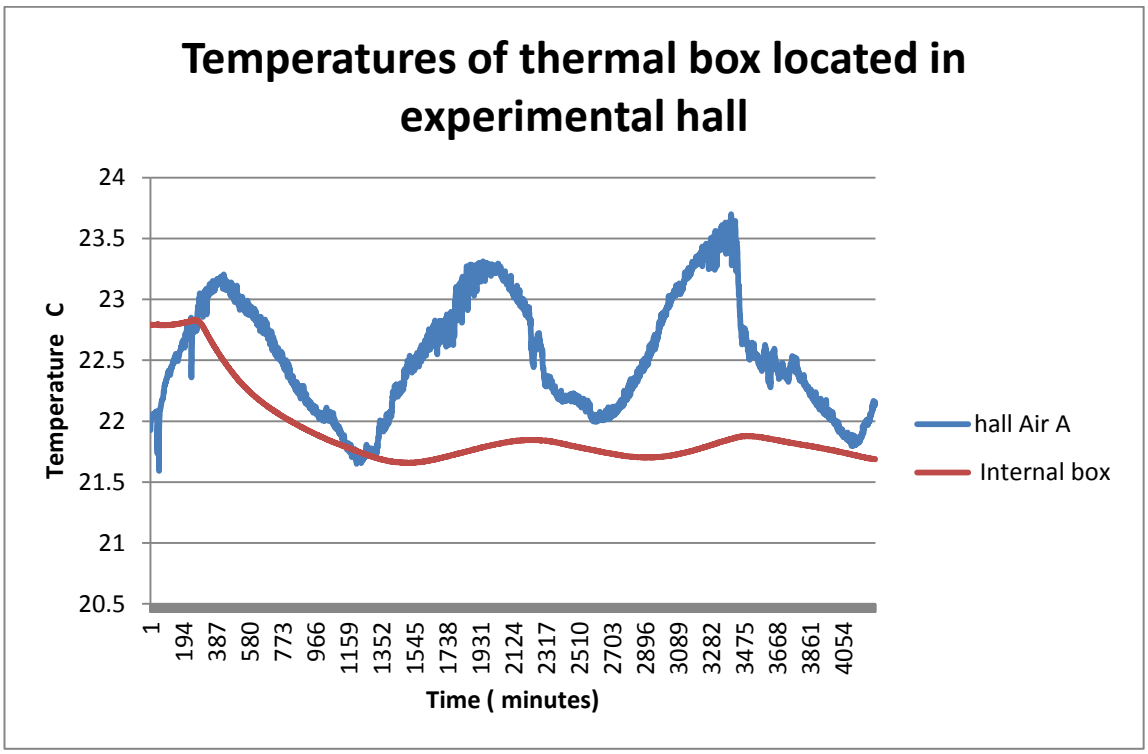


**Figure 120 – Comparison of internal and external temperatures**

These tests showed that the internal temperature stability is highly dependent not only on the temperature variation but the cycle time. This affect could be reduced by applying more thermal insulation but this increase the volume occupied and is not ideal. Tests within the B16 experimental hutch showed similar cycle times to the main experimental hall. The results are shown in Figure 121.

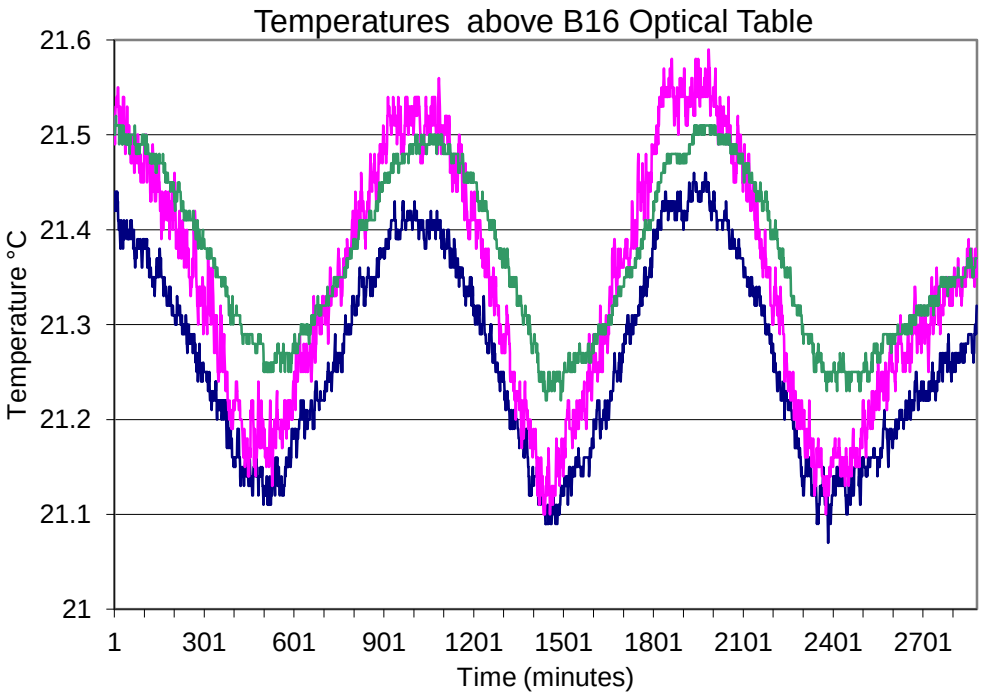


**Figure 121 – B16 Hutch temperature**

The PID settings were changed and the most recent tests within the Experimental hutch were with the internals were fitted with 4 slabs of granite to increase the thermal mass. This produced a standard deviation below 0.6mC over 2 days.

# Appendix F Newport CMM-255 Vibration isolator test

## F.1 Introduction.

A possible method of producing a stable end station is to use piezo actuators to counteract the vibration of the floor. To provide a stable reference measurement point a small vibration isolated platform would be required. This test was to determine if such a small platform could provide a stable reference point.

## F.2 Experimental equipment

A set of 4 Newport Spectra Physics CM-225 compact pneumatic isolators were placed on the floor of the B16 Beamline experiments hutch. These were connected to a compressed air supply. An aluminium plate 360mm x 275mm x 16mm and a granite block was placed onto the isolators. On top of the aluminium plate was placed 2 vibration sensors (1 horizontal and 1 vertical). Next to the isolation system were placed 2 more vibration sensors. The sensors were connected by BNC coaxial cables to a Data physics Quattro data analysis unit which then connected to a PC running Signal Calc Auto power spectrum.

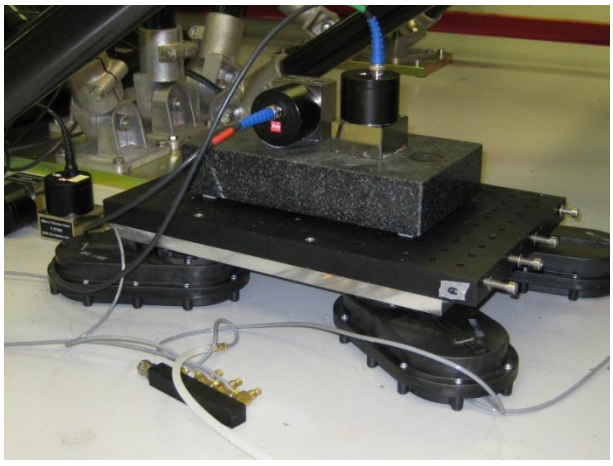

**Figure 122 – Vibration test with 2 aluminium plates and granite block**

## F.3 Sensors

The sensors used were HBA-L1 Ultra low frequency vibration gauges from the Institute of Engineering Mechanics, China Earthquake Administration. Dip switch 2 ON (Small velocity). Bandwidth 1 – 100 Hz

| Input No | Position | Ref No |
|---|---|---|
| 1 | Floor (H) | 07002 |
| 2 | Floor (V) | 07003 |
| 3 | Platform (H) | 07001 |
| 4 | Platform (V) | 06010 |

**Table 41 – Vibration sensors**

## F.4 Data acquisition settings

The settings set in signal calc were as follows: F span 100, Lines 800, 10% overlap, Hanning, T span 8 Seconds, Velocity measurements.

## F.5 Stabilisation

The measurements of the vibrations were observed on the PC screen and the system was allowed time to settle, the sensors placed on the vibration isolators took about 1 hour to settle. The air supply pressure and the load on the isolators were changed to obtain the highest vibration attenuation conditions. The best solution was obtained using 2 plates and a granite block (Total weight 16Kg) and a pressure of 1.5 Bar.

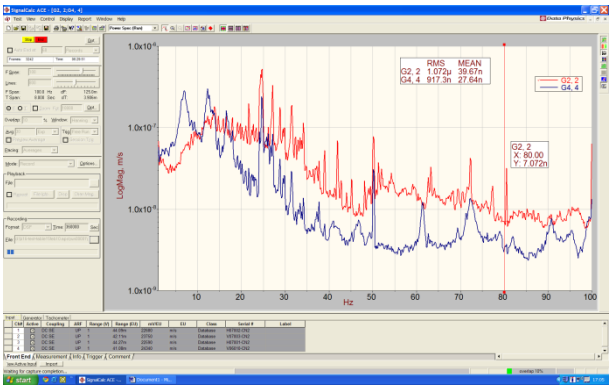


**Figure 123– Screen shot of vertical vibrations during test.**

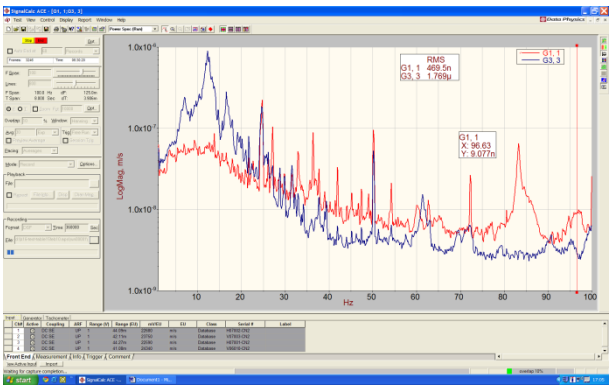


**Figure 124 – Screen shot of horizontal vibrations during test.**

## F.6 Results

The best result was extracted as a text file and then converted into excel and a graph produced.

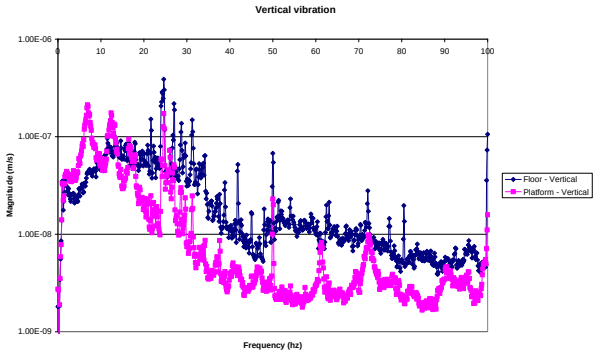


**Figure 125– Vertical vibration.**

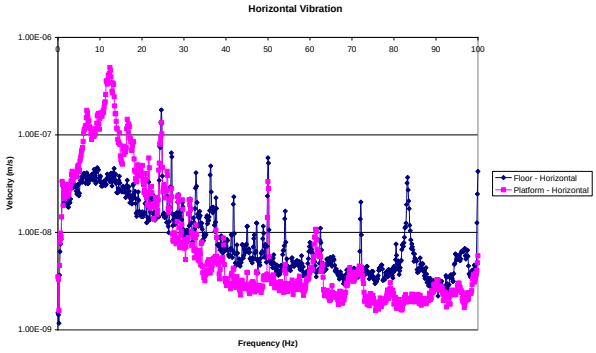


**Figure 126– Horizontal vibrations.**

## F.7 Vertical vibration discussion

The isolator provided vibration damping above 13Hz, but had resonances at 7 and 12Hz which increased vibration levels. The reduction in vibration was best between 30 and 90Hz, except for resonances at 50, 61 and 72Hz the reduction was about 10x.

The CM-225 isolator data sheet shows transmissibility increasing from 1 at 1 Hz to a maximum of 3.5 at 3.5 Hz, reducing to 1 at 5.5Hz and then reducing to 0.2 at 10Hz and 0.01 at 30Hz.

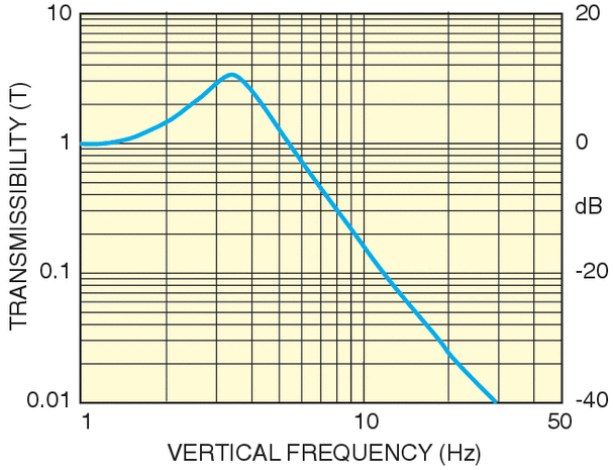


**Figure 127– Data sheet Vertical Transmissibility for a CM-255**

(Newport 1, 2012)

Figure 127 shows the Vertical Transmissibility data supplied by Newport Spectra Physics and Figure 128 shows the transmissibility derived from the measured data. This shows maximum Transmissibility at 7Hz rather than 3.5Hz and generally poorer results.

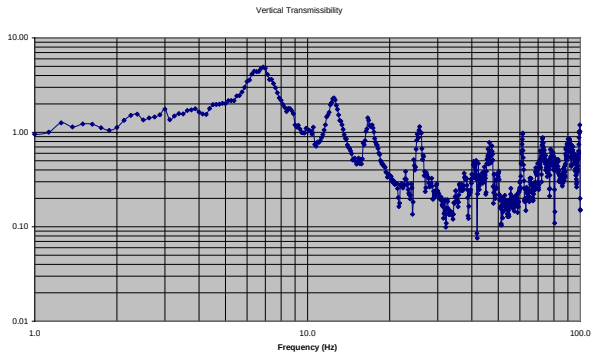


**Figure 128– Measured vertical transmissibility.**

## F.8 Horizontal vibration discussion

The isolator provided vibration damping above 30Hz, but had resonances at 12Hz which increased vibration levels. The reduction in vibration was best between 30 and 100Hz, except for resonances at 50, 61, 69 and 72Hz the reduction was about 2x. However the isolation of a floor vibration at 83 Hz was very good The CM-225 isolator data sheet shows transmissibility increasing from 1 at 1 Hz to a maximum of 3.5 at 3.5 Hz, reducing to 1 at 5.5Hz and then reducing to 0.2 at 10Hz and 0.01 at 40Hz.

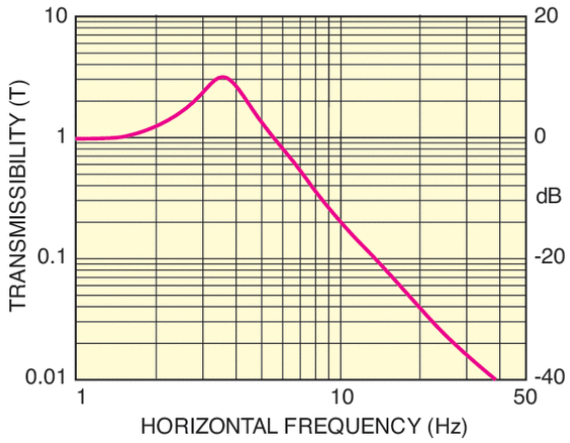


**Figure 129– Data sheet Horizontal Transmissibility for a CM-255**

**(Newport 2, 2012)**

Figure 129 shows the Horizontal Transmissibility supplied by Newport Spectra Physics and Figure 130 shows the transmissibility derived from the measured data. This shows maximum Transmissibility at 12Hz rather than 3.5Hz and generally poor results.

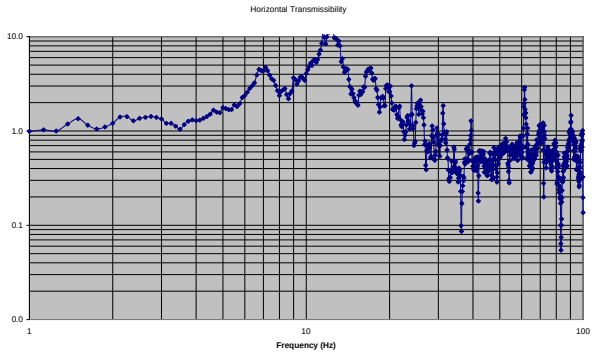


**Figure 130– Measured horizontal transmissibility.**

## F.9 Conclusion

The transmissibility at higher frequencies are larger than predicted by the data sheets. This could be that the background vibration levels are very low and the sensor noise is dominating the signal.

The transmissibility results are poorer, especially in the horizontal direction.

The measured 50Hz resonance is probably from 240v 50Hz ac electrical mains.

The rated maximum load per isolator is 27Kg. This would give a total load of 180Kg. Newport claim the results would be best when the isolators are operating at their maximum rated capacity.

For the low levels of background vibration the CM-255 does not seem to offer a great deal of benefit.

# Appendix G Tests of MinusK table

## G.1 Introduction

MinusK Technology Inc manufacture a range of passive vibration isolation tables that use negative spring coefficient mechanisms. This offers very low frequency resonant frequency. A Bench top vibration isolation platform type BM-10 was tested using four HBA-L1 ultra low frequency vibration gauges.


**Figure 131 – MinusK platform**

## G.2 Test results

Figure 132 shows the measurements of Horizontal vibrations and vertical vibrations for the floor and the MinusK table. The results looked very impressive with very good isolation below 3 Hz. There was good isolation from the known floor vibration at 11,16,18,24.3 and 27 Hz. There was apparent resonance at 50Hz but this could be 50Hz electrical mains pick up on the sensor cables. There was also resonance detected at about 36Hz from the horizontal sensor. The device has an adjustment for setting the payload within the operating range. The platform is very soft and before the platform is touched spacers must be fitted and the top platform clamped down.

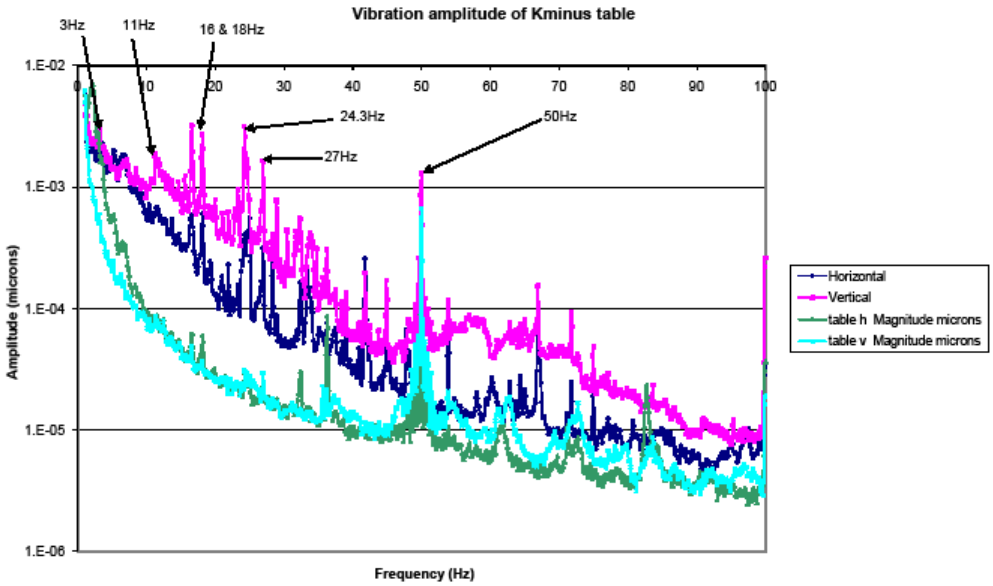


**Figure 132 – MinusK vibration test results**

## G.3 Conclusion

The minusK table offers very god vibration isolation but because it is very soft it needs to be clamped if any external force is applied. A motion stage with a moving mass will affect the table and so it will deflect relative to an external reference. An end station needs to remain aligned with the X-ray source and so this type of device is not ideal. It could however be used as a reference secondary platform from which a primary platform supporting the end station is referenced. This reference could be done using a laser interferometer or capacitive sensor.